ISRAEL TEMPRANO FARIÑA

TOWARDS METATHESIS GROWTH OF INTRINSICALLY CONDUCTING POLYMERS FROM METAL SURFACES

Thèse présentée
à la Faculté des études supérieures de l'Université Laval
dans le cadre du programme de doctorat en Chimie
pour l'obtention du grade de Philosophiae Doctor (Ph.D.)

DÉPARTEMENT DE CHIMIE
FACULTÉ DES SCIENCES ET DE GÉNIE
UNIVERSITÉ LAVAL
QUÉBEC

2010

Abstract

The present thesis tackles the study of alkylidene modified molybdenum carbide as catalyst for surface initiated metathesis polymerization under ultrahigh vacuum (UHV) conditions. The surface science study was carried out using a multianalytical system equipped with reflection absorption infrared spectroscopy (RAIRS), X-ray photoelectron spectroscopy (XPS) and thermal desorption spectrometry (TDS). The first part of this thesis is devoted to the description of the experimental system in terms of a guide for any new student who intends to operate such kind of system.

The study of the characterization and catalytic activity of alkylidene modified molybdenum carbide presented in this thesis is composed of two parts. The first part is devoted to the preparation and characterization of new metal-alkylidene species on the surface of β-Mo_2C. Two new alkylidene species were studied, dimethyl alkylidene ($(CH_3)_2C$=Mo), and vinyl alkylidene (CH_2CHCH=Mo) species. Spectroscopic data for the chemisorption of aliphatic ketones such as acetone, acetone-d_6 and acrolein, indicate that β-Mo_2C induces carbonyl scission at room temperature under ultra high vacuum conditions to form metal alkylidene and oxo species. This reaction also causes the formation of a layer of undefined carbon on the surface which deactivates the otherwise reactive β-Mo_2C towards decomposition of the formed alkylidenes, conferring them with great thermal stability.

The main part of this thesis is dedicated to the study of alkylidenes as initiator species for the surface initiated polymerization towards the formation of polyacetylene. Two polymerization methods were tested. First the ring opening metathesis polymerization of 1,3,5,7-cyclooctatetrarene (COT) was performed at cyclopentylidene and vinyl alkylidene active sites. Then acetylene metathesis polymerization was carried out at cyclopentylidene sites. The results of both methods are comparable, and small differences in the conformation of the polymer are suggested by the vibrational data. Halogenation of the obtained polymers was used as a marker to follow the reaction using X-ray photoelectron spectroscopy.

The adsorption behaviour of the monomers on β-Mo_2C is analyzed at the end of the corresponding chapters. Vibrational data suggest that cyclooctatetraene adopts a planar conformation which could favour the reaction by augmenting the strain of the molecule as well as the residence time which allows the molecule to react at lower temperatures than observed for norbornene and cyclopentene. Acetylene on the other hand undergoes cyclization on the surface of molybdenum carbide at temperatures lower to those required for the polymerization, and thus the formation of benzene and butadiene at the surface of molybdenum carbide enters into competition with the formation of polyacetylene on the alkylidene modified surface.

Résumé

Cette thèse présentera l'étude d'un catalyseur de carbure de molybdène modifié par des alkylidènes dans le but de faire de la polymérisation par réaction de métathèse induite par la surface, le tout dans des conditions de ultra-haut vide (UHV).

Ce système catalytique a été caractérisé par différentes techniques d'analyse utilisées en science des surfaces : la spectroscopie infrarouge par réflexion-adsorption (RAIRS), la spectroscopie des photoélectrons par rayons X (XPS) et la spectrométrie de masse par thermodésorption (TDS). La première partie de la thèse décrira le système expérimental à la manière d'un guide pour les nouveaux utilisateurs de ce type de système multi-analytique.

La caractérisation et l'étude de l'activité catalytique du carbure de molybdène modifié par des alkylidènes sera présentée en deux parties. La première partie sera dédiée à la préparation et à la caractérisation de nouvelles espèces métal-alkylidène sur la surface du β-Mo_2C. Deux nouvelles espèces ont été étudiées, soient le diméthyle alkylidène ($(CH_3)_2C$=Mo) et le vinyl alkylidène (CH_2CHCH=Mo). Des données spectroscopiques sur la chimisorption de cétones aliphatiques telles que l'acétone, l'acétone-d_6 et l'acroléine indiquent que le β-Mo_2C induit un bris du lien carbonyle à température ambiante dans des conditions d'ultra-haut vide pour former les espèces métal-alkylidène et métal-oxo. Cette réaction produit aussi une couche superficielle de carbone de nature indéfinie qui diminue la réactivité de la surface de β-Mo_2C face à la décomposition moléculaire conférant ainsi une très haute stabilité thermique aux espèces formées.

Le principal sujet de cette thèse concerne l'étude de ces alkylidènes comme des espèces initiatrices pour la polymérisation de surface en vue de former le polyacétylène. Deux méthodes de polymérisation ont été testées. Premièrement, la polymérisation par métathèse par ouverture de cycle du 1,3,5,7-cyclooctatétraène (COT) a été effectuée sur des sites actifs de cyclopentylidène et de vinyl alkylidène. Deuxièmement, la polymérisation par métathèse avec l'acétylène a été effectuée sur des sites de cyclopentylidène. Les résultats de ces deux méthodes sont comparables malgré des différences mineures dans la

conformation des polymères, lesquelles sont suggérées par les données des spectres vibrationnels.

Le comportement des monomères adsorbés sur β-Mo_2C est aussi analysé à la fin de chaque chapitre. La spectroscopie vibrationnelle suggère que le cyclooctatétraène adopte une configuration plate qui pourrait favoriser sa réactivité en augmentant la tension moléculaire ainsi que le temps de résidence de la molécule sur la surface. Ces effets pourront être responsables du faite que le cyclooctatétraène réagisse à une plus basse température face à la polymérisation par ouverture de cycle que le norbornène et le cyclopentène. Pour ce qui concerne l'acétylène, il réagit avec lui-même à température plus basse que la température de polymérisation pour donner du benzène et du butadiène sur la surface du carbure de molybdène. Cette réaction est, alors, en compétition avec la formation du polyacétylène sur la surface modifiée avec des espèces alkylidène.

Acknowledgments

I would like to express my appreciation to the president and members of the judging panel for having accepted to be part of the committee and take the time and effort to correct this work.

I would especially like to thank my thesis director, Professor Peter H. McBreen, for all the support and confidence he invested in me over the past years. I am sincerely grateful that he chose to offer me this fantastic opportunity to study under his supervision, turning out to be more than a thesis advisor, an inspiring mentor and a friend. My sincerest hope for this work is that it can make him proud.

Je tiens à remercier tous les membres du groupe de recherche des sciences de surface avec lesquels j'ai partagé mon quotidien ces dernières années. Cela a été un plaisir de travailler dans une ambiance aussi agréable et amicale, ainsi qu'enrichissante.

Je remercie particulièrement Mohamed Siaj pour m'avoir pris *sous son aile* ainsi que pour son amitié sincère, son support et ses précieux conseils. Ses précédents travaux sur ce projet ont été d'une immense inspiration tout au long de mes études.

Un immense merci à Marc-André Laliberté, mon meilleur ami à Québec dès le premier jour, toujours prêt à aider et apporter son inébranlable bonne humeur. Il a été d'une aide inestimable pour moi, tant sur le plan professionnel que personnel.

Gautier Mahieu a également été un extraordinaire support en apportant sa sincère amitié, sa bonne humeur, ainsi que son expérience en tant que post-doc. Merci pour toutes les expériences que nous avons partagées.

Ce fut également un grand plaisir de partager le laboratoire avec Stéphane Lavoie, Nathalie Dubuc, Vincent Demers-Carpentier et Carl Maltais. Qu'ils en soient ici remerciés.

Un grand merci aux membres du Département de Chimie de l'Université Laval, pour leur gentillesse et leur accueil. J'aimerais remercier les professeurs du département pour leurs précieux conseils, leur grande disponibilité et leur collaboration, spécialement

les professeurs Mario Leclerc et Frédéric G. Fontaine pour leur aide et pour l´intérêt qu'ils ont porté à ma carrière.

Merci infiniment à tous les collaborateurs du département, spécialement à Jean Laferrière et André Bilodeau pour venir rapidement à notre secours à chaque fois qu´il y avait quelque chose que ne fonctionnait pas, et ce, avec une patience infinie. À André Demers, parce que sans lui rien ne marcherai en ce bas monde. Sans oublier les gens de l´atelier mécanique et les dames du secrétariat pour être toujours prêts à m'aider avec un sourire et beaucoup de patience par rapport à mon français.

Merci encore à tous les amis que je me suis fait au département. Un merci spécial à Alex Michaud pour m'avoir proposé d'aller jouer au soccer alors que je venais tout juste d´arriver et pour être toujours là encore aujourd'hui. Merci également à Patricia Harding-Lepage pour notre complicité, à Richard Loach pour être mon *"Bro"* depuis son arrivée et à Catherine Lefebvre pour sa compagnie et son support dans les durs moments de la rédaction.

Merci aussi à tous les amis que je me suis fait au Québec et qui m´ont fait sentir entouré et apprécié en tout temps. Votre présence m´a aidé à me sentir vraiment à la maison à Québec. Merci!

Un grand merci à ma famille d'Espagne pour son support inconditionnel dans la distance, mais surtout à celle de Québec, les Fréchette, pour m´avoir accueilli de manière si exceptionnelle. Je me sens comme un membre de plus de votre famille et j'en suis très fier. Si quelqu´un est responsable de mon bien-être à Québec, c´est vous.

Merci enfin à celle qui mérite le plus de remerciements : Christine Fréchette, qui a été une source d'encouragement et un soutien incroyable tout au long de ce travail. Elle a été à mes côtés lorsque je n´étais qu´un petit espagnol perdu au grand Canada à la recherche d´une possibilité de continuer mes études. Elle m´a permis d'avoir cette chance à l´Université Laval et elle est restée à mes côtés tout au long de ce dur travail, dans les bons et mauvais moments, toujours là pour me faire croire en moi-même lorsque j´en avais

besoin. Sans elle, ce travail n´aurait jamais vu la fin. Merci infiniment ma chérie, je ne pourrai jamais asez te remercier pour tout ce que tu as fait pour moi.

À Christine

Table of index

Abstract ..... **i**

Résumé ..... **iii**

Acknowledgments ..... **v**

Figures list ..... **xv**

Schemes ..... **xxi**

1. Introduction **1**

1.1 Motivation 1

1.1.1 Molecular electronics 1

1.1.2 Metal alkylidenes 3

1.1.3 Molybdenum carbide 8

1.2 Overview of results 9

1.3 Bibliography 11

2. Experimental **17**

2.1 Introduction: Surface chemistry and catalysis 17

2.1.1 Surface Science 17

2.1.2 Ultra-High Vacuum Technology 19

2.2 XPS / RAIRS / MS system 21

2.2.1 General characteristics 21

2.2.2 Pumping system 22

2.2.3 Surface analysis 26

2.2.3.1 X-ray photoelectron spectroscopy 27

2.2.3.2 Temperature programmed desorption 30

2.2.3.3 Reflection absorption infrared spectroscopy 31

2.2.3 Preparation of UHV system 33

2.2.4 Surface preparation 34

2.2.4.1 Ion sputtering 36

2.2.4.2 Chemical cleaning 38

2.2.5 Maintenance 38

2.2.5.1 Dry air on the Dewar 38

2.2.5.2 Baking out the gas-handling ramps 39

2.2.5.3 Degassing of internal filaments 40

2.2.5.4 Pumping the infrared detectors 40

2.2.6 Modifications of the system 40

2.2.6.1 Reconfiguration of the gas-handling ramps 40

2.2.6.2 Replacement of the IR system 42

2.3 Bibliography 44

3. Formation of dimethyl alkylidene and vinyl alkylidene species on the surface of molybdenum carbide 45

3.1 Abstract 45

3.2 Dissociative adsorption of carbonyl compounds on β-Mo_2C 46

3.2.1 Dimethyl alkylidene 47

3.2.1.1 Infrared characterization 47

3.2.1.2 Thermally programmed desorption study 54

3.2.1.3 X-ray photoelectron spectroscopy 55

3.2.2 Vinyl alkylidene 58

3.2.2.1 Infrared spectroscopy 59

3.2.2.2 X-ray photoelectron spectroscopy 65

3.2.2.3 Thermally programmed desorption study 69

3.3 Conclusion 70

3.4 Bibliography 71

4. Ring opening metathesis polymerization of 1,3,5,7-cycloocatatetraene on an alkylidene modified β-Mo_2C surface 76

4.1 Abstract 76

4.2 Cyclopentylidene terminated PA 79

4.2.1 IR characterization: "molecular footprint" 80

4.2.2 XPS characterization 91

4.2.3 Absence of polyacetylene oxidation 98

4.3 Vinyl alkylidene modified surface 100

4.3.1 IR characterization 101

4.3.2 XPS characterization 105

4.4 Halogenation of polyacetylene 107

4.4.1 Cyclopentylidene terminated polyacetylene 107

4.4.2 Vinyl alkylidene terminated polyacetylene 112

4.5 Discussion 114

4.5.1 Discussion on the IR data 114

4.5.2 Cyclooctatetraene adsorbed on β-Mo_2C 115

4.6 Bibliography 123

5. Polymerization of acetylene on alkylidene modified β-Mo_2C 131

5.1 Acetylene polymerization 131

5.2 Spectroscopic evidence for acetylene polymerization 132

5.2.1 IR characterization 133

5.2.2 XPS characterization 135

5.3 Acetylene cyclization 139

5.4 Conclusion 146

5.5 Bibliography 146

6. General Conclusion 151

6.1 Conclusion 151

6.2 Future works 154

6.3 Bibliography 155

Tables list

Table 3-1 : Vibrational frequencies (cm^{-1}) observed by RAIRS of acetone and fully deuterated acetone on molybdenum carbide. The mode assignments and data for acetone on Pt(111)[30-33] and for liquid acetone[39] are listed for comparison. 51

Table 4-1 : IR spectra assignment for polyacetylene synthesized from 1) a Ti-based catalyst[40]; 2) a rare-earth-based catalyst[47,48]; 3) highly oriented polyacetylene[50]; and 4) on alkylidene-modified molybdenum carbide.....89

Figures list

Figure 1-1 : Comparison of electrical conductivities of metals, semiconductors, and insulators; *d* indicates doped material. 2

Figure 1-2 : Molecular wire connected to metal electrodes in a sandwich configuration by alkylidene junctions. 4

Figure 1-3 : a) Metal alkylidene bonded on a surface single site on the surface of molybdenum carbide. b) Typical bridge bonded alkylidene on the surface of a pure metal. 5

Figure 2-1 : General view of the multianalytical UHV system used in this study. 20

Figure 2-2 : Cross-section of a pair of *Conflat* flanges used in UHV equipment. The seal is made by bolting together two identical flanges with a flat metal ring gasket between the knife edges. The knife edges press annular grooves in each side of the copper gasket, filling all voids and defects and producing a leak-tight seal. 21

Figure 2-3 : Photographs of the pumping system from below the UHV chamber and from the back of it. 23

Figure 2-4 : Diagram of the design of (a) rotary vane pump, (b) turbomolecular pump, and (c) diffusion pump. 24

Figure 2-5 : Image of a classic ion gauge with all parts indicated. 25

Figure 2-6 : Top view of the system used in this study with the analytical apparatus shown. 27

Figure 2-7 : Diagram of the photoelectric effect, the photon absorption and the deep core electron emission (initial and final states). 28

Figure 2-8 : TPD measurements are performed with the sample placed close to the entrance of the shield of the mass spectrometer. 30

Figure 2-9 : a) Diagram of the IR beam path from the source to the detector; b) Consequence of the electric field reflection of p-polarized and s-polarized radiation; c) Effect of image dipoles on the resultant dipole.....32

Figure 2-10 : Data for O(1s) and S(2p) after several stages of the cleaning process (chemical treatment for oxygen and ion sputtering for the sulphur). The areas are normalized to the area of the Mo($3d_{3/2+5/2}$) peak. 36

Figure 2-11 : Image of a LK Technologies NGI3000 ion gun, the one used in the system, with a leak valve already assembled in position. 37

Figure 2-12 : Background spectra of the clean surface before and after the replacement of the spectrometer and the mirror boxes. Both series of spectra were obtained under the same conditions at 100 K. 43

Figure 3-1 : Acetone as a function of exposure on the surface of β-Mo_2C at 100 K. Evolution of the monolayer is observed from 0.4 L up to ~2 L. Peaks of the multilayer start to appear at ~3 L and are fully visible at 33 L. 48

Figure 3-2 : RAIRS spectra for acetone-d_6 adsorption on molybdenum carbide at 100 K as a function of exposure. Monolayer bands are observed with increasing intensity up to 3 L above which peaks of the multilayer start to appear. The 13 L spectrum reveals the multilayer peaks. 50

Figure 3-3: RAIRS spectra for 30 L acetone adsorbed on β-Mo_2C at 100 K followed by annealing to the indicated temperatures. 53

Figure 3-4 : TPD spectra for multilayer exposure (15 L) of acetone at 100 K on molybdenum carbide. Data for the molecular peak (black spectrum) and CO_2 (red spectrum) are displayed. 54

Figure 3-5 : High-resolution C(1s) data recorded for dimethyl alkylidene species on β-Mo_2C. Reference spectra are shown for the clean carbide sample and for the carbide treated with 10 L ethylene at 600 K to deposit excess surface carbon. The spectrum of a multilayer of acetone (20 L) is also included; the spectra were recorded at the indicated temperatures. 56

Figure 3-6 : RAIRS spectra of acrolein adsorbed on the surface of molybdenum carbide at 100 K as a function of the exposure. 61

Figure 3-7 : RAIRS data for a) acrolein monolayer at 200 K, and b) and c) for vinyl alkylidene species formed after annealing the sample to 300 K and 500 K respectively. 63

Figure 3-8 : RAIRS data for a) multilayer of acrolein at 100 K; b) vinyl alkylidene species formed by annealing the adsorbed acrolein to 300 K; c) vinyl alkylidene species formed by the cross metathesis reaction of cyclopentylidene species on molybdenum carbide with butadiene at 470 K[28]. 64

Figure 3-9 : C(1s) data for acrolein a) as a function of exposure at 100 K, and b) as a function of temperature after dosing the surface with 20 L at 100 K..... 66

Figure 3-10 : Plot of the ratio between alkylidene species (285.8 eV) and surface carbidic carbon (282.8 eV) after annealing acrolein to different temperatures..... 68

Figure 3-11 : TPD data for acrolein adsorption (20 L) at 100 K. The red spectrum corresponds to H_2 desorption and the black one to acrolein desorption..... 70

Figure 4-1 : Different isomers of polyacetylene. 81

Figure 4-2 : RAIRS spectra of a) cyclopentanone at 100 K; b) cyclopentylidene at 300 K; c) The cyclooctatetraene exposed alkylidene modified surface at 470 K and d) cyclooctatetraene at 100 K on the surface of molybdenum carbide..... 83

Figure 4-3 : RAIRS spectra of COT monomer insertion on a cyclopentylidene modified β-Mo_2C surface at a) 350 K and b) 500 K. 87

Figure 4-4 : RAIRS spectra in the ν(CH) region for COT monomer insertion at a cyclopentylidene modified β-Mo_2C surface at c) 350 K and d) 500 K, compared with spectra of a) cyclopentylidene species, and b) species formed by the cross metathesis reaction between cyclopentylidenes and 1,3-butadiene. 90

Figure 4-5 : XPS spectra a) cyclopentylidene species; b) COT insertion as a function of exposure at 350 K. 92

Figure 4-6 : Plot of the proportion of olefinic carbons (284.3 eV) with respect of the amount of alkylidene species (285.8 eV) on the surface as a function of monomer exposure at 350 K. 93

Figure 4-7 : XPS spectra of COT introduction on a clean surface as a function of coverage at a) 100 K and b) 300 K. 95

Figure 4-8 : Relative Mo(3d) intensities for two different treatments of the surface. The black line corresponds to COT deposition on a clean surface. The red line corresponds to monomer insertion on a cyclopentylidene modified surface. Both series were recorded at $5x10^{-9}$ Torr and 350 K. 97

Figure 4-9 : XPS spectra of the a) C(1s) region of the multilayer of cyclopentanone (green), cyclopentylidene (blue) and polyacetylene (black); b) O(1s) region of cyclopentanone (green) and polyacetylene formed by the insertion of different amounts of monomer (COT). 99

Figure 4-10 : Infrared spectra in the C-H region of a) vinyl alkylidene moieties formed from the dissociative adsorption of acrolein on the surface; b) polyCOT formed from these active species, and c) vinyl alkylidene moieties formed from cross metathesis of cyclopentylidene species and 1,3-butadiene. 103

Figure 4-11 : RAIRS spectra in the C-H stretching region for polyacetylene formed at 350 K from a) vinyl alkylidene and b) cyclopentylidene species on β-Mo_2C.....104

Figure 4-12 : C(1s) spectra of the polymerization of COT on a vinyl alkylidene modified surface of molybdenum carbide as a function of monomer introduction at 300 K. 106

Figure 4-13 : Evolution of C(1s) and Br($3d_{5/2}$) peaks during consecutive cycles of polymerization of COT and bromination of the freshly formed polymer. 109

Figure 4-14 : a) TPD spectrum of Br_2 adsorbed on molybdenum carbide, and b) evolution of the Br($3d_{5/2}$) core level spectra for different amounts of bromine adsorbed on the same surface. 111

Figure 4-15 : Evolution of molecular Br on halogenated PA as a function of dosing. Each stage of bromination is made after the insertion of equal amounts of COT at 300 K. 113

Figure 4-16 : Differences in surface accessibility for cyclooctatetraene and norbornene. 116

Figure 4-17 : Configurations of free 1,3,5,7-cyclooctatetraene. 119

Figure 4-18 : IR spectra of adsorbed COT on β-Mo_2C as a function of coverage at 110 K. 121

Figure 4-19 : TPD spectra for m/z=2 and m/z=104 for COT deposition on the surface of molybdenum carbide. 122

Figure 5-1 : IR spectra of acetylene polymerization as a function of monomer insertion. Spectrum a) represents cyclopentylidene species formed at 300 K, whereas spectra b) and c) display acetylene insertion into the metal-alkylidene sites at 350 K when 0.0084 L and 30.9 L of monomer are introduced respectively. 134

Figure 5-2 : Difference spectra of the XPS C(1s) region for acetylene insertion with respect to the spectrum of cyclopentylidene species on the surface of molybdenum carbide as a function of monomer exposure. The temperature was raised from 100 K to 350 K during exposition to the monomer. 137

Figure 5-3 : 3D plot of the C(1s) region when the clean surface was exposed to acetylene. All spectra were taken with intervals of 3 minutes while the pressure of the chamber was maintained at $1x10^{-8}$ Torr. 138

Figure 5-4 : TPD data for exposure of 20 L of acetylene on a clean surface. Data for H_2, C_6H_6 and C_8H_8 moieties desorption was recorded 142

Figure 5-5 : TPD data for masses 39 and 78 as a function of exposure of acetylene at 100 K on the clean surface. 143

Figure 5-6 : TPD data for H_2 desorption as a function of acetylene exposure on a clean surface of molybdenum carbide. 145

Schemes

Scheme 1-1 : Chauvin mechanism for olefin metathesis. 5

Scheme 1-2 : Illustration of the reversible cleavage of the cyclobutanone carbonyl bond mediated by alkylidene-Mo-oxo species[56]. 6

Scheme 1-3 : Cyclopentylidene initiated cross metathesis reactions with a) 1,3-butadiene, b) propene, c) ethylene, and ring opening metathesis polymerization of d) norbornene, and e) cyclopentene.....7

Scheme 1-4 : Formation of dimethyl alkylidene and vinyl alkylidene from the dissociative adsorption of acetone and acrolein respectively. 9

Scheme 1-5 : ROMP of cyclooctatetraene at alkylidene sites and subsequent in-situ bromination of the formed polyacetylene. 10

Scheme 2-1 : Diagram of the gas-handling ramp system used to introduce gas molecules in the UHV chamber. 41

Scheme 3-1 : Proposed pathway for the dissociative adsorption of acetone on the surface of molybdenum carbide including an η^1 adsorption state at low temperatures and an intermediate η^2 state prior to the formation of the oxo=Mo=alkylidene species. 58

Scheme 3-2 : Acrolein adsorption via an η^1 configuration at low temperature (100 K) and the formation of vinyl alkylidene species by carbonyl scission when the temperature is raised above 300 K. 59

Scheme 4-1 : Formation of poly-COT via ROMP. 78

Scheme 4-2 : COT monomer insertion at cyclopentylidene sites on β-Mo_2C. 79

Scheme 4-3 : Formation of polyCOT using vinyl alkylidene species as initiator sites.....101

Scheme 4-4 : Cross metathesis between cyclopentylidene modified molybdenum carbide and 1,3-butadiene. 102

Scheme 4-5 : Bromination of cyclopentylidene initiated polyacetylene..... 112

Scheme 5-1 : Proposed mechanism for metathesis polymerization of acetylene on the surface of molybdenum carbide[16]. 132

Scheme 5-2 : Accepted pathway for acetylene cyclomerization over palladium surfaces. 140

Scheme 6-1 : Formation of dimethyl alkylidene and vinyl alkylidene from the dissociative adsorption of acetone and acrolein respectively. 151

Scheme 6-2 : Metathesis polymerization of acetylene and cyclooctatetraene towards the formation of polyacetylene on the surface of alkylidene modified molybdenum carbide. 152

1. Introduction

1.1 Motivation

1.1.1 Molecular electronics

Molecular transistors are gated three terminal devices in which a semiconducting molecule is sandwiched between two electrodes. These molecular wires are the fundamental building blocks for single-molecule electronics, and are expected to play an important part in the future of technological components[1-3]. Molecular electronics form part of the so-called "bottom up" strategy to achieve nanometer scaled electronic devices as the answer to the demand for smaller components and systems.

Two main challenges arise from this concept. One is the development of organic molecules that possess the electrical, electronic, and optical properties of a metal while retaining the mechanical properties commonly associated with conventional organic components. Polymers with such characteristics are known as "intrinsically conducting polymers", and are based on an extended π-electron system skeleton[4]. The simplest of these conjugated polymers is polyacetylene, which can be described as an unsubstituted $(CH)_x$ molecule. Polyacetylene was first synthesized by Natta and co-workers[5] in 1958 from acetylene, using a $Ti(OBu)_4$-$AlEt_3$ catalyst. However, at the time it was not amenable to most characterization methods and did not possess the interesting electrical properties that were anticipated. Using the same catalyst employed by Natta, but different experimental conditions, Shirakawa and co-workers[6-9] succeeded in preparing free-standing polyacetylene thin films of metallic lustre which upon doping become highly conducting, with a concurrent rise of the room temperature conductivity up to 12 orders of magnitude (Figure 1-1)[10]. Pristine cis-polyacetylene can almost be considered an insulator, whereas trans-polyacetylene has transport properties of a semiconductor, and heavily doped polyacetylenes have metallic conductivities[7].

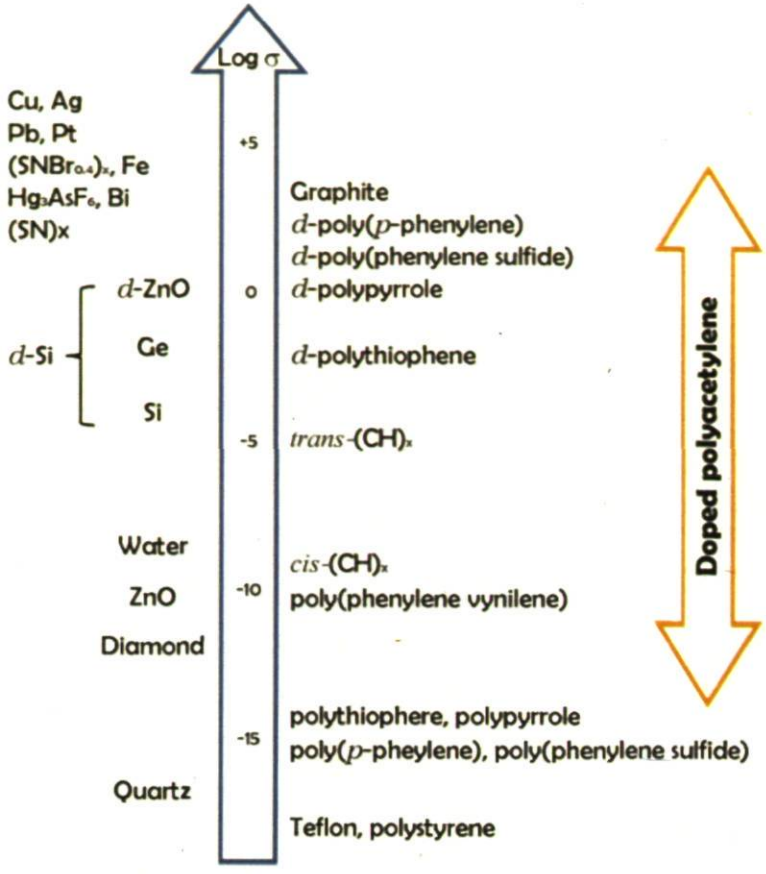

Figure 1-1 : Comparison of electrical conductivities of metals, semiconductors, and insulators; *d* indicates doped material.

Since their discovery, back in the 1970's, conjugated polymers have had a major impact in the scientific community, culminating with the Nobel Prize in chemistry awarded to Alan J. Heeger, Alan G. MacDiarmid, and Hideki Shirakawa in 2000. For almost 30 years now, these intrinsically conducting polymers (ICPs) have been under intensive research and development as new functional materials for electronics, photonics, advanced coatings, and related applications[4,11,12]. Some conjugated polymers such as polypyrrole and polyaniline have already found practical applications in the construction of electronic devices[13].

The second challenge for creating single-molecule electronics is to create suitable metal-molecule contacts. A lot of effort has been invested on the design and synthesis of conducting organic molecules[4,7,11-13]. However, the creation of a suitable metal-molecule

junction is also a very challenging issue. These junctions should allow current to flow effectively between the metal and the molecule, and should posses a good stability in terms of temperature and ambient degradation[3,14-16]. At the same time, a certain chemical activity would allow the use of surface-initiated polymerization to directly grow molecular wires from the surface[17-20].

A number of model surface grafting techniques have been used on planar surfaces and particles. One of the most commonly reported methods involves adsorption of functionalized homopolymers or block copolymers through a linker[21-26]. Commonly conjugated dithiol molecules are used to test candidates for molecular conductor devices when connected to gold electrodes[27-29]. However, discrepancies over the experimentally determined conductivities originate from the lack of atomistic details of the multiple possible gold-thiol adsorption modes[30-32]. Other linker groups, such as amines on gold and silanes on silicon or glass, face the same limitations in terms of lack of detailed atomic structures, subsequent useful chemistry, and an essential conducting channel for electrons and/or holes[18,20,33].

1.1.2 Metal alkylidenes

The conducting characteristics of a molecular junction depend critically on the delocalization of the molecular electronic orbitals. The use of well-defined metal alkylidenes could be a versatile approach towards establishing an efficient electrical contact from metallic surfaces to molecules. These contacts are robust and well-defined, whilst at the same time serving as initiating and propagating sites for olefin metathesis, a powerful synthetic tool[34-38] already used in the polymerization of ICPs[39-44].

Theoretical calculations on the conductivity of metal alkylidene linked polyenes have appeared lately. Tulevsky et al.[20] found that a 1,3-pentadiene chain forms Ru-to-C π bonding that is essentially continuous with the rest of the π-system on the molecule, coupling smoothly with the *d* orbitals in the Ru metal. More recently Ning et al.[33] studied the electron transport properties of 2,4,6-octatriene sandwiched between two Ru(0001)

surfaces, finding that the Ru=C double bonds at both ends of the molecule extend the π states into the leads and couple strongly with the conducting states of the Ru surfaces. They calculated the transmission coefficient for such a molecular junction to be 0.61 at the Fermi level of the metal, confirming that metal carbon double bonds can indeed create an efficient channel for charge carriers (Figure 1-2).

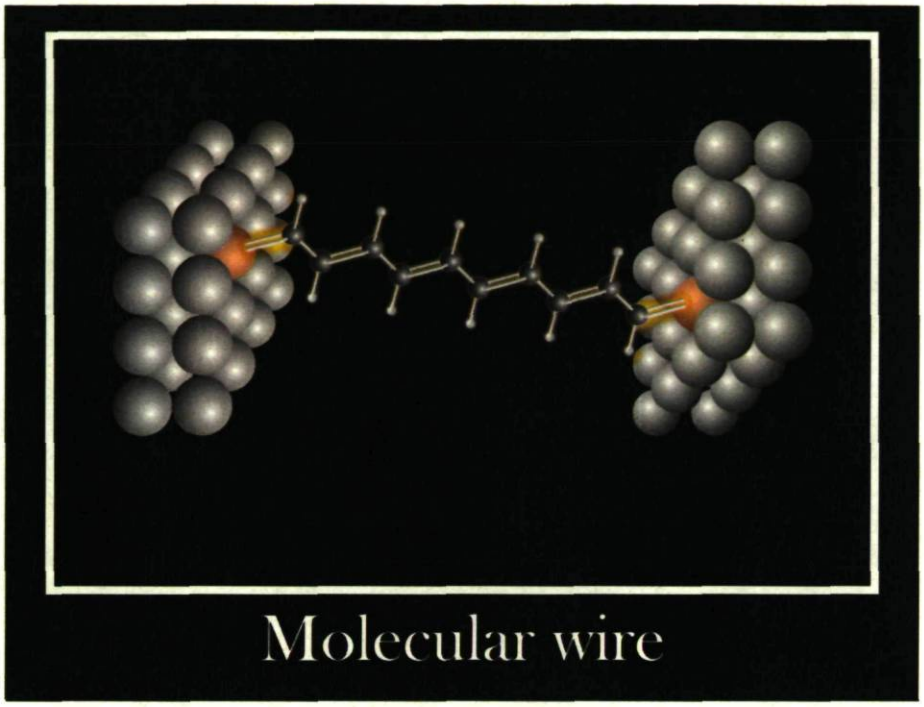

Figure 1-2 : Molecular wire connected to metal electrodes in a sandwich configuration by alkylidene junctions.

Metal alkylidene species have undergone extensive development during the past 30 years as a consequence of the discovery of the mechanism of metathesis reactions involving metal alkylidenes as initiator sites (Scheme 1-1)[45]. However, this development has mainly been achieved on homogeneous systems[23,34-38,46] due to the deep structural knowledge of these systems through their study by nuclear magnetic resonance (NMR) and X-ray diffraction spectroscopy (XRD). These techniques have allowed the study of the structure-activity relationship, and thus led to a continuous improvement in these systems, whereas heterogeneous systems are still for the most part ill-defined.

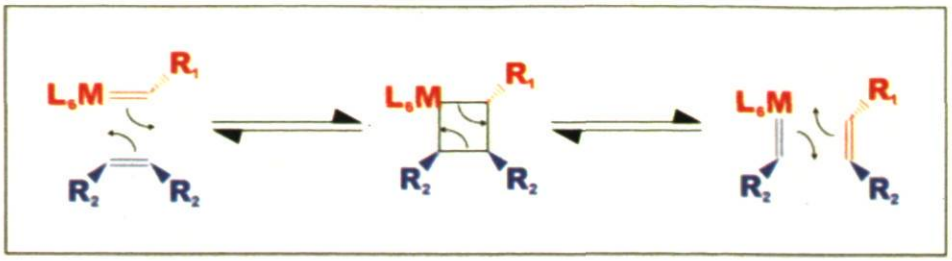

Scheme 1-1 : Chauvin mechanism for olefin metathesis.

Although the metathesis reaction was first observed in heterogeneous systems[47], the development of these systems has been outshone by the easier-to-study organometallic complexes[23,34-38,46]. The principal reason for this slow evolution is the complexity of the heterogeneous systems and the special conditions required for their study. Moreover the small number of active sites on these catalysts complicates the issue severely[48]. Owing to their technological relevance many unsuccessful attempts have been made to characterize heterogeneous metal alkylidenes on pure metals[49-51]. The general outcome of these attempts has been the formation of a bridge-bonded alkylidene (Figure 1-3 (b)), whereby the molecule forms two σ bonds with two metallic atoms, instead of a σ and a π bond to a single surface atom. However, recently surface science studies succeeded in synthesizing and studying the reactivity of single site metal alkylidenes on the surface of molybdenum carbide (Figure 1-3 (a)) under ultra high vacuum (UHV) conditions[17-19,52-56].

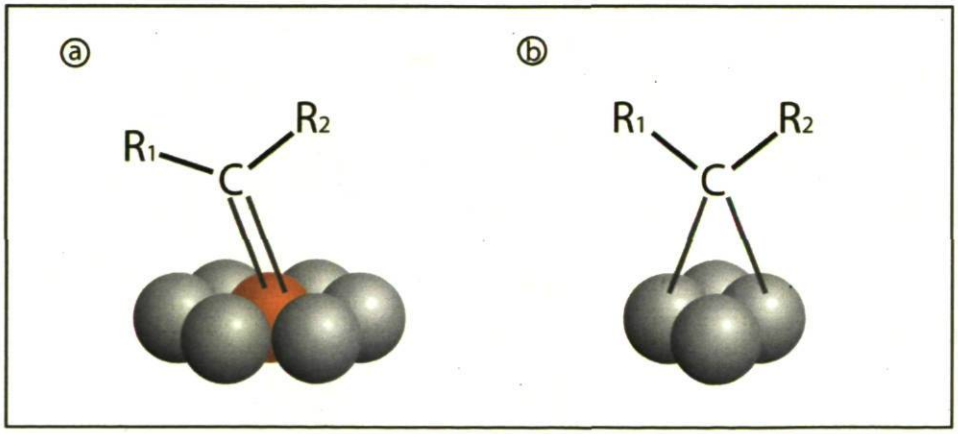

Figure 1-3 : a) Metal alkylidene bonded on a surface single site on the surface of molybdenum carbide. b) Typical bridge bonded alkylidene on the surface of a pure metal.

The formation of molybdenum alkylidenes (Mo=C) from the dissociative adsorption of carbonyl molecules on the surface of molybdenum carbide was first reported by Zahidi et al.[56] They succeeded in characterizing these species for a series of cyclic ketones at 300 K. These surface alkylidene species turned out to be thermally stable, suffering recombination only at temperatures around 1000 K (Scheme 1-2). Siaj et al.[55] then reported the dissociation of acetaldehyde on the same material to yield ethylidene and oxo surface groups, proving that not only cyclic ketones were able to undergo such dissociative adsorption.

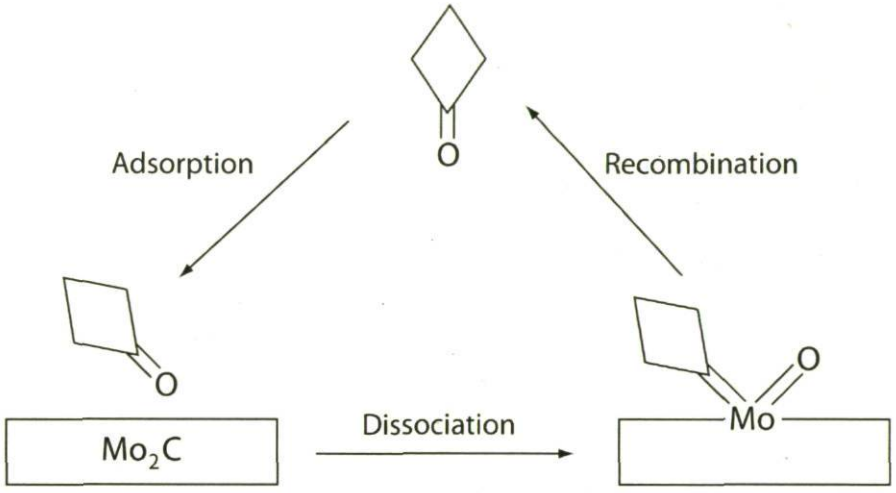

Scheme 1-2 : Illustration of the reversible cleavage of the cyclobutanone carbonyl bond mediated by alkylidene-Mo-oxo species[56].

Subsequent surface science studies on this system helped to deeply characterize these surface molybdenum alkylidene species. Oudghiri-Hassani et al.[52,57], and Siaj et al.[53] found that the relatively high reactivity of a clean β-Mo_2C surface permits both carbonyl bond scission and other less selective processes involving C-C and C-H bond cleavage of adsorbed ketones. These combined processes lead to the deposition of excess carbon and high-coordination oxygen on the surface to form an inert surface on which alkylidenes are thermally stable. Siaj et al.[53] went on to perform extensive studies to fully characterize adsorbed cyclobutanone on the surface of molybdenum carbide and the species resulting from the carbonyl bond scission at temperatures ranging from 300 to 500 K.

The reactivity of the well characterized alkylidene-modified surface of molybdenum carbide was then tested for metathesis reaction by Siaj et al.[17-19]. A series of reflection adsorption infrared spectroscopy (RAIRS) and thermally programmed reaction (TPR) studies under UHV conditions were used to characterize the products of the cross metathesis reaction of surface cyclopentylidene species with short acyclic olefins, and the ring opening metathesis polymerization of strained cyclic olefins (Scheme 1-3).

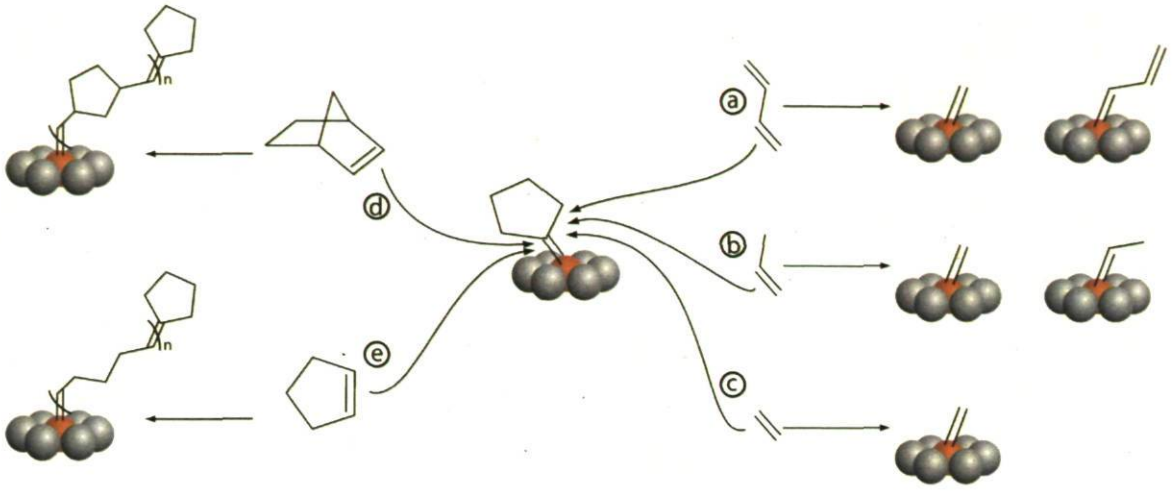

Scheme 1-3 : Cyclopentylidene initiated cross metathesis reactions with a) 1,3-butadiene, b) propene, c) ethylene, and ring opening metathesis polymerization of d) norbornene, and e) cyclopentene.

Recently Nuckolls and co-workers[20,58] succeeded in preparing ruthenium alkylidenes from the dissociative adsorption of diazomethane molecules in solution at room temperature. They performed cross metathesis reactions on an alkylidene-modified thin film surface of Ru with vinyl-trimethylsilane, detecting the corresponding products by gas chromatography (GC)[20]. They subsequently performed ring opening metathesis polymerization of strained cyclic olefins (dicyclopentadiene, norbornene, and trimeric cyclophane) with Ru nanoparticles activated by the alkylidene species[58]. The products of these reactions were characterized by nuclear magnetic resonance (NMR) and transmission electron microscopy (TEM). Although these nanoparticles showed limited reactivity, failing to perform the metathesis reaction with cyclooctatetraene, acetylene and vinyl-

trimethylsilane, they showed the potential of metal alkylidenes to react at ambient conditions.

1.1.3 Molybdenum carbide

Transition metal carbides are produced by dissolving carbon atoms into the metal lattice[59-63]. These carbide materials have unique tribological properties[64], since they demonstrate extreme hardness, high melting temperature, at the same time that they have electronic and magnetic properties similar to their parent transition metals. This combination of characteristics makes them good candidates for various applications in materials science. Moreover, these materials often demonstrate catalytic advantages over their parent metals in activity, selectivity and resistance to poisoning, and have been found to be active for a number of heterogeneous catalytic processes such as hydrodenitrogenation[74-76], aromatization[66,67], deshydrogenation[68-71], hydrogenation[65], and hydrodesulfurization[72,73].

The catalytic performance of transition metal carbides could be considered as tuneable, as it can vary with the nature of the transition metal used, the C/M ratio, and the surface orientation of the carbide[77-79]. Oyama et al.[64] reported that carbide structures suffer an enlargement of metal-metal distances with carbon insertion that can induce an increase in the density of states close to the Fermi level[80]. This electronic effect is known as the *ligand effect*, and is accompanied by a geometric effect since carbon atoms limit the number of metallic atoms at the surface[77,78,81]. These two effects may play an important role in the reactivity of β-Mo_2C to create single site metal alkylidenes from the dissociative adsorption of carbonyl compounds as reported by McBreen and collaborators[19,53-56]. The *ligand effect* can be noticed in that carbon deposition from molecular cracking on the surface lowers the activity of the surface protecting the alkylidene species from decomposition to very high temperatures[52,53,56,57,82].

1.2 Overview of results

The study presented in this thesis intends to develop the knowledge on the characterization and reactivity of metal alkylidenes and oxo groups on the surface of molybdenum carbide. In order to do so, the generation of new aliphatic alkylidenes, and the capability of alkylidenes to perform surface initiated polymerization of conjugated molecules were investigated. These studies have been carried out using surface science techniques. Measurements of the formation of alkylidenes and the reaction products were performed using reflection adsorption infrared spectroscopy (RAIRS), thermal desorption spectrometry (TDS) and X-ray photoelectron spectroscopy (XPS). Chapter 2 will introduce the methodology for the surface science studies, paying special attention to the characteristics of the multianalytical system used in this study. Chapter 2 strives to be a complete guide for anyone who needs to use this or any other UHV system of the surface science laboratory.

The preparation and characterization of new aliphatic alkylidene species on the surface of molybdenum carbide is presented in Chapter 3. Evidence of the formation of dimethyl alkylidene and vinyl alkylidene from the dissociative adsorption of acetone and acrolein will be presented (Scheme 1-4). The characterization of these products is supported by previous studies made on the dissociative adsorption of cyclic ketones and acetaldehyde performed by Zahidi et al.[56], Oudghiri-Hassani et al.[52], and Siaj et al.[17-19,53-55] on the same catalytic system.

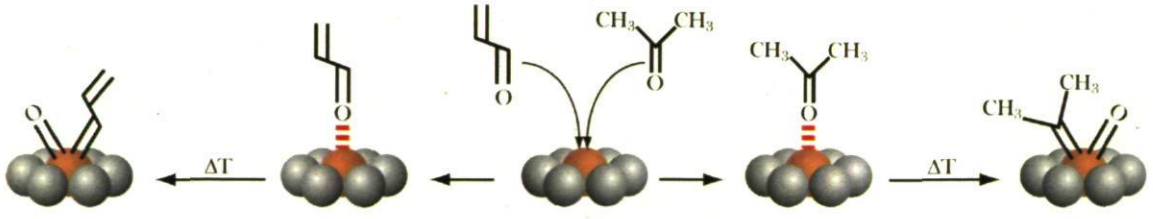

Scheme 1-4 : Formation of dimethyl alkylidene and vinyl alkylidene from the dissociative adsorption of acetone and acrolein respectively.

Chapter 4 presents a new strategy to perform surface initiated polymerization of 1,3,5,7-cyclooctatetraene from metal-alkylidene junctions (Scheme 1-5). Ring opening metathesis polymerization (ROMP) from cyclopentylidene and vinyl alkylidene sites will be discussed and characterized using RAIRS and XPS data, following the example presented by Siaj et al.[18] of the ROMP of strained cycloolefins. The in-situ halogenation of the surface polymer will serve as a further characterization technique, in which the progress of this reaction is followed by XPS using the C-Br bond as a marker. An extensive analysis on the conformational properties of polyacetylene formed by ROMP will be made from data acquired using the conformational sensitive RAIRS technique. Cyclooctatetraene adsorption on molybdenum carbide will be discussed as well in order to analyze its behaviour on the surface and its reactivity in comparison to the ROMP reaction at alkylidene initiator sites.

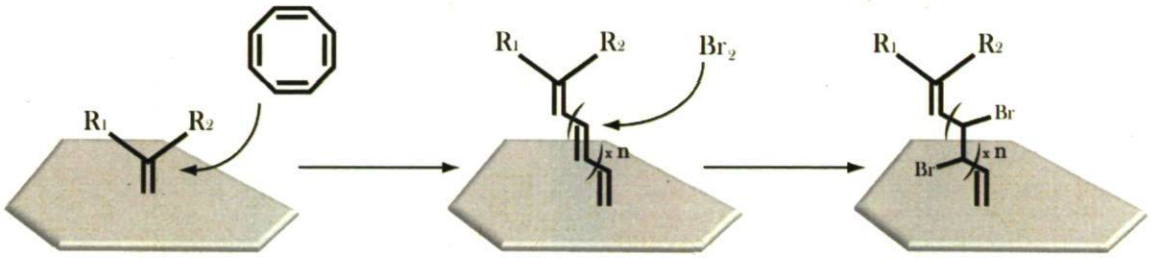

Scheme 1-5 : ROMP of cyclooctatetraene at alkylidene sites and subsequent in-situ bromination of the formed polyacetylene.

An alternative route to surface initiated ring opening metathesis polymerization of cyclooctatetraene to form polyacetylene will be presented in Chapter 5. Acetylene metathesis polymerization was characterized at surface cyclopentylidene sites. The products of this reaction were analyzed using surface science techniques, as well as the products of the halogenation of the formed polyacetylene. A novel reaction on the surface of molybdenum carbide was discovered during the study of the acetylene polymerization, the competitive cyclotrimerization of acetylene. This reaction has been observed in the literature for a number of heterogeneous catalysts[83-92] and will be analyzed by TPD measurements and discussed with respect to the literature.

1.3 Bibliography

(1) Flood, A. H.; Stoddart, J. F.; Steuerman, D. W.; Heath, J. R. *Science* **2004**, *306*, 2055.

(2) Reed, M. A. *Proceedings of the IEEE* **1999**, *87*, 652.

(3) Troisi, A.; Ratner, M. A. *Small* **2006**, *2*, 172.

(4) MacDiarmid, A. G. *Angew. Chem. Int. Ed.* **2001**, *40*, 2581.

(5) Natta, G.; Mazzanti, G.; Corradini, P. *Rend. Accad. Nazl. Lincei* **1958**, *25*, 2.

(6) Ito, T.; Shirakawa, H.; Ikeda, S. *J. Polym. Sci.* **1974**, *12*, 11.

(7) Shirakawa, H. *Rev. of Modern Physics* **2001**, *73*, 713.

(8) Shirakawa, H.; Ikeda, S. *Polym. J.* **1971**, *2*, 231.

(9) Shirakawa, H.; Ikeda, S. *J. Polym. Sci. Chem. Ed.* **1974**, *12*, 929.

(10) Shirakawa, H.; Louis, E. J.; MacDiarmid, A. J.; Chiang, C. K.; Heeger, A. J. *J. C. S. Chem. Comm.* **1977**, 578.

(11) Pearson, D. L.; Jones III, L.; Schumm, J. S.; Tour, J. M. *Synth. Metals* **1997**, *84*, 303.

(12) Shaw, J. M.; Seidler, P. F. *IBM J. Res. & Dev.* **2001**, *45*, 3.

(13) Svoboda, J.; Bláha, M.; Sedlácek, J.; Vohlídal, J.; Balcar, H.; Mav-Golez, I.; Zigon, M. *Acta. Chim. Slov.* **2006**, *53*, 407.

(14) Emberly, E.; Kirczenow, G. *Nanotech.* **1999**, *10*, 285.

(15) Nitzan, A.; Ratner, M. A. *Science* **2003**, *300*, 1384.

(16) Piva, P. G.; DiLabio, G. A.; Pitters, J. L.; Zikovsky, J.; Rezeq, M.; Dogel, S.; Hofer, W. A.; Wolkow, R. A. *Nature* **2005**, *435*, 658.

(17) Siaj, M.; Dubuc, N.; Temprano, I.; Maltais, C.; McBreen, P. H. *J. Phys. Chem.*, Article submitted.

(18) Siaj, M.; McBreen, P. H. *Science* **2005**, *309*, 588.

(19) Siaj, M.; Temprano, I.; Dubuc, N.; McBreen, P. H. *J. Organomet. Chem.* **2006**, *691*, 5497.

(20) Tulevsky, G. S.; Myers, M. B.; Hybertsen, M. S.; Steigerwald, M. L.; Nuckolls, C. *Science* **2005**, *309*, 591.

(21) Bergbreiter, D. E.; Franchina, J. G.; Kabza, K. *Makromol.*. **1999**, *32*, 4993.

(22) Chechik, V.; Crooks, R. M.; Stirling, C. J. M. *Adv. Mater.* **2000**, *12*, 1161.

(23) Copéret, C.; Chabanas, M.; Saint-Arroman, R. P.; Basset, J.-M. *Angew. Chem.* **2003**, *42*, 156.

(24) Edmonson, S.; Osborne, V. L.; Huck, W. T. S. *Chem. Soc. Rev.* **2004**, *33*, 12.

(25) Prucker, O.; Rühe, J. *Langmuir* **1998**, *14*, 6893.

(26) Sullivan, T. P.; Huck, W. T. S. *Eur. J. Org. Chem.* **2003**, 17.

(27) Blumm, A. S.; Kushmerick, J. G.; Pollack, S. K.; Yang, J. C.; Moore, M.; Naciri, J.; Shashidhar, R.; Ratna, B. R. *J. Phys. Chem. B* **2004**, *108*, 18124.

(28) Engelkes, V. B.; Beebe, J. M.; Frisbie, C. D. *J. Phys. Chem. B* **2005**, *109*, 16801.

(29) Monnell, J. D.; Stapleton, J. J.; Dirk, S. M.; Reinerth, W. A.; Tour, J. M.; Allara, D. L.; Weiss, P. S. *J. Phys. Chem. B* **2005**, *109*, 20343.

(30) Xiao, X.; Xu, B.; Tao, N. J. *Nano Lett.* **2004**, *4*, 267.

(31) Ulrich, J.; Esrail, D.; Pontius, W.; Venkataraman, L.; Millar, D.; Doerrer, L. H. *J. Phys. Chem. B* **2006**, *110*, 2462.

(32) Reed, M. A.; Zhou, C.; Miller, C. J.; Burgin, T. P.; Tour, J. M. *Science* **1997**, *278*, 1065.

(33) Ning, J.; Qian, Z.; Li, R.; Hou, S.; Rocha, A. R.; Sanvito, S. *J. Chem, Phys.* **2007**, *126*, 174706.

(34) Buchmeiser, M. R. *Chem. Rev.* **2000**, *100*, 1565.

(35) Buchmeiser, M. R. *New J. Chem.* **2004**, *28*, 549.

(36) Copéret, C. *New J. Chem.* **2004**, *28*, 1.

(37) Furstner, A. *Angew. Chem.Int. Ed.* **2000**, *39*, 3013.

(38) Hoveyda, A. H.; Zhugralin, A. R. *Nature* **2007**, *450*, 243.

(39) Klavetter, F. L.; Grubbs, R. H. *Synth. Metals.* **1989**, *28*, 99.

(40) Korshak, Y. V.; Korshak, V. V.; Danischka, G. H., H. *Mackromol. Chem. Rapid Commun.* **1985**, *6*, 685.

(41) Scherman, O. A.; Grubbs, R. H. *Synth. Metals* **2001**, *124*, 431.

(42) Scherman, O. A.; Rutenberg, I. M.; Grubbs, R. H. *J. Am. Chem. Soc.* **2003**, *125*, 8515.

(43) Schmelmer, U.; Jordan, R.; Geyer, W.; Eck, W.; Gölzhäuser, A.; Grunze, M.; Ulman, A. *Angew. Chem. Int. Ed.* **2003**, *42*, 559.

(44) Vernon, C. G. *Adv. Mater.* **1994**, *6*, 37.

(45) Herisson, J. L.; Chauvin, Y. *Makromol. Chem.* **1971**, *141*, 161.

(46) Thieuleux, C.; Copéret, C.; Dufaud, V.; Marangelli, C.; Kuntz, E.; Basset, J.-M. *J. Mol. Cat. A* **2004**, *213*, 47.

(47) Blanks, R. L.; Bailey, G. C. *I&EC Product Research and Development* **1964**, *3*, 170.

(48) Handzlik, J.; Ogonowski, J. *Catal. Lett.* **2003**, *88*, 119.

(49) Henderson, M. A.; Radloff, P. L.; White, J. M.; Mims, C. A. *J. Phys. Chem.* **1988**, *92*, 4111.

(50) Hills, M. M.; Parmeter, J. E.; Mullins, C. B.; Weinberg, W. H. *J. Am. Chem. Soc.* **1986**, *108*, 3554.

(51) McBreen, P. H.; Erley, W.; Ibach, H. *Surf. Sci.* **1984**, *148*, 292.

(52) Oudghiri-Hassani, H.; Siaj, M.; McBreen, P. H. *J. Phys. Chem. C* **2007**, *111*, 5954.

(53) Siaj, M.; Oudghiri-Hassani, H.; Maltais, C.; McBreen, P. H. *J. phys. Chem. C* **2007**, *111*, 1725.

(54) Siaj, M.; Oudghiri-Hassani, H.; Zahidi, E. M.; McBreen, P. H. *Surf. Sci.* **2005**, *579*, 1.

(55) Siaj, M.; Reed, C.; Oyama, T.; Scott, S. L.; McBreen, P. H. *J. Am. Chem. Soc.* **2004**, *126*, 9514.

(56) Zahidi, E. M.; Oudghiri-Hassani, H.; McBreen, P. H. *Nature* **2001**, *409*, 1023.

(57) Oudghiri-Hassani, H.; Zahidi, E. M.; Siaj, M.; Wang, J.; McBreen, P. H. *App. Surf. Sci.* **2003**, *212*, 4-9.

(58) Ren, F.; Feldman, A. K.; Carnes, M.; Steigerwald, M.; Nuckolls, C. *Makromol.*. **2007**, *40*, 8151.

(59) Leclercq, G.; Kamal, M.; Giraudon, J. M.; Devassine, P.; Feigenbaum, L.; Leckercq, L.; Frennet, A.; Bastin, J. M.; Löfberg, A.; Decker, S.; Dufour, M. *J. Catal.* **1995**, *158*, 142.

(60) Pérez Cadenas, A. F.; Maldonado Hódar, F. J.; Moreno Castilla, C. *Langmuir* **2005**, *21*, 10850.

(61) Pielaszek, J.; Mierzwa, B.; Medjahdi, G.; Marêché, J. F.; Puricelli, S.; Celzard, A.; Furdin, G. *App. Cat. A* **2005**, *296*, 232.

(62) Wang, X.-H.; Hao, H.-L.; Li, W.; Tao, K.-Y. *J. Sol. State Chem.* **2006**, *179*, 538.

(63) Yang, Z.; Cai, P.; Shi, L.; Gu, Y.; Chen, L.; Qian, Y. *J. Sol. State Chem.* **2006**, *179*, 29.

(64) Oyama, S. T. *Catal. Today* **1992**, *15*, 179.

(65) Li, Y.; Fan, Y.; Luo, G. *Ind. Eng. Chem. Res.* **2004**, *43*, 1334.

(66) Ding, W.; Li, S.; Meitzner, G. D.; Iglesia, E. *J. Phys. Chem. B* **2001**, *105*, 506.

(67) Shu, J.; Adnot, A.; Grandjean, P. A. *Ind. Eng. Chem. Res.* **1999**, *38*, 3860.

(68) Solymosi, F.; Németh, R. *Catal. Letters* **1999**, *62*, 197.

(69) Cheekatamarla, P. K.; Thomson, W. J. *J. Power Sourc.* **2006**, *156*, 520.

(70) Oshikawa, K.; Nagai, M.; Omi, S. *J. Phys. Chem. B* **2001**, *105*, 9124.

(71) Potapenko, D. V.; Horn, J. M.; Wihite, M. G. *J. Catal.* **2005**, *236*, 346.

(72) Rodriguez, J. A.; Dvorak, J.; Jirsak, T. *J. Phys. Chem. B* **2000**, *104*, 11515.

(73) Kojima, R.; Aika, K.-I. *App. Cat. A* **2001**, *219*, 141.

(74) Wang, J.; Ji, S.; Yang, J.; Zhu, Q.; Li, S. *Catal. Comm.* **2005**, *6*, 389.

(75) Ramanathan, S.; Yu, C. C.; Oyama, S. T. *J. Catal.* **1998**, *173*, 10.

(76) Ramanathan, S.; Oyama, S. T. *J. Phys. Chem. B* **1995**, *99*, 16363.

(77) Wu, Z. G.; Chen, X. J.; Struzhkin, V. V.; Cohen, R. E. *Phys. Rev. B* **2005**, *71*, 5.

(78) Chen, J. G. *Chem. Rev.* **1996**, *96*, 1477.

(79) Hwu, H. H.; Chen, J. G. G. *Chem. Rev.* **2005**, *105*, 185.

(80) Kitchin, J. R.; Nørskov, J. K.; Barteau, M. A.; Chen, J. G. *Catal. Today* **2005**, *105*, 66.

(81) Fukui, K.-I.; Lo, R.-L.; Iwasawa, Y. *Chem. Phys. Lett.* **2000**, *325*, 275.

(82) Siaj, M.; Maltais, C.; Zahidi, E. M.; Oudghiri-Hassani, H.; Wang, J.; Rosei, F.; McBreen, P. H. *J. Phys. Chem. B* **2005**, *109*, 15376.

(83) Abdelrehim, I. M.; Thornburg, N. A.; Sloan, J. T.; Caldwell, T. E.; Land, D. P. *J. Am. Chem. Soc.* **1995**, *117*, 9509.

(84) Eng, J.; Chen, J. G.; Abdelrehim, I. M.; Madey, T. E. *J. Phys. Chem. B* **1998**, *102*, 9687.

(85) Kyriakou, G.; Kim, J.; Tikhov, M. S.; Macleod, N.; Lambert, R. M. *J. Phys. Chem. B* **2005**, *109*, 10952.

(86) Lee, A. F.; Baddeley, C. J.; Hardacre, C.; Lambert, R. M. *J. Am. Chem. Soc.* **1995**, *117*, 7719.

(87) Ormerod, R. M.; Baddeley, C. J.; Lambert, R. M. *Surf. Sci. Lett.* **1991**, *259*, L710.

(88) Pacchioni, G.; Lambert, R. M. *Surf. Sci.* **1994**, *304*, 208.

(89) Rucker, T. G.; Logan, M. A.; Gentle, T. M.; Muetterties, E. L.; Somorjai, G. A. *J. Phys. Chem.* **1986**, *90*, 2703.

(90) Sesselmann, W.; Woratschek, B.; Ertl, G.; Küppers, J.; Haberland, H. *Surf. Sci.* **1983**, *130*, 245.

(91) Vollhardt, K. P. C. *Acc. Chem. Res.* **1976**, *10*, 3344.

(92) Xu, C.; Peck, J. W.; Koel, B. E. *J. Am. Chem. Soc.* **1993**, *115*, 751.

2. Experimental

2.1 Introduction: Surface chemistry and catalysis

2.1.1 Surface science

Many chemical reactions are activated or accelerated by the use of heterogeneous catalysts[1]. These reactions occur in systems in which two, or more, phases are present, precisely at the interface between the phases. Liquid-solid and gas-solid interfaces where the solid is the catalyst are of particular interest because they can ensure that the catalyst is not washed away and lost in the stream of products. The surface of a solid is inherently different than the rest of the solid (the bulk) since surface atoms simply cannot satisfy their bonding requirements in the same way as bulk atoms. Therefore, surface atoms will always want to react in some way, either with each other or with foreign atoms, to satisfy their bonding requirements, and therefore, we should expect the chemistry of the surface to be unique[2].

In a surface catalytic process, the reaction occurs repeatedly by a sequence of elementary steps that includes adsorption, surface diffusion, chemical rearrangements (bond breaking, bond forming, molecular rearrangement) of the adsorbed reaction intermediates, and desorption of the formed products. The characterization of a solid surface on an atomic level implies unambiguously that the surface composition remains essentially unchanged over the duration of an experiment. In order to study atomically clean surfaces, we must then work under so-called ultrahigh vacuum (UHV) conditions[3], a region between 10^{-9} and 10^{-12} Torr. This region has its sense of being in the following rough calculation: For a bulk density of 1 g/cm^3 (such as ice or water), the molecular density ρ is $\approx$ 5x10^{22} molecules/cm^3. The surface concentration of molecules σ (molecules/cm^2) is proportional to $\rho^{2/3}$, assuming a cube-like packing, and is thus on the order of 10^{15} molecules/cm^2. Because the densities of most solids or liquids are all within a factor of 10 or so of each other, 10^{15} molecules/cm^2 is a good order-of-magnitude estimate of the surface concentration of atoms or molecules for most solids or liquids. Of course, the

surface atom concentration of crystalline solids may vary by a factor of two or three, depending on the type of packing of atoms at a particular crystal face.

This is a very weak concentration if we compare it with the 10^{22} molecules/cm^3 for liquids, which can help to imagine the complexity of extracting any information on these types of systems. Especially if we consider that chemical processes take place at the monolayer scale. This fact forces us to study atomically clean surfaces (< 1% of a monolayer), because contaminants not only reduce catalytic activity, but mask information as well. Agreeing then that the density of atoms on the surface of a solid is on the order of 10^{15} cm^{-2}, to keep the surface clean for 1 second, the flux of molecules incident on the initially clean surface must therefore be less than $\approx 10^{15}$ molecules/cm^2/s assuming that each incident gas molecule "sticks", the worst scenario possible, the pressure in the chamber to keep the surface clean for a second should be 10^{-6} Torr. At pressures on the order of 10^{-7} Torr it may take thus 10 seconds to complete monolayer coverage, at 10^{-8} 100 seconds, and so on. Thus, ultrahigh vacuum conditions (< 10^{-9} Torr) are required to maintain a clean surface for about 1 h, the time usually needed to perform experiments on clean surfaces. However our base pressure is usually on the order of 10^{-11} Torr, so we can work on a wide margin of utilisation. Working under these conditions, a 10^{-6} Torr second^{-1} exposure, which is called *langmuir* (L), will cover a surface with a monolayer amount of gas molecules, again assuming a sticking coefficient of unity. This is the exposure or dosing unit used in surface science.

A large number of techniques have been developed to study various surface properties under UHV conditions[4,5], including structure, composition, oxidation states, and changes of chemical, electronic, and mechanical properties. The frontiers of surface instrumentation are constantly being pushed toward detection of finer detail: atomic spatial resolution, ever smaller energy resolution, and shorter time scales. Because no one technique provides all the necessary information about surface atoms, the tendency is to use a combination of techniques. In this thesis X-ray photoelectron spectroscopy (XPS), thermal desorption spectrometry (TDS), and reflection adsorption infrared spectroscopy (RAIRS) are used to analyze the behaviour of surface atoms and adsorbed molecules on β-Mo_2C.

2.1.2 Ultra-High Vacuum Technology

Conducting experiments in ultra-high vacuum conditions necessitates special instrumentation[6-8]. Any UHV system for surface science experiments integrates a chamber (or several interconnected chambers), a pumping stack, valves, process equipment (such as load lock facilities, sample manipulators, heaters, and dosers), and facilities for surface analysis. The experimental system used in this study is shown in Figure 2-1.

UHV systems are built with very specific materials that have to fulfil special requirements such as low vapour pressure and the ability to endure bake-out, alongside with the use of non-magnetic materials when low-energy electrons are employed as analytical probes. The most common material for vacuum chambers and associated components is *304 stainless steel* due to its low gas permeability, resistance to corrosion, and ability to take a high polish (since the less roughness, the easier a system can be pumped). Other commonly used materials are copper (especially for gaskets), aluminium, and refractory metals like tantalum, tungsten, and molybdenum, especially used for the construction of evaporators and sample holders. Glass is also a common material used in UHV, as many types of glass have low permeability (except for helium) and good vacuum characteristics. However, glass is more susceptible to damage, and its use should be reduced to minimum. For electrical insulation inside the UHV chamber various types of ceramics are employed.

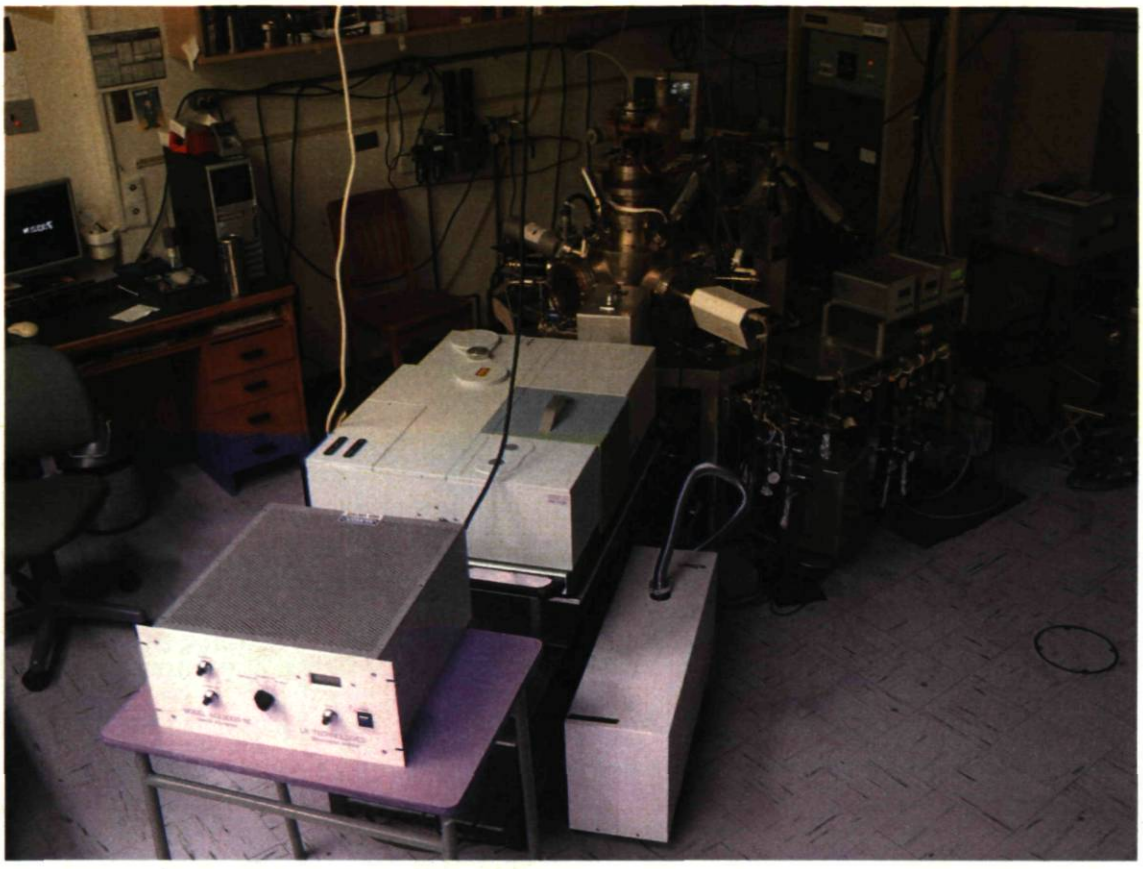

Figure 2-1 : General view of the multianalytical UHV system used in this study.

The analysis chamber is usually the central part of the vacuum system, precisely where the UHV experiments are conducted. It is typically made of stainless steel and has a number of ports with different sizes to attach the other chambers (preparation or load-lock), analytical instruments, deposition systems, sample manipulators, windows and so on. Each port has a flange also made of stainless steel (metal seal flanges as shown in Figure 2-2). Standard copper gaskets are made from high purity and oxygen-free copper and are for one-time use only. These flanges are usually referred to as *Conflat* (CF) flanges and are the most widely used for applications, though *Viton* sealed flanges can be used in some external parts of the system as well. The CF sealing mechanism is suitable for pressures from atmosphere to 10^{-13} Torr, and can be baked to 450° C and cooled to -200° C. Modular design of UHV systems and compatibility of UHV components give the possibility of easy

exchange of the different parts and permits versatile upgrading. Likewise, worn or damaged components may be replaced easily and quickly.

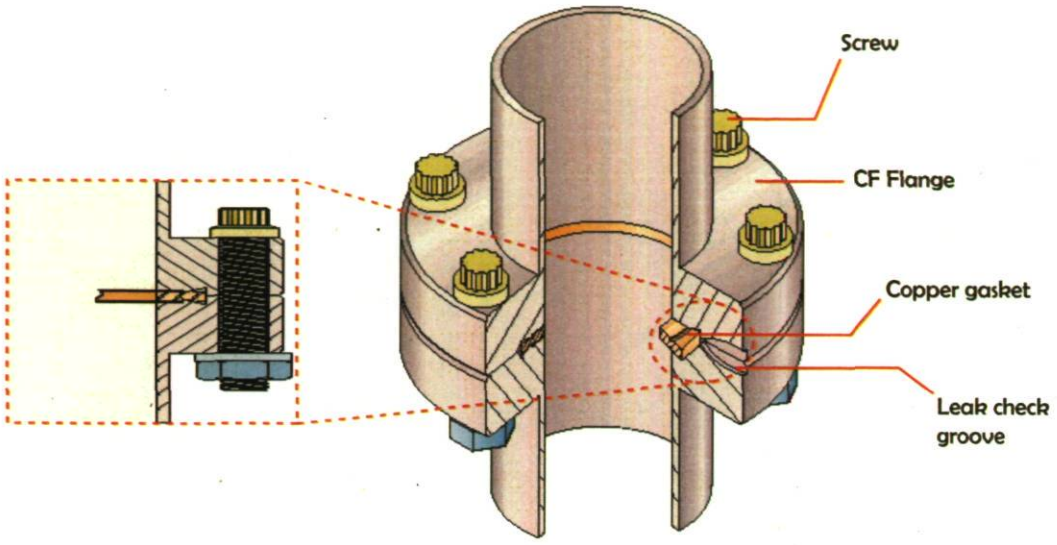

Figure 2-2 : Cross-section of a pair of *Conflat* flanges used in UHV equipment. The seal is made by bolting together two identical flanges with a flat metal ring gasket between the knife edges. The knife edges press annular grooves in each side of the copper gasket, filling all voids and defects and producing a leak-tight seal.

2.2 XPS / RAIRS / MS system

2.2.1 General characteristics

The ultra high vacuum system used in this work is built up from a compact central chamber with different parts connected to this central piece. The multianalytical experimental system is fitted with three surface analysis techniques, reflection absorption infrared spectroscopy (RAIRS), X-ray photoelectron spectroscopy (XPS), and thermal desorption spectrometry (TDS). The system is also fitted with an ion gun to sputter clean the surface, an ion gauge to measure the pressure, as well as a dosing system consisting of three leak valves connected to three gas-handling ramps. The dosing system is also used to eliminate surface impurities via chemical treatment.

The system is able to produce and hold a vacuum in the range of ~10^{-11} Torr. Such a low base pressure is reached after a day of full power pumping followed by 1-2 days of bake-out at temperatures around 140 K, and then allowing for another 2-3 days of pumping after degassing all internal components including the sample. This base pressure assures fine control of surface conditions, and allows one to work without taking into consideration possible contaminations coming from the surroundings. It also allows dosing of the sample in a very accurate way, since an introduction of less than 1 monolayer (habitually 2-3 langmuirs) can be achieved at pressures 100-1000 times higher than the base pressure in an useful scale of time (usually between 100 and 1000 seconds). It also provides an excellent control of the quality of the gas introduced in the chamber by using the quadrupole mass spectrometer.

2.2.2 Pumping system

A number of pumps are responsible for reaching and maintaining the low pressure on the system. The main turbomolecular pump (pump number 1 in Figure 2-3) is responsible for pumping down the system and maintaining the pressure. It is backed up by a rotary vane pump (number 2) which evacuates the gases pumped by the main turbomolecular pump. Diffusion pump (pump number 3) and the auxiliary rotary vane pump (number 4) are responsible for the two stage differential pumping of the rotary part of the sample manipulator, along with rotary pump (number 5) which pumps the outer part. A smaller turbomolecular pump (number 6) assisted by a rotary vane pump (number 7) is used to pump the gas-handling ramps. Additionally, another rotary vane pump (number 8) has been added to this pumping system through a three-way valve to protect the turbomolecular pump in case of over pressure of the in-let system.

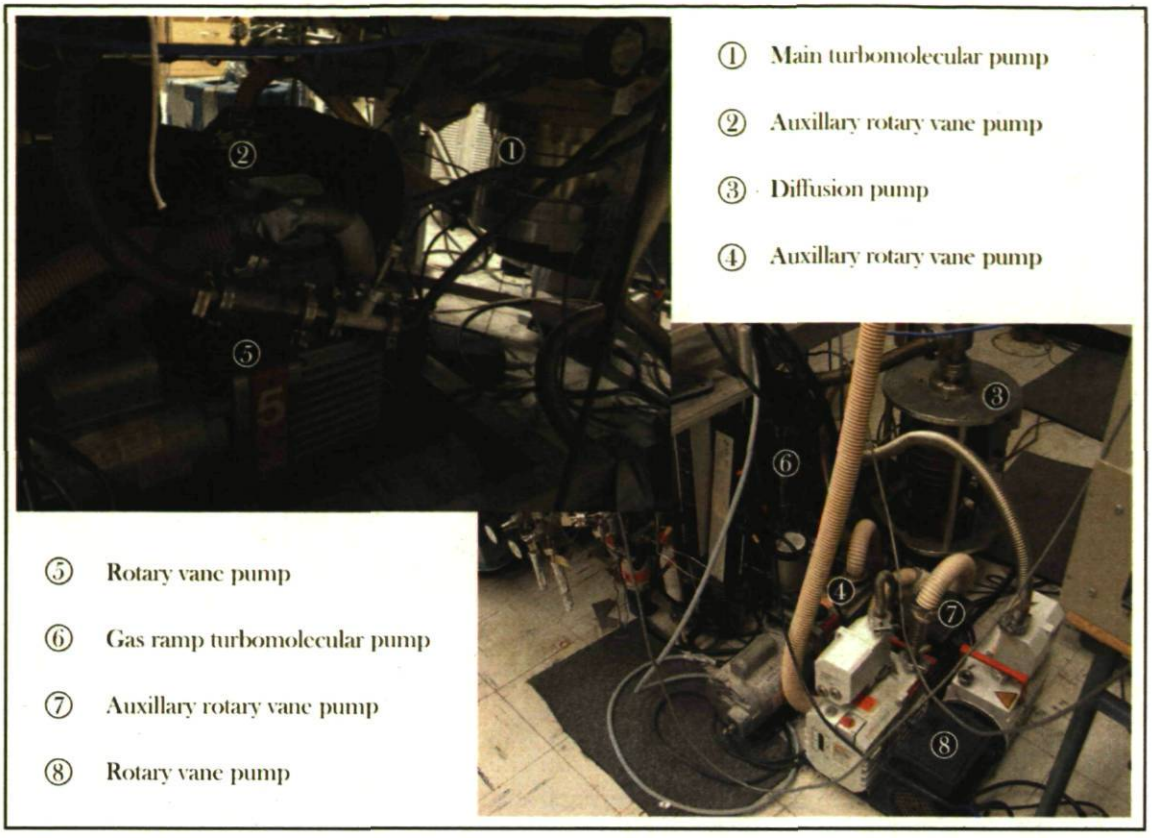

Figure 2-3 : Photographs of the pumping system from below the UHV chamber and from the back of it.

The combined action of these pumps is to obtain and maintain the vacuum in the chamber. This process has to be done through a sequence of steps since the transition from atmospheric pressure (760 Torr) to UHV (~10^{-11} Torr) means changing the pressure value by ~13-14 orders of magnitude, which is well beyond the pumping characteristics of any single pump. That is the reason why two or more different types of pumps are needed. Preliminary pumping is effected in this system by the rotary vane pumps whereas those used to reach the UHV level are turbomolecular pumps and diffusion pumps.

Rotary vane pumps (pumps 2, 4, 5, 7 and 8) are employed for pumping from atmospheric pressure down to about 10^{-3} Torr, as well as for backing the turbomolecular and diffusion pumps. The principle of operation of a rotary vane pump is illustrated in Figure 2-4 (a). Gas enters the inlet port and becomes trapped in the volume between the rotor vanes and the stator. Upon rotation of the eccentrically mounted rotor, the gas is

compressed and then expelled into atmosphere through the exhaust discharge valve. The pumps usually employ vacuum oil as a sealant and lubricant.

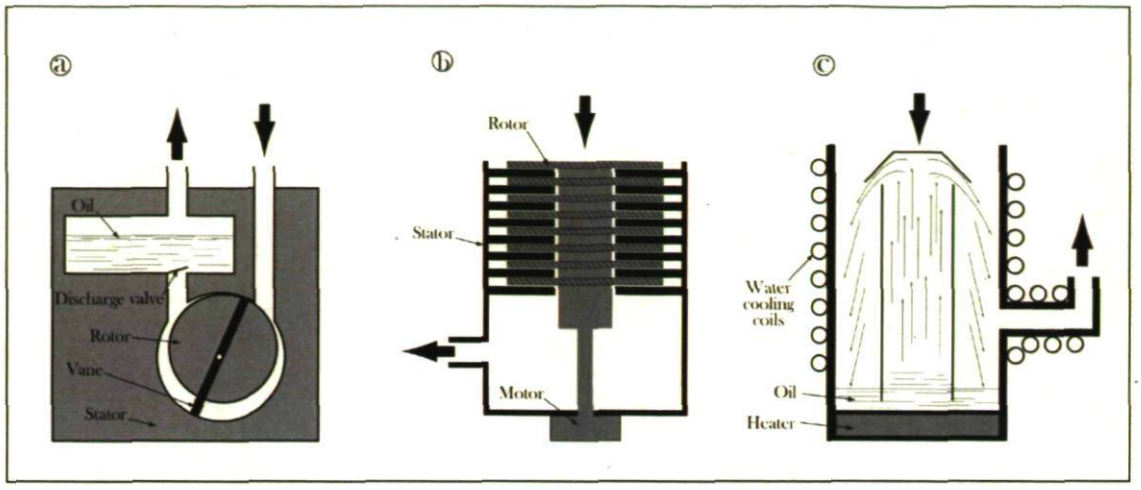

Figure 2-4 : Diagram of the design of (a) rotary vane pump, (b) turbomolecular pump, and (c) diffusion pump.

Pumps with UHV capabilities used in this system are turbomolecular (1 and 6) and diffusion pumps (3). Turbomolecular pumps are the most popular UHV pumps. Operating in the 10^{-4} to 10^{-11} Torr range, a turbomolecular pump resembles a jet engine: a stack of rotors with multiple blades with angled leading edges, which are rotated at very high speed (5000-20000 Hz) and sweep the gas molecules in the direction of the exhaust connected to the foreline (Figure 2-4 (b)). The turbomolecular pump is backed up typically by a rotary vane pump or sometimes by combination with an additional small turbo pump and rotary pump (when ultimate UHV is required). These kinds of pumps are clean and reliable, but due to induced vibrations they are not suitable in systems with precise positioning, like those for microscopy or surface microanalysis. Diffusion pumps are vapour jet pumps requiring a mechanical pump connected in series as well, and are used when constant high speeds for all gases are desired for long periods of time without attention. Diffusion pumps consist on the generation of an oil vapour produced in the boiler and is expanded through a nozzle achieving high velocity (Figure 2-4 (c)). Then the jet vapour is directed down and traps gas molecules which are also deflected downward after colliding with much heavier

vapour molecules and are pumped by the backing pump. The upper part of the pump is cooled by cooling coils welded to the body to condense and preserve the pump fluid.

Pressure measurement in the main chamber is achieved by an ion gauge. As with pumps, there is no universal gauge which can operate in the whole range from atmospheric pressure down to UHV. Thermocouple and Pirani gauges measure a vacuum in the range of 10^{3}-10^{-3} Torr, and ionization gauges cover the range lower than 10^{-4} Torr. The operation of this kind of gauge is based on the ionization of molecules of a gas system. As the ionization rate and, hence the ion current, are directly dependent on the gas pressure, the pressure can be determined. The ion gauge used in our system is a hot-filament gauge, which use thermionic emission of electrons from a hot filament to ionize the molecules which are then attracted towards the fine-wire grounded collector situated at the centre of the gauge. Finally, the collector current is converted into a pressure reading (Figure 2-5).

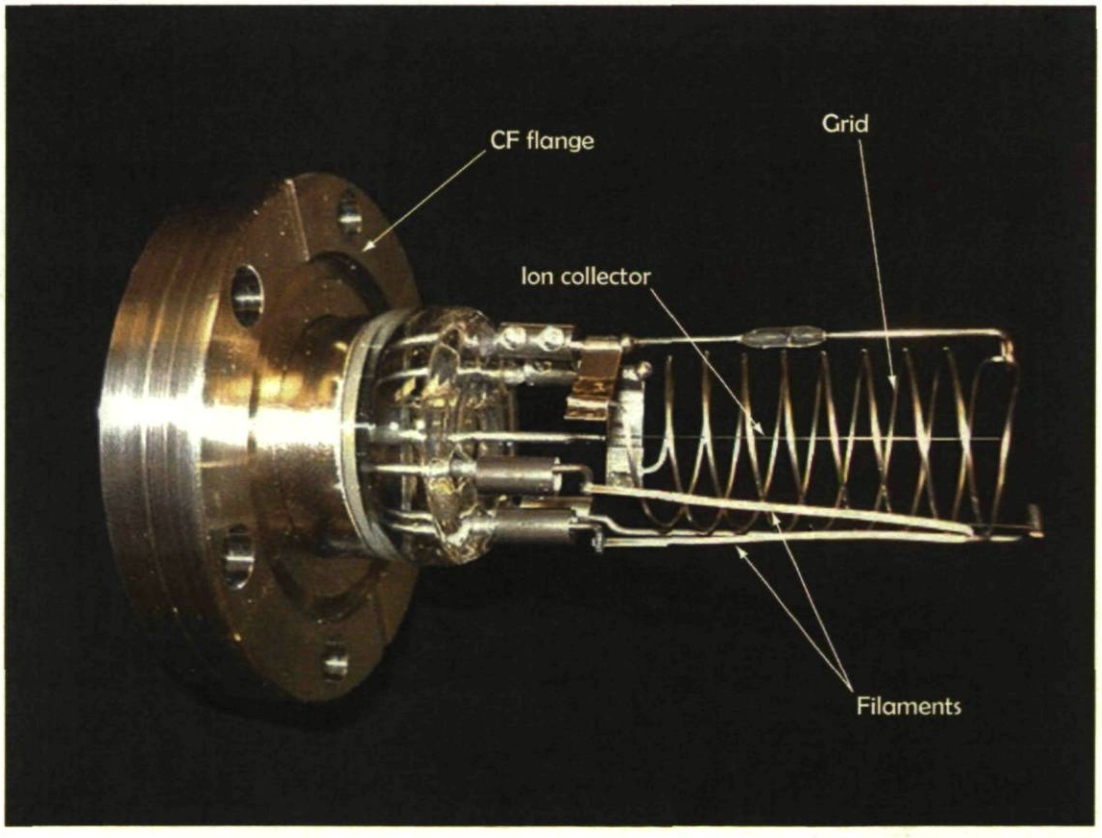

Figure 2-5 : Image of a classic ion gauge with all parts indicated.

The gas introduction system is fitted with Pirani gauges in every independent part. In this type of gauge, the pressure is determined from the change in resistance of the filament, often platinum. The resistance is measured using a Wheatstone bridge scheme, where the reference filament is immersed in a permanently evacuated chamber, while the measurement filament is exposed to the system gas. Both filaments are heated by a constant current through the bridge, and when the pressure in the system volume is equal to that of the reference filament, the current between the two arms of the bridge is zero. The higher the pressure in the system volume, the lower the resistance of the measurement filament, and subsequently, the higher the electrical current between the arms of the bridge that is later converted to pressure units.

2.2.3 Surface analysis

In this section the different surface analysis techniques used for data acquisition will be reviewed, namely X-ray photoelectron spectroscopy (XPS), reflection absorption infrared spectroscopy (RAIRS) and thermal desorption spectrometry (TDS). Figure 2-6 shows a top view of the multianalytical system showing the different surface science analytical apparatus peripherally connected to the central chamber. As shown at the top of the photograph, the XPS source is placed at right angles with respect to the hemispherical analyser. The photograph also shows the IR source connected to the focalizing mirror box placed at grazing angle with respect to the detector box. The quadrupole mass spectrometer is shown in the bottom of the photograph.

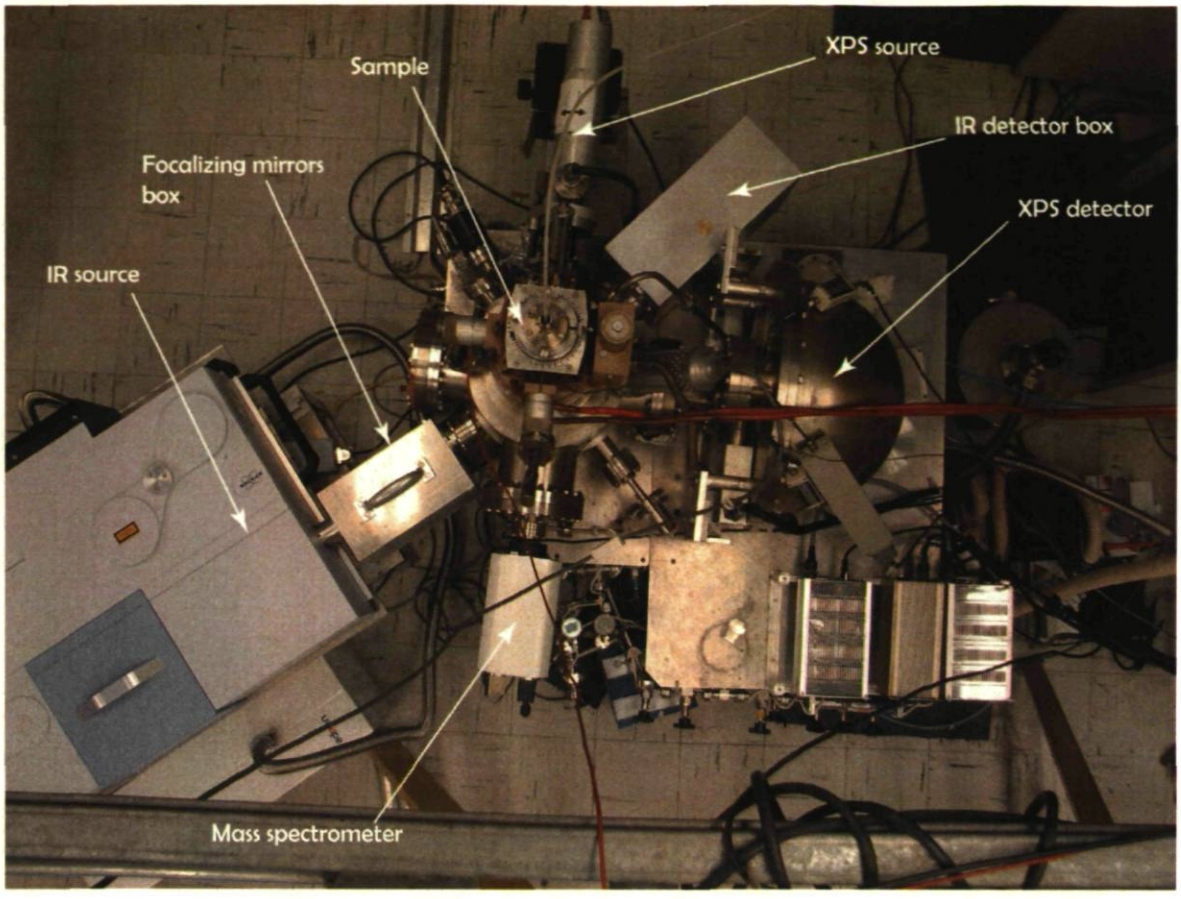

Figure 2-6 : Top view of the system used in this study with the analytical apparatus shown.

2.2.3.1 X-ray photoelectron spectroscopy

Surface analysis by X-ray photoelectron spectroscopy (XPS), also known as electron spectroscopy for chemical analysis (ESCA), is accomplished by irradiating a sample with soft X-rays and analyzing the kinetic energy of the electrons emitted. These photons have a penetrating power in a solid of the order of 1-10 micrometers. However, the energy dependent escape depth of the photoelectrons is typically less than 50 Å. Hence, the study can be confined to the surface. In order to understand the theoretical basis of this technique we use the *frozen orbital approximation*, in which the photoelectric effect (Figure 2-7) causes electrons to be emitted with a kinetic energy given by:

$$KE = h\nu - BE - \phi_s$$

Where $h\nu$ is the energy of the photon, BE is the binding energy of the atomic orbital from which the electron originates, and ϕ_s is the spectrometer work function.

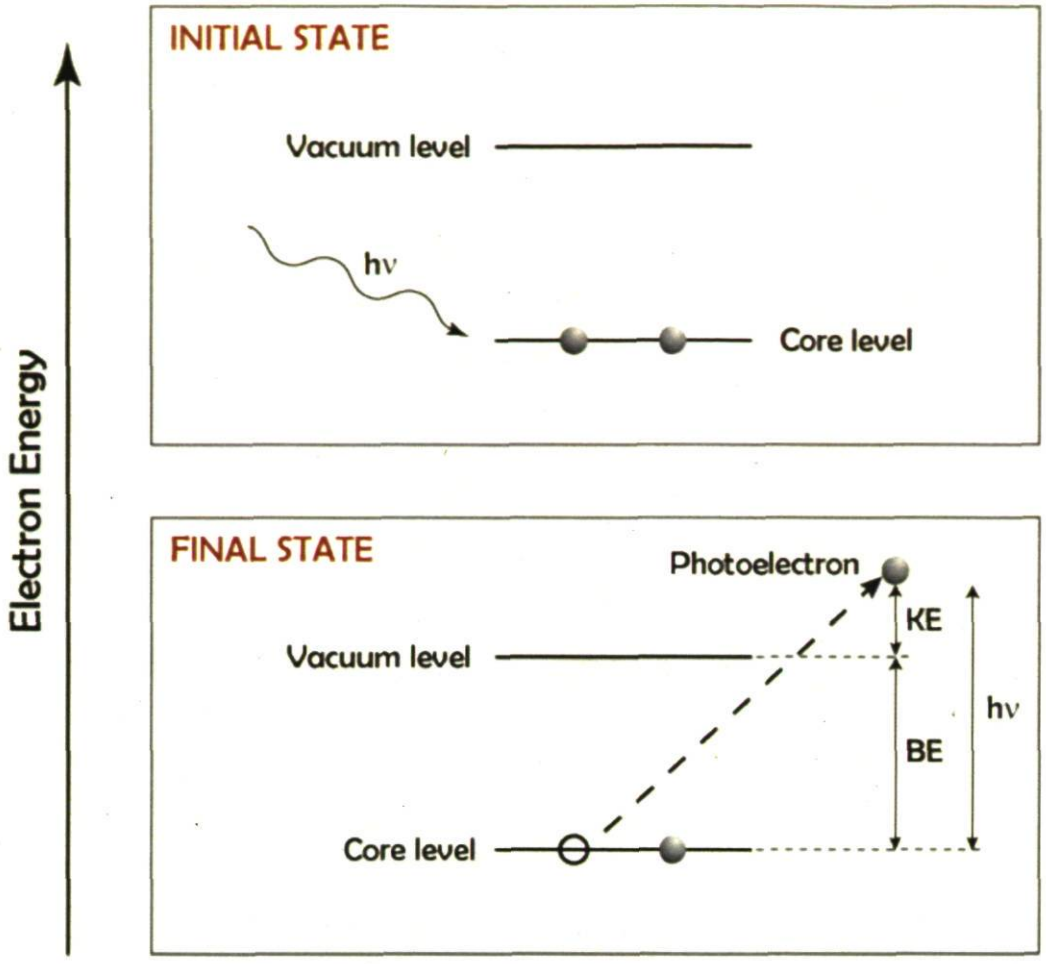

Figure 2-7 : Diagram of the photoelectric effect, the photon absorption and the deep core electron emission (initial and final states).

In addition to the electrons emitted in the photoelectric process, Auger electrons are emitted as well, due to relaxation of the energetic ions left after photoelectron. In this process an outer electron falls into the inner orbital vacancy, and a second electron is emitted, carrying off the excess energy. The Auger electron possesses kinetic energy equal to the difference between the energy of the initial ion and the doubly-charged final ion. Thus, photoionization normally leads to two emitted electrons, a photoelectron and an

Auger electron. The relaxation energy effect, describing the final state causes a positive shift in the kinetic energy with respect to the *frozen orbital approximation.*

Deep-core electrons have binding energies corresponding to the energies of photons that lie in the X-ray region. These electrons do not participate in bonding, and their energies are characteristic of the atom from which they originate. To a first approximation, the energy of core electrons does not depend on the environment of the atom. However, when energies of core levels are investigated in more detail it is found that small but easily detected shifts do occur. These shifts, known as chemical shifts, depend on the bonding environment around the atom and in particular on its oxidation state. Generally as the oxidation state increases the binding energy increases, since the greater the electron withdrawing power of the substituents bound to an atom, the higher the binding energy. Similarly, the higher the effective positive charge on the atom, the higher the binding energy of the photoelectron. Therefore, XPS is particularly useful for elemental analysis of a sample.

One of the great strengths of XPS is that it can be used not only for elemental analysis but also for quantitative analysis. XPS peak areas are proportional to the amount of material present because the photoionization cross-section of core levels is virtually independent of the chemical environment surrounding the element. In this study XPS was used to verify the conditions of the surface prior to experiments. Molybdenum carbide is a quite complex material, with a temperature-dependent surface composition, but also with rather important amounts of contaminants, oxygen and sulphur principally. XPS is then used to control the proportions between those elements on the surface and to decide whether the surface needs treatment, and which kind, or if it is suitable for performance of an experiment. Further explanation of this use of the XPS will be given on the *surface preparation* section.

2.2.3.2 Temperature programmed desorption

One of the most widely used and versatile techniques for the study of adsorbed species on surfaces is temperature programmed desorption (TPD), often called thermal desorption spectrometry (TDS). In this technique, the temperature of an adsorbate-covered sample is raised at a constant rate (in this study, 1 K/s typically) and the increase of pressure induced by adsorbate or product desorption is simultaneously recorded as a function of temperature.

The collection of TPD data has progressed from the early use of ionization gauges to the almost universal employment of quadrupole mass spectrometers (QMS) for the detection of desorbing gases. Using the mass spectrometer in the multiplex mode, one can simultaneously measure the evolution of various gas products as the temperature of the crystal is raised. This can also be extended to the study of isotopic mixing between labelled adsorbates.

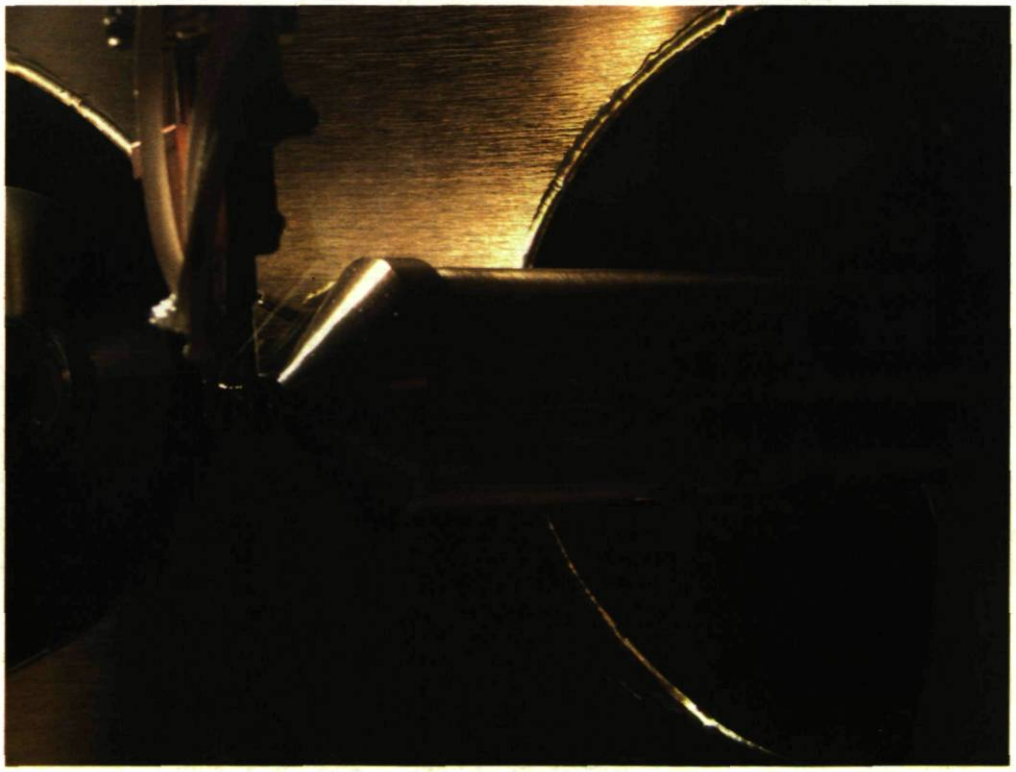

Figure 2-8 : TPD measurements are performed with the sample placed close to the entrance of the shield of the mass spectrometer.

The early work with single crystals employed unshielded mass spectrometers that sampled the random flux of desorbing gases originating from the front of the crystal, from the electrical support leads to the crystal, and from the back of the crystal disk. These effects could be eliminated to various degrees by using a differentially pumped and shielded mass spectrometer that preferentially collects gases desorbing only from the front of the crystal, as shown in Figure 2-8. This technique allows measurement of molecular desorption from the surface, as well as the study of surface reactions by detecting new fragments desorbed after a chemical reaction. The latter experiment is called temperature programmed reaction (TPR).

2.2.3.3 Reflection absorption infrared spectroscopy

Vibrational spectroscopy has developed into one of the most powerful tools for the study of the adsorption of molecules on a variety of surfaces from single crystal metals to supported catalysts. In particular, reflection absorption infrared spectroscopy (RAIRS)[9] permits high sensitivity (typically 1/1000 of a CO monolayer) at high resolution (1-5 cm^{-1}). It also offers the possibility to work from ultra high vacuum to atmospheric pressure. This technique makes possible a systematic understanding of the adsorption behaviour of molecules on defined surfaces, and reference spectra can be directly correlated with spectra obtained from catalysts under ambient pressure conditions. The necessity of working with single crystal metals, which are non transparent in contrast to supported catalysts, requires the use of this reflection method.

RAIRS works on the principle of a polarized IR light focalized on the surface at grazing incidence. A fraction of this incident infrared light is absorbed by vibrational excitation of molecules adsorbed on the surface through interaction with the dipole moment of the molecule[10]. The specularly reflected IR light is then directed towards the detector and re-focalized with the help of another set of mirrors (Figure 2-9 (a)).

As shown in Figure 2-9 (b), only the p-polarized radiation causes a significant electromagnetic field near the metallic surface for near grazing incidence (>80°).

Furthermore, the conduction band electrons of the metal will rearrange in the surface to counteract the dynamic dipoles created in the excited adsorbates by the IR radiation (Figure 2-9 (c)). As a result, only vibrations with dipole components perpendicular to the surface can be observed with this technique. This is known as the *surface selection rule*.

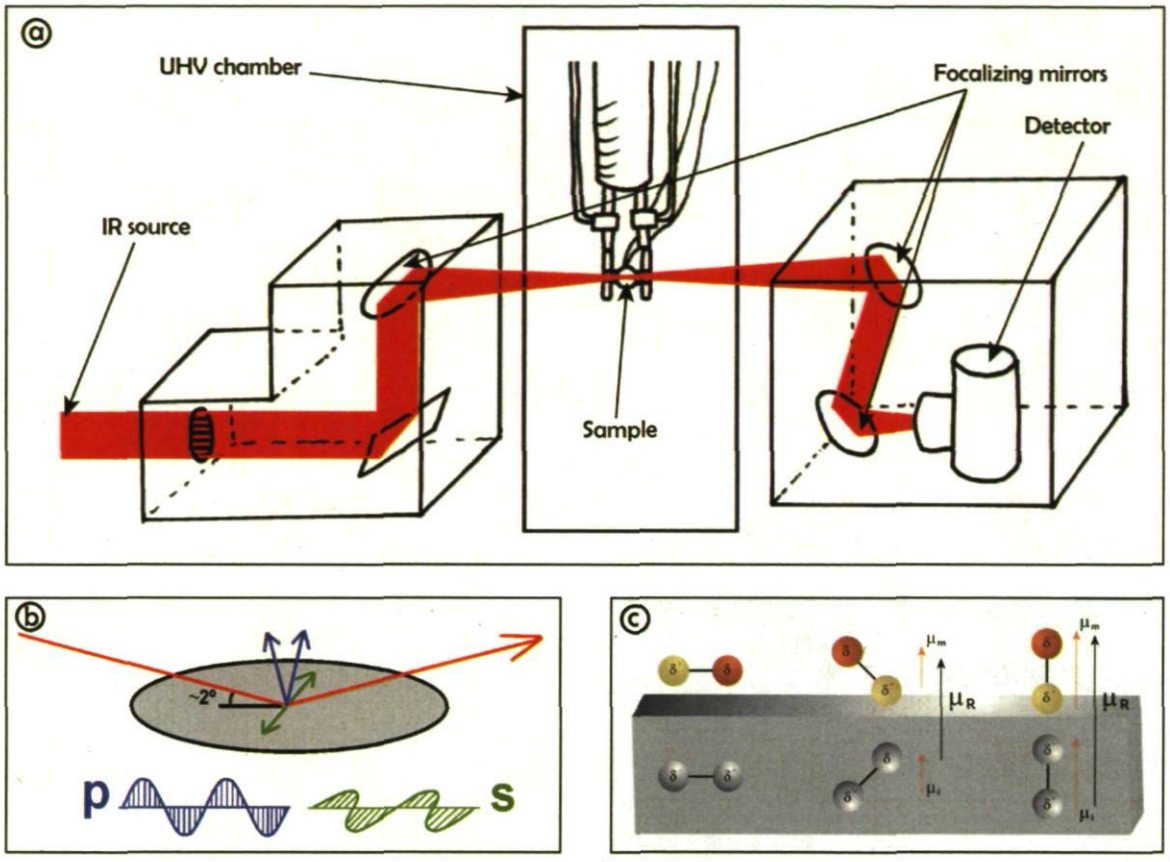

Figure 2-9 : a) Diagram of the IR beam path from the source to the detector; b) Consequence of the electric field reflection of p-polarized and s-polarized radiation; c) Effect of image dipoles on the resultant dipole.

RAIRS experiments are started by filling the detector with liquid nitrogen one hour and a half to two hours before the beginning of the experiment to allow the base signal of the detector to stabilize. Then a series of background spectra of the clean surface are recorded at the acquisition temperature (100 K) to ensure the stability of the system and thus the reproducibility of the experiment. Once the baseline of the background is stable enough, the molecule under study is introduced into the chamber followed by the annealing of the surface when required. Typically the system is cooled down to the acquisition

temperature to obtain the corresponding spectra with the same parameters used in the background acquisition; usually 600-800 scans with a scan speed of 20 kHz.

2.2.3 Preparation of UHV system

After securing all ports in the chamber, rough pumping using mechanical pump n°1 (Figure 2-4) is carried out for a period of 30-45 minutes. An initial gurgling noise indicating pumping around ambient pressure is followed by a gradual "normalization" of the noise of the pump. In this stage no direct observation of the pressure inside of the chamber is possible, however several indications can be observed. First the behaviour of the turbomolecular pump in the early working stages may indicate some kind of leak or malfunction. Secondly, allowing the pumped gas-handling ramp to have access to the chamber (fully opening a leak valve) allows a rough estimation of the pressure by reading the Pirani gauge. Although this gauge is placed quite far from the chamber and the connections are through very thin tubes and a leak valve, it can provide useful information in order to ensure protection of the turbomolecular pump.

After the main turbomolecular pump reaches maximum rotor speed, an hour or two should be enough to reach pressures in the order of 10^{-6}-10^{-7} Torr and within 5-6 hours later the 10^{-8} Torr range. Any difficulty for the system to reach these pressures in this order of time should be considered as an indication of a possible leak or malfunction in the system. At this stage, it is completely secure to turn the ion gauge on (from $P \leq 10^{-4}$ Torr) and degassing of the two filaments should be performed for at least 30 minutes of uninterrupted use of each one, being cautious that the pressure does not rise above the operation limit of the gauge.

A leak test could be performed at this point of the pump down process prior to the bake-out, in order to verify the correct installation of all components and flanges of the UHV chamber. For this, a start-up procedure for the quadrupole mass spectrometer is required, including the degassing of both filaments keeping the pressure below the maximum operating pressure (10^{-4} Torr). Once the mass spectrometer is fully operational,

the leak testing mode should be switched on and then a low flow of helium might be directed close to the flanges of the chamber, especially on those that have been installed after the last venting of the system, and preferentially from the upper part to the bottom of the system since helium is lighter than air and it may go up as it comes off the pipe. If a leak is detected, the system should be vented, first switching off all filaments and allowing them to cool down for at least half an hour, then turning off the UHV pumps (turbomolecular, ionic and diffusion pumps), and lastly turning off the rough pumps. It is then possible to replace the damaged parts or to close correctly the leaky flange, paying attention to change the copper gasket for a new one.

If no leak is detected, the bake-out process can start. First all fragile parts should be covered with aluminium foil in order to dissipate heat all around them (view ports, electrical plugs, bellows, IR windows, etc.). Then thermometers should be installed in strategic places in order to control the temperature in all parts of the chamber. Usual places where the thermocouples are installed are both KBr windows, and the bellows. Once all this equipment is secured, heating plates are placed on the table of the system in the best way possible to ensure the uniform heating of the whole chamber. The plates are plugged to current regulators (*Variacs*) in order to control the heat emitted by each one. Finally a thermally insulating cover is placed and secured over the whole system. The temperature must be kept between 100 °C and 150 °C, in order to prevent damage of the IR windows, for 1-2 days time. After that time all bake-out components should be removed, and the final installation of the components can take place (XPS gun, electronic components of the XPS detector, IR mirror and detector boxes, and ion gun electronics). The process finishes with the degassing of all filaments and the sample manipulator, the alignment of all components that require it (XPS source and IR mirrors mainly) and surface preparation.

2.2.4 Surface preparation

Once UHV conditions are ensured and all the analytical tools are tuned up, one can start with experiments. The first thing to be done is to prepare a clean surface. Before installation into the UHV system, the sample undergoes a set of various cleaning

treatments, such as mechanical polishing, chemical etching, boiling in organic solvents, rising in deionized water, etc. However, all this processing constitutes rather a pre-treatment stage, as the final preparation of an atomically clean surface (i.e., a surface which contains foreign species in amounts of a few per cent of a monolayer) can be conducted only *in situ* under UHV conditions. The most common methods of the *in situ* cleaning are cleavage, heating, chemical processing, and ion sputtering.

Cleanliness in surface chemistry is essential since only molecules directly in contact with the surface will display interesting properties for study. To ensure reproducibility of results then, a certain quality of the surface is required, and a cleaning and verification of the stoichiometry of the surface with help of the XPS is always carried out prior to experiments. From experience it has been decided that 0.05, < 0.008 and < 0.004 of the area of the molybdenum ($3d_{3/2+5/2}$) peak of carbon, oxygen, and sulphur, respectively, are required in order to proceed with experiments. These values have been chosen empirically, after noting that surfaces with that quality give reproducible results. This does not mean a less clean surface will not be reactive enough, but it rather would make observations more difficult. In order to verify the correct stoichiometry established for the surface, data of the O(1s), S(2p), C(1s), and Mo($3d_{3/2+5/2}$) regions of the XPS are acquired by scanning in the 535-525 eV, 156-166 eV, 285-295 eV, and 230-245 eV energy regions, respectively.

As pointed out before there are two cleaning processes used in this study; ion sputtering and chemical treatment, which combined allow achieving the required quality of the surface. It has been noticed that ion bombardment is an efficient process to eliminate sulphur from the surface of molybdenum carbide, one of the principal natural impurities of this material, whereas cycles of dosing of carbon rich molecules, and high temperature annealing are ideal to eliminate oxygen by desorption of CO and CO_2.

Figure 2-10 shows an example of XPS data for oxygen and sulphur at different conditions of the surface. The values displayed for each spectrum make reference to the ratio between its area and the area of the Mo($3d_{3/2+5/2}$) peak. In both cases a drop in intensity can be clearly seen after each cycle of the cleaning process, chemical treatment in the case of oxygen, and ion sputtering for sulphur removing, to the point where the surface

matches the conditions required to perform an experiment (0.0032, and 0.0029 of the $Mo(3d_{3/2+5/2})$ peak respectively).

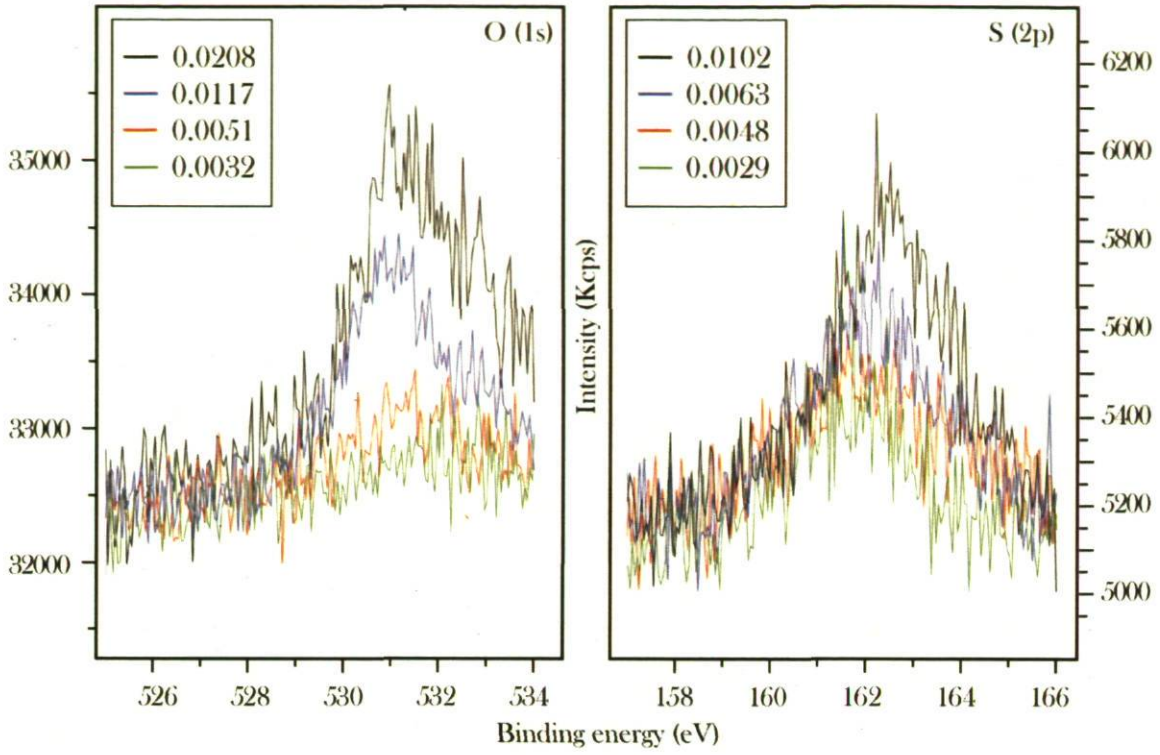

Figure 2-10 : Data for O(1s) and S(2p) after several stages of the cleaning process (chemical treatment for oxygen and ion sputtering for the sulphur). The areas are normalized to the area of the $Mo(3d_{3/2+5/2})$ peak.

2.2.4.1 Ion sputtering

Surface contaminants can be sputtered off together with the substrate top layer by bombardment of the surface by noble gas ions (in this case Ar^+) through kinetic energy transfer. To produce an ion beam, Ar gas is admitted through a leak valve (at a pressure of $\sim 10^{-6}$ Torr) directly into the ion gun. Ionization of the gas atoms proceeds via electron impact in the ionizer of the gun. Electrons are then emitted from the cathode (Figure 2-11). The produced ions are extracted from the ionizer, accelerated to the desired energy (2.5 keV in this case) and directed towards the sample.

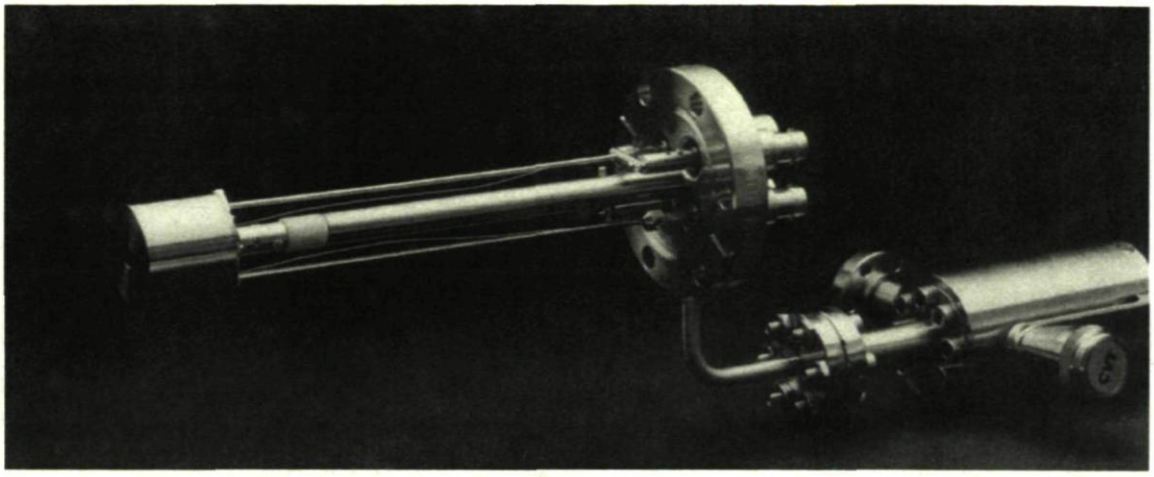

Figure 2-11 : Image of a LK Technologies NGI3000 ion gun, the one used in the system, with a leak valve already assembled in position.

Ion bombardment is performed for cleaning the surface of molybdenum carbide at 700 K for different periods of time depending on the condition of the surface previously analyzed by XPS, but a minimum of 15 minutes and a maximum of 60 minutes are used. The surface is placed at ~10 cm from the ion gun and at an angle of 45° of the incident ion beam. Then the temperature is set and the Ar^+ flux is controlled by increasing the pressure in the chamber; 10^{-6} Torr is the typical pressure used to ensure sufficient ion flux to the surface. After all these parameters are set, emission is raised gradually to a value of 20 mA and then the energy of the beam is set to 2.5 kV. After the bombardment process, the current is turned off gradually and then the leak valve is closed. The side effect of ion bombardment is the degradation of the surface structure. Therefore, subsequent annealing is required to restore the surface crystallography and to remove embedded Ar. For that, a number of temperature flashes are made to 1400 K at a rate of 10 K/s. The process concludes with allowing the surface to cool down and performing XPS spectra of the surface in the O(1s), C(1s), S(2p), and Mo($3d_{3/2+5/2}$) regions in order to verify the stoichiometry and establish the success of the sputtering.

2.2.4.2 Chemical cleaning

In order to eliminate adsorbed oxygen from the surface and dissolved oxygen in the bulk of the material, cleaning cycles are performed. Regardless off the position of the surface in the UHV system, a certain exposure to a molecule (typically 5-10 L) with a high percentage of carbon (usually ethylene or propylene, but also acetylene or even 1,3,5,7-cyclooctatetraene) is introduced at low temperatures to ensure high coverages on the surface, and then a rapid annealing of the surface, usually 2-3, to 1400 K (10 K/s) is performed. These annealings are accompanied by CO_2 desorption peaks in the mass spectrum at 600 K and 1200 K and a CO desorption peak at 900 K. After repeating cycles of dosing/annealing, a period of time is allowed to let the system pump down, and XPS data is collected again to verify the stoichiometry of the surface, usually observing a drop in intensity of the oxygen peak. If the drop doesn't occur or is not enough to satisfy quality standards, the process will be repeated until the desired stoichiometry is achieved.

It is worth noting that after opening the system or after large periods of inactivity a large number of ion sputtering/redox cycles may be needed, and the process of cleaning the surface may take as long as 2 or 3 days.

2.2.5 Maintenance

In order to keep the system in working order, a few easy operations must be done regularly. The multianalytical system is composed of many different components, and all its parts must be in perfect condition in order to be able to perform spectroscopic measurements successfully.

2.2.5.1 Dry air on the Dewar

In order to control the temperature of the sample, experiments are always carried with the Dewar tube filled with liquid nitrogen. As experiments often last a few hours, a

thick layer of ice is formed on the upper part of the manipulator and the bellows. These parts are thus in danger of suffering corrosion over the time, especially the bellows since the thickness of the steel in this moveable part of the system is critically thin. At the same time, if liquid nitrogen is left on the Dewar overnight, ice layers can also be formed at the bottom of the tube, putting in danger the ceramic-metal feedthrough part of the system if the tube is filled the following day when water is still in the bottom. In order to prevent all these negative effects, ice must be removed, especially from the bellows, by applying a current of dry air with a high flow rate, and then a tube with a lower dry air flow must be introduced in the Dewar and kept overnight to dry the bottom of the tube.

The introduction of the dry air tube into the Dewar must be performed carefully, and with a very low flow of air since otherwise the liquid nitrogen will be projected upwards and fall, like rain, over the system and the operator, being especially dangerous if some drops fall into the eyes.

2.2.5.2 Baking out the gas-handling ramps

Since multiple products are used in the experiments, different gases are introduced in the system via the gas-handling ramps. These ramps are composed of very thin long steel tubes with multiple connections and angles which make them very hard to be effectively pumped down, even though a turbomolecular pump is assigned to the task. In order to ensure the accuracy of measurements, the products introduced must be of the highest purity, and thus the gas-handling ramps must be degassed from adsorbed gases prior to adding any new product to be tested. For that reason periodic bake-outs of the ramps must be performed using wire heaters rolled over the tubes. This operation is usually performed overnight with the path to the pump fully opened, and allowing the ramps to cool down prior to the introduction of any product in it.

2.2.5.3 Degassing of internal filaments

Degassing all components from time to time is an operation required for the correct functioning of every internal device. The two filaments of the ion gauge and the two filaments of the quadrupole mass spectrometer must be degassed periodically, whereas the X-ray gun and the sample manipulator only require degassing after venting the system and after long periods of inactivity. Every component has its own protocol for degassing, and following instructions from the manual is strongly recommended.

2.2.5.4 Pumping the infrared detectors

IR detectors work under vacuum conditions. The photoreceptor material must be kept under vacuum and cooled down with liquid nitrogen in order to be photoactive. For that reason the detectors must be pumped down regularly (about twice a year) by connecting them to a turbomolecular pump until pressures on the 10^{-4} -10^{-5} Torr range are reached, whereas after long periods of use, pressures usually rise to the range of the 10^{-2} Torr. This rise in pressure can affect to the stability of the measurements as well as to the intensity of the signal, and to the lifetime of the photosensitive materials.

2.2.6 Modifications of the system

A few modifications have been performed in the system in order to adapt it to new studies, as well to upgrade the equipment to ensure the best possible results.

2.2.6.1 Reconfiguration of the gas-handling ramps

Reconfiguration of the ramps was done in order to optimize pumping capacity and to ensure the purity of the products prior to introduction into the chamber, essentially by shortening the paths to the turbomolecular pump.

The gas-handling ramp is divided into three parts, each having direct access to the turbomolecular pump. One exclusively dedicated to argon (top part on Scheme 2-1) is connected to the leak valve assembled to the ion sputter gun. This part of the ramp usually supports higher pressures than the other two since argon needs to be introduced in higher quantities than the other products (higher pressure for longer periods of time), and thus needs to be pumped down carefully since the turbomolecular pump could be damaged. A second part of the gas-handling ramp is dedicated for carbonyl products, which are used to form the alkylidene species on the surface so as to functionalize it for metathesis reactions, whereas the third part of the gas-handling ramp contains olefin products for treatment of the surface by redox cycles and for performing the above mentioned metathesis reactions.

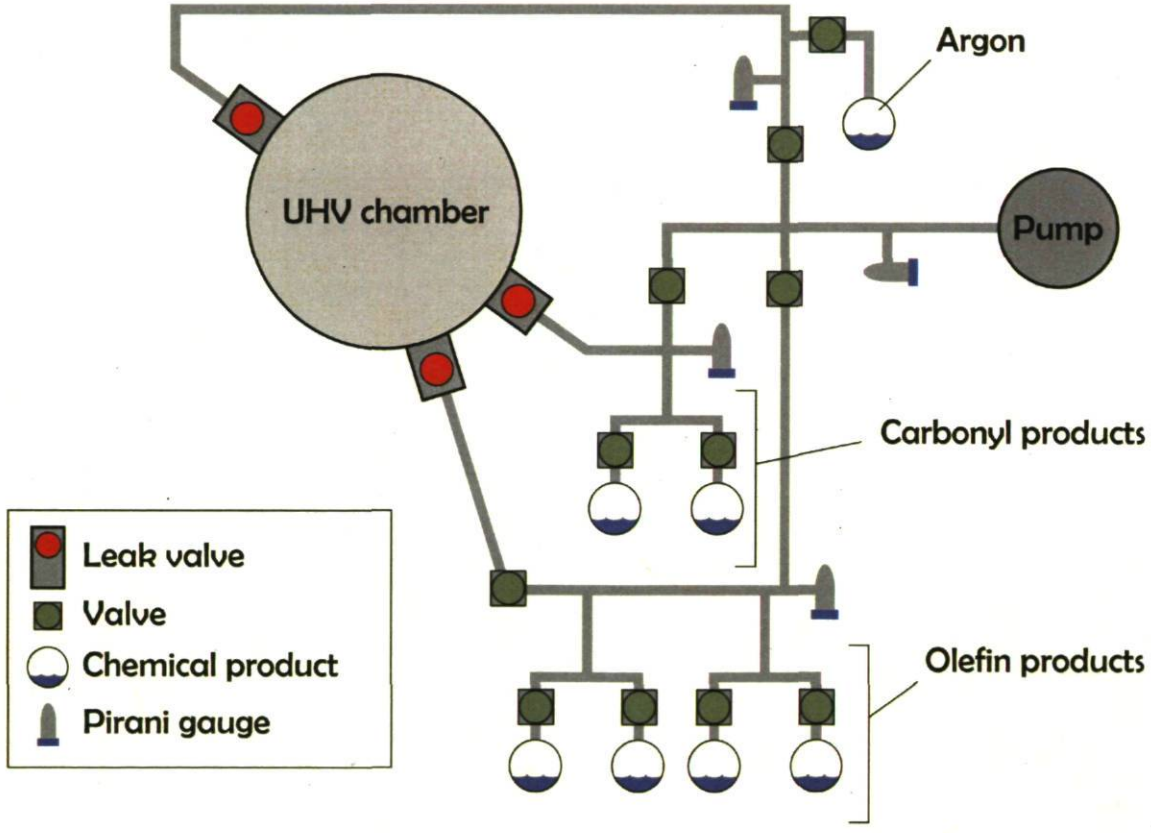

Scheme 2-1 : Diagram of the gas-handling ramp system used to introduce gas molecules in the UHV chamber.

Both parts of the gas-handling ramp containing reactive products should be baked-out regularly to ensure the purity of the products introduced into the UHV chamber, as discussed in section 2.2.5.2. However since the only product of the third gas-handling ramp is argon, and this gas is very stable and easy to pump down there is no need for this part of the gas-handling ramp to be baked-out.

2.2.6.2 Replacement of the IR system

Replacement of the IR spectrometer and the mirror boxes allowed an improvement of the stability of the spectra. The new spectrometer (Bruker Vertex 80V) is pumped to a pressure of ~2 Torr, and it has been directly connected to a focalizing mirrors box, sealed with *Viton* flanges, so it can be pumped as well, through the spectrometer. The detector box for its part has the same sealing system, and it is pumped through the same pump by a bypass. However, the presence of the detector required the development of special devices for the electronic connections and the LN_2 (liquid nitrogen) cooling system. The electronic connection was secured by applying a special resin (*Torrseal*) capable of ensuring UHV sealing to the spot welded connector on the wall of the box, allowing plugging and unplugging the detector when required without the necessity of venting the box. The LN_2 required for the detector to work is guaranteed by a double *Viton* sealed connection which allows filling the Dewar tube of the detector while keeping the vacuum in the rest of the box.

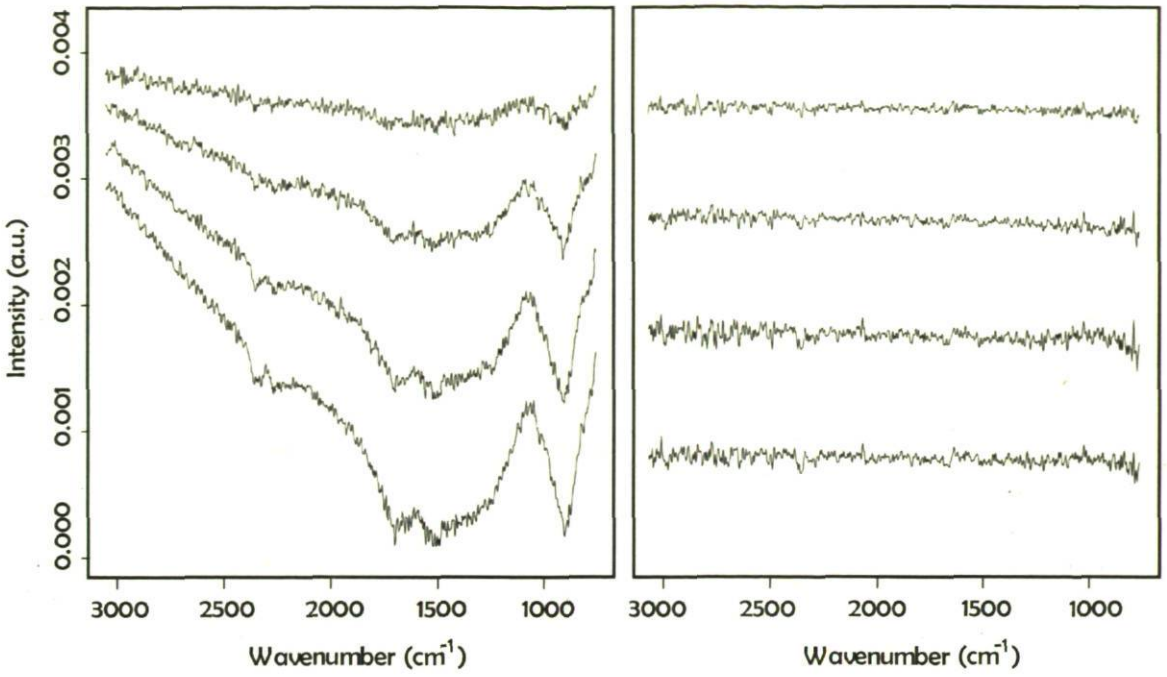

Figure 2-12 : Background spectra of the clean surface before and after the replacement of the spectrometer and the mirror boxes. Both series of spectra were obtained at the same intervals of time, under the same conditions at 100 K.

As we can see in Figure 2-12, the background spectra are much more stable over time with the new equipment. Both series of spectra were obtained under the same conditions, with a clean sample at 100 K, 800 scans per spectrum with a scan speed of 20 kHz, in the same intervals of time. It can be clearly seen that there is an improvement of the signal to noise ratio and stability especially in the 1200-1800 cm^{-1} region due to elimination of external contamination in the IR beam path outside the vacuum chamber. This improvement eliminates variations due to ambient conditions, especially in the detector box.

2.3 Bibliography

(1) Ma, Z.; Zaera, F. *Surf. Sci. Reports* **2006**, *61*, 229.

(2) Zangwill, A. *Physics at Surfaces*; 1st edition ed.; Cambridge university press, **1988**.

(3) Somorjai, G. A. *Surface chemistry and catalysis*; 1st edition ed.; John Wiley & sons, inc., **1994**.

(4) Kolasinski, K. W. *Surface science*; 1st edition ed.; John Wiley & sons, ltd, **2002**.

(5) Yates, J. T. *Experimental innovations in surface science*; 1st edition ed.; Springer, **1998**.

(6) Holland, L.; Steckelmacher, W.; Yarwood, J. *Vacuum manual*; 1st edition ed.; E. & F. N. SPON London, **1974**.

(7) Moore, J. H.; Davis, C. C.; Coplan, M. A. *Building scientific apparatus*; 2nd edition ed.; Addison-Wesley publishing company, inc., **1989**.

(8) Oura, K.; Lifshits, V. G.; Saranin, A. A.; Zotov, A. V.; Katayama, M. *Surface science*; 1st edition ed.; Springer, **2003**.

(9) Hoffmann, F. M. *Surf. Sci.Reports* **1983**, *3*, 107.

(10) Silverstein, R. M.; Webster, F. X. *Spectrometric Identification of Organic Compounds*; 6th edition ed.; John Wiley & Sons, Inc., **1998**.

3. Formation of dimethyl alkylidene and vinyl alkylidene species on the surface of molybdenum carbide

3.1 Abstract

Although there are a few reports of olefin metathesis from the 1950s[1-3], notably the polymerization of ethylene by Ziegler[4], the first complete study of this reaction may be attributed to Robert L. Banks and Grant C. Bailey[5]. Their 1964 paper described disproportionation reactions of olefins containing from two to eight carbon atoms, observed during studies of molybdenum hexacarbonyl-alumina and molybdena-alumina catalysts prepared *in situ* and commercial cobalt oxide-molybdena-alumina catalysts. In its simplest form the olefin metathesis reaction consists of a redistribution of alkylidene components of olefins. It was known to be promoted by tungsten, molybdenum, and rhenium; although at the time the reactions were an enigma with nothing known about the mechanism or the detailed nature of the catalyst.

The discovery by Yves Chauvin and his student at the French Petroleum Institute, Jean-Louis Hérrison[6], of the mechanism for this reaction changed the direction of the development of new metathesis catalysts. Until that moment catalysts were essentially inorganic metallic salts. However, the discovery by Hérrison and Chauvin that olefin metathesis was initiated by a metal carbene, which reacts with an olefin through a metallacyclobutane intermediate, led to a rapid change in the way chemists looked at the reaction. Since then preparing and characterizing metal carbenes has become a major activity in organometallic chemistry[7-10]. The initiating and propagating intermediates in homogeneous olefin metathesis are metal alkylidenes, as described by the Hérrison-Chauvin mechanism. It is generally assumed that the same mechanism holds for heterogeneously catalyzed olefin metathesis[11-17].

In the past 40 years homogeneous catalysis has undergone a rapid development and has outshone heterogeneous catalysts[18]. One reason stems from the level of understanding of molecular chemistry, which can readily help to identify the key requirements for better catalytic systems (design of active sites through structure-activity relationships), hence their

rapid development. In contrast, heterogeneous catalysts are often more ill-defined (with unknown and multiple active sites). The low percentage of active sites, the special conditions in which surface science studies are typically carried out, and the difficulty to perform accurate theoretical studies as a consequence of the number of atoms of the solid, have also severely complicated the task.

3.2 Dissociative adsorption of carbonyl compounds on β-Mo_2C

Surface science studies have proven extremely successful in revealing fundamental details on several catalytic reactions[19,20]. However, the characterization of terminal alkylidenes on pure metal surfaces has been unsuccessful[21-23], with the exception of the work by Nuckolls and collaborators[13,17] on ruthenium surfaces. Previous studies have demonstrated that carbonyl molecules undergo carbonyl bond specific dissociation on β-Mo_2C to yield surface alkylidene-oxo species[24-27], which have proven to be active for metathesis reactions[14,15,28,29]. The case of the metathesis activity of the alkylidene-modified surface of molybdenum carbide presents then a rare case, and can be considered as a step forward in the study of heterogeneous active sites.

The formation of new alkylidene species on the surface of molybdenum carbide might be regarded in the same way as the modification of a homogeneous catalyst, in which the substitution of one of its ligands can have a large effect on its properties and catalytic activity. Thus a study of the structure-activity relationship can be attempted with the help of surface science technology.

3.2.1 Dimethyl alkylidene

3.2.1.1 Infrared characterization

The adsorption of acetone to the surface of metal single crystals, such as Pt(111)[30-33], Ru(001)[30,34], Pd(111)[35], Rh(111)[36], and Ni(111)[37] has been used as a basic model system to study the adsorption and reaction of ketones on some catalytically relevant heterogeneous materials. This database provides a valuable starting point to compare with new data obtained using reflection absorption infrared spectroscopy (RAIRS) in our system, and makes acetone an excellent candidate to explore the mechanism for the dissociative adsorption of carbonyl containing molecules on the surface of β-Mo_2C.

A vibrational study of acetone behaviour when adsorbed at low temperature on the surface of molybdenum carbide could provide insight on how the molecule is positioned prior to carbonyl bond cleavage. RAIRS spectra were obtained for acetone exposures from 0.4 to 33 L at 100 K on the clean surface. The most significant feature in the spectra up to 3 L (~ 1 monolayer) displayed in Figure 3-1 is a relatively low frequency C=O stretching vibration, observed at 1660 cm^{-1} with respect to the higher frequency (1716 cm^{-1}) obtained when the multilayer is present on the surface, at coverages of 3 L and higher. This feature reveals the presence of a weakened carbonyl bond characteristic of a η^1 state monolayer assigned to acetone species bonding end-on via the lone pair electrons on the oxygen. This adsorption state places the plane of the molecule roughly perpendicular to the surface, allowing RAIRS to detect the C=O stretching vibration as an intense signal, even from a very low coverage, and has also been reported for acetone adsorbed on Pt(111)[30-33] surfaces at low temperatures and submonolayer coverages.

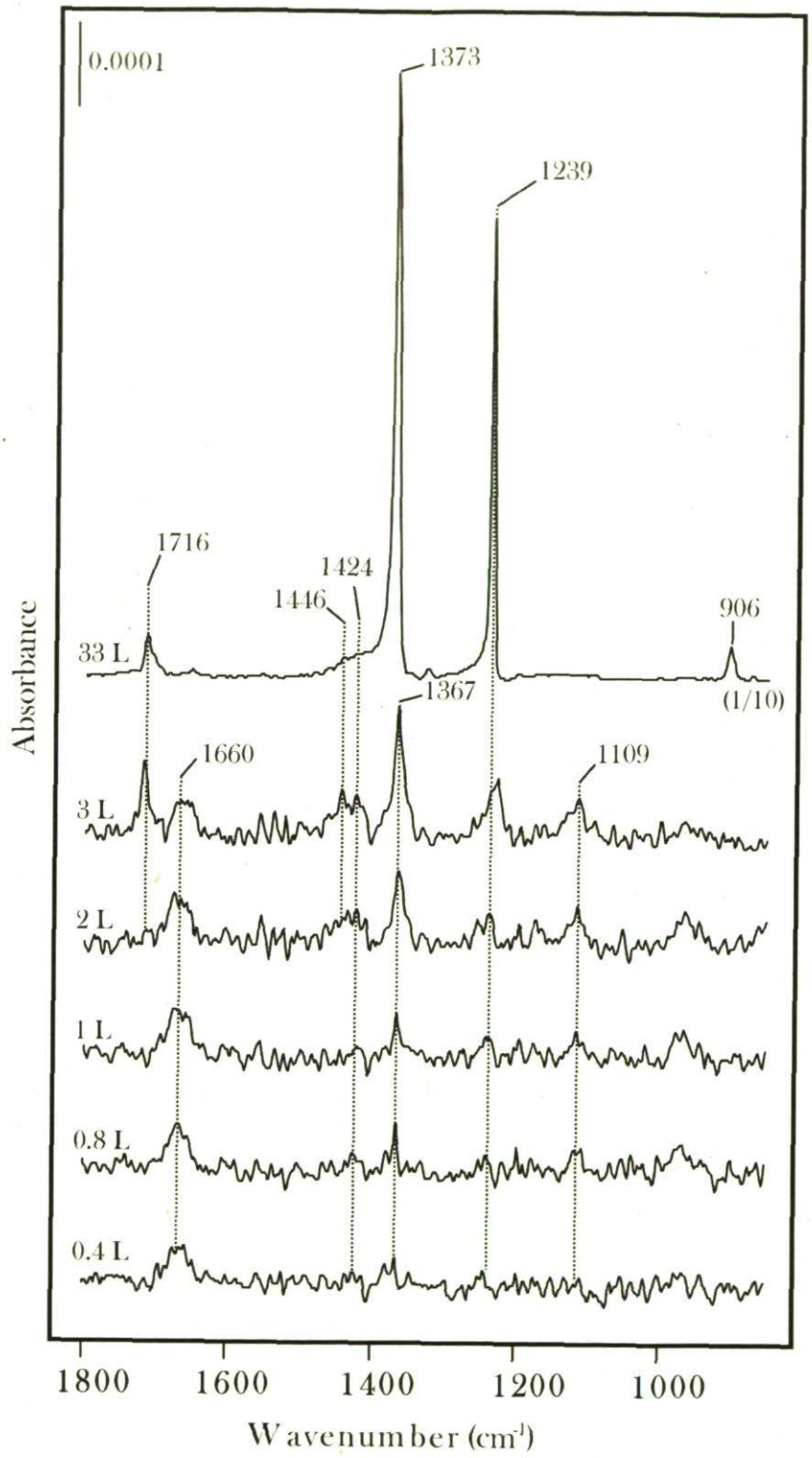

Figure 3-1 : Acetone as a function of exposure on the surface of β-Mo_2C at 100 K. Evolution of the monolayer is observed from 0.4 L up to ~2 L. Peaks of the multilayer start to appear at ~3 L and are fully visible at 33 L.

Apart from the carbonyl stretching vibration, the adsorbed monolayer of acetone also presents weaker bands appearing at ~1424, 1367, 1239 and 1109 cm^{-1}. Features observed at 1424 and 1367 cm^{-1} are assigned to the asymmetric deformation ($\delta_{a\ Me}$) and symmetric deformation ($\delta_{s\ Me}$) modes of the methyl groups, whereas the bands detected at 1239 and 1109 cm^{-1} correspond to the C-C-C asymmetric stretching ($\nu_{a\ C\text{-}C\text{-}C}$) and methyl rocking ($\rho_{Me}$) modes respectively. Near completion of the monolayer (~3 L), the previously mentioned $\nu_{C=O}$ band emerges at 1716 cm^{-1}. Upon multilayer formation, bands grow in at 1373 ($\delta_{s\ Me}$) and 906 cm^{-1} (δ_{Me}).

Isotopic substitution studies were performed in order to confirm the adsorption state of acetone as a function of coverage. Thus, spectra for fully deuterated acetone (AcD_6) were obtained under conditions identical to those used for non-deuterated acetone. Figure 3-2 shows an increase in intensity of bands corresponding to a η^1 adsorption state with increasing exposure of deuterated acetone at 100 K up to monolayer completion. As for non-deuterated acetone, a downshifted frequency of the C=O stretching band for the η^1 adsorption state (1654 cm^{-1}), with respect to the multilayer (1710 cm^{-1}), is observed. This vibrational mode has also been detected at 1638, 1670, 1665, 1655, and 1690 cm^{-1} on Pt(111)[30-33], Pd(111)[35], Rh(111)[36], Ni(111)[37] and Ru(001)[34] respectively; and at 1680-1694 cm^{-1} for a range of $[M((bz)_2SO)_4$ (η^1(O)-acetone$)_2]^{2+}$ complexes (M= Mn, Fe, Co, Ni, Zn, or Cu)[38]. These observations confirm that the η^1 state is the more energetically favoured adsorption configuration at low temperatures for almost all transition metals. Table 3-1 enables a comparison of spectra observed for acetone and acetone-d_6 on β-Mo_2C, with the assigned spectrum of both molecules in the liquid phase and adsorbed on Pt(111)[30-33].

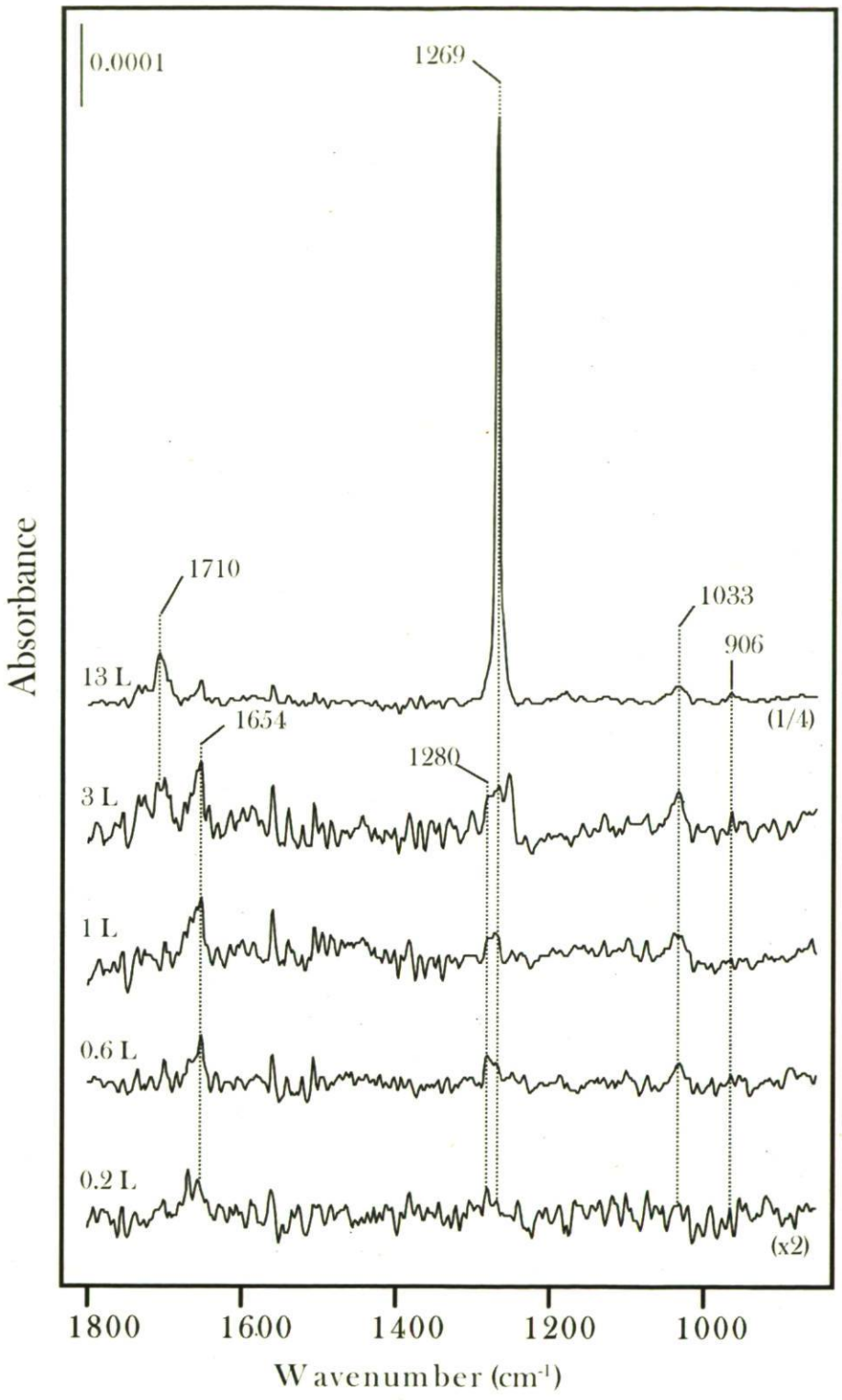

Figure 3-2 : RAIRS spectra for acetone-d_6 adsorption on molybdenum carbide at 100 K as a function of exposure. Monolayer bands are observed with increasing intensity up to 3 L above which peaks of the multilayer start to appear. The 13 L spectrum reveals the multilayer peaks.

AcD_6					AcH_6				AcH_6	Assignment
Liquid IR	Pt (111)		β-Mo_2C		Liquid IR	Pt (111)	β-Mo_2C		β-Mo_2C	
	Multilayer	η¹ acetone	Multilayer	η¹ acetone		Multilayer	η¹ acetone	Multilayer	η¹ acetone	
					900	900		906		δ(Me)
									982	ν(Mo=O)
960	960	958	906	965	1090	1094	1086	1115	1109	ρ(Me)
									1120	ν(Mo-C)+ν_a(C-C)
1245	1261	1280	1269	1280	1220	1239	1238	1239	1239	1238	ν_a(C-C-C)
1085	1090				1360	1373	1350	1373	1367	1380	δ_s(Me)
		1025			1428	1422	1426	1424	1424	1415	δ_a(Me)
1035	1036	1040	1033	1033	1445	1443		1446		1445	δ_a(Me)
1700	1710	1626	1710	1654	1712	1716	1638	1716	1660		ν(CO)

Table 3-1 : Vibrational frequencies (cm^{-1}) observed by RAIRS of acetone and fully deuterated acetone on molybdenum carbide. The mode assignments and data for acetone on Pt(111)[30-33] and for liquid acetone[39] are listed for comparison.

The η^1 state was also observed for adsorption of 30 L acetone followed by annealing over the multilayer desorption temperature (150 K). This behaviour is also observed for the other surfaces studied, and shows that this adsorption state is still present as the monolayer state even when multilayer is present. The principal difference between molybdenum carbide and the other surfaces studied for the adsorption of acetone is the behaviour of the carbonyl molecule at higher temperatures. Whereas acetone suffers desorption at relatively low temperatures, or dehydrogenates on most of studied surfaces[30-33], acetone undergoes carbonyl bond scission on molybdenum carbide.

The RAIRS spectrum for acetone on β-Mo_2C at 200 K displayed in Figure 3-3 is still characteristic of an η^1 adsorption state. However, the intense downshifted ν(CO) band at 1660 cm^{-1}, typical of chemisorption via the carbonyl oxygen, as discussed above, is eliminated by annealing to 300 K. Despite the disappearance of the ν(CO) band, all of the bands characteristic of the CH_3CCH_3 moiety are observed in the 300 and 500 K spectra. As shown in Figure 3-3, new bands grow in when temperature is raised to 300 K and higher. Notably, two new relatively intense peaks at 982, 1120 cm^{-1} corresponding to oxo (Mo=O) surface species and to a combination of Mo=C, and C-C stretching vibrations, respectively. These new bands, as well as the absence of the carbonyl band, suggest the formation of an oxo-Mo-dimethylidene complex on the surface of β-Mo_2C. The intense peak at 1120 cm^{-1} is very close in frequency to bands detected for deuterium-labelled $TiNp_4$ (Np=neopentylidene) adsorbed on Cu(111)[40] (1121 cm^{-1}) assigned to metal-carbon double bond stretches at temperatures from 235 to 350 K, and for cyclobutylidene[25,27] (1130 cm^{-1}), cyclopentylidene[14,28,29] (1146 cm^{-1}) and ethylidene[26] (1120 cm^{-1}) species on β-Mo_2C at temperatures from 300 K. These observations provide the first database for the attribution of the very elusive terminal alkylidene vibrational modes in heterogeneous catalysis.

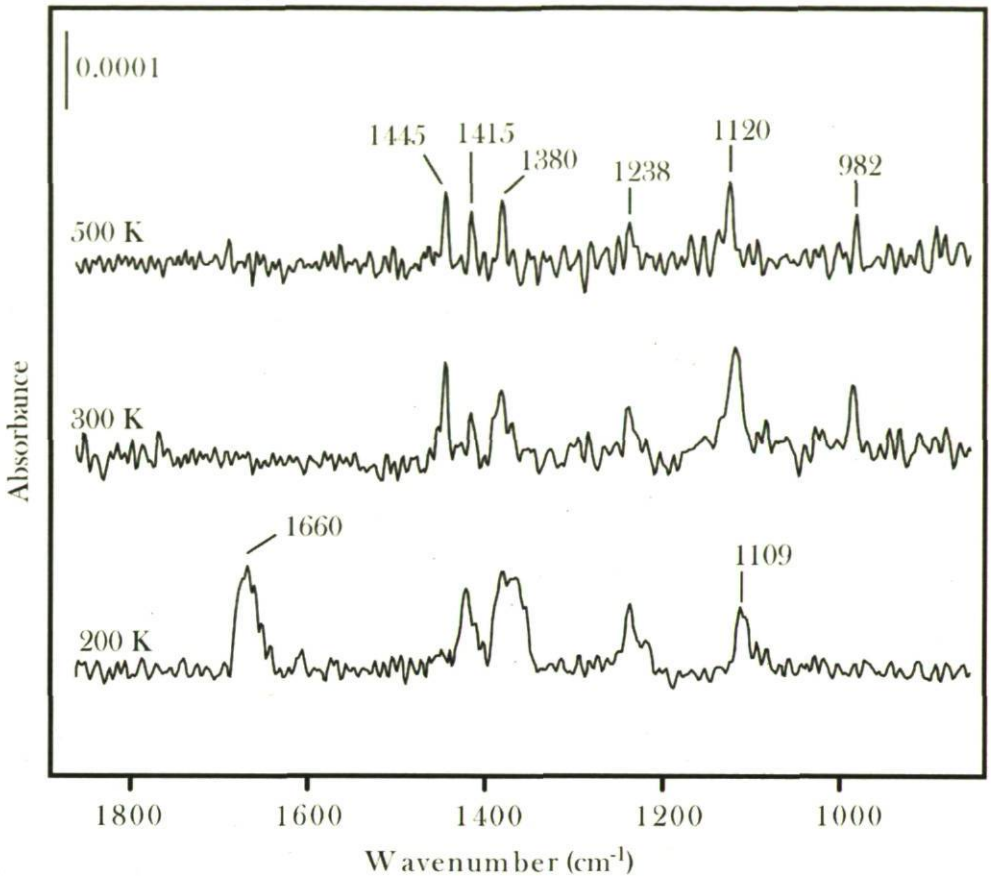

Figure 3-3: RAIRS spectra for 30 L acetone adsorbed on β-Mo_2C at 100 K followed by annealing to the indicated temperatures.

The formation of a terminal alkylidene on the surface of molybdenum carbide suggests the formation of a strongly chemisorbed η^1 state, as evidenced by the observation of the characteristic ν(CO) band above 200 K. The strong chemisorption bond keeps the η^1 state intact on the surface of β-Mo_2C until it can undergo carbonyl bond dissociation, presumably via η^2 intermediate, since in order to dissociate the bond should be placed parallel to the surface. This η^2 adsorption state has been suggested in other examples of surface adsorbed acetone[30-37]. However, it has shown itself very elusive and spectroscopic evidence of its existence has not yet been observed on carbonyl molecules adsorbed on molybdenum carbide.

3.2.1.2 Thermally programmed desorption study

Thermally programmed desorption (TPD) spectra were obtained for acetone adsorbed on a clean β-Mo_2C surface. For acetone the most abundant peak, 43 amu, and CO_2 desorption, 28 amu, were monitored. Figure 3-4 shows the TPD spectra for multilayer (15 L deposition) coverage of acetone using a heating rate of 0.5 K/s. The multilayer phase desorbs at 150 K, followed by small peaks, probably due to molecular rearrangements, until a bigger peak at 270 K that may be attributed to transition from the η^1 state, to an η^2 state involving a species adsorbed with its C=O bond parallel to the surface (see Figure 3-1), bonding to the metal atoms of the surface either by a π-bonding or a di-σ-bonding. No spectroscopic evidence was reported for these species adsorbed on molybdenum carbide. However, in order to undergo C=O bond scission, a parallel orientation of this bond with respect to the surface plane would be required.

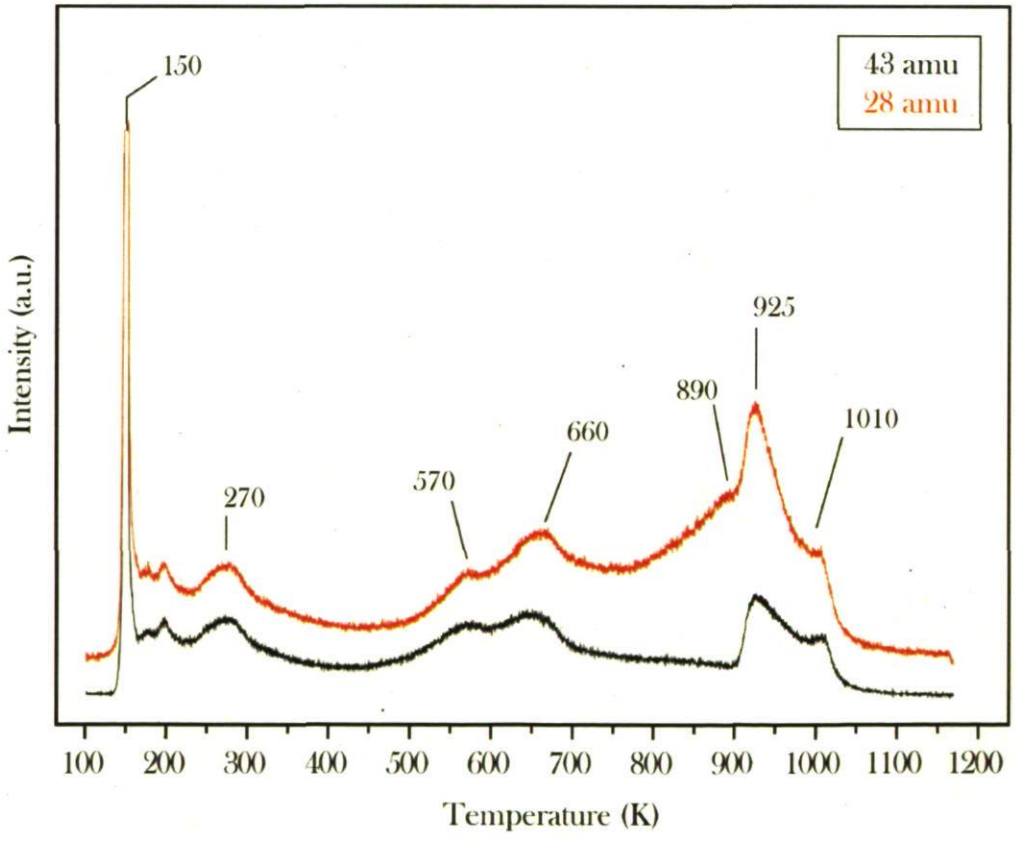

Figure 3-4 : TPD spectra for multilayer exposure (15 L) of acetone at 100 K on molybdenum carbide. Data for the molecular peak (black spectrum) and CO_2 (red spectrum) are displayed.

A double peak observed at temperatures between 510 and 660 K in Figure 3-4 may be attributed to desorption of molecular decomposition fragments. These peaks are accompanied by a CO_2 desorption peak at 890 K suggesting some molecular decomposition, probably from unreacted carbonyl molecules. A second feature consisting on a double desorption peak at high temperatures (925 and 1010 K) is characteristic of molecular recombination of carbonyl molecules on β-Mo_2C. This has been previously recorded for cyclic ketones after recombination of the alkylidene species and adsorbed oxo moieties at high temperatures[27], in opposition to the low temperature desorption observed for acetone adsorbed on Pt(111)[30-33].

3.2.1.3 X-ray photoelectron spectroscopy

High surface-sensitivity XPS C(1s) data for acetone are presented in Figure 3-5. Reference spectra for clean β-Mo_2C and for the surface following decomposition of 10 L ethylene at 600 K to deposit excess carbon[15,41] are displayed to support peak assignment for the alkylidene spectrum. The clean surface displays a single peak at 282.8 eV, and the ethylene treated surface is characterized by a peak at 283.4 eV. Two molecular peaks at 288.2 eV and 285.3 eV are observed after deposition of 20 L of acetone at 100 K, due to the carbonyl carbon and the two CH_3 moieties. Heating the acetone multilayer to 400 K leads to a C(1s) complex spectrum that may be deconvoluted into the already established features with energies of 282.8 and 283.4 eV, due to the metal carbide and to carbon deposited on the surface, and two new peaks at 284.8 and 285.8 eV, with peak areas presenting a ratio of 2:1, attributed respectively to the two methyl carbons and the alkylidene carbon of the surface alkylidene. These assignments are supported by previous observations on high-resolution synchrotron XPS data of cyclopentylidene species on β-Mo_2C reported by Siaj and co-workers[15,25,41], and Oudghiri-Hassani and co-workers[24,42], in which the 4 sp^3 carbons are detected at 284.7 eV and those directly bonded to the surface sp^2 carbon at 285.8 eV. Similar assignment for the sp^3 carbon groups were observed by Fuhrman et al.[43] at 284.0 eV for ethylidene moieties adsorbed on Rh(111). Nowak et al.[44]

reported a binding energy of 285.8 eV for C atoms in hydrocarbons adsorbed on the surface of deposited Cr films identified as a mixture of Cr_2O_3 and Cr_3C_2.

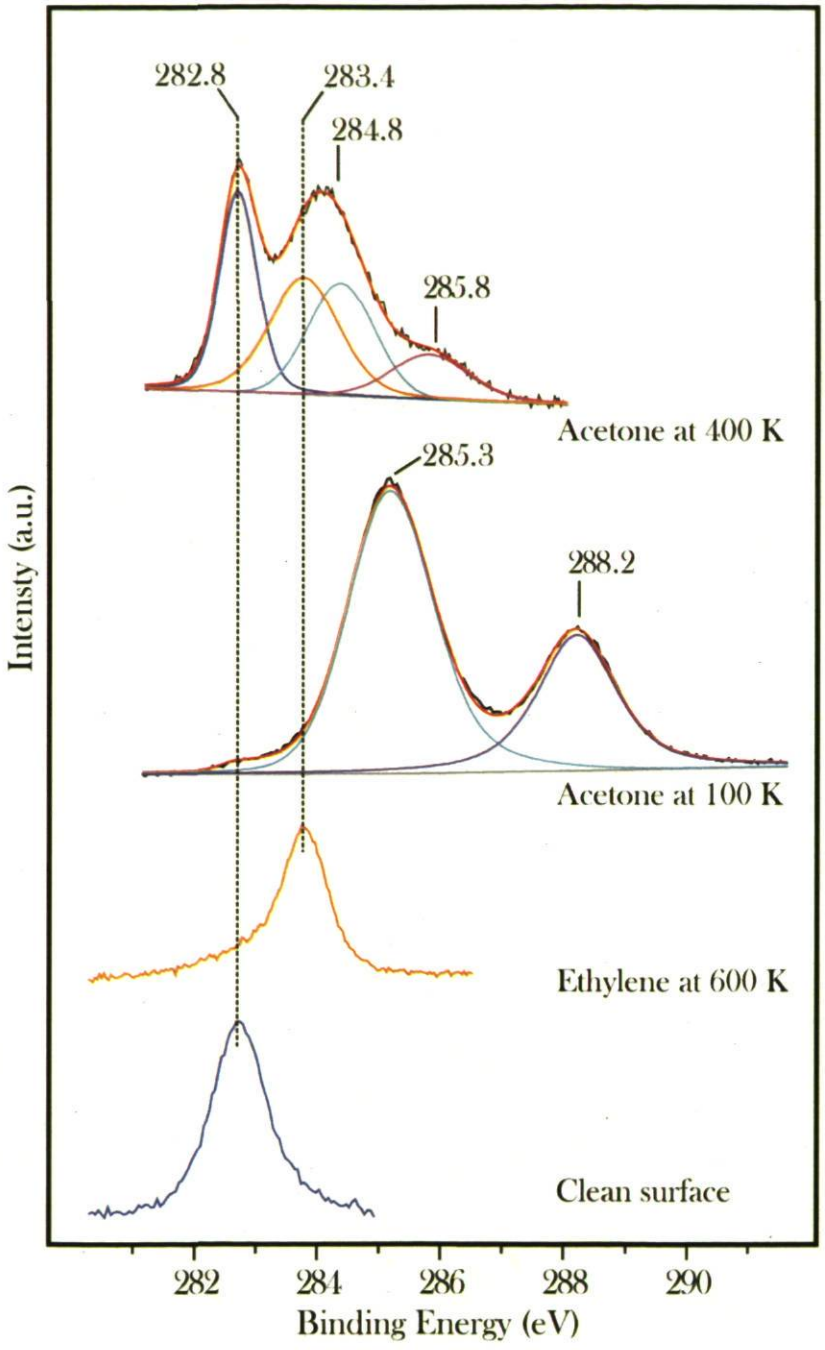

Figure 3-5 : High-resolution C(1s) data recorded for dimethyl alkylidene species on β-Mo_2C. Reference spectra are shown for the clean carbide sample and for the carbide treated with 10 L ethylene at 600 K to deposit excess surface carbon. The spectrum of a multilayer of acetone (20 L) is also included; the spectra were recorded at the indicated temperatures.

An estimation of the amount of dimethylidene species present on the surface at 400 K was made by comparing the relative intensities of the 285.8 eV peak, corresponding to the surface alkylidene sp^2 carbon (C_{alk}), and the 282.8 eV peak, characteristic of the inorganic carbidic carbon in the surface (C_{surf}). It is found a ratio between the adsorbed carbon and the surface carbon of ~0.4. It has to be taken into account that XPS can reach a certain depth into the bulk of the material, and thus the measure of the carbidic carbon is based on more than one layer. For this reason, this measure of the ratio C_{alk}/C_{surf} serves as an estimation of the lower limit of alkylidenes per carbide carbon at the surface. Knowing that these surface carbons are assumed to be in an invariable proportion to the Mo atoms (1:2), it is found that at least 20 % of molybdenum atoms at the surface are covered by alkylidene species. Similar results have been previously estimated for the fraction of cyclobutylidene species present at 900 K by comparing the C(1s) intensity to the O(1s) intensity for saturation coverage of dissociated O_2 (2 L) at 100 K on this material[15,65]. This astonishingly high coverage of alkylidene species on the surface of molybdenum carbide may be the main reason why this system can be studied in detail. In comparison, the number of active sites in supported metathesis catalysts is very low. In fact, a dynamic chemical counting study made by Handzlik et al.[45] resulted in an estimation of the percentage of the active sites for MoO_3/Al_2O_3 catalysts, in the range of 0.1 to 0.4%.

The experimental data presented above were used to characterize dimethyl alkylidene species formed by dissociative adsorption of acetone on the surface of molybdenum carbide. The process is summarized in Scheme 3-1, where an approximate positioning of the molecule with respect to the surface is displayed. Adsorption at low temperature occurs through an η^1 state where the molecule is bonded to the surface through the lone pair of electrons of the oxygen atom. This interaction forces the molecule to adopt a configuration with a component perpendicular to the surface. When the temperature is increased over room temperature the surface selectively dissociates the carbonyl bond to form two new species, dimethyl alkylidene and oxo moieties, strongly adsorbed to the metallic atoms of the surface through double bonds. The dissociation of the carbonyl bond, however, cannot take place with the molecule in an η^1 configuration. Thus, an η^2 configuration is proposed based on a much more suitable positioning of the molecule with

respect to the surface, the weaker carbonyl bond of the η^2 state, and spectroscopic evidences of this species in the literature[30-33].

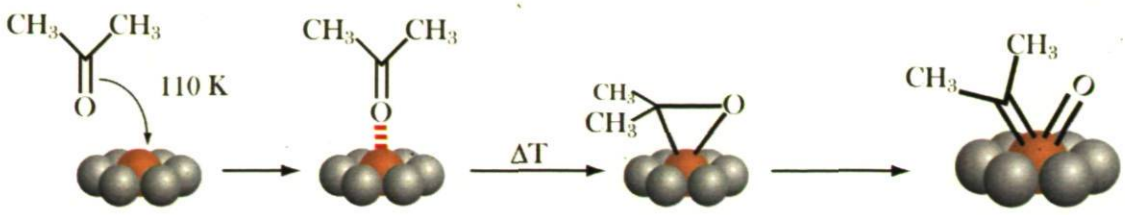

Scheme 3-1 : Proposed pathway for the dissociative adsorption of acetone on the surface of molybdenum carbide including an η^1 adsorption state at low temperatures and an intermediate η^2 state prior to the formation of the oxo=Mo=alkylidene species.

The dimethyl alkylidene modified surface of molybdenum carbide was found to display no activity, or at least very poor activity, for metathesis reactions. No significant amount of product for the metathesis reaction was detected under UHV condition in a series of thermally programmed reaction (TPR), RAIRS, and XPS experiments. This fact, though disappointing, demonstrates the importance of the environment of the metal-alkylidene bond. The factors giving rise to such poor catalytic activity could be either electronic or steric on the molecular side of the active site. Since there is very little variation on electronic properties between cyclopentyl and dimethyl groups, the reason for such low activity may be due to steric hindrance caused by the two CH_3 groups, or a close packing of alkylidene domains disallowing the reacting molecules to reach the active sites.

3.2.2 Vinyl alkylidene

In this section we will discuss the behaviour of acrolein adsorbed on the surface of molybdenum carbide at different temperatures. The thermal dissociation of acrolein on molybdenum carbide is expected to lead to the formation of surface vinyl alkylidene and oxo groups (Scheme 3-2), consistent with carbonyl bond scission, also reported for other carbonyl compounds[14,15,25-29,41], mostly ketone molecules. Siaj et al.[26] also reported the dissociative adsorption of acetaldehyde molybdenum carbide to form ethylidene.

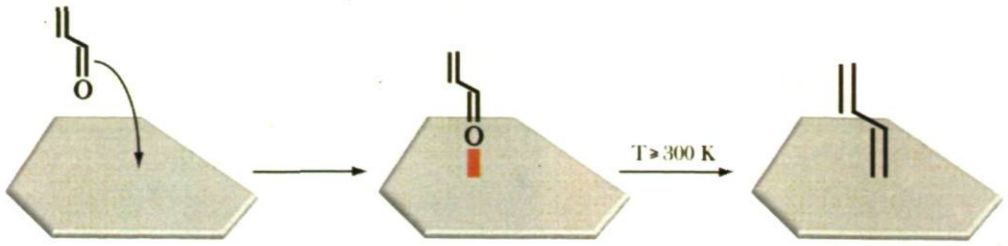

Scheme 3-2 : Acrolein adsorption via an η^1 configuration at low temperature (100 K) and the formation of vinyl alkylidene species by carbonyl scission when the temperature is raised above 300 K.

Vinyl alkylidene species would be of great interest as they are the shortest linear oligoene possible bonded through a double bond to a metallic surface (Scheme 3-2) in this case the surface of β-Mo_2C. Linear oligoenes have been extensively studied spectroscopically and structurally by a number of authors for many years[46-48]. They are relevant as the simplest series of molecules having π-electron conjugation, which show very interesting electrical and optical properties, and as models to characterize polyacetylene. Outside the viewpoint of heterogeneous catalysis, this could provide insights on the vibrational spectroscopic characterization of molecules with conjugated π-systems directly bonded to a metallic surface via a double bond. Such molecular contacts could allow very efficient electron transport between a conducting bulk material and a semiconducting molecule[17,49].

3.2.2.1 Infrared spectroscopy

The selective hydrogenation of unsaturated aldehydes, such as α,β-unsaturated aldehydes, has been recognized as an important step in a number of synthetic industrial processes[50,51]. For that reason, a number of spectroscopic studies have been performed on the chemisorption of acrolein on metal surfaces with catalytic properties, such as Pt(111)[52-54], Ni(111) and Pt-Ni-Pt(111) bimetallic surfaces[55], evaporated Ag films on a mirror-finished Cu plate[56,57], Rh(111)[58] and Au(111) surfaces[59].

RAIRS data for the adsorption of acrolein at low temperatures on the surface of molybdenum carbide as a function of exposure are displayed in Figure 3-6. Monolayer completion is observed at exposure of ~2 L and can be characterized principally by the appearance of a free carbonyl peak at 1699 cm^{-1}, in contrast to the lower frequency band observed at 1635 cm^{-1} for chemisorbed acrolein. This low energy vibrational mode for the carbonyl bond on the monolayer has been related to an orientation of the molecule in an η^1 state, with a perpendicular component of the molecular chain with respect to the surface. However, relatively weak bands for the monolayer of acrolein may suggest a high degree of tilting in the chemisorbed state, possibly due to some interaction of the alkene group with the surface. This proposal is based on observations and calculations for acrolein adsorbed on Au(111)[59] and evaporated Ag films[56,57], which suggest an initial adsorption in a η^2 (C=O) configuration at low temperatures, with a subsequent change to a η^4 (C-C-C-O) configuration as the temperature increases.

Spectra for monolayer adsorption of acrolein also display bands at 887, 1015, 1175, and 1425 cm^{-1} with increasing intensity as the monolayer goes to completion. These bands are in agreement with literature reports[52-57] and have been identified as $\rho(CH_2)$ rocking, γ(CH) out-of-plane bending, ν(C-C) stretching, and δ(CH) in-plane bending due to the aldehyde part of the molecule, respectively. Multilayer formation is accompanied by the appearance of new bands at 921, 989, 1160, 1364, and the already discussed 1699 cm^{-1} carbonyl band. These bands are assigned to (CH_2) wagging, γ(CH) out-of-plane bending, ν(C-C) stretching, and δ(CH) in-plane bending, respectively. Most of these bands should also be present in the monolayer spectra, and the fact that they are not observed may be due to their low intensity, suggesting, as mentioned above, a tilted positioning of the molecules with respect to the surface.

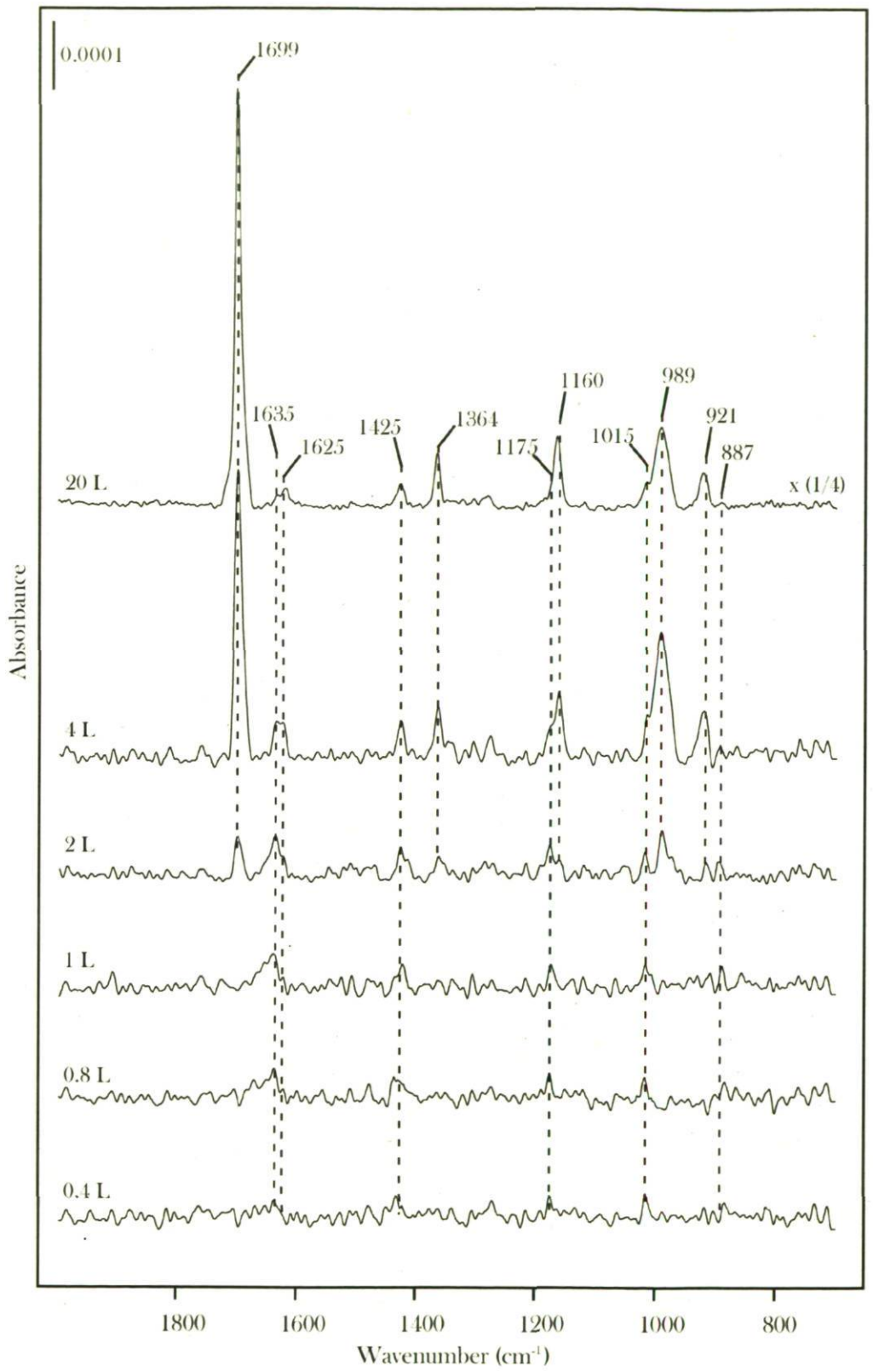

Figure 3-6 : RAIRS spectra of acrolein adsorbed on the surface of molybdenum carbide at 100 K as a function of the exposure.

RAIRS data for alkylidene species formed from annealing acrolein adsorbed on molybdenum carbide are displayed on Figure 3-7. The spectrum of the monolayer of adsorbed acrolein obtained after thermal desorption of the multilayer at 200 K displays all of the bands discussed above, including the low frequency carbonyl stretching vibration at 1635 cm^{-1}. A further annealing to above room temperatures leads to the loss of the carbonyl vibrational mode, as well as the appearance of a new peak at 990 cm^{-1} that can be attributed to a metal-oxo species. Interestingly, few changes in the molecular vibrational modes can be reported after the carbonyl cleavage leading to the formation of the surface alkylidene species. The most significant changes are a shift in the peak at 1175 cm^{-1} of chemisorbed acrolein to 1155 cm^{-1} in the vinyl alkylidene species, as a result of a mixing of the ν(C-C) and Mo=C stretching vibrations[14,25,26]. The disappearance of the peak at 1425 cm^{-1} along with the development of three new bands at 1430, 1460, and 1517 cm^{-1} corresponding to the CH rocking, CH_2 scissoring, and ν(C=C) out of phase stretching vibrations respectively, whereas the wagging CH_2 vibration (887 cm^{-1}), the CH wagging vibration (1015 cm^{-1}), and the ν(C=C) in-phase stretching vibration (1625 cm^{-1}) remain invariable with respect to spectrum of adsorbed acrolein[52-57]. No significant differences apart from a slight rise in intensities are observed at higher temperatures and all bands characteristic of the alkylidene species are present in the 300-500 K temperature range.

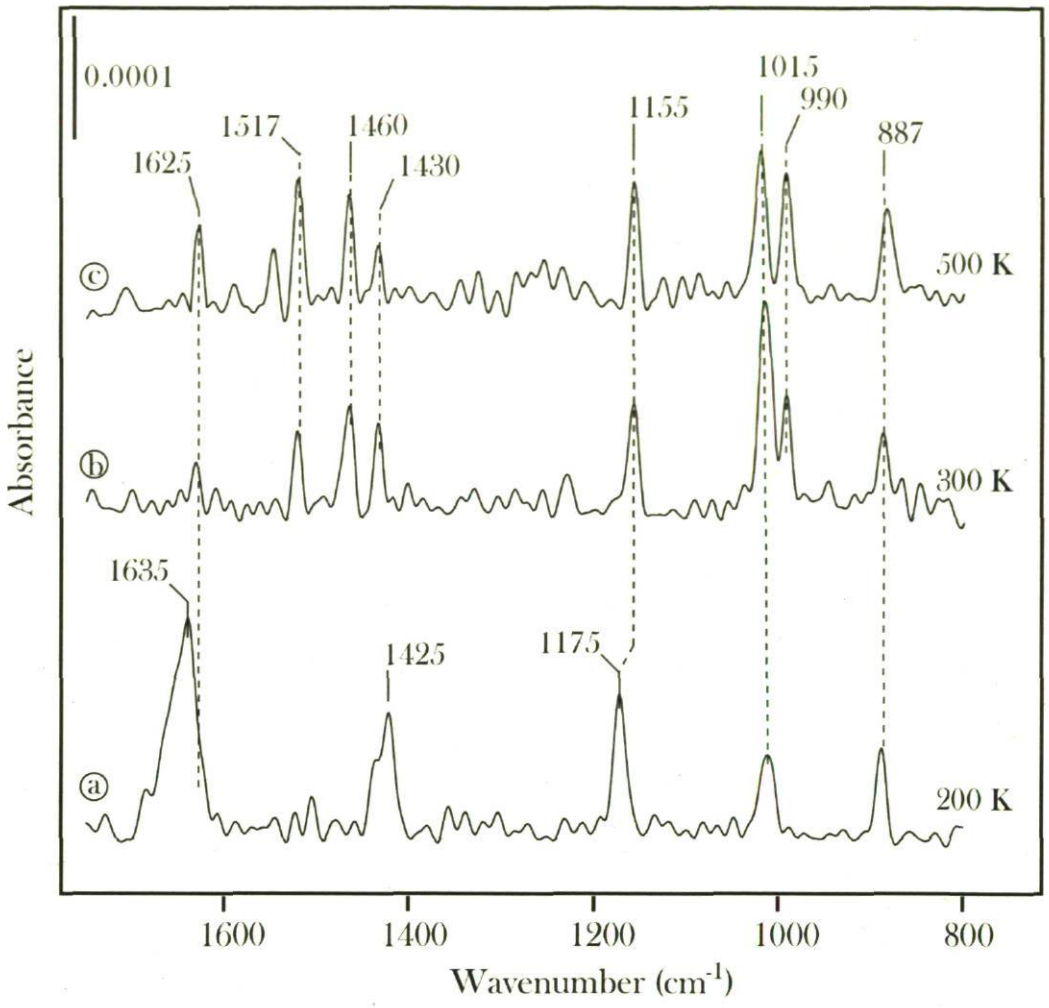

Figure 3-7 : RAIRS data for a) acrolein monolayer at 200 K, and b) and c) for vinyl alkylidene species formed after annealing the sample to 300 K and 500 K respectively.

The high frequency mode of the ν(C=C) in-phase stretching vibration (1625 cm^{-1}) is in agreement with the literature[52-57]. This peak is characteristic of short linear olgoenes and is an interesting result, since the conjugation length dependence of this band is very well documented[46-48,50-63]. This peak has been found at 1643 and 1661 cm^{-1} for 1,3-butadiene[61,62] and at 1629 and 1632 cm^{-1} for 1,3,5-hexatriene[47], whereas it appears at 1613 cm^{-1} for 1,3,5,7-octatetraene and as low as 1593 cm^{-1} for 1,3,5,7,9-decapentaene[60]. The relatively low frequency of this band in the vinyl alkylidene species on the surface of molybdenum carbide, may be a consequence of the conjugation C=C-C=Mo being different from the all-carbon conjugation on the free 1,3 butadiene molecule.

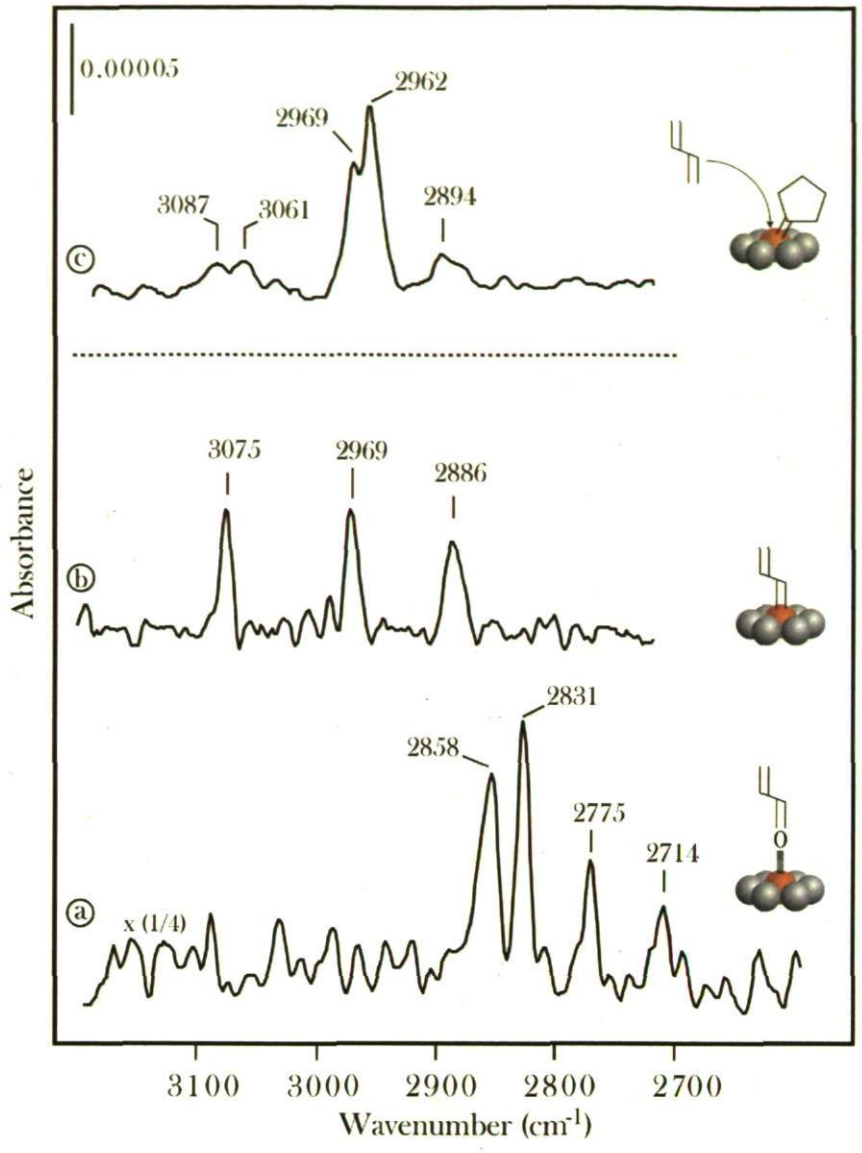

Figure 3-8 : RAIRS data for a) multilayer of acrolein at 100 K; b) vinyl alkylidene species formed by annealing the adsorbed acrolein to 300 K; c) vinyl alkylidene species formed by the cross metathesis reaction of cyclopentylidene species on molybdenum carbide with butadiene at 470 K[28].

C-H stretching region spectra for vinyl alkylidene species formed by the dissociative adsorption of acrolein present more information about the structure of the adsorbed species. Spectrum 3-8(a), corresponding to a multilayer phase of acrolein adsorbed on molybdenum carbide at 100 K, displays bands at 2714, 2775, 2831, and 2858 cm^{-1}, in agreement with liquid and gas-phase IR data for acrolein[54]. The spectrum obtained

on annealing the acrolein multilayer to 300 K displays new peaks at 2886, 2969, and 3075 cm^{-1} (Spectrum 3-8(b)). The latter sharp peak at 3075 cm^{-1} is characteristic of sp^2 C-H bonds. The proximity of the surface may explain the high frequency of this band, observed between 3030 and 3065 cm^{-1} for liquid and gas acrolein[54].

This behaviour is also observed for the vinyl alkylidene species formed from cross metathesis using cyclopentylidene species as active sites on the surface of molybdenum carbide (spectrum 3-8(c)). Acrolein is however essentially *transoid* and thus, the observed high frequency peak at 3075 cm^{-1} could be due to essentially *trans* sp^2 C-H bonds, whereas for the case of cross metathesis production of vinyl alkylidene species, both *cis* and *trans* isomers are expected due to the utilization of 1,3-butadiene. So the doublet at 3087 and 3061 cm^{-1}, should be, respectively, assigned to *cis* and *trans* vinyl alkylidene species, as well as to the presence of methylidene species ($=CH_2$) also formed in the cross metathesis reaction.

3.2.2.2 X-ray photoelectron spectroscopy

XPS data of acrolein adsorption as a function of coverage at 100 K is displayed in Figure 3-9(a). We can observe the evolution of two peaks at 288.2 and 284.3 eV that are assigned to the carbonyl sp^2 carbon and to the two sp^2 carbons of the alkene group respectively, with a relative intensity of 1:2 as expected. The evolution of these two peaks is accompanied by the progressive masking of the inorganic surface-carbidic carbon peak at 282.8 eV. These three peaks have been previously reported for carbonyl compounds adsorbed on molybdenum carbide[15,24,25,41,42], notably cyclopentanone and cyclobutanone with the help of high resolution synchrotron spectroscopy, and acetone, and acetone-d_6 under the same experimental conditions and using the same equipment as in this case. No variation whatsoever on the positioning of the peaks could be observed between those different cases for the different sp^2 and sp^3 species. Here though, the allyl part of the molecule displays a peak at 284.3 eV, instead of the 284.8 eV peak of the sp^3 carbons of both cyclic ketones and acetone, 0.5 eV lower in energy, in agreement with data obtained by Freyer and co-workers[64] for ethylene adsorbed on Pt(111) at low temperature.

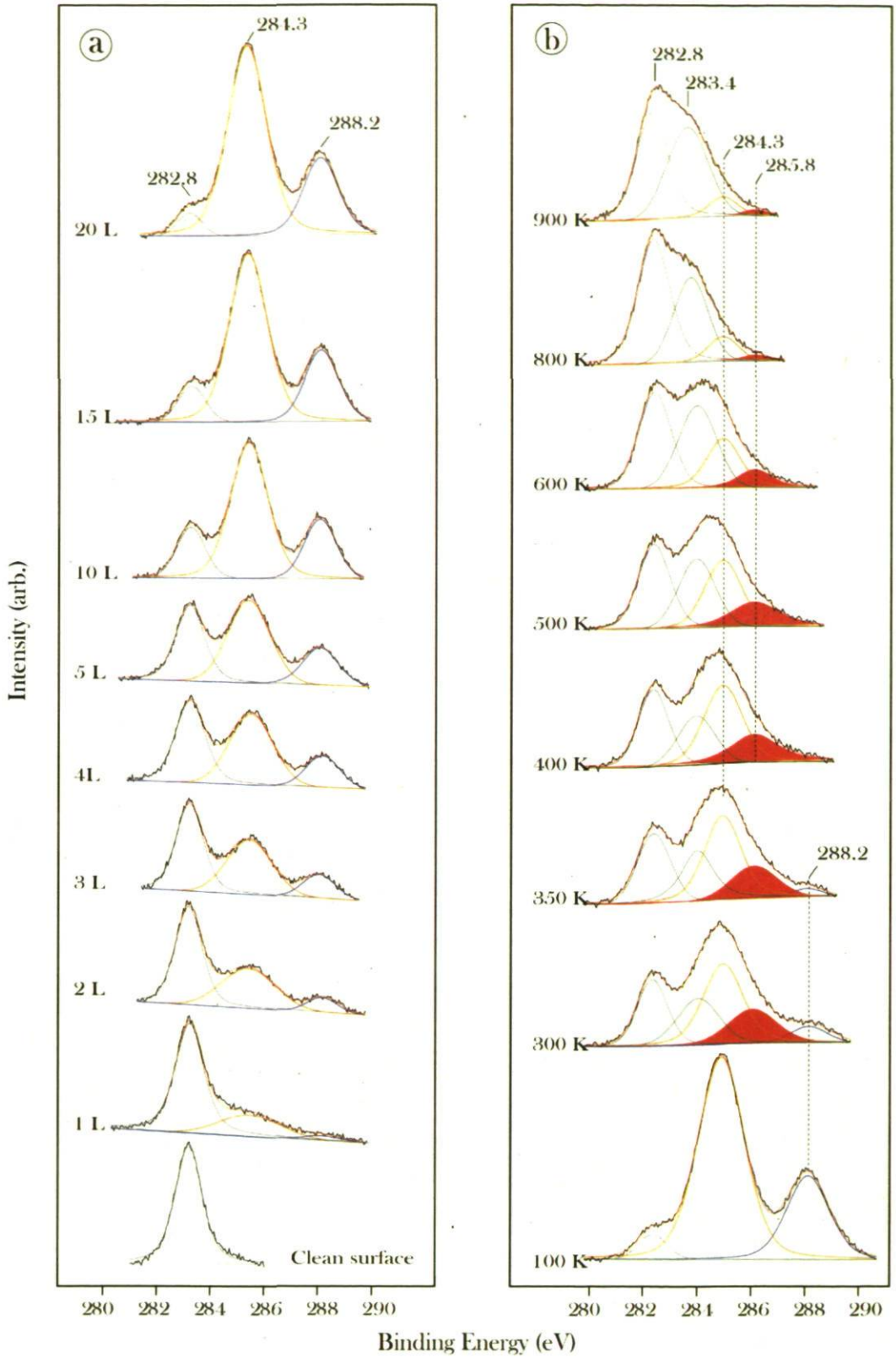

Figure 3-9 : C(1s) data for acrolein a) as a function of exposure at 100 K, and b) as a function of temperature after dosing the surface with 20 L at 100 K.

The evolution of the C(1s) spectrum of the multilayer of acrolein as a function of temperature is shown in Figure 3-9(b). We can observe from the transition between 100 K and 300 K that multilayer desorption leads to a significant reduction of the general intensity of the spectrum with the only exception being the surface-carbidic peak (282.8 eV) which is now less attenuated by the molecular layers. Especially noticeable is the drop of intensity of the peak at 288.2 eV corresponding to the carbonyl carbon in comparison to the drop in the alkenyl carbons (284.3 eV) alongside with the appearance of a new peak with a binding energy of 285.8 eV, which partly compensates the difference in lost intensity between the carbonyl and the alkenyl carbons. This new peak corresponds to the partial transformation of adsorbed acrolein into vinyl alkylidene species through the dissociation of the carbonyl bond.

The evolution has its continuity at 350 K in which even more carbonyl carbons are transformed into alkylidenyl carbons bonded to the surface metal atoms. Carbonyl carbons are then completely transformed at temperatures above 400 K into these new alkylidenyl carbons. The alkylidene sp^2 C(1s) peak (shaded) is detected on the surface up to 900 K, and its maximum intensity appears to be at 400 K, slowly decreasing in its intensity from temperatures as low as 500 K, due to molecular decomposition on the surface of small amounts of alkylidene species. This decrease in intensity becomes dramatic at 800 K, in agreement with the TPD data displayed in Figure 3-11, where a recombinative desorption peak is observed from around 800 K. This decrease of the molecular peak intensities is accompanied by an increase in intensity of the peak observed at 283.4 eV corresponding to carbon deposition on the surface as a consequence of molecular cracking above 300 K.

An estimation of the amount of alkylidene species present on the surface at each temperature can be achieved by comparison of the areas for the peaks corresponding to the alkylidene sp^2 carbon with a binding energy of 285.8 eV, and the surface carbon which appears at 282.8 eV. This is lower limit estimation as mentioned for the case of dimethyl alkylidene species. Figure 3-10 displays the ratio between alkilydene carbons and carbidic carbons for each temperature. Alkylidene species appear from 300 K as seen in Figure 3-10, and the population of these species grows from just below 0.2 at 300 K to over 0.4 at 400 K, then a continuous decrease is observed in agreement with TPD data (Figure 3-11).

The TPD spectra show a broad feature above 400 K due to molecular cracking of a small quantity of molecules on the surface. These data show that the amount of vinyl alkylidene species formed from the dissociative adsorption of acrolein is comparable with the amount of dimethyl alkylidene species formed from adsorbed acetone.

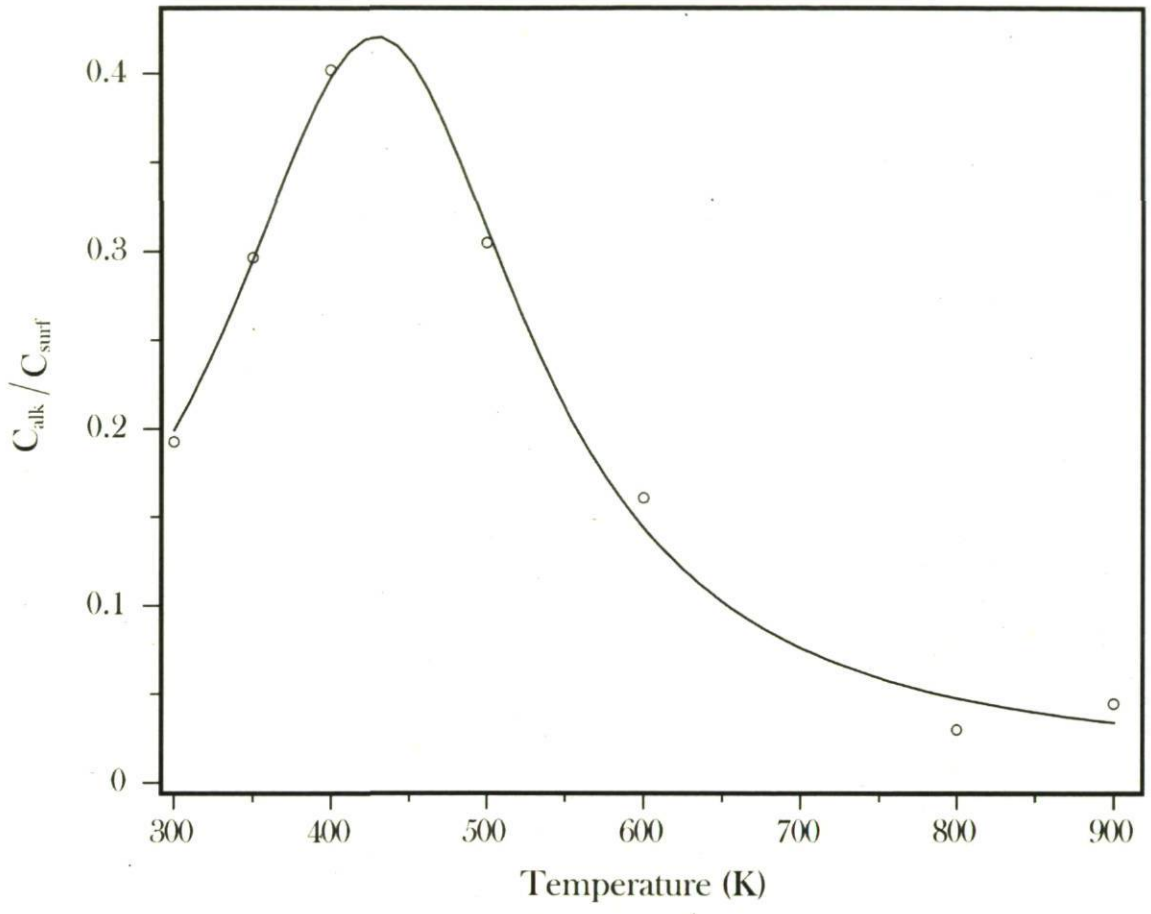

Figure 3-10 : Plot of the ratio between alkylidene species (285.8 eV) and surface carbidic carbon (282.8 eV) after annealing acrolein to different temperatures.

The molecular cracking yielding to carbon deposition on the surface is characterized by a new peak at 283.4 eV in the C(1s) spectra. The decrease in the population of alkylidene species on the surface is accentuated from temperatures near 800 K where a large decrease in the alkylidene peak intensity occurs. However this drop in intensity is not accompanied by a rise in intensity of the 283.4 eV peak indicating that this loss of species is not due to molecular decomposition, but to molecular desorption instead. This high

temperature molecular desorption is also observed in the TPD spectra (Figure 3-11) and has been reported previously for cyclic ketones[24,27] and acetone (section 3.2.1.2) on molybdenum carbide.

3.2.2.3 Thermally programmed desorption study

The gas-phase products of acrolein desorption were studied using TPD by monitoring the mass desorption patterns that belong to the parent molecule and fragments. The TPD spectra of 55 and 2 amu are shown in Figure 3-11 after dosing the surface with 20 L acrolein at 100 K. The 55 amu trace is due to molecular desorption, and the 2 amu to hydrogen desorption. A first analysis of the data reveals that both spectra are basically similar, with the sole difference of a feature in the H_2 spectrum at temperatures higher than 1000 K. This fact indicates that no sub-products are obtained upon desorption, and acrolein suffers no major transformations that cause new gas-phase products. We can observe multilayer desorption at 150 K followed by a small sharp peak at 227 K probably due to an adsorption state transformation. Adsorption studies of acrolein on Pt(111), Ni(111), and Pt-Ni-Pt(111) surfaces[55] suggested multiple possible adsorption states, from an η^1 state with the molecule adsorbed through the carbonyl bond, an η^2 state with a contribution of both C and O atoms of the carbonyl bond in the adsorption, and an η^4 state with the whole molecule placed flat on the surface and all molecular atoms contributing directly to the chemisorption bonds. Any of these states could be possible on the surface of molybdenum carbide, but vibrational results suggest the formation of metal-alkylidene species, possibly via an η^2 adsorption state.

The high temperature feature, centered at 920 K, displayed in both spectra is related to the recombination of surface alkylidene and oxo species to desorb as acrolein. This feature has been reported previously for cyclic ketones and acetone (section 3.2.1.2) adsorbed on molybdenum carbide. A difference in this case can be observed in the shape of this recombinatorial desorption, as the peaks in those cases where sharp doublets, assigned to recombination with two different oxygen sources leading to desorption at different temperatures. In the case of vinyl alkylidene species, a wide asymmetrical peak centred at

920 K is observed instead. The H_2 spectrum shows a broad feature at temperatures inmediatly above the first peak (~1150 K). In combination, these two spectra suggest molecular decomposition is taking place instead of recombination between vinyl alkylidene and oxo species diffusing on the surface from the bulk of the material at temperatures higher than 100 K.

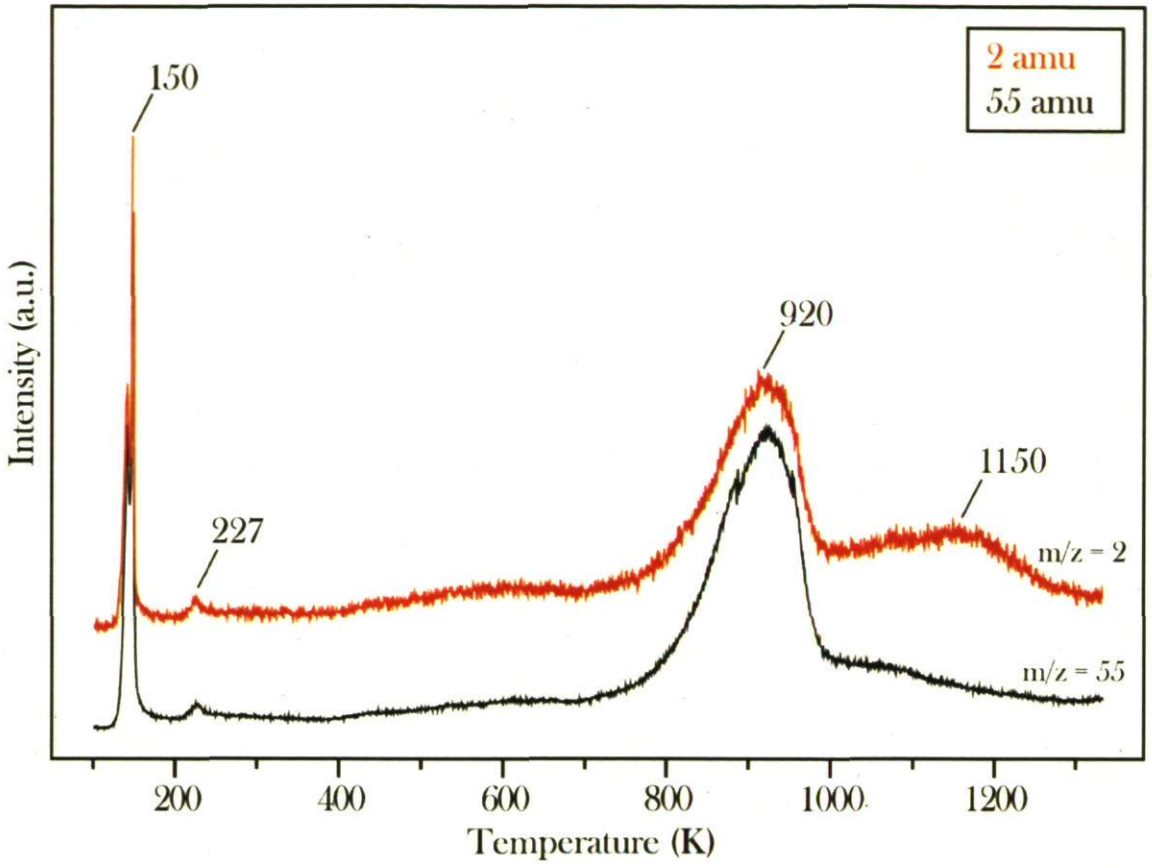

Figure 3-11 : TPD data for acrolein adsorption (20 L) at 100 K. The red spectrum corresponds to H_2 desorption and the black one to acrolein desorption.

3.3 Conclusion

Two new alkylidene species have been detected on the surface of molybdenum carbide under UHV conditions. Dimethyl alkylidene species were formed through the dissociative adsorption of acetone and were characterized by RAIRS, XPS and TPD spectroscopies. However, no catalytic activity towards metathesis reaction was observed

for this alkylidene species. Adsorption of acetone-d_6 at low temperature was used in an effort to characterize via RAIRS the adsorption states of chemisorbed acetone prior to alkylidene formation.

Vinyl alkylidene species have also been characterized on the surface of β-Mo_2C. This species was formed by the dissociative adsorption of acrolein (allyl aldehyde), in a similar fashion to that previously reported by Siaj et al.[26] using acetaldehyde on the same surface. Again RAIRS, XPS, and TPD were used to fully characterize adsorption states of the carbonyl compound at low temperatures, as well as the alkylidene species formed at higher temperatures. XPS data show the dissociation of the carbonyl bond above 300 K. However, a fraction of the carbonyl bond still remains intact until 400 K. From this temperature on, only alkylidene species are detected. The recombination of the alkylidene-oxo species around 900 K in a single stage process causes an irreversible decrease of the population, and no alkylidenes are detected on the surface at temperatures higher than 1000 K. The metathesis activity of vinyl alkylidene species on this surface will be studied in chapters 4 and 5 of this thesis.

3.4 Bibliography

(1) Natta, G.; Dallasta, G.; Mazzanti, G.; Motroni, G. *Makromol. Chem.* **1963**, *69*, 163.

(2) Natta, G.; Mazzanti, G.; Corradini, P. *Rend. Accad. Nazl. Lincei* **1958**, *25*, 2.

(3) Truett, W. L.; Johnson, D. R.; Robinson, I. M.; Montague, B. A. *J. Am. Chem. Soc.* **1960**, *82*, 2337.

(4) Ziegler, K. *Angew. Chem. Int. Ed.* **1959**, *71*, 623.

(5) Blanks, R. L.; Bailey, G. C. *I&EC Product Research and Development* **1964**, *3*, 170.

(6) Herisson, J. L.; Chauvin, Y. *Makromol. Chem.* **1971**, *141*, 161.

(7) Fürstner, A. *Angew. Chem. Int. Ed.* **2000**, *39*, 3012.

(8) Hoveyda, A. H.; Zhugralin, A. R. *Nature* **2007**, *450*, 243.

(9) McLain, S. J.; Schrock, R. R. *J. Am. Chem. Soc.* **1978**, *100*, 1315.

(10) Schrock, R. R.; Messerle, L. W.; Wood, C. D.; Guggenberger, L. J. *J. Am. Chem. Soc.* **1978**, *100*, 3793.

(11) Buchmeiser, M. R. *New J. Chem.* **2004**, *28*, 549.

(12) Copéret, C. *New J. Chem.* **2004**, *28*, 1.

(13) Ren, F.; Feldman, A. K.; Carnes, M.; Steigerwald, M.; Nuckolls, C. *Makromol.*. **2007**, *40*, 8151.

(14) Siaj, M.; McBreen, P. H. *Science* **2005**, *309*, 588.

(15) Siaj, M.; Oudghiri-Hassani, H.; Maltais, C.; McBreen, P. H. *J. Phys. Chem. C* **2007**, *111*, 1725.

(16) Thieuleux, C.; Copéret, C.; Dufaud, V.; Marangelli, C.; Kuntz, E.; Basset, J.-M. *J. Mol. Cat. A* **2004**, *213*, 47.

(17) Tulevsky, G. S.; Myers, M. B.; Hybertsen, M. S.; Steigerwald, M. L.; Nuckolls, C. *Science* **2005**, *309*, 591.

(18) Buchmeiser, M. R. *Chem. Rev.* **2000**, *100*, 1565.

(19) Barlow, S. M.; Raval, R. *Surf. Sci. Reports* **2003**, *50*, 201.

(20) Ma, Z.; Zaera, F. *Surf. Sci. reports* **2006**, *61*, 229.

(21) Henderson, M. A.; Radloff, P. L.; White, J. M.; Mims, C. A. *J. Phys. Chem.* **1988**, *92*, 4111.

(22) Hills, M. M.; Parmeter, J. E.; Mullins, C. B.; Weinberg, W. H. *J. Am. Chem. Soc.* **1986**, *108*, 3554.

(23) McBreen, P. H.; Erley, W.; Ibach, H. *Surf. Sci.* **1984**, *148*, 292.

(24) Oudghiri-Hassani, H.; Siaj, M.; McBreen, P. H. *J. Phys. Chem. C* **2007**, *111*, 5954.

(25) Siaj, M.; Oudghiri-Hassani, H.; Zahidi, E. M.; McBreen, P. H. *Surf. Sci.* **2005**, *579*, 1.

(26) Siaj, M.; Reed, C.; Oyama, T.; Scott, S. L.; McBreen, P. H. *J. Am. Chem. Soc.* **2004**, *126*, 9514.

(27) Zahidi, E. M.; Oudghiri-Hassani, H.; McBreen, P. H. *Nature* **2001**, *409*, 1023.

(28) Siaj, M.; Dubuc, N.; Temprano, I.; Maltais, C.; McBreen, P. H. *J. Phys. Chem.*, Article submitted.

(29) Siaj, M.; Temprano, I.; Dubuc, N.; McBreen, P. H. *J. Organomet. Chem.* **2006**, *691*, 5497.

(30) Avery, N. R.; Weinberg, W. H.; Anton, A. B.; Toby, B. H. *Phys. Rev. Lett.* **1983**, *51*, 683.

(31) Jeffery, E. L.; Mann, R. K.; Hutchings, G. J.; Taylor, S. H.; Willock, D. J. *Catalysis Today* **2005**, *105*, 85.

(32) Vannice, M. A.; Erley, W.; Ibach, H. *Surf. Sci.* **1991**, *254*, 1.

(33) Villegas, I.; Weaver, M. J. *J. Am. Chem. Soc.* **1996**, *118*, 458.

(34) Anton, A. B.; Avery, N. R.; Toby, B. H.; Weinberg, W. H. *J. Am. Chem. Soc.* **1986**, *108*, 684.

(35) Davis, J. L.; Barteau, M. A. *Surf. Sci.* **1989**, *208*, 383.

(36) Houtman, C.; Barteau, M. A. *J. Phys. Chem.* **1991**, *95*, 3755.

(37) Sim, W.-S.; Li, T.-C.; Yang, P.-W.; Yeo, B.-S. *J. Am. Chem. Soc.* **2002**, *124*, 4970.

(38) Weber, J. H. *Inorg. Chem.* **1969**, *8*, 2813.

(39) Dellepia.G; Overend, J. *Spectrochimica Acta* **1966**, *22*, 593.

(40) Cheon, J.; Dubois, L. H.; Girolami, G. S. *J. Am. Chem. Soc.* **1997**, *119*, 6814.

(41) Siaj, M.; Maltais, C.; Zahidi, E. M.; Oudghiri-Hassani, H.; Wang, J.; Rosei, F.; McBreen, P. H. *J. Phys. Chem. B* **2005**, *109*, 15376.

(42) Oudghiri-Hassani, H.; Zahidi, E. M.; Siaj, M.; Wang, J.; McBreen, P. H. *App. Surf. Sci.* **2003**, *212-213*, 4.

(43) Fuhrman, T.; Kinne, M.; Trankenschuh, B.; Papp, C.; Zhu, J. F.; Denecke, R.; Steinruck, H.-P. *New J. Phys.* **2005**, *7*, 107.

(44) Nowak, R.; Hess, P.; Oetzmann, H.; Schmidt, C. *App. Surf. Sci.* **1989**, *43*, 11.

(45) Handzlik, J.; Ogonowski, J. *Catal. Lett.* **2003**, *88*, 119.

(46) Kofranek, M.; Lischka, H.; Karpfen, A. *J. Chem, Phys.* **1992**, *96*, 982.

(47) Langkilde, F. W.; Wilbrandt, R.; Nielsen, O. F.; Christensen, D. H.; Nicolaisen, F. M. *Spectrochim. Acta A* **1987**, *43*, 1209.

(48) Schaffer, H. E.; Chance, R. R.; Silbey, R. J.; Knoll, K.; Schrock, R. R. *J. Chem, Phys.* **1991**, *94*, 4161.

(49) Ning, J.; Qian, Z.; Li, R.; Hou, S.; Rocha, A. R.; Sanvito, S. *J. Chem, Phys.* **2007**, *126*, 174706.

(50) Mäki-Arvela, P.; Hájek, J.; Salmi, T.; Murzin, D. Y. *Appl. Catal. A* **2005**, *292*, 1.

(51) Marinelli, T. B. L. W.; Nabuurs, S.; Ponec, V. *J. Catal.* **1995**, *151*, 431.

(52) Bournel, F.; Laffon, C.; Parent, P.; Tourillon, G. *Surf. Sci.* **1996**, *359*, 10.

(53) De Jesus, J. C.; Zaera, F. *Surf. Sci.* **1999**, *430*, 99.

(54) Loffreda, D.; Jugnet, Y.; Delbecq, F.; Bertolini, J. C.; Sautet, P. *J. Phys. Chem. B* **2004**, *108*, 9085.

(55) Murillo, L. E.; Chen, J. G. *Surf. Sci.* **2008**, *602*, 919.

(56) Fujii, S.; Misono, Y.; Itoh, K. *Surf. Sci.* **1992**, *277*, 220.

(57) Fujii, S.; Osaka, N.; Akita, M.; Itoh, K. *J. Phys. Chem.* **1995**, *99*, 6994.

(58) Brown, N. F.; Barteau, M. A. *J. Am. Chem. Soc.* **1992**, *114*, 4258.

(59) Akita, M.; Osaka, N.; Itoh, K. *Surf. Sci.* **1998**, *405*, 172.

(60) Hirata, S.; Yoshida, H.; Torii, H.; Tasumi, M. *J. Chem, Phys.* **1995**, *103*, 8955.

(61) Panchenko, Y. N. *Spectrochim. Acta A* **1975**, *31*, 1201.

(62) Rasmussen, R. S.; Brattain, R. R. *J. Chem. Phys.* **1947**, *15*, 131.

(63) Yoshida, H.; Tasumi, M. *J. Chem, Phys.* **1988**, *89*, 2803.

(64) Freyer, N.; Pirug, G.; Bonzel, H. P. *Surf. Sci.* **1983**, *126*, 487.

(65) Wang, J.; Castonguay, M.; Deng, J.; McBreen, P. H. *Surf. Sci.* **1997**, *374*, 197.

4. Ring opening metathesis polymerization of 1,3,5,7-cycloocatatetraene on an alkylidene modified β-Mo_2C surface

4.1 Abstract

The coating of relevant materials with polymers is a versatile and effective technique for tailoring their properties. Polymer films with thicknesses in molecular dimensions attached to solid substrates are expected to be very useful for a wide range of applications ranging from protective coatings to improvement of the biocompatibility of materials[1], chemical sensing[2,3], and electronics[4], among many other applications. A common approach for polymer coatings is through surface initiated polymerization using self assembled monolayers (SAMs) as linkers and initiators of the reaction. This strategy has rapidly evolved over the last few years, and all the major controlled polymerization methods have been used to grow polymer brushes from surfaces using this technique. Examples of living ring opening polymerization[5-7], living anionic[8,9] and cationic polymerization[10] or atom transfer radical polymerization[11,12] are numerous in the literature, as well as in several reviews on the subject[13-15].

The use of Surface-Initiated Ring-Opening Metathesis Polymerization (SI-ROMP)[16-18] has attracted a lot of attention as a strategy for offering a high degree of control over a surface polymerization process that occurs in mild conditions, and some reviews on supported metathesis catalysts has been published[19-21]. Following this approach, a number of research groups have focussed on the use of several Grubbs first generation ruthenium-based catalysts to polymerize a large variety of monomers in a living fashion from SAM coated surfaces[17,22-24], especially strained cyclic monomers with useful electrical properties. Liu et al. have proven the controllability of this approach by using dip-pen nanolithography (DPN), patterning thiol linked SAMs on a gold substrate by bringing a tip coated with norbornenylthiol in contact with the surface[25]. The subsequent reaction of these SAMs with a Grubbs first generation metathesis catalyst permitted ROMP of norbornenyl-

functionalized monomers to obtain polymer brush dots of 78(±4) nm in diameter and 5(±1) nm in height.

The use of SAMs has, however, its limitations as initiators for surface-initiated polymerization since the spacing created by the SAM prevents direct growth from the surface. A direct contact between the polymer and the surface might be preferred in order to pursue electronic and electro-optic properties on polymer modified materials. In the past years two strategies for the *in situ* growth of polymers directly from a reactive surface have been reported. Nuckolls and collaborators have established that alkylidene activated ruthenium thin films are active for olefin metathesis[26] and that alkylidene functionalized ruthenium nanoparticles are able to perform ROMP with strained olefins such as dicyclopentadiene and norbornene[27]. However, neither unstrained olefins, such as 1,3,5,7-cyclooctatetraene, nor acetylenes appear to react with these ruthenium systems. The second strategy, continued in this work, explores the use of alkylidene functionalized Mo_2C to initiate growth directly from the surface. Earlier work demonstrated the reactivity of alkylidene modified molybdenum carbide towards ROMP with norbornene and cyclopentene[28].

Metathesis polymerization of 1,3,5,7-cyclooctatetraene (COT) as a route for obtaining polyacetylene was first investigated by Korshak and co-workers[29], using tungsten based homogeneous catalysts, reporting low yields (40% max). Since then, this reaction has been investigated by the group of Grubbs first, using tungsten catalysts[30,31] and more recently, using more reliable (even commercially available) ruthenium catalysts[32,33]. They found the ring opening metathesis polymerization of COT to be an effective route to high quality polyacetylene and derivatives, using unsubstituted and substituted cyclooctatetraene[34] as monomer for homopolymerization and a number of mono- and polycyclic olefins for copolymerization[30]. This approach towards polyacetylene offers the convenience of polymerization at ambient conditions (pressure and temperature), due principally to the versatility of mild catalysis and a monomer such as cyclooctatetraene which displays many polymerizable derivatives. Poly-COT films are shown to have physical and spectral properties very similar to polyacetylene prepared by the Shirakawa methodology[35]. When these silvery films of the semiconducting trans-polyacetylene are

halogen-doped, the conductivity increases markedly (over seven orders of magnitude in the case of iodine doping) reaching in some cases conductivities greater than 300 $\Omega^{-1}cm^{-1}$ at room temperature[36-38]. Most of the catalysts used for the process are, however, air and moisture sensitive, and thus, all polymerizations performed to date have been carried out under inert atmosphere. In addition the reaction requires purification of monomers prior to reaction and manipulation and storage of the polymer films in an inert atmosphere due to the tendency of polyacetylene to undergo oxidation. Usually a high pressure stream of nitrogen is used to protect the samples from air.

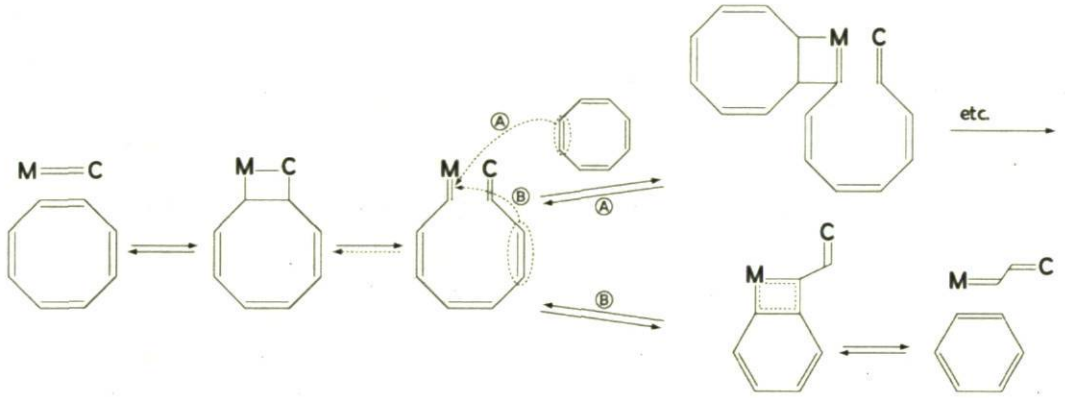

Scheme 4-1 : Formation of poly-COT via ROMP.

Polymerization of COT is considered still as an important achievement due to the very low ring strain of COT (2.5 kcal/mol) compared to monomers such as norbornene (27.2 kcal/mol) or 1,5 cyclooctadiene (13.3 kcal/mol), usually used as reference monomers to study the reactivity of new metathesis catalysts. However, at room temperature and using high monomer/catalyst ratios, the transformation from liquid to film occurs in 10 to 30 seconds, and lower monomer/catalyst ratios produce films exothermically within even shorter times. The formation of block copolymers from norbornene (NBE) and COT[39] by the group of Grubbs, reveal that because of the much greater ring strain of NBE than COT, near instantaneous polymerization of NBE first produces long block copolymers of polynorbornene. As the NBE concentration in the reaction mixture rapidly decreases, COT begins to polymerize. The much slower polymerization of COT produces the final block of polyacetylene. These results, however indicate that both polymerizations occurs equally

under reaction conditions; that the difference in ring-strain between monomers only affects the kinetics of the reaction, confirming the ring opening metathesis polymerization of cyclooctatetraene as a powerful tool towards the formation of polyacetylene. Ring opening metathesis polymerization of cyclic conjugated olefins appears to be an ideal route to form such polymers since interchain meshing seems to be crucial to the formation of polyacetylene films with good mechanical properties[31,40]. This is due to the capacity of the polymer backbone itself to undergo cross metathesis reaction with the catalyst through ring closing metathesis reactions (Scheme 4-1 path (b)). In particular, the absence of side groups in polyacetylene formed by unsubstituted COT, make this polymer highly suitable for crosslinking.

4.2 Cyclopentylidene terminated PA

Cyclopentylidene moieties formed on a planar surface of β-Mo_2C from the dissociative adsorption of cyclopentanone has been extensively characterized by RAIRS, XPS and TPD, and confirmed as active alkylidenes for the cross metathesis of different linear olefins[28,41-43], and ROMP of norbornene and cyclopentene monomers[28,43] under UHV conditions. Due to their high ring strain, these monomers are usually used in control tests to verify the reactivity of a catalyst. Given the reactivity for ROMP reactions of norbornene and cyclopentene of the cyclopentylidenyl modified β-Mo_2C, the ring opening reaction of COT at alkylidene sites was attempted.

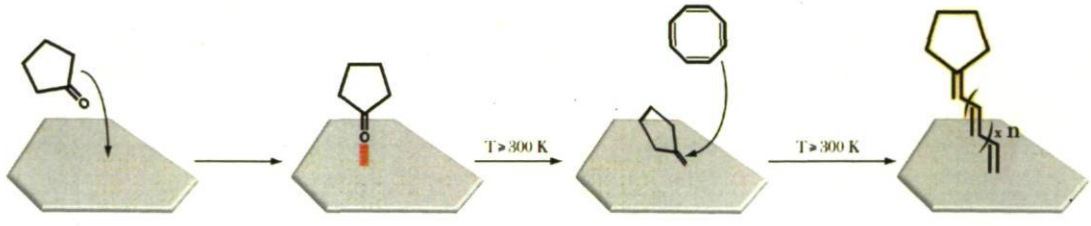

Scheme 4-2 : COT monomer insertion at cyclopentylidene sites on β-Mo_2C.

Surface initiated polymerization of cyclooctatetraene was carried out on the modified surface of a ~1 cm^2 flat polycrystalline molybdenum carbide sample. The surface modification was performed by exposing the clean surface to cyclopentanone at 100 K. The multilayer is then removed by annealing to over 200 K, and further annealing to 300-500 K drives to the formation of cyclopentylidene species on the surface. This active modified surface was subsequently exposed to different doses of monomer (1,3,5,7-cyclooctatetraene) at different temperatures. Different analytical techniques were used to characterize the resulting surface species.

4.2.1 IR characterization: "molecular footprint"

An infrared (IR) spectroscopic study on structure and properties of Ti-PA prepared from a Ziegler-Natta catalyst was first reported by Shirakawa in 1971[40]. Many vibrational spectroscopy studies, both theoretical[44-46] and experimental[40,47-51], have been reported for both *cis*- and *trans*-PA isomers since then. Nevertheless, in spite of its apparent simplicity, PA is a rather complex molecule, having multiple possible configurations and oxidation states (it is highly air and moisture sensible) which makes it hard to analyze vibrationally, and as a consequence, no full agreement has yet been achieved on the features of the spectra and their assignment. In fact, experimental information of the structure of large, unsubstituted polyenes is not available to date, and fairly complete experimental vibrational spectra, together with a detailed assignment of the normal modes are available only up to decapentaene[52-57].

An important part of its complexity comes from the fact that there are four pure isomeric structures available for polyacetylene (Figure 4-1), and none of them has already been obtained as a 100% pure crystalline form. Each path to polyacetylene gives a different mixture of isomers. For example, polyacetylene prepared by the Shirakawa method[40] results in the mostly *trans* configuration (structure IV) for the polymers prepared at temperatures higher than 423 K, and mostly *cis-transoid* (or *trans-cisoid*) configurations (structures II and III) for the polymers prepared at temperatures below 195 K. Polymers obtained between those two temperatures, contain both *cis-transoid* (or *trans-cisoid*) and

trans configurations. However, annealing the *cis* polymer over 423 K produces the thermodynamically-favoured *trans* isomer (IV). Even though the *cis-cisoid* helical (structure I) prevents extended planarity, there is X-ray evidence for its existence in soluble diblock copolymers[58].

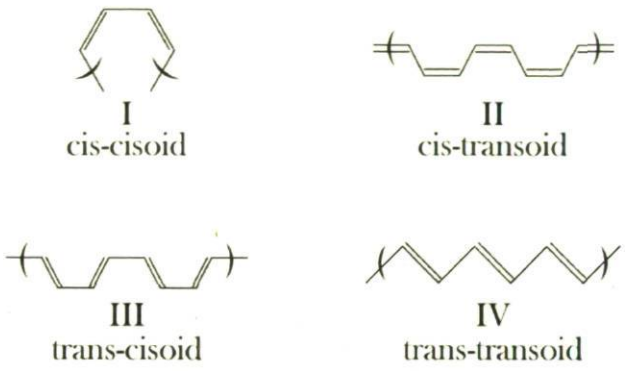

Figure 4-1 : Different isomers of polyacetylene.

As pointed out above, the interpretation of the IR spectrum of polyacetylene has not yet been fully established. The two major discussion points to date in the interpretation of the vibrational spectroscopic data are the double bond conjugation effect, characterized by an inconsistency in placing and assigning the C=C stretching band between 1450 and 1690 cm^{-1}, and the length distribution of *cis* and/or *trans*-PA and its effect in the C-H stretching region over 3000 cm^{-1}. Despite this lack of unanimity on the characterization of polyacetylene spectra, infrared spectroscopy remains a powerful tool for polymer characterization, and thus, it will be used here to investigate the surface initiated polymerization of PA on molybdenum carbide. Surface science studies under controlled UHV conditions can, in principle, study monomer insertion in a living way, one step at a time, using infrared spectroscopy, which is sensitive to chain length, orientation and conformation. This, in principle, should allow the study of the initial steps of polymer growth. RAIRS is commonly used as a standard to characterize adsorbed molecules on surfaces, being especially useful in conformational studies of small molecules either physisorbed or chemisorbed on well defined metallic surfaces by bias of its selection rule

(Figure 2-9(c)). These facts combine to make RAIRS an ideal technique for the study of COT monomer insertion at surface alkylidene sites.

Figure 4-2 shows infrared data recorded of the interaction of COT with cyclopentylidene modified β-Mo_2C. The experiments were performed by first forming a cyclopentanone multilayer at 100 K. The multilayer formed by 20 L cyclopentanone displays, spectrum 4-2(a), a characteristic very strong feature at 1731 cm^{-1}, corresponding to the carbonyl bond. An annealing of this multilayer to 300 K (spectrum 4-2(b)) leads to the development of new bands, especially at 1338, 1124, 1017, and 971 cm^{-1}. The latter band is characteristic of a surface oxo group[43,59-62] indicating that carbonyl scission has taken place. In contrast, the absence of new bands in the 1600-2000 cm^{-1} region suggests that decarbonylation leading to the formation of adsorbed CO does not occur. Apart from the oxo band, all of the clearly resolved bands observed in this spectrum are characteristic, by comparison to vibrational data for cyclopentanone, of a C_5H_8 ring. Hence, the subtle changes detected over 300 K are attributed to the conversion of one 5 membered-cyclic species into another. That is, the results are consistent with the transformation of adsorbed cyclopentanone into a surface cyclopentylidene-oxo species.

Spectrum 4-2(c) shows infrared spectroscopy data for monomer insertion on the functionalized carbide surface. Exposure to gas-phase cyclooctatetraene at 100 K followed by annealing to 470 K leads to the appearance of several new peaks, notably at 1675, 1240, 1860 and 3063 cm^{-1}. These changes can be observed from 350 K (Figure 4-3), however heating to 470 K leads to more clearly resolved peaks, and thus this spectrum is chosen for discussion. For sake of comparison, spectrum 4-2(d) shows the adsorption of cyclooctatetraene at 100 K when surface-alkylidenes are not present on the surface.

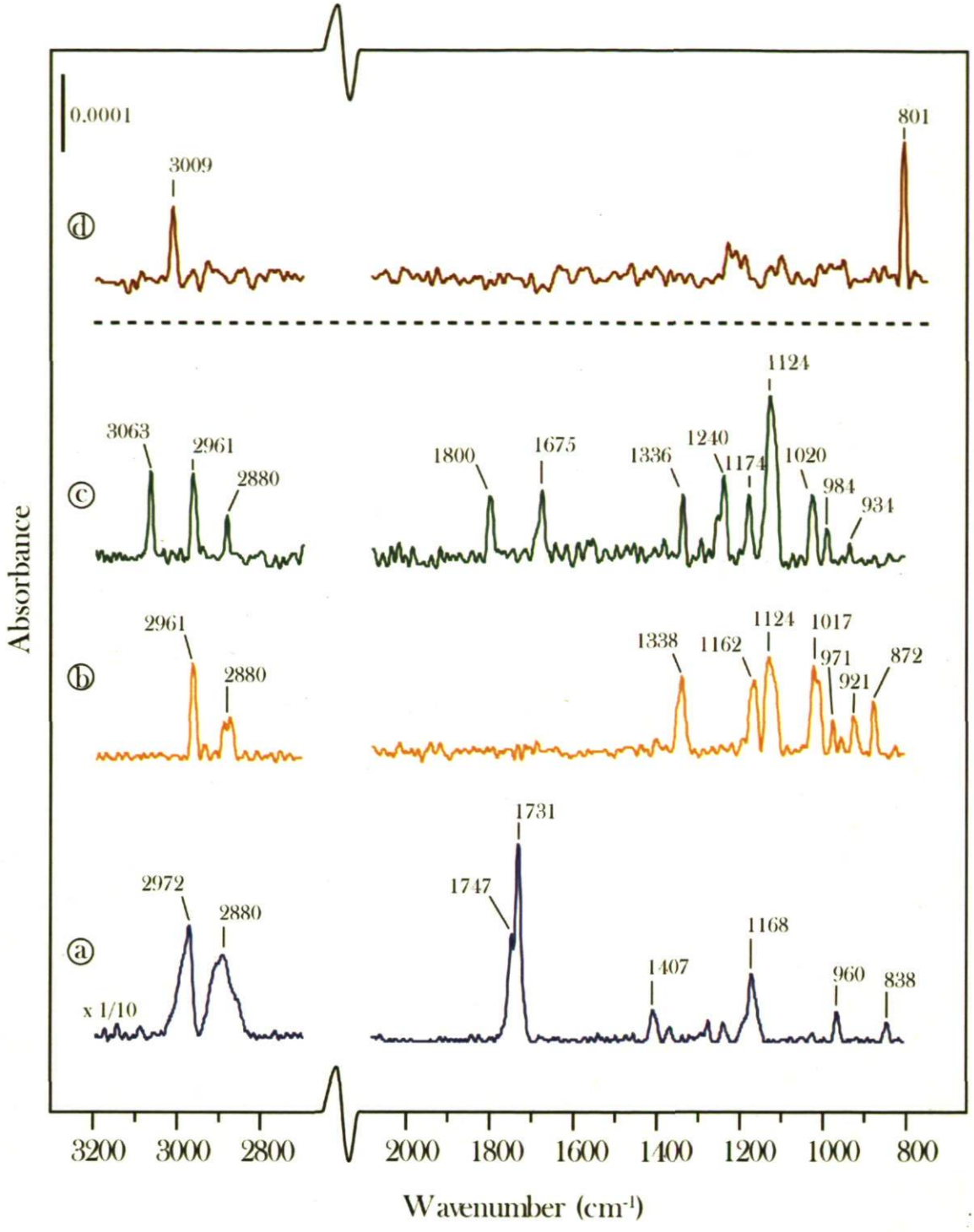

Figure 4-2 : RAIRS spectra of a) cyclopentanone at 100 K; b) cyclopentylidene at 300 K; c) The cyclooctatetraene exposed alkylidene modified surface at 470 K and d) cyclooctatetraene at 100 K on the surface of molybdenum carbide.

The most notable new features in spectrum 4-2(c), recorded after interaction of cyclooctatetraene with cyclopentylidene modified Mo_2C at 470 K, are two peaks at 1800 and 1675 cm^{-1}. The first peak has been observed consistently in most of spectroscopic studies of polyacetylene and is usually attributed to a combination of two modes, C-C=C wagging deformation and C-H in plane deformation[47,48,50], in long chain *cis* polyacetylenes (conjugation effect). The 1675 cm^{-1} band corresponds to the C=C stretching vibration. Although this band has been reported in all theoretical calculations[44-46,63], its assignation is still open to debate and it has shown to be very elusive in a number of experimental studies. This band has been observed and predicted (theoretically) in the very wide range between 1450 and 1690 cm^{-1}. It is expected to decrease with increasing conjugation lengths, and it has been predicted to be as low as 1470 cm^{-1} for long chain polyacetylene[63]. Thus, the interpretation of this high frequency C=C stretching vibration may have some implications concerning the length, conformation, and interactions of the formed polymer chain. The high frequency observed in this study could imply either the formation of short chains, a stabilizing role of the surface on the polymeric chain by π donation interactions from the double bonds to the metal centres of the surface, or a combination of all of the above.

The possibility of a certain interaction between the chains and the surface has to be taken into account, since examples of π interaction between olefinic molecules and several metallic surfaces are very well documented[64,65]. As revealing as the position of this C=C stretching vibration is its shape; a distribution of chain lengths may cause a wide adsorption band, but instead a very sharp peak is observed in spectrum 4-2(c). The sharpness of the peak reveals a very low polydispersity, as expected for metathesis polymerization, but in this case the difference between a single and a double monomer insertion is quite big in terms of polymer length. A single monomer insertion may form a 4 double bond molecule, whereas double insertion may form a molecule double the size. The difference is thus significant enough to lead to two separate peaks rather than a single broad peak, in the case where both molecules are attached to the surface. In a study of the conjugation length dependence of Raman scattering in a series of linear polyenes, Schaffer and co-workers[56] have reported a variation of this vibration from over 1600 cm^{-1} for a 4 double bond molecule to below 1550 cm^{-1} for an 8 double bond oligoene. This fact, along with the

analysis of this peak, suggests that single monomer insertion has mainly occurred on the modified surface of the carbide.

Along with the two above discussed high frequency bands, there is a new band at 1240 cm^{-1} corresponding to the C-H in-plane deformation that is not present in the cyclopentylidene spectrum. In addition, there is a dramatic increase in intensity of the C-C stretching vibration observed at 1124 cm^{-1}. Both changes are characteristic of the formation of *cis*-rich polyacetylenes[40]. The increase in intensity of the band at 1124 cm^{-1} is attributed to the insertion of a number of new C-C bonds corresponding to the backbone of the surface-initiated polyacetylene. Once again, the sharpness of this peak suggests a high monodispersity in the polyacetylene obtained, since this vibrational mode displays the same behaviour as the C=C stretching vibration discussed above, shifting to the red with increasing conjugation length[63]. The relatively high intensities of both the C-C and C=C stretching vibrations at 1120 and 1675 cm^{-1} may suggest, as well, some degree of vertical orientation with respect to the surface.

A further characterisation of the products from COT insertion was made in the C-H stretching region of the IR spectra using an InSb detector. Figure 4-2 (left part) shows the appearance of a new peak at 3063 cm^{-1} arising from the shift of the 3009 cm^{-1} all-*cis* sp^2 C-H stretching vibration of the physisorbed COT monomer (spectrum 4-2(d)), by strain release in the ring-opening process. This high frequency band is totally absent in the cyclopentylidene spectrum since there are no sp^2 C-H bonds on these species, and is characteristic of *cis*-rich polyacetylenes[40,47,48], agreeing with the information extracted from the MTC region of the spectrum. This sp^2 C-H vibration mode has been already observed in the region of 3060-3090 cm^{-1} for alkylidene propagator species formed by transalkylidenation reactions between cyclopentylidene species on β-Mo_2C and simple gas-phase olefins such as ethylene, propylene and 1,3-butadiene[28,41]. It is also observed for vinyl alkylidenes formed from the dissociative adsorption of acrolein on the same surface (Figure 3-8). The lower frequency of the sp^2 C-H vibration (3009 cm^{-1}) of the adsorbed monomer on the clean surface can be explained in terms of out-of-the-plane bending of the C-H bonds of a planarized COT molecule as a consequence of the strong $4\pi\rightarrow$ interactions between the molecule and the carbide surface, as already observed for benzene adsorbed on

Pt(111)[66]. Moreover, the feature at 2880 cm^{-1} corresponding to the ν(CH) vibration of the 4 sp^3 carbons of the cyclopentylidene species seems to be narrower and more intense. The evolution of this peak could be attributed to sp^3 impurities in the polyene molecule as has been previously observed in polyacetylene[50]. Hence, by comparing the IR spectra of the activated surface after monomer insertion (spectrum 4-2(c)) with both the spectra of cyclopentylidene moieties on β-Mo_2C and the 1,3,5,7-cyclooctatetraene monomer (both in liquid/gas form and adsorbed on the same surface), we can conclude that ring opening metathesis polymerization can be carried out at cyclopentylidene initiator sites on the surface of β-Mo_2C.

Figure 4-3 shows polyacetylene spectra on β-Mo_2C formed at two different temperatures (350 and 470 K). This comparison allows us to observe a further increase in intensity of both C-C and C=C stretching vibrations at 1124 and 1675 cm^{-1} respectively, when further monomer insertion occurs at higher temperatures. The rest of the bands undergo smaller variations and no new bands appear on the spectrum. However, the growth of the C-C and C=C stretching vibration bands indicates either some change in the polymer conformation or that a further polymerisation has taken place. The incipient peak at 1120 cm^{-1}, characteristic of *cis*-rich polyacetylenes, alongside with the low intensity of the C-H out of plane bend for *trans*-rich polyacetylenes, at 1020 cm^{-1}, suggests the formation of a fair amount of *cis*-polyacetylene[40,47,48] at both temperatures. This suggestion though initially supported by the use of all *cis*-cyclooctatetraene as monomer in the reaction[29,31,32], is somehow unexpected due to the very well known tendency of free polyacetylene to isomerise towards the formation of the thermodynamically more stable *trans*-form at temperatures higher than room temperature[37,40,47,48,51]. Isomerisation seems to be somehow affected by the proximity of the metallic surface at temperatures as high as 500 K, probably due to a strong interaction between the polyacetylene chain and the surface. The fact that further polymerization takes place, suggested by the growth of both C=C and C-C stretching bands shows the living character of this reaction, characteristic of the ring opening metathesis polymerization[67-69]. This living character makes this polymerization step-controllable, a very interesting characteristic when molecular electronic applications are desired.

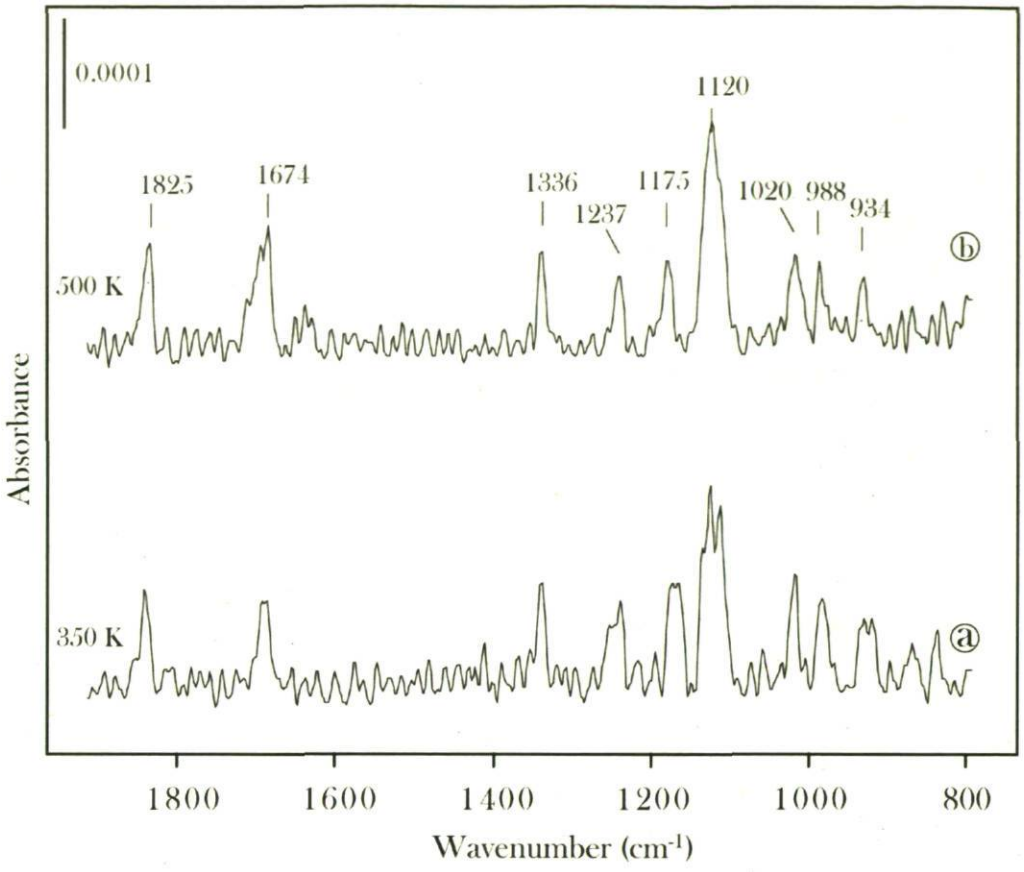

Figure 4-3 : RAIRS spectra of COT monomer insertion on a cyclopentylidene modified β-Mo_2C surface at a) 350 K and b) 500 K.

Spectrum 4-3(a) is also very relevant in order to discuss the activity of the catalytic system. This spectrum shows that polymerization reaction takes place at relatively low temperatures (350 K in this case). This fact is very interesting when taking into account practical considerations for industrial applications. Moreover, the fact that low temperature polymerization is possible shows the high reactivity of this catalytic system considering the low strain energy of the COT ring, since release of strain tension is the driving force for ring opening polymerization[70]. It is worth mentioning that previous work on metathesis reactions on the alkilydene modified surface of molybdenum carbide[28,41,43] show reactivity only over 500 K for cross-metathesis with mono-olefin molecules, and ring opening metathesis polymerization with norbornene and cyclopentene. Grubbs and co-workers[33] struggled also to form polyCOT using their 1st generation Ru catalyst, and the reaction only

took place when a more reactive 2nd generation catalyst was used. Here, the monomer-surface interaction may have a significant effect on reducing activation barriers for the reaction, favouring the reactive collision of the COT monomer with surface alkylidenes. This fact will be discussed below.

It is seen that the major absorption bands characteristic of *cis*-rich polyacetylene are present in both spectra. The wavenumbers of the major bands are summarized in Table 4-1. Also presented in the table are the band locations and assignments of the spectra observed by Shirakawa and Ikeda[40] of mixed *cis* and *trans*-PA films, as well as the observations made by Chen and co-workers[47,48] on highly oriented PA with high ratios of *cis* and *trans*-PA. It can be seen that the polyacetylene directly connected to the surface of molybdenum carbide through an alkylidene bond, obtained under ultra-high vacuum conditions from the ring opening metathesis polymerization of cyclooctatetraene, is in total agreement with previous observations in the literature on polyacetylene obtained under different conditions. This fact opens the possibility of using of conducting polymers directly bonded to the surface of technologically relevant materials for applications in molecular electronics.

Ti - $(CH)_x$ [1]	rare-earth-$(CH)_x$ [2]		highly oriented-$(CH)_x$ [3]		β-Mo_2C-$(CH)_x$	Assignment
	(high Z)	(high E)	trans $(CH)_x$	cis $(CH)_x$		
940	935 (vw)			937 (vw)	**934**	CH=CH trans in $(CH=CH)_n$ cis
980	982 (vw)				**984**	CH=CH trans in $(CH=CH)_n$ cis
1015	1013 (w)	1012,5 (s)	1014 (vs)		**1020**	CH out of plane trans
1118	1119 (m)		1108 (vvw)	1114 (m)	**1124**	(C-C) stretching
	1165 (w)		1170 (vvw)		**1174**	C-C, C-O (oxidative degradation)
1249	1247 (w)	1247 (w)	1248 (w)	1246 (m)	**1240**	-
	1253 (w)			1256 (w)		CH in plane def. cis
1292		1295 (w)	1293 (w)			CH in plane def. trans
1329	1329,2(s)			1328 (s)	**1336**	CH in plane def. cis
1690	1686,5(m)		1672 (vw)	1689 (sh)	**1675**	(C=C) stretching
1800	1802,6(m)		1720(mw)		**1800**	1336 + 438 cis
			2884 (vw)		**2880-90**	υ_s(CH) sp^3 trans
			2980 (sh)		**2961**	υ_{as}(CH) sp^3 trans
3013		3013,1 (s)	3011 (s)		**3033**	CH stretching trans
3044	3044,5(m)			3044 (m)	**3055**	CH stretching cis
3057	3057 (w)				**3063-69**	CH stretching cis

Table 4-1 : IR spectra assignment for polyacetylene synthesized from 1) a Ti-based catalyst[40]; 2) a rare-earth-based catalyst[47,48]; 3) highly oriented polyacetylene[50]; and 4) on alkylidene-modified molybdenum carbide.

Further analysis can be done of the structure of the polyene molecules obtained by taking a closer look to the assignment of the CH region spectra obtained with the InSb detector. By comparison we can distinguish the appearance of a single and very narrow band at 3065 cm^{-1} assigned to a *cis*-PA C-H sp^2 stretching vibration[40,47,48], also observed in a 1,3-propylidiene[41] species obtained by the cross metathesis reaction between a cyclopentylidene modified surface and 1,3-butadiene (spectrum 4-4(b)), as a wider band with two peaks at 3061 and 3087 cm^{-1}. Therefore the presence of a single high frequency band supports the observations made using the MCT spectra of the presence of mostly *cis*-PA, whereas the wider band of spectrum 4-4(b) suggests the presence of an unresolved mixture of both conformers, alongside with the presence of methylidene species also obtained in the cross metathesis reaction, which typically displays a very high frequency C-

H stretching vibration (~3080 cm^{-1})[28,41]. The short *trans* and *cis* segment C-H stretching vibrations are of quite high frequency in the case of vinylene species on the surface of molybdenum carbide. These bands have been observed around 3013 cm^{-1} for *trans*-polyacetylenes, and 3044 cm^{-1} for short *cis* segments in mostly mixed polyacetylenes, but is in clear agreement with previously reported short alkylidenes with sp^2 C-H bonds on β-Mo_2C. The high frequency of these peaks could be explained in terms of the strong interaction of the surface metal electronic states with the π system of the molecule[26,71].

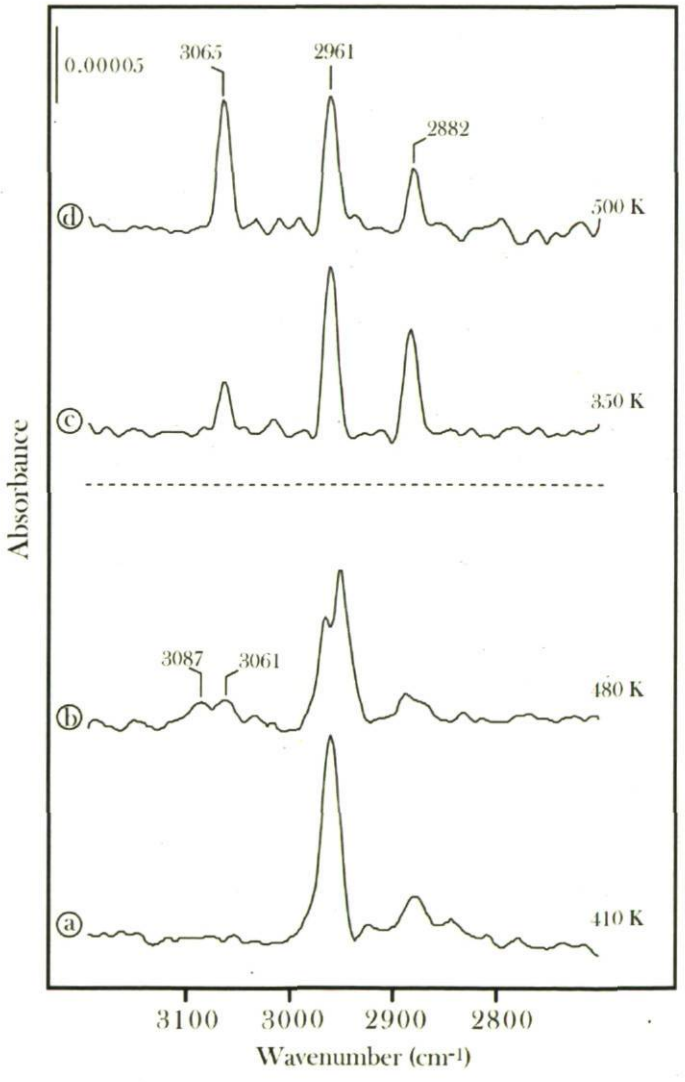

Figure 4-4 : RAIRS spectra in the ν(CH) region for COT monomer insertion at a cyclopentylidene modified β-Mo_2C surface at c) 350 K and d) 500 K, compared with spectra of a) cyclopentylidene species, and b) species formed by the cross metathesis reaction between cyclopentylidenes and 1,3-butadiene.

The high frequency of the 3065 cm^{-1} band may indicate a certain mixture of *cisoid* and *transoid* segments of the polyacetylene chain. It's well known that short *cis* segments between two *trans* segments of PA may cause a higher frequency peak than long ones (3057 *vs* 3044 cm^{-1} in the literature)[40,47,48]. However, no significant amount of *trans*-PA has been recorded as shown by the absence of the lower frequency peak (3013 cm^{-1}) typical of the *trans*-polyacetylene C-H sp^2 stretching vibration. It has to be taken in consideration that it is difficult to establish whether the surface has a strong contribution to the shifts of these peaks due to interactions between the surface and the polymer backbone. What seems clear is that the surface may have some kind of interaction that disallows thermal isomerisation from happening over 350 K since no *trans* C-H, or short length *cis* C-H stretching vibration are detected.

4.2.2 XPS characterization

Monomer insertion of 1,3,5,7-cyclooctatetraene through ring opening metathesis reaction on cyclopentylidene moieties on β-Mo_2C was also monitored by X-ray photoelectron spectroscopy. Spectrum 4-5(a) shows the C(1s) data after cyclopentylidene moieties have been formed. In it we can distinguish four peaks. The first two at energies of 282.8 and 283.4 eV are assigned to the surface carbidic atoms and to C deposition on the surface during the alkylidene formation via molecular cracking. This deposition of essentially undefined carbon species on the surface has been observed in a number of studies on molybdenum carbide[42,59,72]. The two other peaks are due to molecular species, notably the four sp^3 carbons of the C_5 cycle, and the disubstituted sp^2 carbon bonded to the surface, the alkylidene carbon. The relative intensities of the peaks at 284.8 and 285.8 eV is 4:1 as expected for a C_5 group containing 4 sp^3 and 1 sp^2 carbons.

As we can see in Figure 4-5(b), the C(1s) spectrum a new peak grows in at 284.3 eV after annealing to 350 K when COT is introduced in the presence of Mo=C active sites. The appearance of this incipient peak at 284.3 eV reveals the appearance of new C sp^2 species different from those directly bonded to the surface when COT is introduced and the system is annealed to 350 K.

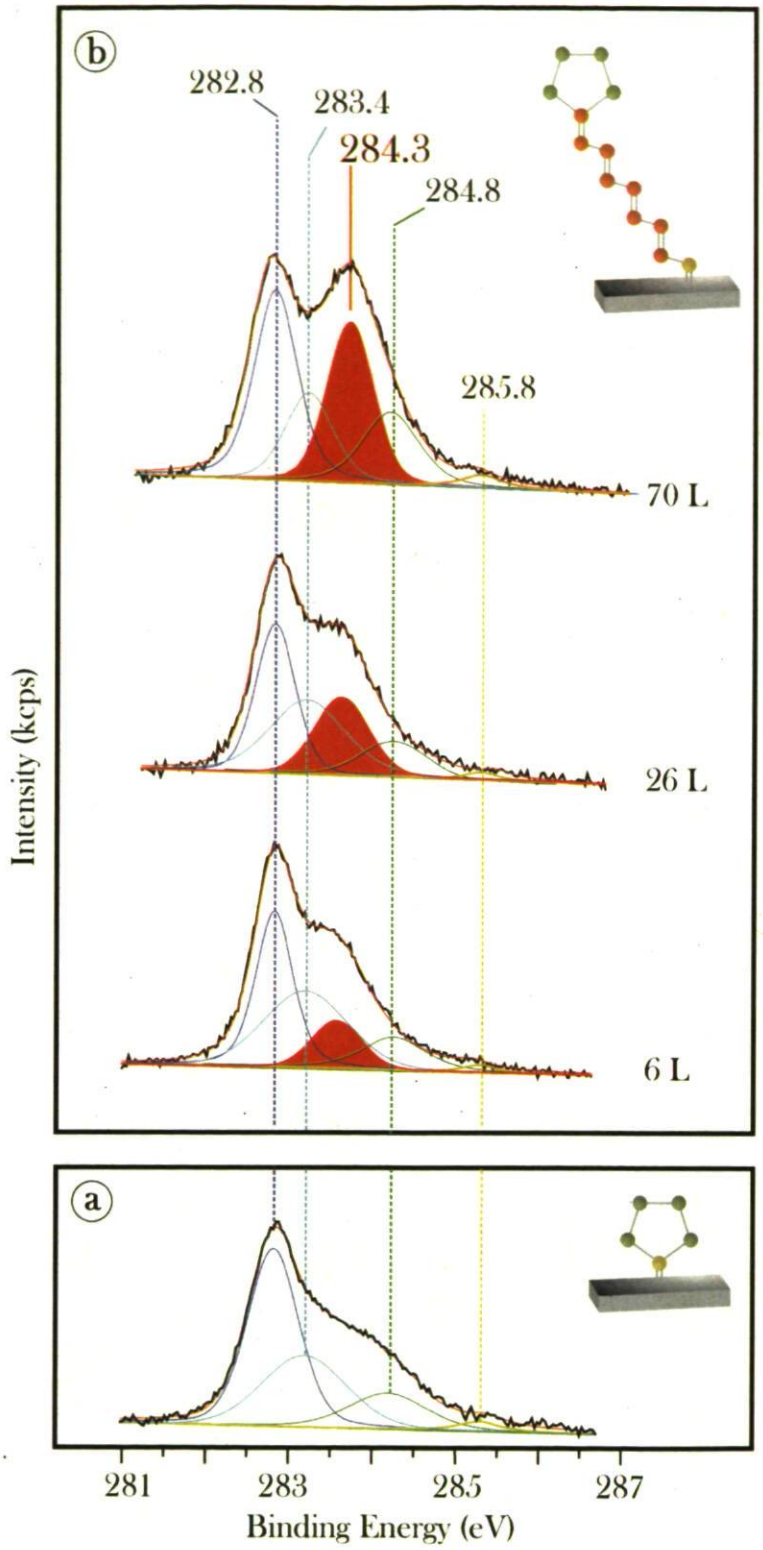

Figure 4-5 : XPS spectra a) cyclopentylidene species; b) COT insertion as a function of exposure at 350 K.

This new peak at 284.3 eV grows when further monomer is introduced step by step, as would be expected in a living polymerization process such as ring opening metathesis polymerization, and can be attributed to the sp^2 carbon backbone of newly formed polyene chains. The assignment of this C sp^2 peak at 284.3 eV, as due to monomer insertion, is well supported in the literature. Notably, Rochet et al.[73] have assigned a peak in the C(1s) region at ~284.7 eV to a multilayer of cyclooctatetraene adsorbed on Si(001) at 300 K by photoelectron spectroscopy (PES) using synchrotron radiation. Freyer et al.[74] detected a signal centred at 284.3 eV when ethylene was deposited on Pt(111) at 100 K.

Figure 4-6 monitors the area evolution of this new peak at 284.3 eV compared to the amount of alkylidene species (285.8 eV) on the surface, as a function of the exposure of monomer at 350 K. The shape of this curve reveals that in the early stages of monomer introduction the rate of formation of new sp^2 carbon is considerably higher than in the later stages. This behaviour has already been observed for homogeneously catalyzed formation of polyacetylene from ROMP of cyclooctatetraene[29] suggesting that the same mechanism is occurring for both catalytic systems.

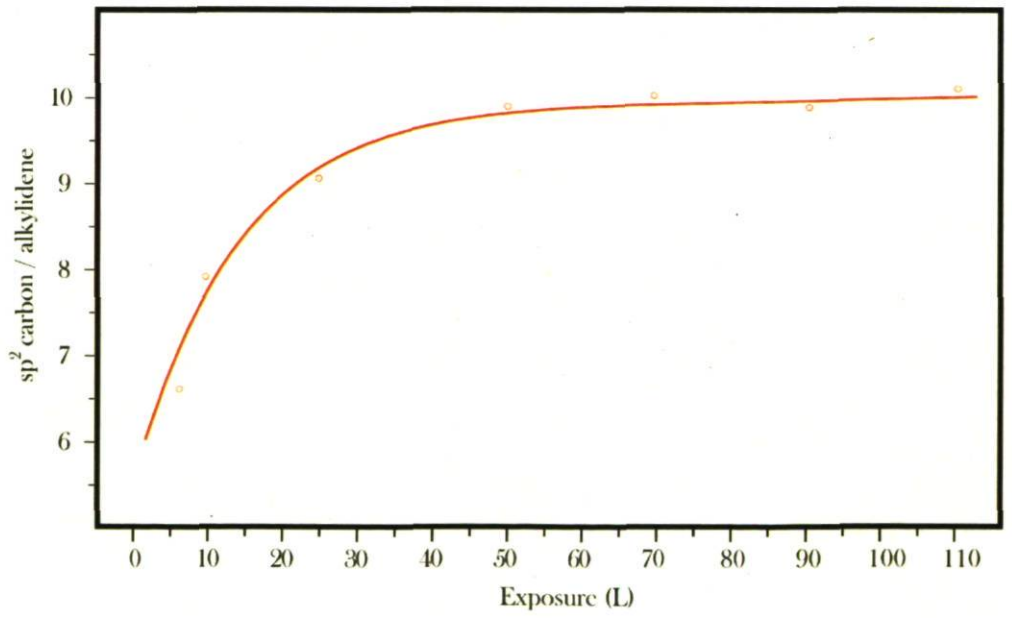

Figure 4-6 : Plot of the proportion of olefinic carbons (284.3 eV) with respect of the amount of alkylidene species (285.8 eV) on the surface as a function of monomer exposure at 350 K.

Figure 4-6 provides extra quantitative information about monomer insertion. By comparing the new peak at 284.3 eV with the alkylidene peak at 285.8 eV, which remains constant with time, we can quantify the evolution of this conjugated olefinic carbon species to a maximum of ~10 times the amount of alkylidene species. Considering that every monomer insertion adds 8 sp^2 carbons to the surface, the fact that 10 of these sp^2 atoms are detected per alkylidene suggests that more than one monomer molecule on average has been inserted per active site. This observation however has to be taken carefully, since it does not mean that each cyclopentylidene site undergoes monomer insertion, but refers to average measurements. Although ROMP is well known to produce polymers with polydispersities very close to 1, a possible effect of the surface in this aspect cannot be neglected. RAIRS observations appear to support the idea that polyacetylene molecules with lengths close to 8 carbon atoms are formed regarding the already discussed high frequency of the C=C stretching vibration. These data suggest not only that metal-alkylidenes can perform ring opening metathesis polymerization of cyclooctatetraene at temperatures close to room temperature, but multiple turnovers could be achieved by this catalytic system, as observed in previous studies of cross metathesis reactions[41].

Figure 4-7 sheds light on the question as to whether this peak is indeed due to the additional carbon arising from polymer formation and not due to simply monomer deposition on the surface, since the carbon atoms of the cyclic monomer should be of the same binding energy as those of the polymer. In this figure we can see the evolution of the C(1s) region of the XPS spectrum when monomer is introduced at different temperatures in the absence of the alkylidene active sites. All spectra were taken with intervals of 1 minute while the pressure in the chamber was maintained at $5x10^{-8}$ Torr.

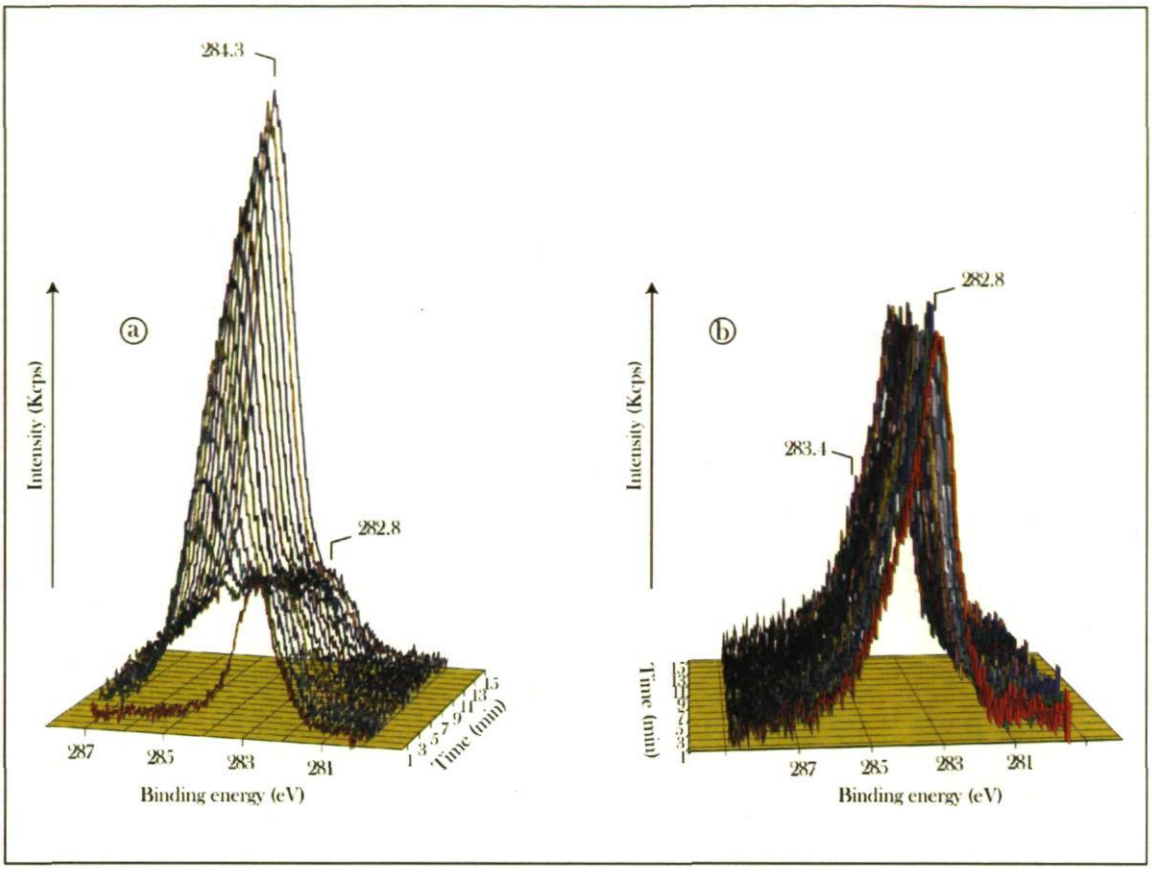

Figure 4-7 : XPS spectra of COT introduction on a clean surface as a function of coverage at a) 100 K and b) 300 K.

We can observe in spectrum 4-7(a), the formation of a multilayer of COT at 100 K characterized by the appearance and further evolution of a peak at 284.3 eV as a function of the coverage. This peak corresponds to the 8 sp^2 carbons of the cyclic molecule. This result is in complete agreement with the previous assignment of this region since only two carbon species are expected and both of them appear in the COT multilayer, the inorganic carbon of the metal-carbide surface with a disappearing peak at 282.8 eV as a consequence of the masking effect caused by the incipient molecular multilayer, and the already discussed molecular sp^2 carbon of the cycle. Figure 4-7(b) displays the same experiment repeated at 300 K, and reveals that no new peak develops in the region around 284 eV, only a small shoulder at 283.4 eV is observed due to molecular decomposition of the COT molecule. Spectrum 4-7(b) confirms that no deposition of COT occurs on the surface at temperatures above 150 K, contrary to the monomer behaviour at lower temperatures where we can see a

multilayer formation. This absence of monomer accumulation shows that the new peak observed in the C(1s) region of the XPS spectrum at 300 K as a function of monomer introduction when alkylidene species are present in the surface (Spectra 4-5 (b)) is, as suggested above, due to the formation of polyacetylene through ring opening metathesis polymerization, and not to monomer stacking.

The monitoring of the reduction in intensity of the molybdenum ($3d_{3/2 + 5/2}$) peak (doublet at 227.8 and 230.7 eV) under monomer introduction is another way of following the reaction in real-time. We can clearly see in Figure 4-8 that the area of this peak decreases more rapidly on the early stages under COT introduction at 300 K when cyclopentylidene species are present on the surface (red line), compared with the same conditions in the absence of cyclopentylidenes (black line). In this case, we can observe a sharp drop in the Mo(3d) signal, due to the already discussed carbon deposition, from molecular decomposition, on the surface leading to a peak at 283.4 eV (Figure 4-5). There is however, a sharper drop of the signal when alkylidenes are present on the surface (red line) caused mostly by the formation of the polymer. In this case due to previously deposited carbon on the surface, caused by partial decomposition of cyclopentanone, COT decomposition is expected to happen in a very small proportion, since the surface has already been partially deactivated, as the relative intensities of the first peaks of both curves may indicate. It is clearly seen that the intensity of the Mo(3d) peak for the first peak of the red series is much lower than the first of the black one, indicating that at that point of the experiment molybdenum atoms on the surface are already covered by carbon through thermal decomposition of cyclopentanone.

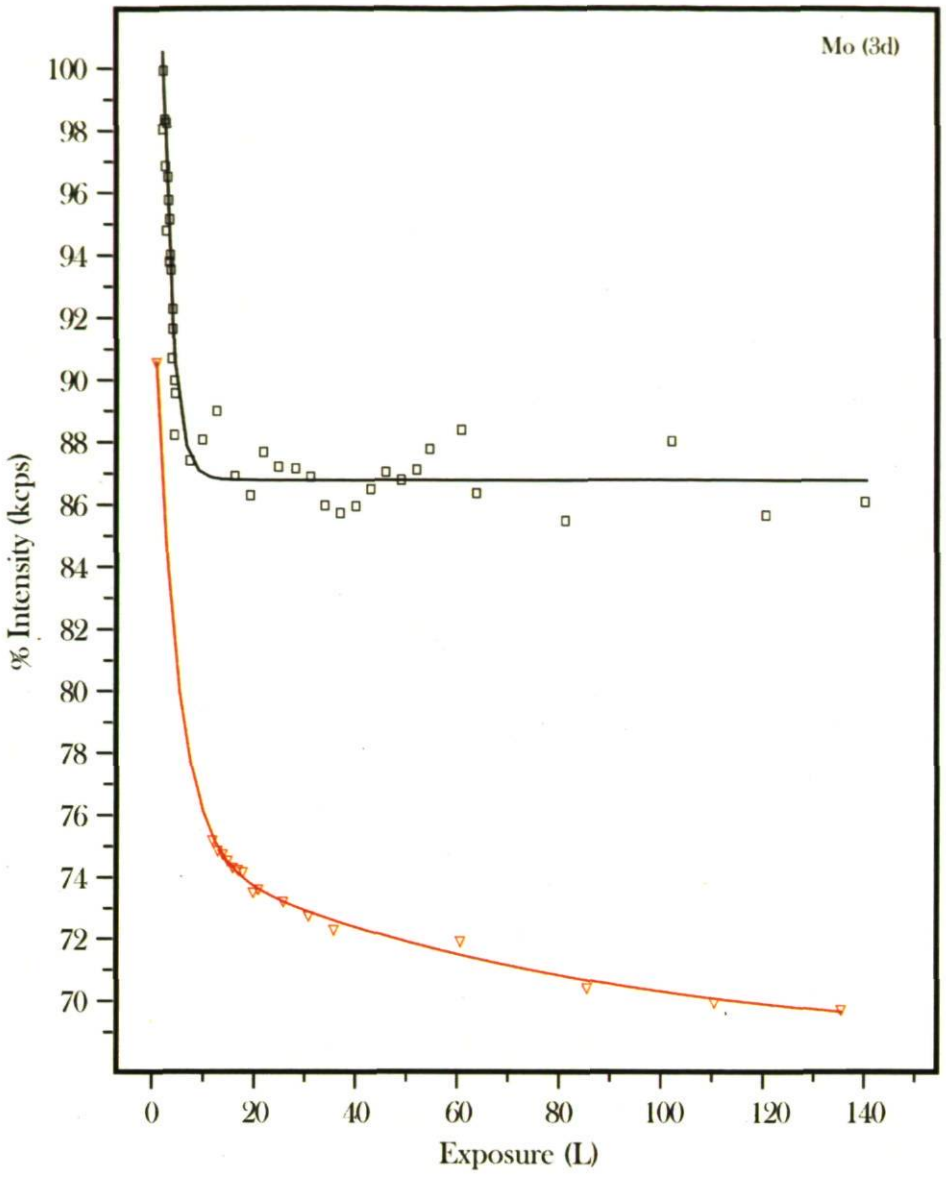

Figure 4-8 : Relative Mo(3d) intensities for two different treatments of the surface. The black line corresponds to COT deposition on a clean surface. The red line corresponds to monomer insertion on a cyclopentylidene modified surface. Both series were recorded at $5x10^{-9}$ Torr and 350 K.

This early stage of the introduction of monomer when cyclopentylidenes are on the surface shows that more carbon is being placed over the molybdenum atoms despite the fact that the surface is already passivated through partial thermal decomposition of cyclopentanone molecules, leaving polymerization as the only plausible explanation for the

decrease in Mo(3d) intensity. Following a rapid decrease of the intensity in both experiments, the Mo(3d) peak then remains constant in the case of monomer introduction to a clean surface, although more monomer is introduced (black line). In contrast, the attenuation of the Mo(3d) signal continues in the presence of active sites on the surface (red line), though now slower as in the case of the increase of the polyacetylene sp^2 backbone carbon peak. Thus, the evolution of the Mo(3d) spectrum matches the behaviour of the surface carbidic C(1s) peak (282.8 eV) presented in Figure 4-5b.

4.2.3 Absence of polyacetylene oxidation

As outlined before, there are still some disagreements and differences in the IR and Raman characterization of polyacetylene, especially concerning the C=C stretching vibration. In regards to the region in which this peak is expected, some groups have assigned a peak around 1670 cm^{-1} to the oxidation of polyacetylene (PA) chains exposed to air. Will and co-workers[51] have assigned this band to C=O stretching vibrations in α,β-unsaturated ketones on highly oxidized (over 2,5% O) PA powders. Piaggio et al.[50] were less specific when assigning as impurities and different oxidation states a series of peaks between 1494 and 1775 cm^{-1} in polarized IR spectra of highly stretched *trans* polyacetylene samples. Chen et al.[47] assigned a peak at 1720 cm^{-1} to a ν(C=O) vibration when polymerizing acetylene using a coordination catalyst solution of neodymium naphthenate/triisobutyl aluminium in toluene.

No C-O bond whatsoever has been found in the polyacetylene formed from ring opening metathesis polymerization of cyclooctatetraene under UHV conditions. Such a bond could possibly arise because oxygen is deposited onto the surface during the alkylidene preparation process[42,60,61,75,76]. As shown in Figure 4-9(a) there is an absence of a signal for a carbonyl carbon in the C(1s) region when polymerization occurs, in contrast with a very intense peak at 288.2 eV when cyclopentanone is adsorbed on the surface at low temperature (green spectrum). This peak corresponding to the carbonyl group of the ketone is in a 1:4 proportion to the peak at 285.3 eV corresponding to the other 4 sp^3 carbon atoms of the C_5 ring. Note that the peak of the surface carbidic C at 282.8 eV is highly

masked by the cyclopentanone multilayer. However, no peak arising from a C-O bond is observed after annealing cyclopentanone over 300 K (blue spectrum). At the same time, a series of peaks arise in the 284-285 eV range corresponding to the deposition of graphitic C on the surface, and molecular sp^3 C from the 5-membered cycle. Once the polymerization is initiated (black spectrum), there is still a total absence of any peak above 285 eV, indicating that despite the formation of PA, no C=O species has been formed.

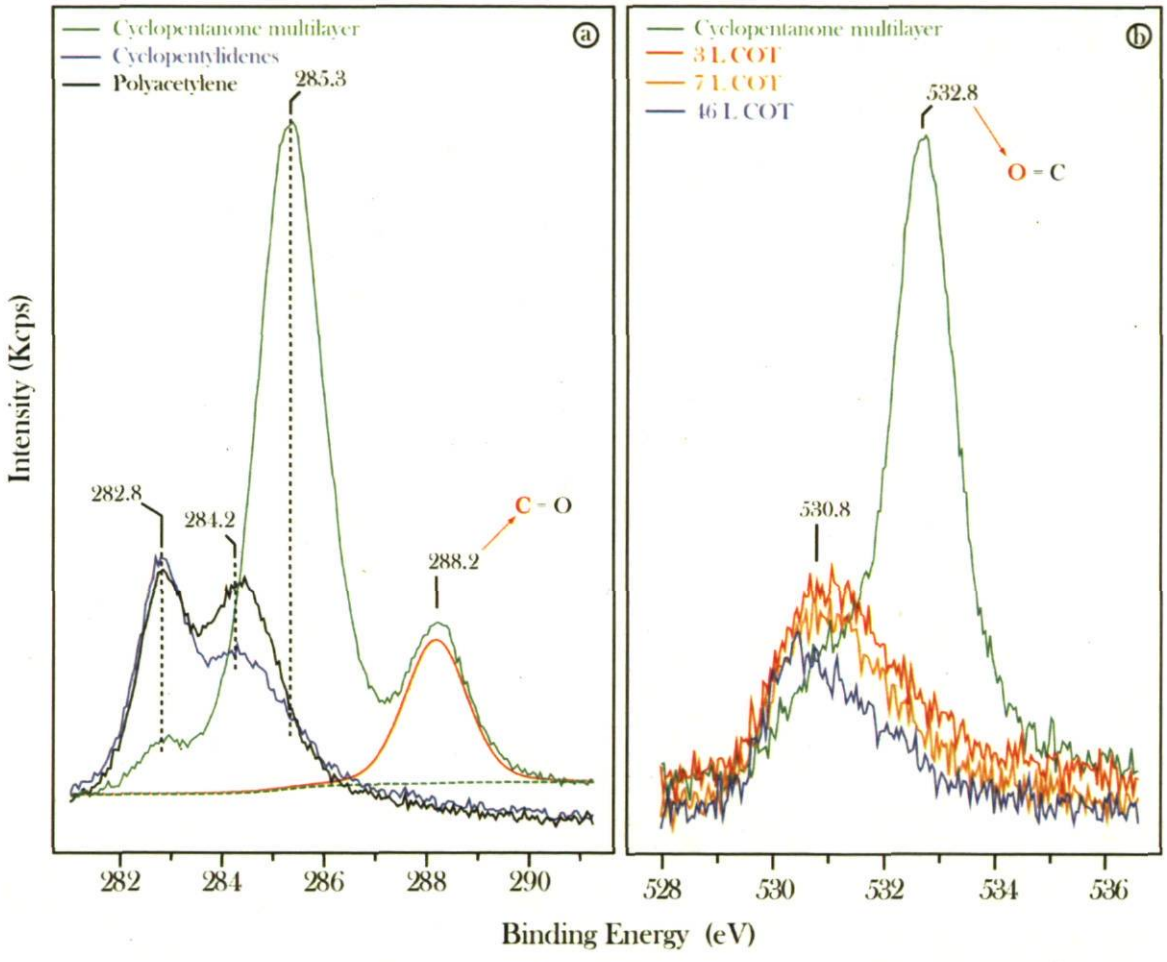

Figure 4-9 : XPS spectra of the a) C(1s) region of the multilayer of cyclopentanone (green), cyclopentylidene (blue) and polyacetylene (black); b) O(1s) region of cyclopentanone (green) and polyacetylene formed by the insertion of different amounts of monomer (COT).

Figure 4-9(b) displays the O(1s) region of the XPS spectra. The cyclopentanone multilayer spectrum (green) is characterized by an intense molecular oxygen peak

appearing at 532.8 eV and a smaller peak appearing as a shoulder at 530.8 eV. This latter peak has already been observed in previous studies carried in this surface and has been attributed to an inorganic surface oxo (Mo=O) species[42,59-61,72,75,76]. The molecular oxygen peak disappears when cyclopentylidene is formed by carbonyl bond scission, at the same time that a rise of the peak at 530.8 eV occurs, due to the conversion into surface atomic oxygen due to the oxophilicity of molybdenum. No molecular oxygen, however, is observed in the polyacetylene spectra at any level. The weak peak from atomic oxygen decreases its intensity as polymerization takes place, indicating that O stays at the surface or subsurface and is being masked by the polymer. In addition no oxygenated products have ever been reported for any metathesis reaction on β-Mo_2C at temperatures below 900 K under ultrahigh vacuum conditions[28,41,43]. These XPS observations, as well as the assumption that ideal conditions are achieved under UHV agree with the IR data concerning the absence of oxidized states of polyacetylene, and it confirms the assignment of the peak at 1675 cm^{-1} as ν(C=C).

4.3 Vinyl alkylidene modified surface

As discussed above, despite its apparent simplicity polyacetylene is a rather complex molecule. The interpretation of spectroscopic results for this conjugated polymer proved to be difficult because no 100% crystalline structures have been obtained. Furthermore, inhomogeneities caused by strongly varying degrees of polymerization, and various other defects such as crosslinks, sp^3 impurities, *cis-trans* isomerism, and conformational disorder, complicate the issue severely[35,37,40,47,48,50,51].

In order to help with characterisation of polyacetylene formed from the alkylidene-modified molybdenum carbide catalytic system, the substitution of cyclopentylidene active species by vinyl alkylidenes has been attempted. This strategy would in principle yield to a pure conjugated chain from the surface, instead of carrying the C_5 cycle all throughout the reaction. The cyclopentyl end of the polyene chain obtained through the use of cyclopentanone as starting material to create the active sites on the surface of molybdenum carbide can complicate the characterization, as well as somehow interfere in the reactivity

by steric hindrance at the surface active sites. Thus pure polyene chains are suitable both for easier and better characterization as well as for conformational studies. The vinyl alkylidene species on the surface of the metallic carbide could provide, at the same time, another model to compare polyacetylene, being itself a short oligoene with three carbons and two double bonds linked directly to the surface. The characterization of these species could be used as a reference to identify and assign vibrational modes in the RAIRS spectra of polyCOT, and as an aid in interpreting the C(1s) data.

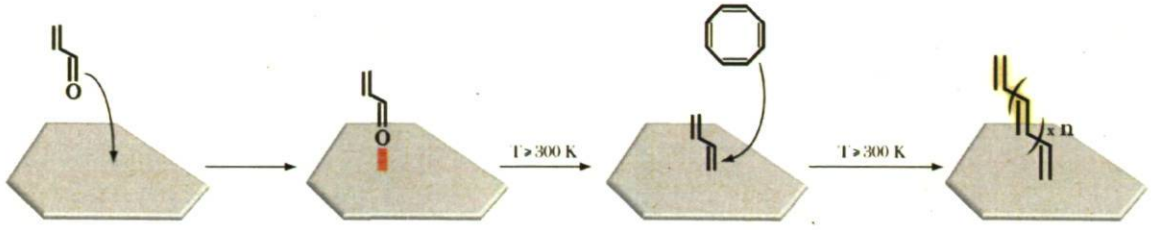

Scheme 4-3 : Formation of polyCOT using vinyl alkylidene species as initiator sites.

The formation of vinyl alkylidene species on the surface of molybdenum carbide was achieved through the dissociative adsorption of acrolein (acrylaldehyde) on the same bulk β-Mo_2C sample, under UHV conditions. The characterization of the surface-vinyl alkylidene species was extensively discussed in Chapter 3, and here it will be compared to polyacetylene spectra formed from both cyclopentylidene and from the vinyl alkylidene species itself, as well as to vinyl alkylidene species formed from the cross metathesis reaction of 1,3-butadiene with surface cyclopentylidene species.

4.3.1 IR characterization

IR spectroscopy of the C-H stretching region of vinyl alkylidene species formed by the dissociative adsorption of acrolein (spectrum 4-10(a)) show a sharp peak at 3075 cm^{-1} characteristic of a sp^2 C-H bond, as already discussed above. The proximity of the surface may explain the high frequency of this band, observed between 3030 and 3065 cm^{-1} for liquid and gas-phase acrolein[77]. This behaviour is also observed for the vinyl alkylidene

species formed from cross metathesis using the reaction of 1,3-butadiene with cyclopentylidene species as active sites on the surface of molybdenum carbide[41] (spectrum 4-10(c)). Acrolein is however, essentially *transoid* and thus, the observed high frequency peak at 3075 cm^{-1} is due to the *trans* sp^2 C-H bond, whereas for the case of cross metathesis production of vinyl alkylidene species, both *cis* and *trans* isomers are expected. This reaction will also produce surface methylidene species (Scheme 4-4), and the mixture of products may be the responsible for the broad band produced in this spectrum. The doublet at 3087 and 3061 cm^{-1} may then be assigned to *cis* and *trans* vinyl alkylidene species, following the same reasoning used above.

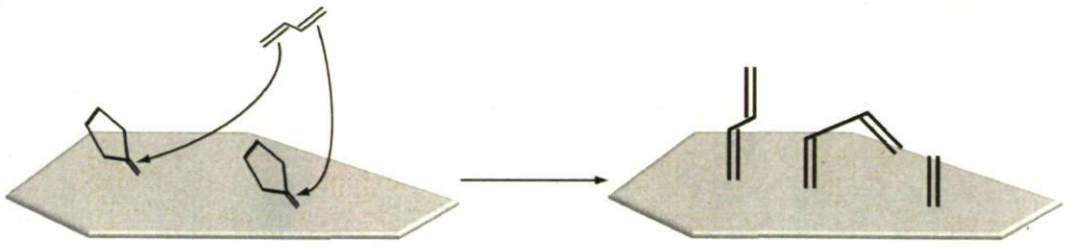

Scheme 4-4 : Cross metathesis between cyclopentylidene modified molybdenum carbide and 1,3-butadiene.

The IR spectrum of polyene species obtained from the ring opening metathesis polymerization of cyclooctatetraene with vinyl alkylidene species on β-Mo_2C (spectrum 4-10(c) shows a very sharp and very intense doublet at 3064 and 3033 cm^{-1}. The evolution of the sp^2 C-H bond of the original *trans*-vinyl alkylidene species observed at 3075 cm^{-1} shifts to significantly lower frequencies (3033 cm^{-1}) suggesting the evolution of this *trans* segments away from the surface. The appearance of the new peak at 3064 cm^{-1}, more characteristic of *cis*-polyacetylene, indicates the development of a vinyl chain with a configuration different from the initial *trans* configuration of the vinyl alkylidene species, matching the position of the peak observed for polyacetylene formed on cyclopentylidene active sites, and assigned to *cis* segments of the conjugated chain. The assignment of this peak is in agreement, as discussed above, with the fact that poly-cyclooctatetraene is expected to be formed initially in mostly a *cis*-configuration when thermal isomerisation does not take place. It may be tempting to compare quantitatively the height of both peaks

for the sp^2 C-H bonds corresponding to the two isomers. However, it should be kept in mind that due to the selection rule for RAIRS the intensity of the peak does not necessarily scale with the species population.

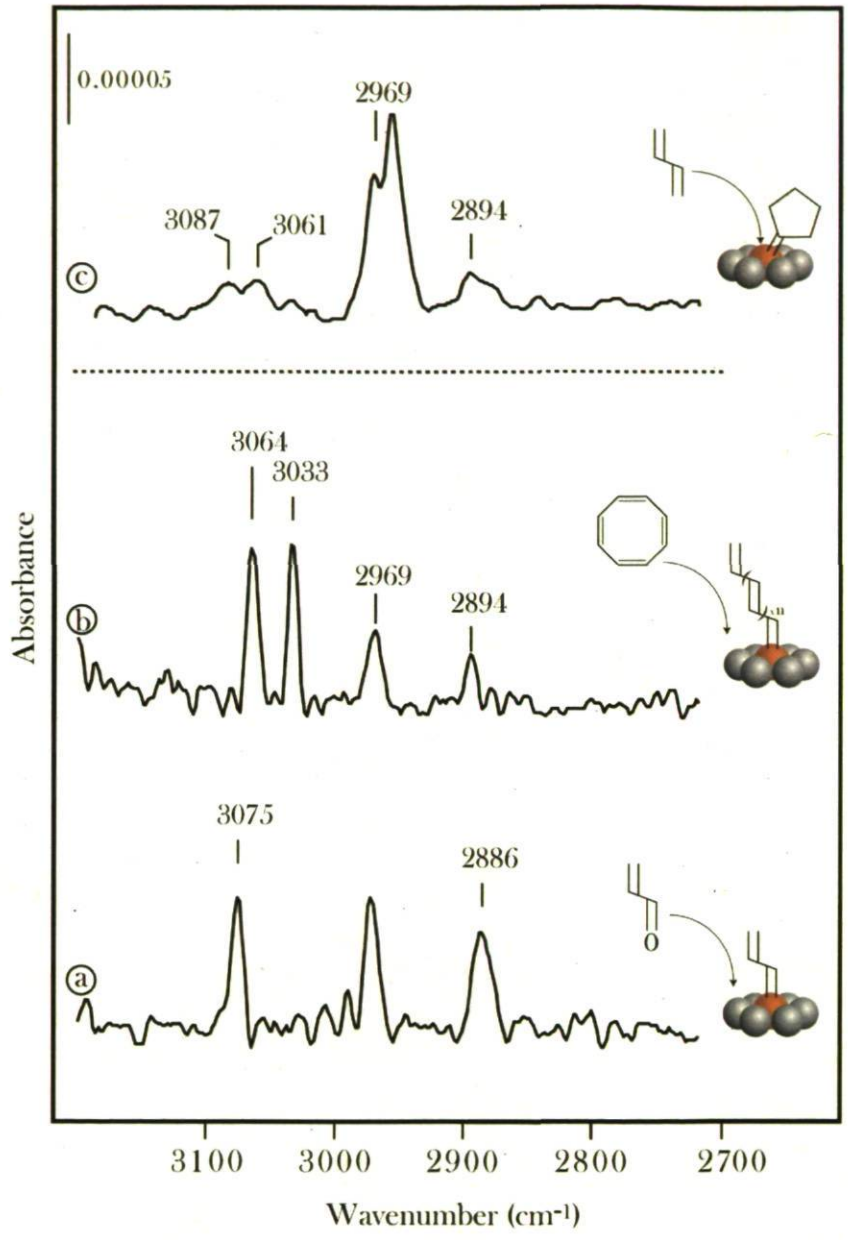

Figure 4-10 : Infrared spectra in the C-H region of a) vinyl alkylidene moieties formed from the dissociative adsorption of acrolein on the surface; b) polyCOT formed from these active species, and c) vinyl alkylidene moieties formed from cross metathesis of cyclopentylidene species and 1,3-butadiene.

An evident difference, concerning the sp^2 C-H band, between the polyCOT spectra derived from cyclopentylidene and vinyl alkylidene species can be observed in Figure 4-11. Spectrum 4-11(a) reveals a double peak at 3033 and 3064 cm^{-1} for this stretching vibration in the vinyl alkylidene initiated polyacetylene, whereas the cyclopentyl alkylidene initiated polyacetylene presents a single peak at 3065 cm^{-1} (spectrum 4-11(b)). The other two peaks of the spectra at ~2960 and ~2890 cm^{-1}, attributed to the $\nu_{as}(CH_2)$ and $\nu_s(CH_2)$ vibrations[28,41-43,60-62], suffer few variations. These two bands are present in polyacetylene formed using vinyl alkylidene as initiator sites due to the CH_2 end group, as well as in sp^3 impurities as discussed above, whereas the 4 sp^3 carbons of the cyclopentyl group, as well as any sp^3 impurities of the polymeric chain, are the responsible for these bands in spectrum 4-11(b).

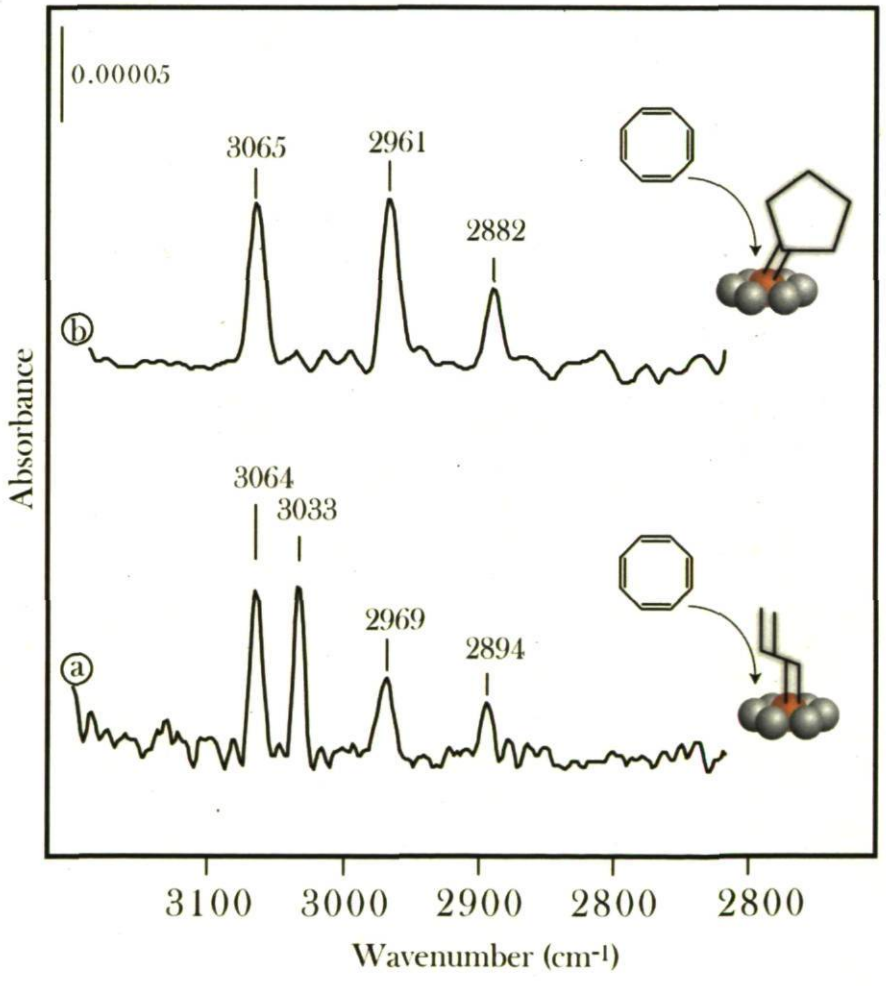

Figure 4-11 : RAIRS spectra in the C-H stretching region for polyacetylene formed at 350 K from a) vinyl alkylidene and b) cyclopentylidene species on β-Mo_2C.

Variations in the sp^2 C-H band must be of a different nature than that for the CH_2 stretching vibrations, since this band arises from the backbone of the polymeric chain, and thus, in principle there should be no difference between both spectra. However, as discussed above, the sp^2 C-H stretching vibration is conformationally sensitive for polyene molecules, a fact that has been extensively reported in the literature[40,47,48,51]. These observations seem then to point to a difference in the conformation between both polyacetylene chains, possibly caused by a difference in the surroundings of the active sites, either electronic or steric, which could induce to a difference in reactivity and thus differences in the conformation of the polyacetylene formed. This phenomenon should however require an extensive study to clarify the nature of this difference in the reactivity of both alkylidene species, and in the conformation of the polyacetylene formed.

4.3.2 XPS characterization

Figure 4-12 displays the evolution of the C(1s) region of the XPS spectra during polymerization as a function of monomer introduction. All spectra are subtracted to the spectrum of vinyl alkylidene moieties prior to reaction, and show the development of the polyacetylene chain on the surface. The spectra in Figure 4-12 show the evolution of a peak at a binding energy of 284.3 eV, corresponding to the accumulation of sp^2 C species on the surface. This evolution has already been observed in the case of the SI-ROMP of COT using cyclopentylidene moieties as active sites, and has been discussed above (Section 4.2.2).

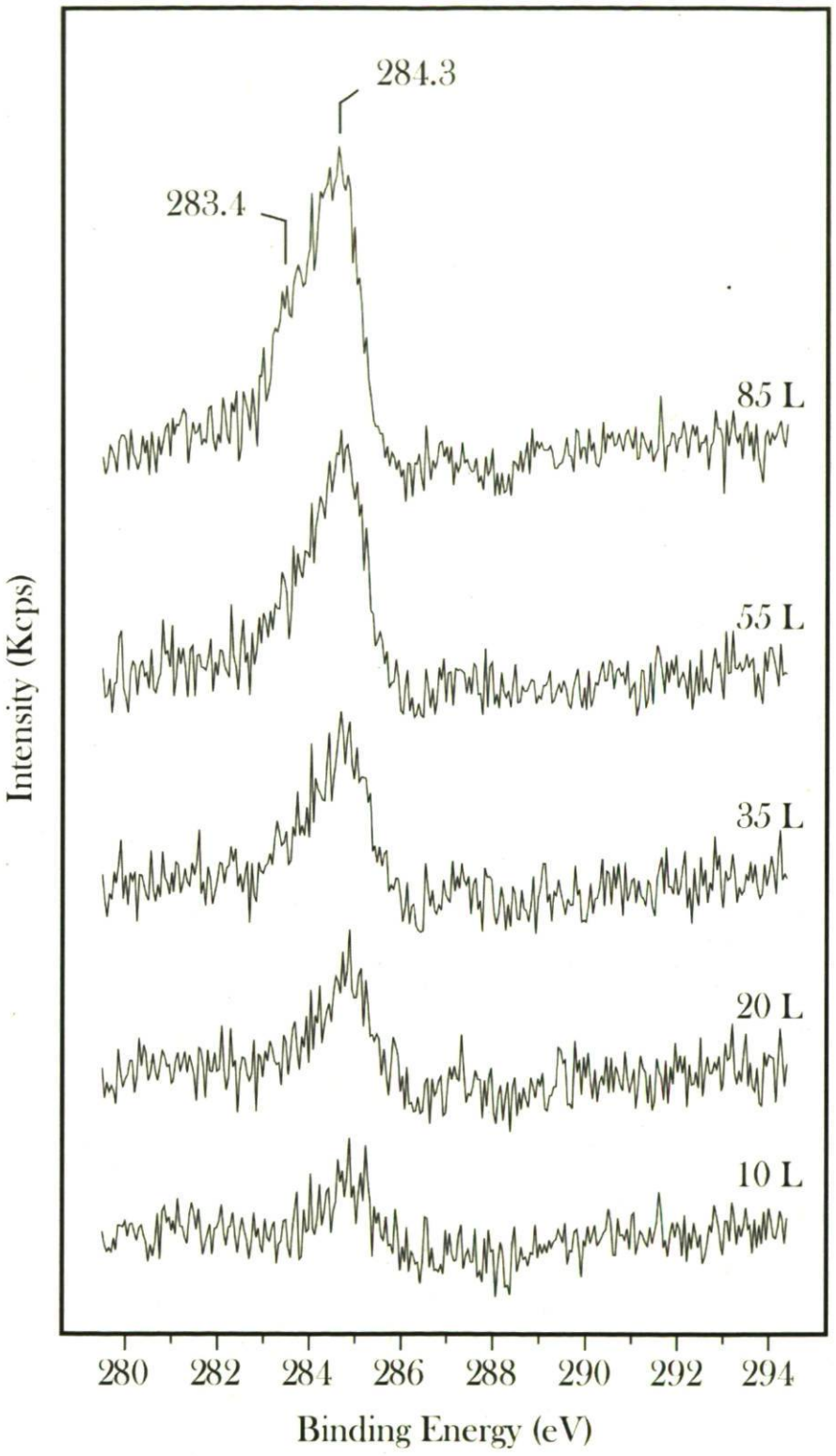

Figure 4-12 : C(1s) spectra of the polymerization of COT on a vinyl alkylidene modified surface of molybdenum carbide as a function of monomer introduction at 300 K.

Alongside with the appearance of the peak at 284.3 eV there is the development of a shoulder at 283.4 eV. This peak has been observed in all XPS studies of the C(1s) region of this material, and has been assigned to an excess of carbon due to molecular decomposition[42,59,60]. This differs from data obtained for polymerization of COT using surface cyclopentylidene as initiators in that no growth of the 283.4 eV peak was observed. In the case of the cyclopentylidene initiated reaction, this peak reaches saturation after the formation of the initiator sites, and no further growth of this peak is observed during monomer insertion, whereas when acrolein is used to form vinyl alkylidene moieties less molecular decomposition seems to occur, and thus the surface is not fully deactivated through molecular cracking, which appears to occur to the molecules of cyclooctatetraene as they are adsorbed on the surface. This behaviour is also observed when COT is introduced into the chamber over 200 K in absence of initiator sites (Figure 4-7(b)). There we can see that after a period of development this peak saturates once the surface deactivates itself by deposition of excess of carbon. As we can observe in Figure 4-12, although there appears to be a competition between both polymerization and monomer decomposition, the polymerization seems to prevail. This fact suggests that even if it is in less proportion than for cyclopentanone, the introduction of acrolein and further annealing of the surface passivates the surface to a certain degree, and thus when monomer is added, the principal reaction taking place is the ring opening metathesis polymerization.

4.4 Halogenation of polyacetylene

4.4.1 Cyclopentylidene terminated polyacetylene

The synthesis and study of metallic covalent polymers such as polyacetylene has known considerable interest for a long time. Combinations of experimental observations on relatively short oligoenes, and theoretical studies have been appearing since the 1930s[78-82]. These early studies expected infinitely long one-dimensional π electron systems to form a half filled band, due to the overlap of the HOMO and LUMO orbitals, leading to metallic behaviour. However, when Natta and co-workers[83] first synthesized polyacetylene in 1958

it was found to be a non-conducting black powder from which it was very difficult to make specimens in a shape suitable for spectroscopic measurements of various properties because of its insolubility and infusibility. This fact made the subject unattractive for some time. The discovery made by Ikeda and co-workers[40] of a way to synthesize polyacetylene directly in the form of thin films made it suitable for spectroscopic studies. However, the electrical resistivity of films obtained by the so-called Shirakawa method were very poor (comparable of those obtained with the Natta powder)[37]. It was not until the well known meeting between Shirakawa, Heeger, and MacDiarmid, that the synthesis of electrically conducting organic polymers was achieved[38]. Those were halogen deriatives of polyacetylene with electric conductivities up to seven orders of magnitude higher than that of polyacetylene. These doped polyacetylenes have conductivities as high as 560 $\Omega^{-1}cm^{-1}$, and opened a new era of conducting polymers. This achievement was recognized by the award of the Nobel Prize 2000 to Shirakawa, MacDiarmid and Heeger.

However, the use of halogens on polyacetylene did not start with the intention of doping this molecular semiconductor. Ikeda and co-workers[37], after realizing that their polyacetylene films didn't show any improvement in electrical conductivity, tried to convert them to graphite, first by heating the films, and then by a combination of electrophilic addition of halogens such as chlorine and bromine at mild conditions and elimination of hydrogen halide from adjacent carbon atoms in the halogenated polyacetylene.

The halogenation of polyacetylene under UHV conditions and its characterization by XPS were attempted in order to add more proof of its synthesis by surface initiated ring opening metathesis polymerization at alkylidene sites of β-Mo_2C by detecting organic Br species on the surface after bromination of the conjugated molecules.

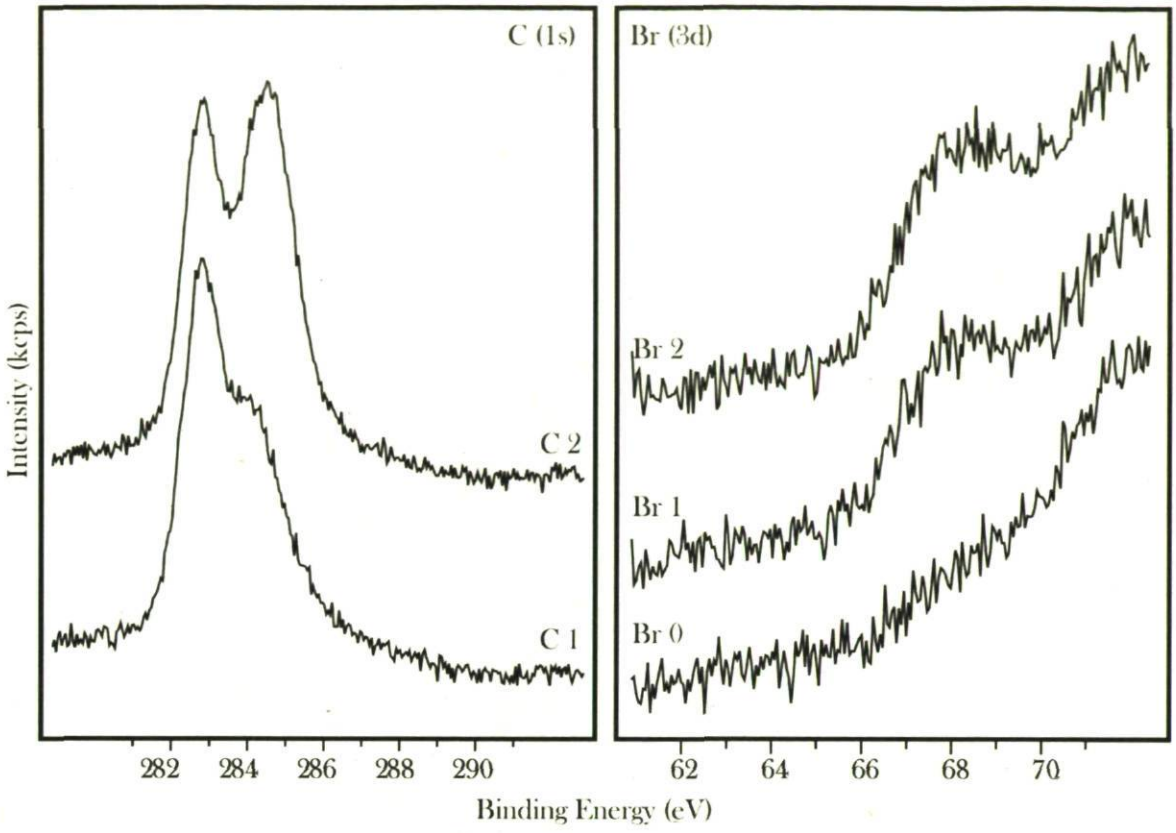

Figure 4-13 : Evolution of C(1s) and Br($3d_{5/2}$) peaks during consecutive cycles of polymerization of COT and bromination of the freshly formed polymer.

The experiments followed by XPS where made in a series of consecutive cycles of polymerization of cyclooctatetraene and subsequent bromination. All steps where performed at 350 K and spectra of C(1s), Br($3d_{5/2}$), Mo($3d_{3/2+5/2}$) and O(1s) where recorded after each step. Functionalization of the surface was performed as usual by introduction of cyclopentanone (~10 L) at 100 K, and then annealing the surface to 350 K at a rate of 1 K/s to form cyclopentylidene moieties. The surface polymerization reaction starts by the introduction of cyclooctatetraene monomer at a pressure of $1x10^{-8}$ Torr for 240 s (2.4 L) at 350 K. The C(1s) spectrum corresponding to this stage of the process is displayed as C1 in Figure 4-13, and we can distinguish in it the incipient peak at 284.3 eV, corresponding to the C sp^2 of the polymer's backbone discussed above (section 4.2.2). A look to the Br(3d) region of the spectra (spectrum 4-13 Br0) reveals a clean spectrum as expected for the undoped polyacetylene molecule. The introduction of $1x10^{-9}$ Torr for 240 s (0.24 L) of Br_2

at this stage however (spectrum 4-13 Br1), shows the appearance of two peaks, one corresponding to a molecular C-Br bond at 68.5 eV, and one corresponding to the adsorption of Br to the surface at 76.3 eV (displayed in Figure 4-14(b)). The characterization of the peak at a binding energy of 68.5 eV as C-Br from the halogenated polymer is supported by observations in the literature. Notably, Ikemoto et al.[112] found a binding energy of 69.3 eV for the Br(3d) peaks of several polyacetylene films of different bromine content, whereas Kang et al.[113] observed a wide peak with two components, one at 68.8 eV which they attributed to bromine anions, and another at 70.5 eV corresponding to bromine covalently bonded to polyacetylene. Moreover, these values are typical for the $Br(3d_{5/2})$ region in molecular bromine compounds and bromide ionic salts respectively[84,85].

A further introduction of monomer at $1x10^{-7}$ Torr for 400 s (40 L) and subsequent introduction of Br_2 at $1x10^{-8}$ Torr for 400 s (4 L), illustrated in Figure 4-13 as spectra C2 and Br2, shows not only the growth of the molecular Br peak at 68.5 eV and the sp^2 C peak of the polymer, but a shift towards higher binding energy of 0.4 eV of this peak now placed at 284.7 eV. This shift of the C(1s) core binding energy is attributed to charge transfer from the polymer to the dopant, and has also been observed for iodine doped (+ 0.2 eV)[86-89] and AsF_5 doped (+ 0.6 eV)[90] polyacetylene.

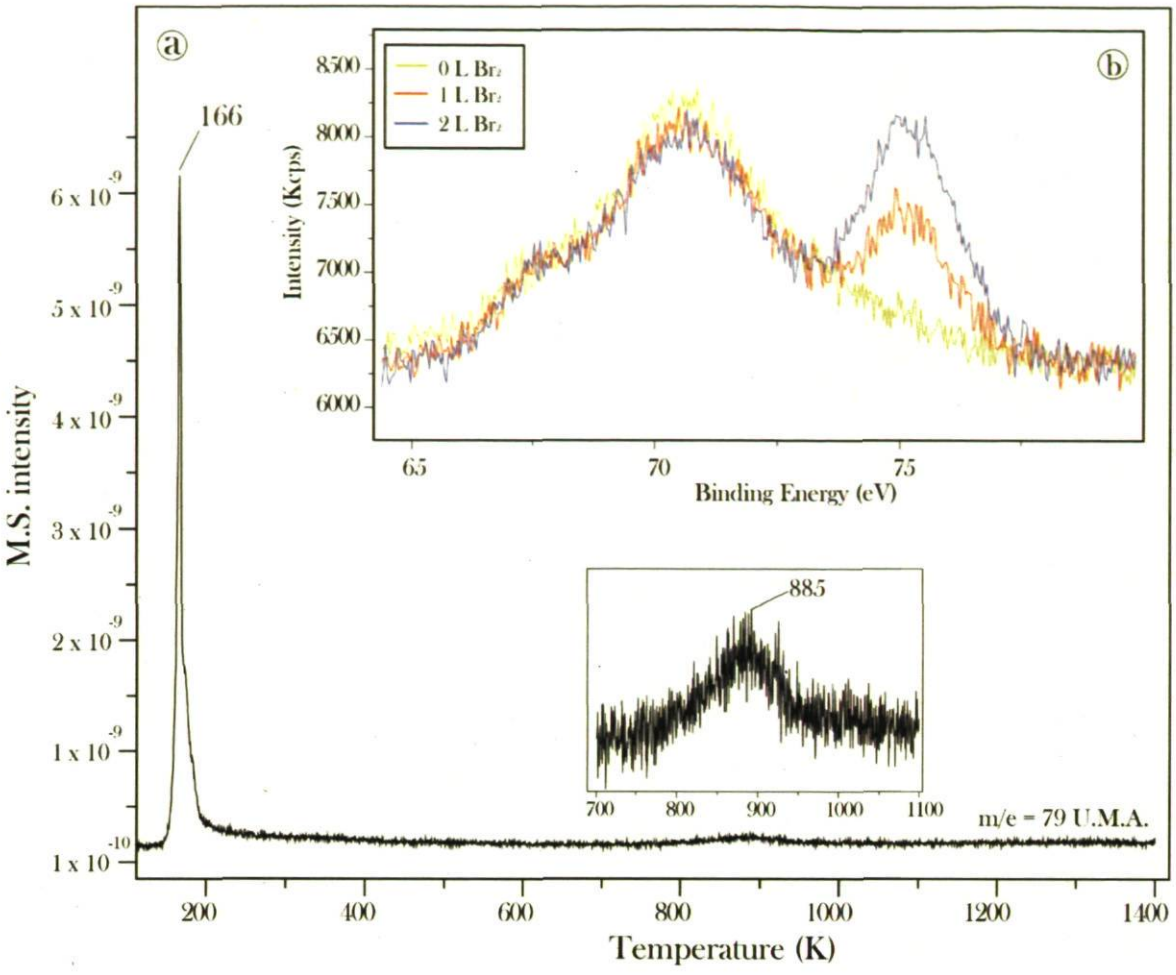

Figure 4-14 : a) TPD spectrum of Br_2 adsorbed on molybdenum carbide, and b) evolution of the Br($3d_{5/2}$) core level spectra for different amounts of bromine adsorbed on the same surface.

Control experiments consisting on XPS and TPD spectra of bromine adsorption with and without the presence of cyclooctatetraene were performed. Figure 4-14(a) displays a thermally programmed desorption of 10 L of bromine (79 uma) introduced at 100 K. We can clearly distinguish the presence of the multilayer desorption peak at 166 K and a small desorption peak (amplified in the centre of the figure) centred at 885 K. This figure is due to desorption of atomic Br chemically bonded to the surface. Figure 4-14(b) shows the Br($3d_{5/2}$) region of the XPS spectrum after the introduction of 1 L of bromine on the clean surface (red spectrum) under the same conditions as used in the polyacetylene bromination experiments described above. We can observe the appearance of a peak centred at 76.3 eV

corresponding to the dissociative adsorption of Br to the surface. This is characteristic of the adsorption of Br_2 in absence of any other molecular compound. A further introduction of 1 L of bromine (blue spectrum) causes this peak to double its size without the development of any other peak in the region. This behaviour is also maintained when cyclooctatetraene is previously deposited on the clean surface at conditions similar to those used during the polymerization (data not showed). It is worth noting, as discussed above, that no COT deposition is observed in these conditions in the absence of alkylidenes on the surface, and thus, no C-Br species could be formed.

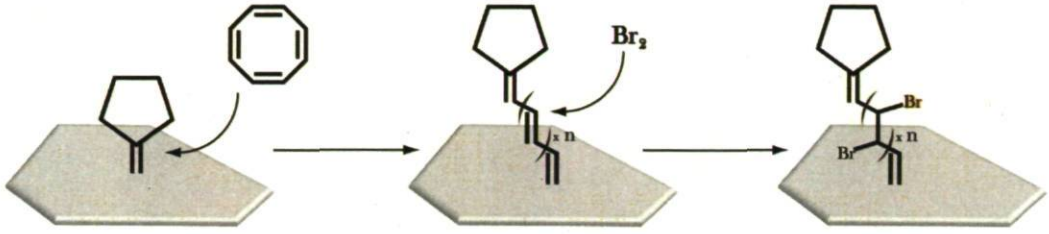

Scheme 4-5 : Bromination of cyclopentylidene initiated polyacetylene.

These data suggest the bromination of the polyene chain formed by ring opening metathesis polymerization on the surface of cyclopentylidene modified molybdenum carbide, following scheme 4-5. This bromination reaction of the double bonds of the polyene chain provides direct insight on the polymerization of cyclooctatetraene since these are the only places where the bromination reaction can take place.

4.4.2 Vinyl alkylidene terminated polyacetylene

Halogenation of polyacetylene formed on vinyl alkylidene sites on the surface of molybdenum carbide was also attempted. A series of bromine introductions were performed on the polyacetylene modified surface of molybdenum carbide. First vinyl alkylidene moieties were prepared on the surface by the introduction of 20 L acrolein at 100 K followed by an annealing of the surface to 300 K at a rate of 10 K/s. Polymerization of COT was performed by introduction of COT (110 L) while annealing from 100 K to a

temperature of 500 K with the same rate of 10 K/s. Then, introduction of different amounts of bromine at 300 K lead to the sequence of spectra shown in Figure 4-15. The evolution of the Br($3d_{5/2}$) peak at 68.5 eV peak corresponding to the C-Br bond is the same as that previously discussed. One can see that the introduction of just 0.3 L of bromine in the chamber where freshly made undoped polyacetylene is present produces a fair amount reaction compared with subsequent larger exposures due to the fact that polyacetylene is already halogenated in some proportion.

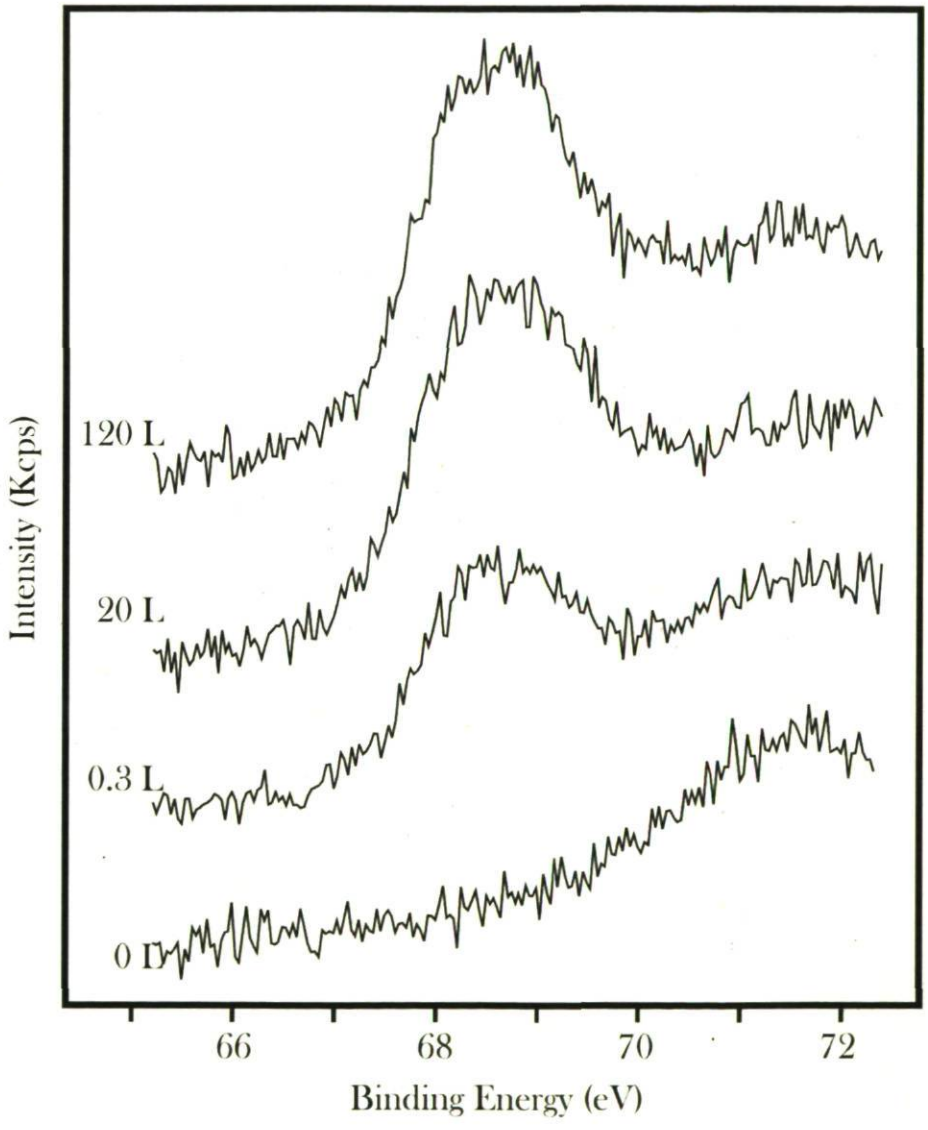

Figure 4-15 : Evolution of molecular Br on halogenated PA as a function of dosing. Each stage of bromination is made after the insertion of equal amounts of COT at 300 K.

Figure 4-15 confirms the results obtained for the bromination of polyacetylene at sites formed by acrolein. This fact provides a further characterization of the polyCOT molecules, and suggests that the polyene species formed both from cyclopentylidene and vinyl alkylidene initiator sites have similar reactivities.

4.5 Discussion

4.5.1 Discussion on the IR data

As referred to above, some theoretical studies have shown that the growth of the polyene chain results in a shift to lower energy of the first optically allowed and optically forbidden electronic transitions, as well as a decrease of the lowest totally symmetric C=C stretching frequency. This was shown by Kofranek et al.[63] using SCF structure optimizations for the polyenes $C_{2n}H_{2n+2}$ with n=1-7,9 and for infinite PA. The prediction was verified experimentally by Schaffer et al.[56], using solid state Raman scattering spectra of a homologous series of all-*trans* polyenes from 3 to 12 double bonds. The critical point, as far as vibrational spectroscopy is concerned, is the experimentally firmly established red shift of the C=C stretching frequency by about 170 cm^{-1} going from *trans*-1,3-butadiene to polyacetylene. Possible explanations for this strong red shift with increasing chain length are: (i) a sufficiently strong reduction of the C=C stretching force constant; (ii) an increase in the absolute value of the coupling constants between C=C bonds; (iii) an increase in anharmonic contributions, and most probably a combination of all these three effects.

In another paper, Korshak et al.[63] showed that electronic correlation has a profound effect on some of the coupling force constants between C-C bonds. These off-diagonal force constants play a key role in the correct description of the vibrational spectra of polyenes, in particular, for the C=C stretching region, and determine the shape of the phonon dispersion curve for that mode. In the case of surface polyenes, there could be a possible role for the metallic surface in causing electron transfer, through π-donation of the C=C double bond, from the polymer at some points (maybe isolated single points) that partially breaks the π-conjugation, thus reversing the red shift. The C=C stretching band

appears at 1675 cm^{-1} for short polyacetylene chains formed by ROMP on the surface of molybdenum carbide (Figure 4-2) . At the same time this π-donation to the surface would act as positive (+) doping, making some holes in the conduction band of the polymer that could improve electronic conductivity without a need for a further chemical doping.

A distribution of conjugation lengths within a given sample of PA when prepared from acetylene is assumed. This fact may cause dispersion in the vibrational spectra of *trans*-PA. This is correlated with a bimodal distribution of conjugation lengths, due to the well known fact that PA contains crystalline and amorphous regions[50,56,91]. However the very well defined peak corresponding to the C=C stretching vibration from the polymerization of cyclooctatetraene on the modified surface of molybdenum carbide suggests that high monodispersity has been achieved. Besides, data obtained using X-ray photoelectron spectroscopy indicates that polyene species of 4 double bonds (8 sp^2 carbons) are probably the most common on this system. Thus, the high frequency C=C stretching mode (1675 cm^{-1}) is in agreement with the formation of short length polymer chains. Short *cis* intervals between some *trans* modes, or electronic transfer from the polymer to the surface might also be in part responsible for this high frequency position of this vibrational mode. For *trans* chains of different lengths, the absorption band and the C-C stretch frequencies should shift to lower energy with increasing length. However the effect of the surface may not be completely ruled out, thus normally a coordination of the double bond by the metal atoms of the surface can help to stabilize the polymeric chain.

4.5.2 Cyclooctatetraene adsorbed on β-Mo_2C

The previously discussed fact that the ring opening metathesis reaction for cyclooctatetraene is kinetically more favoured than for norbornene and cyclopentene on the alkylidene modified surface of molybdenum carbide might be explained by the different interaction of these monomers with the surface. This fact can be extended to cross metathesis of small mono-olefinic molecules also studied in the same catalytic system. All these molecules have in common a single double bond, whereas cyclooctatetraene has four double bonds. Double bonds are known linkage points to metallic surfaces via π-donation

from the molecule to the metal (and in some cases back donation from the metal to the molecule). Thus, the number of linkage points between the molecule and the metal could play an important role in the dynamics that make this reaction possible, since diffusion time should be crucial (residence time) to help a monomeric molecule to find an active species on the surface in the correct geometry to make the reaction possible. Moreover, two extra π-donations from the molecule to the surface take place, forcing the molecule to flatten itself and thus raising its ring strain which could help to the polymerization.

Cyclopentylidene modified β-Mo_2C surface has been found to be an active phase for both cross metathesis and ROMP for norbornene and cyclopentene monomers at temperatures above 450 K under UHV conditions[28,41]. These monomers have higher ring strain than COT, and thus they are expected to be more reactive through ring opening metathesis polymerization. However surface dynamics could favourize the adsorption of four double-bonded COT molecules on the surface, and thus facilitate diffusion paths to find active species. In addition, its symmetry will allow the reaction to take place regardless the side of the molecule approaches the metal-alkylidene bond (Figure 4-16), and thus, it may explain why it forms polyacetylene at 350 K.

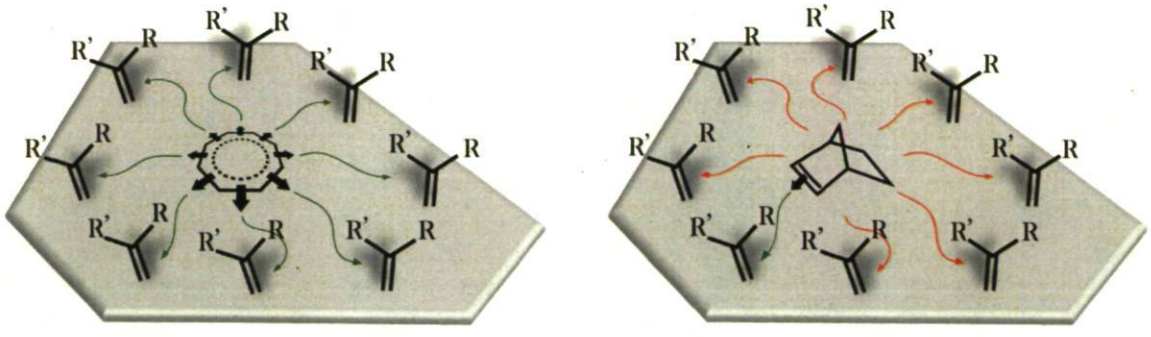

Figure 4-16 : Differences in surface accessibility for cyclooctatetraene and norbornene.

Polymerization of cyclooctatetraene has previously performed by Korshak and co-workers[29] by using a tungsten based catalyst ($W[OCH(CH_2Cl)_2]_n\ Cl_{6-n}$ / $Al(C_2H_5)_2Cl$ (n=2 or 3)), and by Grubbs and co-workers using 1st and 2nd generation Grubbs catalysts in mild conditions[32]. The synthesis of block copolymers of polyNBE/polyCOT and random

copolymers formed from copolymerization of COD and COT[39], as well as the syntheses of soluble, end-functionalized polyenes and polyacetylene block copolymers[33] has also been achieved by Grubbs et al. without varying the conditions between polymerizations. All these successful synthesis suggest that the low ring strain of COT does not make much of a difference in reactivity. Instead the flatness of the COT adsorbed on the surface of molybdenum carbide, may help it to stick better so it can diffuse further on the surface to find an active site, and its high symmetry assures it a perfect approach direction (Figure 4-16) to put a double bond close enough to an initiator or a propagator.

These surface effects may explain the relatively low temperature at which the polymerization takes place. The difference in reactivity is thus kinetic and not thermodynamic because both polymerizations of norbornene and cyclooctatetraene take place at the same temperature and conditions in homogeneous conditions. PolyNBE only forms faster. Then, the difference is due to surface processes favorising the formation of polyCOT over polyNBE by having 4 C=C and being planarized by the action of the surface. Adsorption and diffusion of cyclooctatetraene on the surface should be much greater than in the case of norbornene speeding up the polymerization of COT. Also the π-donation from the 4 double bonds should weaken more the molecule than in the case of NBE and the fact that either side of the molecule is suitable to be attacked by the alkylidenes should also help to favourize the formation of polyCOT. In fact both polymerization of polyCOT and polyNBE takes place at room temperature with Grubbs catalysts. In the case of the surface reactions it is an intriguing question as to why polyNBE does not (as well as poly-cyclopentene and cross metathesis with ethylene and propylene)[28,41] and it does for polyCOT. A plausible answer is suggested by the study of aromatic chiral modifiers on Pt(111) for the stereoselective hydrogenation of α,β-diketones (Orito reaction). The authors found that single-ring aromatics do not stick strongly enough on the surface to perform the 1:1 docking complex with substrate whereas double-ringed aromatics do[92]. By analogy, molecules with one (or 2) double bonds could desorb easier, or more likely, diffuse much shorter distances because they stick less effectively than COT on the carbide surface. Also more molecules could remain on the monolayer, so the polymerization could take place at lower temperatures because each molecule would have to cover less distance to diffuse to find alkylidene species.

The COT molecule has been considered a classic prototype of a cyclic antiaromatic (8 π electrons) hydrocarbon. Many experimental[93-95] and theoretical[85,96-99] studies have been performed concerning the structure, photo-, and thermal chemistry of free COT. It is by now firmly established that the most stable conformer of the free molecule has a tub-like structure with D_{2d} symmetry. This structure was first determined by the X-ray diffraction study of Kaufman et al.[100] and then confirmed by electron diffraction studies in the vapour phase[94,101,102]. Despite the fact that this molecule is highly symmetrical, the vibrational spectral features of this molecule are still not completely understood and there is still some disagreement concerning mode assignments. The D_{2d} structure is found to be a true minimum on the potential energy surface. Hence, the theoretical results are consistent with experimental evidence supporting this structure for the free COT molecule, with alternating single and double bonds and small conjugation interaction between the π bonds.

Dynamic processes (ring inversion and π-bond shift) have been experimentally observed (Figure 4-17), and planar COT conformations were proposed to be the transition states of these two processes. The planar D_{4h} conformation is generally accepted to be the transition state of the ring inversion, whereas the D_{8h} conformation seems to be the transition state of the π-bond shift. Moreover, COT derivatives that have planar ground states can be produced by the annelation of strained three- or four-membered rings to the COT skeleton[103,104], by the replacement of endocyclic double bonds with triple bonds[105], or by halogen substitution[106]. These structural modifications cause an expansion of the endocyclic bond angles and hence the planarization of the COT skeleton. However, even when strain effects cancel the tendency to pucker, bond alternation is still unambiguously observed, and thus, these effects do not overcome antiaromaticity. Apart from strain induced planarization, COT can also suffer large conformational changes to the planar form due to ionisation. The anion (COT^-) adopts a D_{4h} symmetry, as well as when the loss of an electron leads to an increase of the folding angle in the cation. Both doubly charged ions are planar and aromatic with D_{8h} symmetry, as expected for 10 and 6 π-electron cyclic molecules.

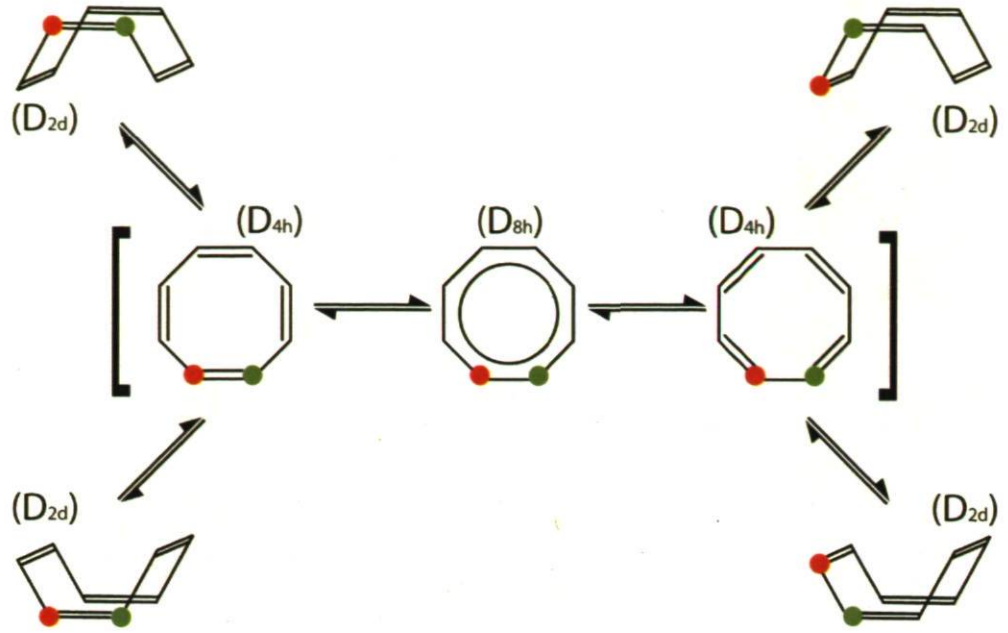

Figure 4-17 : Configurations of free 1,3,5,7-cyclooctatetraene.

Surface science studies on adsorbed COT have also been performed on Pt(111)[66,107], Pd(111)[108], Ag(110)[109], Si(001)[73,110], and Ru(001)[111] surfaces. In a very interesting paper, Hostetler and co-workers[66] studied the structure-reactivity correlations of cyclic C_8 hydrocarbons on a Pt(111) surface. In this paper they established that cyclooctene, 1,3-cyclooctadiene, 1,5-cyclooctadiene and cyclooctatetraene convert into benzene. The process is however, at least, as interesting as the result itself. First both cyclooctene and cyclooctadienes transform in cyclooctatetraene via dehydrogenation on the surface, and then the tub-shaped η^4 cyclooctatetraene is converted to a planar η^8 structure at higher temperatures prior to undergoing decomposition into benzene and acetylene. A neutral planar COT molecule (D_{8h}) is well known to be an unstable conformer. Formation of a stable planar aromatic species is allowed upon charge transfer to form either the dianion (10 π-electrons) or dication (6 π-electrons). The formation of the dianion has been proposed for a COT monolayer adsorbed on clean Ag(110), while on an oxygen precovered Ag(110) surface COT bonds in a tub-shaped structure[109] since the presence of electron-withdrawing oxygen limits the extent of charge transfer to COT and therefore the formation of the aromatic species. The adsorption of COT on Ru(001)[111] happens in a similar fashion as on Pt(111)[66,] forming a neutral planar D_{8h} species, however no formation of benzene nor

desorption of the complete molecule has been observed for the monolayer, but dehydrogenation occurs instead.

The study of the adsorption of cyclooctatetraene on a clean surface of β-Mo_2C would help to understand the mechanism in which the ring opening metathesis polymerization takes place. Reflection adsorption infrared spectroscopy is a powerful tool in surface chemistry for establishing the relative geometry of molecules adsorbed on metallic surfaces with help of its selection rule. RAIRS is thus, a very attractive tool to verify the conformation of cyclooctatetraene when adsorbed on the surface of molybdenum carbide. Figure 4-18 shows adsorption of cyclooctatetraene on molybdenum carbide at low temperature (110 K) as a function of coverage. There is a total absence of peaks corresponding to a monolayer of cyclooctatetraene (~3 L), and only two peaks corresponding to a multilayer of monomer on the surface, a CCC ring distortion mode at 802 cm^{-1} and a C-H stretching mode at 3009 cm^{-1}, both well established in the literature[85,95].

The absence of ν(C=C), ν(C-C), and ν(C-H) modes in the monolayer is consistent with a flat-lying geometry for the adsorbed molecule on the surface of molybdenum carbide, similar to the adsorption of COT on Pt(111)[66] and Pd(111)[108] surfaces. At higher coverages the vibrational spectra clearly indicates that the molecule undergoes a substantial change in adsorption geometry which is accompanied by the appearance of a C-H stretching mode at 3009 cm^{-1} and a CCC deformation at 802 cm^{-1} featuring the appearance of a tub-like configuration of the multilayer adsorbed molecule (D_{2d} symmetry).

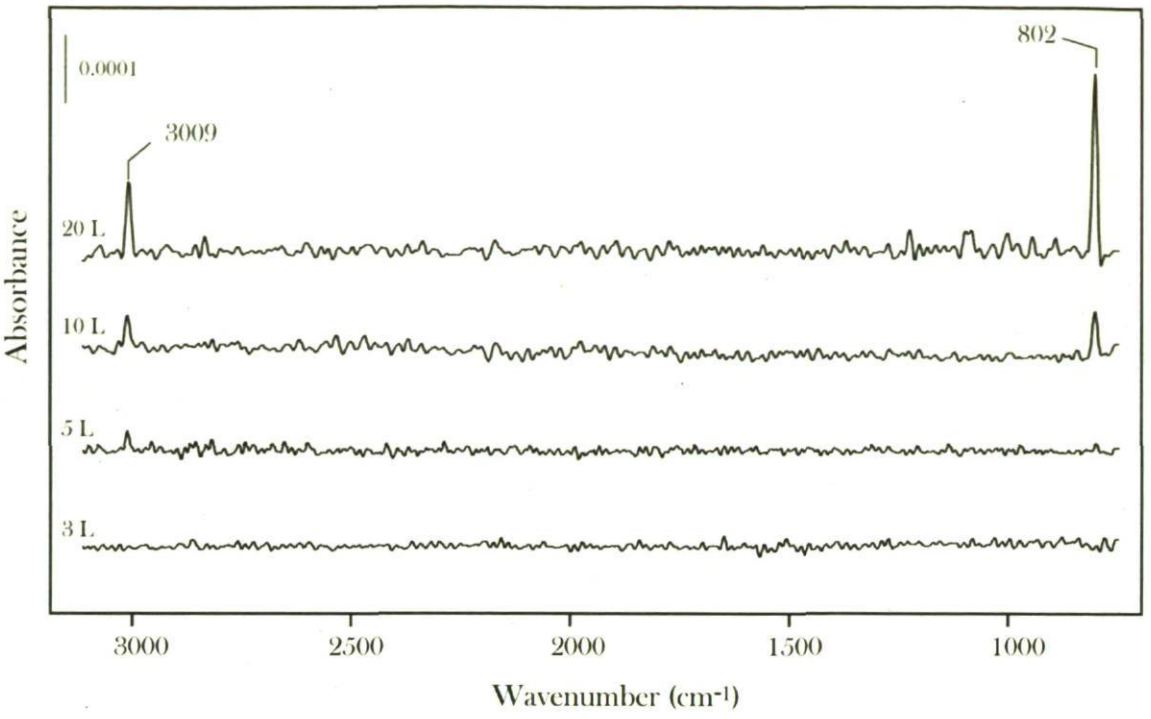

Figure 4-18 : IR spectra of adsorbed COT on β-Mo_2C as a function of coverage at 110 K.

Unlike the adsorption on Pt(111)[66], COT does not undergo decomposition into benzene and ethylidene species when adsorbed on molybdenum carbide, as shown by TPD data displayed in Figure 4-19. Instead the strongly adsorbed η^8 species undergoes decomposition on this surface as we can see regarding to the m/z=2 spectra. We can observe a sole desorption of molecular cyclooctatetraene (m/z=104) corresponding to multilayer desorption at ~180 K, whereas no desorption at all is observed for submonolayer coverages of the molecule (< 3 L). The same peak is observed in the m/z=2 spectra as well as a broad peak from ~300 K to ~1000 K corresponding to hydrogen desorption due to molecular decomposition on the strongly adsorbed monolayer. The hydrogen desorption grows from 1 L deposition to 3 L, behaviour opposite to the peak attributed to the multilayer desorption that appears only at 3 L and grows as the coverage is further increased. COT decomposition at higher temperatures is consistent with the previously discussed carbon deposition on the surface due to molecular decomposition observed consistently in XPS spectra. However, the presence of alkylidene species on the surface

seems to act as an inhibitor to this decomposition since carbon deposition on the surface happens as a side reaction to the dissociative adsorption of carbonyl compounds.

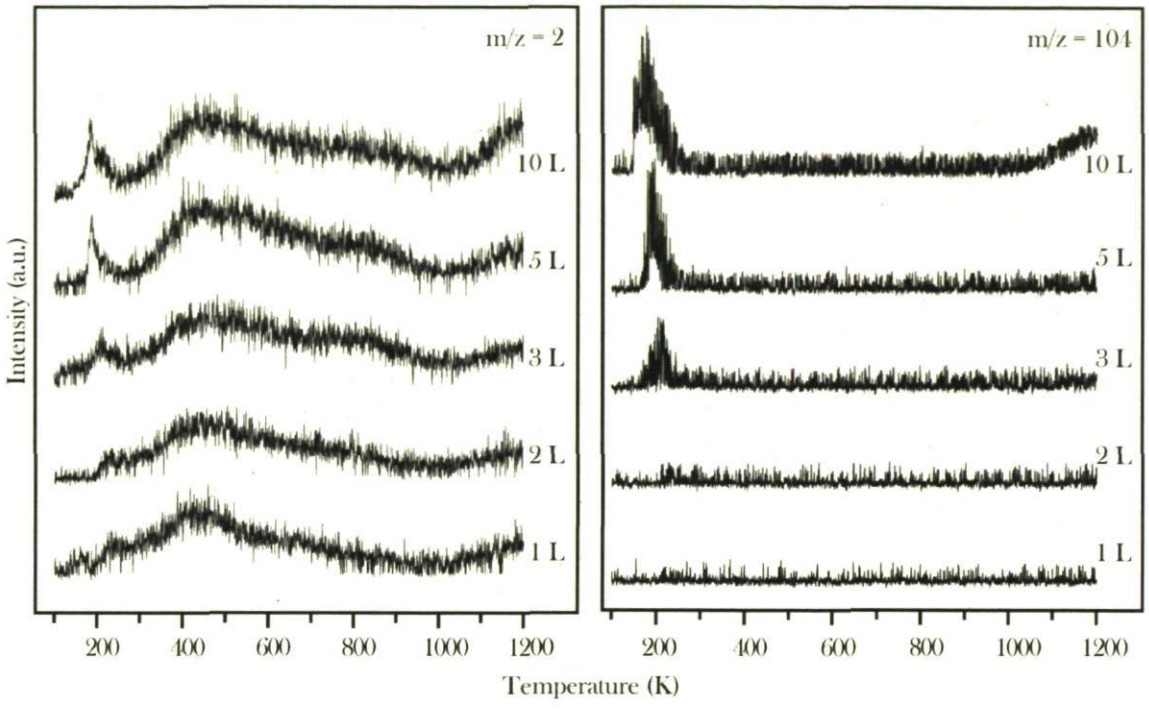

Figure 4-19 : TPD spectra for m/z=2 and m/z=104 for COT deposition on the surface of molybdenum carbide.

Since planarized cyclooctatetraene is possibly less stable than the free molecule, we propose that adsorbed COT on the surface of molybdenum carbide is both weakened because of the increase in strain, and more strongly adsorbed to the surface, two very important factors to favourize the ring opening metathesis reaction. These factors could be the responsible for the low temperature reaction of polymerization of COT on the surface of molybdenum carbide.

4.6 Bibliography

(1) Ratner, B. D. *Biosensors & Bioelectronics* **1995**, *10*, 797.

(2) Everhart, D. S. *Chemtech* **1999**, *4*, 30.

(3) Ricco, A. J.; Crooks, R. M.; Osbourn, G. C. *Acc. Chem. Res.* **1998**, *31*, 289.

(4) Mirkin, C. A.; Ratner, M. A. *Ann. Rev. Phys. Chem.* **1992**, *43*, 719.

(5) Choi, I. S.; Lager, R. *Makromol.ecules* **2001**, *34*, 5361.

(6) Husseman, M.; Mecerreyes, D.; Hawker, C. J.; Hedrick, J. L.; Shah, R.; Abbott, N. L. *Angew. Chem. Int. Ed.* **1998**, *38*, 647.

(7) Jordan, R.; Ulman, A. *J. Am. Chem. Soc.* **1998**, *120*, 243.

(8) Advincula, R.; Zhou, Q. G.; Park, M.; Wang, S. G.; Mays, J.; Sakellariou, G.; Pispas, S.; Nadiichristidis, N. *Langmuir* **2002**, *18*, 8672.

(9) Jordan, R.; Ulman, A.; Kang, J. F.; Rafailovich, M. H.; Sokolov, J. *J. Am. Chem. Soc.* **1999**, *121*, 1016.

(10) Zhao, B.; Brittain, W. J. *Makromol.ecules* **2000**, *33*, 342.

(11) Huang, W.; Kim, J.-B.; Buening, M. L.; Baker, G. L. *Makromol.ecules* **2002**, *35*, 1175.

(12) Jones, D. M.; Huck, W. T. S. *Adv. Mater.* **2001**, *13*, 1256.

(13) Chechik, V.; Crooks, R. M.; Stirling, C. J. M. *Adv. Mater.* **2000**, *12*, 1161.

(14) Copéret, C.; Chabanas, M.; Saint-Arroman, R. P.; Basset, J.-M. *Angew. Chem.* **2003**, *42*, 156.

(15) Edmonson, S.; Osborne, V. L.; Huck, W. T. S. *Chem. Soc. Rev.* **2004**, *33*, 12.

(16) Kim, N. Y.; Leon, N. L.; Choi, I. S.; Takami, S.; Harada, Y.; Finnie, K. R.; Girolami, G. S.; Nuzzo, R. G.; Whitesides, G. M.; Laibinis, P. E. *Makromol.ecules* **2000**, *33*, 2793.

(17) Luang, A.; Scherman, O. A.; Grubbs, R. H.; Lewis, N. S. *Langmuir* **2001**, *17*, 1321.

(18) Moon, J. H.; Swager, T. M. *Makromol.ecules* **2002**, *35*, 6086.

(19) Buchmeiser, M. R. *New J. Chem.* **2004**, *28*, 549.

(20) Copéret, C. *New J. Chem.* **2004**, *28*, 1.

(21) Thieuleux, C.; Copéret, C.; Dufaud, V.; Marangelli, C.; Kuntz, E.; Basset, J.-M. *J. Mol. Cat. A* **2004**, *213*, 47.

(22) Bazzi, H. S.; Sleiman, H. F. *Makromol.ecules* **2002**, *35*, 624.

(23) Mingotaud, A.-F.; Reculusa, S.; Mingotaud, C.; Keller, P.; Sykes, C.; Duguet, E.; Ravaine, S. *J. Mater. Chem.* **2003**, *13*, 1920.

(24) Weck, M.; Jackiw, J. J.; Rossi, R. R.; Weiss, P. S.; Grubbs, R. H. *J. Am. Chem. Soc.* **1999**, *121*, 4088.

(25) Liu, X.; Guo, S.; Mirkin, C. A. *Angew. Chem. Int. Ed.* **2003**, *42*, 4785.

(26) Tulevsky, G. S.; Myers, M. B.; Hybertsen, M. S.; Steigerwald, M. L.; Nuckolls, C. *Science* **2005**, *309*, 591.

(27) Ren, F.; Feldman, A. K.; Carnes, M.; Steigerwald, M.; Nuckolls, C. *Makromol.*. **2007**, *40*, 8151.

(28) Siaj, M.; McBreen, P. H. *Science* **2005**, *309*, 588.

(29) Korshak, Y. V.; Korshak, V. V.; Danischka, G. H., H. *Mackromol. Chem. Rapid Commun.* **1985**, *6*, 685.

(30) Klavetter, F. L.; Grubbs, R. H. *J. Am. Chem. Soc.* **1988**, *110*, 7807.

(31) Klavetter, F. L.; Grubbs, R. H. *Synth. Metals.* **1989**, *28*, 99.

(32) Scherman, O. A.; Grubbs, R. H. *Synth. Metals* **2001**, *124*, 431.

(33) Scherman, O. A.; Rutenberg, I. M.; Grubbs, R. H. *J. Am. Chem. Soc.* **2003**, *125*, 8515.

(34) Gorman, C. B.; Ginsburg, E. J.; Mardel, S. R.; Grubbs, R. H. *Angew. Chem. Int. Ed. Engl. Adv. Mater.* **1989**, *28*, 1571.

(35) Shirakawa, H.; Ikeda, S. *j. polym. Sci. Chem. Ed.* **1974**, *12*, 929.

(36) Chiang, C. K.; Fincher, C. R.; Park, Y. W.; Heeger, A. J.; Shirakawa, H.; Louis, E. J.; Gau, S. C.; MacDiarmid, A. J. *Phys. Rev. Lett.* **1977**, *39*, 1098.

(37) Shirakawa, H. *Rev. of Modern Physics* **2001**, *73*, 713.

(38) Shirakawa, H.; Louis, E. J.; MacDiarmid, A. J.; Chiang, C. K.; Heeger, A. J. *J. C. S. Chem. Comm.* **1977**, 578.

(39) Klavetter, F. L.; Grubbs, R. H. *Synth. Metals.* **1989**, *28*, 105.

(40) Shirakawa, H.; Ikeda, S. *Polym. J.* **1971**, *2*, 231.

(41) Siaj, M.; Dubuc, N.; Temprano, I.; Maltais, C.; McBreen, P. H. *J. Phys. Chem.*, Article submitted.

(42) Siaj, M.; Oudghiri-Hassani, H.; Maltais, C.; McBreen, P. H. *J. Phys. Chem. C* **2007**, *111*, 1725.

(43) Siaj, M.; Temprano, I.; Dubuc, N.; McBreen, P. H. *J. Organomet. Chem.* **2006**, *691*, 5497.

(44) Parente, V.; Fredriksson, C.; Selmani, A.; Lazzaroni, R.; Bredas, J. L. *J. Phys. Chem. B* **1997**, *101*, 4193.

(45) Schettino, V.; Gervasio, F. L.; Cardini, G.; Salvi, P. R. *J. Chem. Phys.* **1999**, *110*, 3241.

(46) Takeuchi, H.; Furukawa, Y.; Harada, I.; Shirakawa, H. *J. Chem. Phys.* **1986**, *84*, 2882.

(47) Chen, Z.; Liu, M.; Shi, M.; Shen, Z.; Hummel, D. O. *Mackromol. Chem.* **1987**, *188*, 2687.

(48) Chen, z.; Liu, M.; Shi, M.; Shen, Z.; Hummel, D. O. *Mackromol. Chem.* **1987**, *188*, 2697.

(49) Furukawa, Y. *App. Spectroscopy* **1993**, *47*, 1405.

(50) Piaggio, P.; Dellepiane, G.; Piseri, L.; Tubino, R.; Taliani, C. *Sol. State Comm.* **1984**, *50*, 947.

(51) Will, F. G.; McDonald, R. S.; Gleim, R. D.; Winkle, M. R. *J. Chem, Phys.* **1983**, *78*, 5847.

(52) Hirata, S.; Yoshida, H.; Torii, H.; Tasumi, M. *J. Chem, Phys.* **1995**, *103*, 8955.

(53) Lippincott, E. R.; White, C. E.; Sibilia, J. P. 1958; Vol. 80, p 2926.

(54) Panchenko, Y. N. *Spectrochim. Acta A* **1975**, *31*, 1201.

(55) Rasmussen, R. S.; Brattain, R. R. *J. Chem. Phys.* **1947**, *15*, 131.

(56) Schaffer, H. E.; Chance, R. R.; Silbey, R. J.; Knoll, K.; Schrock, R. R. *J. Chem, Phys.* **1991**, *94*, 4161.

(57) Yoshida, H.; Tasumi, M. *J. Chem, Phys.* **1988**, *89*, 2803.

(58) Bates, F. S.; Baker, G. L. *Makromol.ecules* **1983**, *16*, 342.

(59) Siaj, M.; Maltais, C.; Zahidi, E. M.; Oudghiri-Hassani, H.; Wang, J.; Rosei, F.; McBreen, P. H. *J. Phys. Chem. B* **2005**, *109*, 15376.

(60) Siaj, M.; Oudghiri-Hassani, H.; Zahidi, E. M.; McBreen, P. H. *Surf. Sci.* **2005**, *579*, 1.

(61) Siaj, M.; Reed, C.; Oyama, T.; Scott, S. L.; McBreen, P. H. *J. Am. Chem. Soc.* **2004**, *126*, 9514.

(62) Zahidi, E. M.; Oudghiri-Hassani, H.; McBreen, P. H. *Nature* **2001**, *409*, 1023.

(63) Kofranek, M.; Lischka, H.; Karpfen, A. *J. Chem, Phys.* **1992**, *96*, 982.

(64) Deng, R.; Jones, J.; Trenary, M. *J. Phys. Chem. C* **2007**, *111*, 1459.

(65) Eng, J.; Chen, J. G.; Abdelrehim, I. M.; Madey, T. E. *J. Phys. Chem. B* **1998**, *102*, 9687.

(66) Hostetler, M. J.; Nuzzo, R. G.; Girolami, G. S.; Dubois, L. H. *J. Phys. Chem.* **1994**, *98*, 2952.

(67) Buchmeiser, M. R. *Chem. Rev.* **2000**, *100*, 1565.

(68) Fürstner, A. *Angew. Chem. Int. Ed.* **2000**, *39*, 3012.

(69) Hoveyda, A. H.; Zhugralin, A. R. *Nature* **2007**, *450*, 243.

(70) De Clercq, B.; Smellinickx, T.; Hugelier, C.; Maes, N.; Verpoort, F. *App. Spectroscopy* **2001**, *55*, 1564.

(71) Ning, J.; Qian, Z.; Li, R.; Hou, S.; Rocha, A. R.; Sanvito, S. *J. Chem, Phys.* **2007**, *126*, 174706.

(72) Oudghiri-Hassani, H.; Siaj, M.; McBreen, P. H. *J. Phys. Chem. C* **2007**, *111*, 5954.

(73) Rochet, F.; Bournel, F.; Gallet, J. J.; Dufour, G.; Lozzi, L.; Sirotti, F. *J. Phys. Chem. B* **2002**, *106*, 4967.

(74) Freyer, N.; Pirug, G.; Bonzel, H. P. *Surf. Sci.* **1983**, *126*, 487.

(75) Oudghiri-Hassani, H.; Zahidi, E. M.; Siaj, M.; Wang, J.; McBreen, P. H. *App. Surf. Sci.* **2003**, *212-213*, 4.

(76) Wang, J.; Castonguay, M.; Deng, J.; McBreen, P. H. *Surf. Sci.* **1997**, *374*, 197.

(77) Loffreda, D.; Jugnet, Y.; Delbecq, F.; Bertolini, J. C.; Sautet, P. *J. Phys. Chem. B* **2004**, *108*, 9085.

(78) Bayliss, N. S. *Q. Rev. Chem. Soc.* **1952**, *6*, 319.

(79) Bohlmann, F.; Manhardt, H. *Chem. Ber.* **1956**, *89*, 1307.

(80) Kuhn, H. *Helv. Chim. Acta* **1948**, *31*, 1441.

(81) Kuhn, R. *Angew. Chem.* **1937**, *34*, 703.

(82) Sondheimer, F.; Ben-Efraim, D. A.; Wolovsky, R. *J. Am. Chem. Soc.* **1961**, *83*, 1675.

(83) Natta, G.; Mazzanti, G.; Corradini, P. *Rend. Accad. Nazl. Lincei* **1958**, *25*, 2.

(84) Wagner, C. D. *J. Vac. Sci. Technol.* **1978**, *15*, 518.

(85) Zhou, X.; Liu, R.; Pulay, P. *Spectrochim. Acta* **1993**, *49A*, 953.

(86) Hsu, S. L.; Signorelli, A. J.; Pez, G. P.; Baughman, R. H. *J. Chem, Phys.* **1978**, *69*, 106.

(87) Salaneck, W. R.; Thomas, H. R.; Bigelow, R. W.; Duke, C. B.; Plummer, E. W.; Heeger, A. J.; MacDiarmid, A. G. *J. Chem, Phys.* **1980**, *72*, 3674.

(88) Salaneck, W. R.; Thomas, H. R.; Duke, C. B.; Paton, A.; Plummer, E. W.; Heeger, A. J.; MacDiarmid, A. G. *J. Chem, Phys.* **1979**, *71*, 2044.

(89) Salaneck, W. R.; Thomas, H. R.; Duke, C. B.; Plummer, E. W.; Heeger, A. J.; MacDiarmid, A. G. *Synth. Metals* **1979**, *1*, 133.

(90) *Polyacetylene: Chemistry, Physics, and Material Science*; Chien, J. C. W., Ed., 1984.

(91) Balzaretti, N. M.; Perottoni, C. A.; Herz da Jornada, J. A. *J. Raman Spectosc.* **2003**, *34*, 259.

(92) Lavoie, S.; Laliberte, M. A.; Temprano, I.; McBreen, P. H. *J. Am. Chem. Soc.* **2006**, *128*, 7588.

(93) Bastiansen, O.; Hedberg, L.; Hedberg, K. *J. Chem, Phys.* **1957**, *27*, 1311.

(94) Karle, I. L. *J. Chem, Phys.* **1952**, *20*, 65.

(95) Lippincott, E. R.; Lord, R. C.; McDonald, R. S. *J. Am. Chem. Soc.* **1951**, *73*, 3370.

(96) Andrés, J. L.; Castaño, O.; Morreale, A.; Palmeiro, R.; Gomperts, R. *J. Chem, Phys.* **1997**, *108*, 203.

(97) Frutos, L. M.; Castaño, O.; Andrés, J. L.; Merchán, M.; Acuña, A. U. *J. Chem, Phys.* **2004**, *120*, 1208.

(98) McLachlan, A. D.; Snyder, L. C. *J. Chem, Phys.* **1962**, *36*, 1159.

(99) Stevenson, C. D.; Brown, E. C.; Hrovat, D. A.; Borden, W. T. *J. Am. Chem. Soc.* **1998**, *120*, 8864.

(100) Kaufman, H. S.; Fankuchen, I.; Mark, H. *Nature* **1947**, *161*, 165.

(101) Bastiansen, O.; Hasse, O. *Acta Chem. C. Scand.* **1949**, *3*, 209.

(102) Traetteberg, H. *Acta Chem. C. Scand.* **1966**, *20*, 1724.

(103) Klärner, F.-G. *Angew. Chem. Int. Ed.* **2001**, *40*, 3977.

(104) Trindle, C. *Int. J. Quantum Chem.* **1998**, *67*, 367.

(105) Huang, N. Z.; Sondheimer, F. *Acc. Chem. Res.* **1982**, *15*, 96.

(106) Einstein, F. W. B.; Willis, A. C. *J. Chem. Soc. Chem. Commun.* **1981**, 526.

(107) Hitchcock, A. P.; Newbury, D. C.; Isii, I.; Stöhr, J.; Horsley, J. A.; Redwing, R. D.; Johnson, A. L.; Sette, F. *J. Chem, Phys.* **1986**, *85*, 4849.

(108) Lee, A. F.; Baddeley, C. J.; Hardacre, C.; Lambert, R. M. *J. Am. Chem. Soc.* **1995**, *117*, 7719.

(109) Merrill, P. B.; Madix, R. J. *Surf. Sci.* **1996**, *365*, 701.

(110) Hovis, J. S.; Hamers, R. J. *J. Phys. Chem. B* **1998**, *102*, 687.

(111) Tegeder, P.; Danckwerts, M.; Hagen, S.; Hotzel, A.; Wolf, M. *Surf. Sci.* **2005**, *585*, 177.

(112) Ikemoto, I.; Cao, Y.; Yamada, M.; Kuroda, H.; Harada, I.; Shirakawa, H.; Ikeda, S. *Bull. Chem. Soc. Jpn.* **1982**, *55*, 721.

(113) Kang, E. T.; Neoh, K. G.; Tang, K. L.; Tang, B. T. G. *J. Polym. Sci. B* **1989**, *27*, 2061.

5. Polymerization of acetylene on alkylidene modified β-Mo_2C

5.1 Acetylene polymerization

Acetylene was first polymerized by Natta et al.[1] to a linear conjugated Makromol.ecule via chain-growth polymerization using the $Ti(OBu)_4$-$AlEt_3$ catalyst. A breakthrough came when Ito et al.[2] succeeded in preparing high-quality free-standing films employing a very high concentration of the same catalyst. This modification allowed the production of polyacetylene as a film that could be washed, sliced, and manipulated for experimental investigations.

Acetylene polymerization has also been initiated by anionic polymerization[3], cationic polymerization[4], and by a variety of transition[5,6] and rare earth metal catalysts[7-9]. Aoky and co-workers[10] have also discovered that acetylene undergoes solid-state polymerization at pressures above 3.5 GPa at room temperature. A number of transition metal acetylacetonates have been compared for acetylene polymerization[5]. Titanium and vanadium complexes were found to be more active than the others: Ti, V >> Cr > Fe > Co. A number of side reactions were found in all these processes, which vary depending on the method of initiation, as for instance cyclization to benzene. Other processes lead to low molecular weight oligomers, branched polymers, and cross-linked polymers.

Different catalysts based on molybdenum and tungsten have been used to polymerize acetylene, and monosubstituted derivatives. Woon and Farona[11] studied the polymerization of phenylacetylene with $ArM(CO)_3$ (Ar = arene or mesilene, and M = Cr, Mo, or W). More recently Schuehler and co-workers[12] polymerized acetylene using a well defined ruthenium metathesis catalyst, in a very fast reaction at ambient temperature giving a black solid precipitate of *trans*-polyacetylene.

However no attempts seem to have succeeded in performing surface-initiated polymerization of acetylene on technologically interesting solid materials through direct metal-molecule junctions[13]. Such structures could be very interesting in regards to the

electronic properties of polyacetylene for the creation of molecular electronic devices. A new strategy to create such a device will be attempted in this chapter by the metathesis polymerization of acetylene on an alkylidene modified surface of molybdenum carbide.

5.2 Spectroscopic evidence for acetylene polymerization

Having established in the previous chapter, that cyclooctatetraene insertion through ring opening metathesis polymerization can be carried out on β-Mo_2C, the direct route of acetylene metathesis polymerization was investigated. The mechanism of such a polymerization on the surface is believed to be the same established for this polymerization in homogeneous catalysis[14,15]. As displayed in Scheme 5-1, monomer insertion is expected to take place through a metallacyclobutene intermediate following the mechanism proposed by Hérrison and Chauvin[16].

The general procedure for the surface initiated polymerization of acetylene on alkylidene modified molybdenum carbide follows the same general path as for ROMP of cyclooctatetraene. First, cyclopentylidene modification of the surface is achieved by the dissociative adsorption of cyclopentanone after the introduction of 20 L at low temperature (110 K) and then annealing the system to 300 K. Once the alkylidenes are formed, acetylene polymerization is carried out by introducing different amounts of acetylene at low temperature, and then the system is again annealed to the chosen temperature.

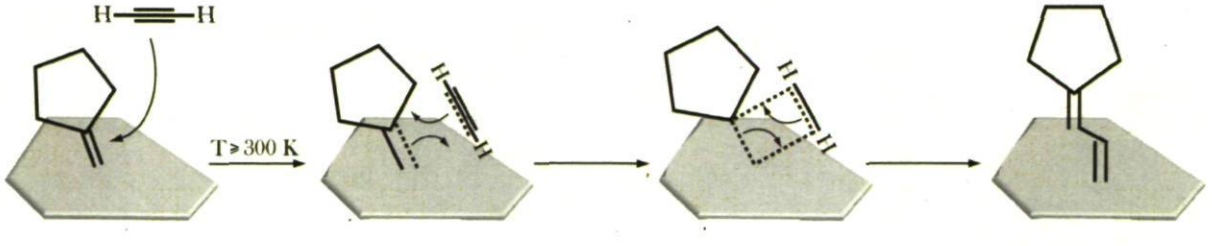

Scheme 5-1 : Proposed mechanism for metathesis polymerization of acetylene on the surface of molybdenum carbide[16].

5.2.1 IR characterization

The high resolution of RAIRS, combined with the high sensitivity the technique has in the C-H stretching region, makes it possible to more definitively characterize surface hydrocarbon species. Figure 5-1 shows data for the introduction of acetylene on the cyclopentylidene initiator sites on the surface of β-Mo_2C at different exposures of monomer at 350 K. Exposure to gas-phase acetylene leads to the replacement of the cyclopentylidene spectrum (spectrum 5-1(a)) with bands at 3069, 3055, 3035, 2963 and 2886 cm^{-1} through monomer insertion (spectra 5-1(b) and (c)). The 2886 and 2963 cm^{-1} peaks are assigned to ν_s and $\nu_{as}(CH_2)$ vibrations for sp^3 carbons respectively[17-24], and are also observed in the cyclopentylidene spectrum, so it may be assumed they are due to unreacted cyclopentilidene species remaining in the surface or due to C_5 end groups of the newly formed polyene molecules, or due to sp^3 impurities in the polyene chain.

More relevant are the appearance of the new peaks at high frequency (>3000cm^{-1}), notably at 3069 and 3055 cm^{-1} and a shoulder formed at 3035 cm^{-1}. Spectrum 5-1(a) shows acetylene exposure (0.0084 L) to a cyclopentylidene modified surface at 350 K, displaying a single feature on this region at 3055 cm^{-1}, whereas spectrum 5-1(b) corresponds to a further exposure of 30.9 L of acetylene at the same temperature and displays a wide feature containing the three peaks previously mentionned. These three bands have been assigned in the literature as C-H stretching vibrations of the different isomers of the polyacetylene[8,9,25-28]. Notably, three bands are usually assigned to this C-H stretching band at 3013, 3044 and 3057 cm^{-1}, for long chain polyacetylenes. The lower frequency one has been characterized as a C-H stretching vibration of the *trans* configuration, whereas the other two higher frequency bands are related to long and short *cis* segments respectively. Bands in the same region have been reported for some alkylidene species on the surface of molybdenum carbide, notably methylidene species, formed from the cross metathesis reaction of a cyclopentylidene modified surface with gas-phase ethene and propene[18,19]. Frequencies in the same range are also observed in vinyl alkylidene species[18] formed from cross metathesis reaction of the same modified surface with 1,3-butadiene and from the dissociative adsorption of acrolein (Section 3.2.2.1 on this thesis). In addition, this band has

already been observed in the ROMP of cyclooctatetraene and was discussed in the previous chapter (Sections 4.2.1 and 4.3.1) of this thesis.

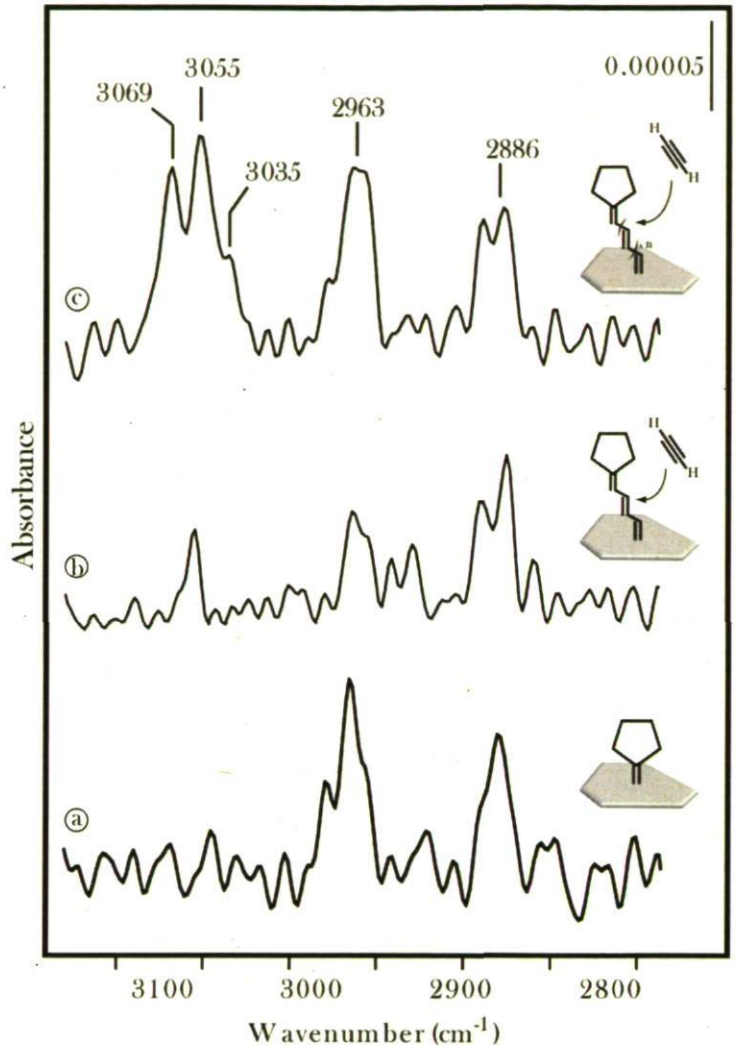

Figure 5-1 : IR spectra of acetylene polymerization as a function of monomer insertion. Spectrum a) represents cyclopentylidene species formed at 300 K, whereas spectra b) and c) display acetylene insertion into the metal-alkylidene sites at 350 K when 0.0084 L and 30.9 L of monomer are introduced respectively.

The bands corresponding to the C-H stretching vibrations, could also shed some light on the conformation form of the polyacetylene formed from acetylene insertion on molybdenum carbide. Spectrum 5-1(a) shows polyacetylene formation from a low exposure of acetylene at 350 K of the alkylidene modified surface. The new band at 3055 cm^{-1} may

be assigned to C-H stretching vibration on *cis* segments of the polyacetylene molecule according to the literature[8,9,27]. This band suggests that polymerization at these conditions leads to mostly *cis*-polyacetylene. A further evolution of the reaction at the same temperature, shown in spectrum 5-1(b), induces the developpment of a new band at higher frequency (3069 cm^{-1}) and a shoulder towards lower frequency (~3035 cm^{-1}) characteristic of C-H stretching vibration of short *cis* segments and *trans* segments of polyacetylene respectively.

These results, though in agreement with previously reported ROMP of cyclooctatetraene on the alkylidene modified molybdenum carbide, present some differences. ROMP reaction of COT with the cyclopentylidene modified surface displays a single peak at 3065 cm^{-1}, and with the vinyl alkylidene modified surface shows two peaks at 3064, and 3033 cm^{-1}. These differences point out a certain difference in the activity of these reactive sites for the same monomer, as well as within the same active sites for different monomers.

RAIRS results for acetylene polymerization on the cyclopentylidene modified molybdenum carbide suggest that in the early stages mostly *cis*-polyacetylene is formed at 350 K, whereas as the monomer insertion continues, *trans* segments became more present, presumably as the polymeric chain grows in length. It is also worth noting that even though *trans* segments are detected, *cis* polyacetylene seems to be the major species present on the surface at 350 K. *Cis-trans* isomerization is expected to happen close to room temperature for polyacetylene[9,12,26,28]. This behaviour, also observed for the polyacetylene formed by ROMP, may suggest a certain role of the surface as inhibitor of the isomerization process, possibly through inmobilisation of the polyene chain via interaction between the double bonds of the molecular π system and the surface.

5.2.2 XPS characterization

Acetylene insertion on the alkylidene modified surface was also monitored by XPS on the C(1s) region. Figure 5-2 displays a series of difference spectra, for a sequence of

acetylene introductions, with respect to the spectrum of cyclopentylidene species. After the formation of cyclopentylidene species, by exposing the clean surface to 10 L of cyclopentanone at 100 K and further annealing to 300 K. The exposure to the monomer was performed by keeping the pressure at $5x10^{-8}$ Torr during the corresponding amount of time, while annealing from 100 K to 350 K, leading to monomer coverages equivalent to 2.34, 37, 125, 223, and 321 L. The corresponding spectrum for each step of the reaction, after monomer insertion, was then subtracted from the spectrum of the cyclopentylidene species, to eliminate the peaks of the other C species which remain unvariable, such as the carbide, the carbon deposited on the surface, and the molecular peaks of the cyclopentilydene moieties.

A new peak arising at 284.3 eV as monomer insertion occurs can be clearly seen in all of the spectra of this series. This peak has already been attributed to the sp^2 carbon of polyacetylene in the case of ring opening metathesis polymerization of cyclooctatetraene on cyclopentylidene and vinyl alkylidene modified surfaces, as well as in the case of cyclooctatetraene deposition on the clean surface at 100 K (Sections 4.2.2 and 4.3.2). The assignment of this new C sp^2 peak is also well supported by numerous examples in the literature. Rochet and co-workers have found a peak at 284.75 eV when they exposed a Si(001) surface to COT[29]. Hitchcock et al.[30] attributed a peak at 284.6 eV to C_2H_4 species on Pt(111) after cyclobutane decomposition. Solomon et al.[31] reported a binding energy for benzene adsorbed on Pt(111) of 284.7 eV. Similarly, spectrum 4-10(a) on the Chapter 4 of this thesis shows the development of a peak at a binding energy of 284.3 eV when COT is adsorbed on the surface of molybdenum carbide at 100 K.

The evolution of this peak appears to occur in the absence of further carbon deposition on the surface, characterized by the absence of a peak at 283.4 eV[17,20,21,32], suggesting that the cyclopentylidene modified surface is reactive enough to undergo metathesis polymerization, but stable enough not to induce monomer decomposition at these temperatures.

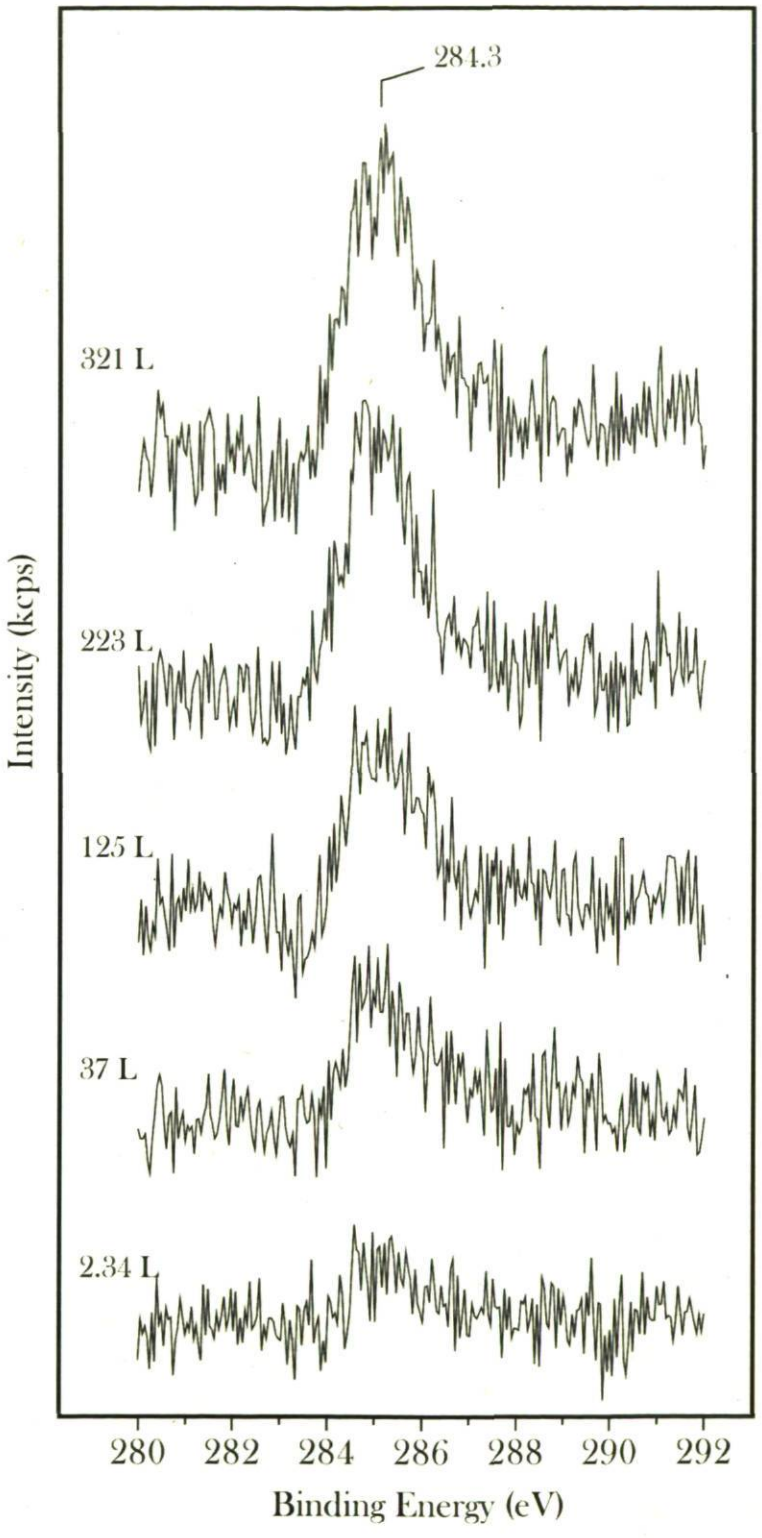

Figure 5-2 : Difference spectra of the XPS C(1s) region for acetylene insertion with respect to the spectrum of cyclopentylidene species on the surface of molybdenum carbide as a function of monomer exposure. The temperature was raised from 100 K to 350 K during exposition to the monomer.

Figure 5-3 rules out the possibility that the peak observed at 284.3 eV through acetylene exposure of the cyclopentylidene modified surface at 350 K is due to acetylene deposition on the surface. In this Figure we can see the evolution of the C(1S) region of the XPS spectrum when monomer is introduced at 300 K on the clean surface.

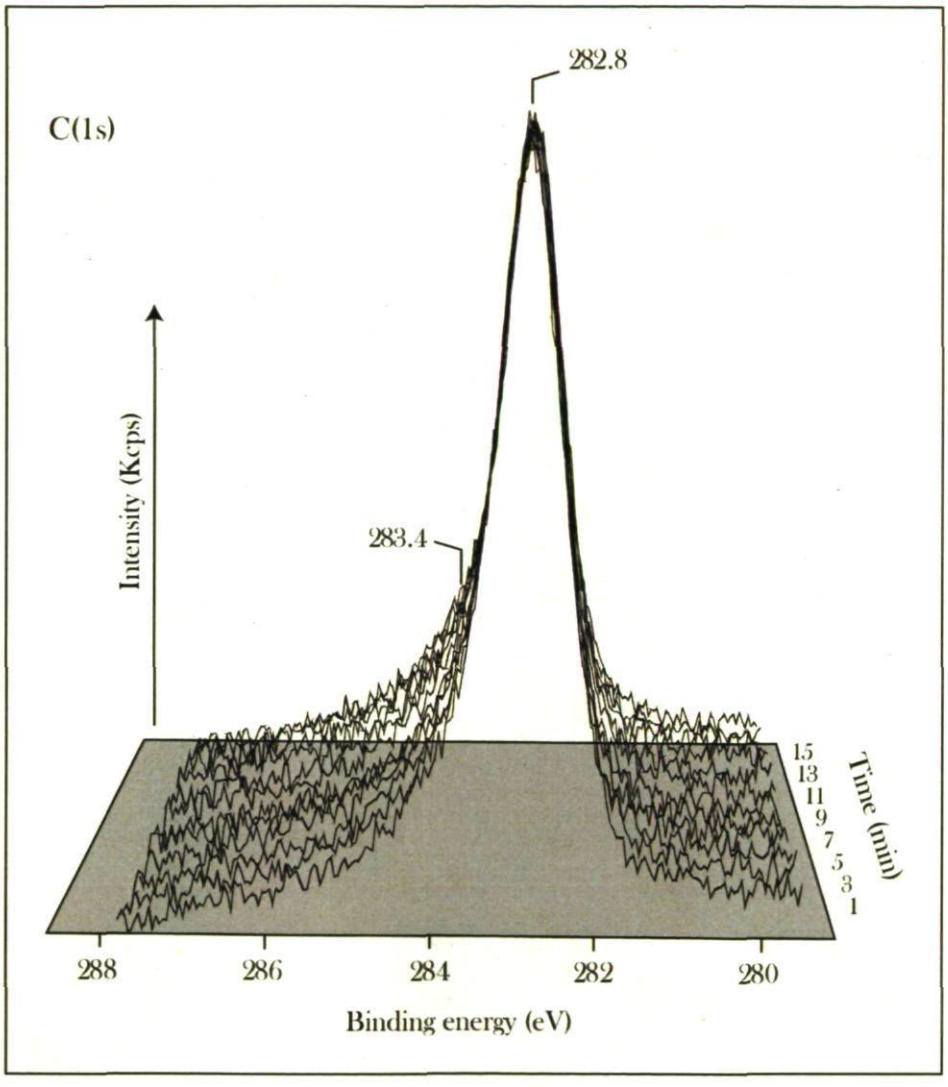

Figure 5-3 : 3D plot of the C(1s) region when the clean surface was exposed to acetylene. All spectra were taken with intervals of 3 minutes while the pressure of the chamber was maintained at $1x10^{-8}$ Torr.

Figure 5-3 shows that no new peak develops in the region around 284 eV when the clean surface is exposed to acetylene, in opposition to the observation of a new peak at 284.3 eV when the alkylidene modified surface is exposed to acetylene under the same

conditions. It can be clearly seen that the only peak present is the 282.8 eV corresponding to the carbide C of the surface, with a small shoulder at higher energy 283.4 eV, which has been previously observed and assigned to carbon deposition on the surface due to molecular cracking[17,20,21,32]. The total absence of any peak development leaves the acetylene polymerization as the only possible explanation for data recorded when acetylene is introduced in the presence of alkylidene species on the surface of molybdenum carbide displayed in Figure 5-2.

5.3 Acetylene cyclization

An unexpected behaviour of several peaks in the mass spectra was observed during acetylene polymerization reactions, notably the appearance of a peak at m/z=78 when acetylene was introduced into the chamber at temperatures equal or higher than room temperature. Immediately the idea of acetylene cyclo-oligomerization on several metal catalysts came to mind, and a battery of TPD measurements were carried out to verify if this reaction could take place on the surface of molybdenum carbide.

There is a strong tendency for acetylenic molecules to cyclo-oligomerize to cyclobutadiene, benzene, cyclooctatetraene, or even higher annulenes[33-38]. This reaction, first reported over 100 years ago[39], probably accounts, at least in part, for the pronounced difficulty for acetylenes to polymerize linearly to high molecular weights. This reaction has been systematically observed, as a side reaction, in a number of processes to form polyacetylene, and has been usually described as a competing reaction. Moreover, a large variety of transition metal compounds have been used to cyclotrimerize mono- and disubstituted acetylenes to benzene derivatives. Nevertheless, in the absence of metals, this reaction has also been observed, needing relatively high temperatures (~670 K), and leading to a wide variety of products[40].

Heterogeneously catalyzed acetylene to benzene cyclization has been reported on a number of different surfaces. First reported by Reppe and co-workers[41], cyclization of acetylene on various Ni based homogeneous and heterogeneous catalysts, including mono

crystalline Ni(111), leads to the co-production of benzene and cyclooctatetratene in different proportions varying with the catalyst and reaction conditions[42,43]. This reaction has also been reported to take place over Cu(111)[44], Au/Pd[34] and Sn/Pt(111)[38] surface alloys. However, the most extensively studied heterogeneous system for this reaction is on Pd surfaces[36,45-47]. The process is particularly interesting because it can be operated under widely different conditions: single crystals under UHV conditions, evaporated films, and dispersed Pd catalysts supported on alumina at atmospheric pressure are all effective. Mechanistic studies[48,49] have shown that the reaction involves an associative mechanism with an adsorbed C_4 metallocycle as the key intermediate and proceeds without scission of either C-H or C-C bonds (Scheme 5-2). The crucial C_4H_4 surface intermediate has been identified as a tilted metallocycle by a number of surface science techniques[50-52].

$$2C_2H_{2\,(a)} \longrightarrow C_4H_{4\,(a)} \xrightarrow{C_2H_{2\,(a)}} C_6H_{6\,(a)}$$

Scheme 5-2 : Accepted pathway for acetylene cyclomerization over palladium surfaces.

Some alloys have also shown activity in this reaction. Ormerod and co-workers[34] have demonstrated that although Au(111) is totally inert towards acetylene cyclization, Au/Pd surface alloys are very active. Sn-doped Pt(111) also produces benzene from acetylene under UHV conditions[38]. This catalytic system is very interesting since in contrast to Pd, Pt does not show any reactivity for the cyclotrimerization of acetylene due to the higher reactivity compared to Pd. As concerns Pt surfaces, it has been well-established that acetylene adsorbed at low temperatures converts to ethylidyne (CCH_3) upon annealing to room temperature or above on the Pt(111)[33,53,54] surface as well as on other transition metal surfaces[55-57].

This correlation between reactivity of the surface and the type of reaction that occurs on it is very well pointed out by Eng and co-workers[58]. They have shown that acetylene decomposes between 100 and 450 K on a clean W(211) surface, ultimately forming carbidic carbon and gaseous hydrogen. However, when a less reactive carbide-modified W(211) surface is used the C-H bond activation is suppressed, leading to

stabilisation of acetylene decomposition intermediates between 300-450 K. This increased stability of the intermediates on the carbide-modified surface, as compared to the clean one, suggests that there is a difference in the abilities of clean W(211) and C/W(211) to activate C-H bonds. This tuneable character of carbide surfaces makes molybdenum carbide suitable to perform complex chemical reactions on it, since the surface is initially reactive enough to break the very strong carbonyl bond and form the surface alkylidenes at low temperatures, but not so reactive that it decomposes the resultant surface species at higher temperatures[18-20,23,24].

Figure 5-4 displays TPD spectra for masses 2, 78, and 104 when 30 L of acetylene are introduced in the chamber at 100 K in the presence of a clean surface of β-Mo_2C. Those masses correspond to molecular peaks of hydrogen, benzene and cyclooctatetraene respectively. We can observe that there is a desorption peak centred at 273 K at the m/z=78 spectrum, corresponding to benzene, whereas no cyclooctatetraene desorption is observed in all the range of temperature. It is worth noting that m/z=78 is also a peak of a fragment of cyclooctatetraene, but the absence of the COT parent peak confirms that the feature observed at 273 K on the spectrum of m/z=78 is indeed due to benzene desorption.

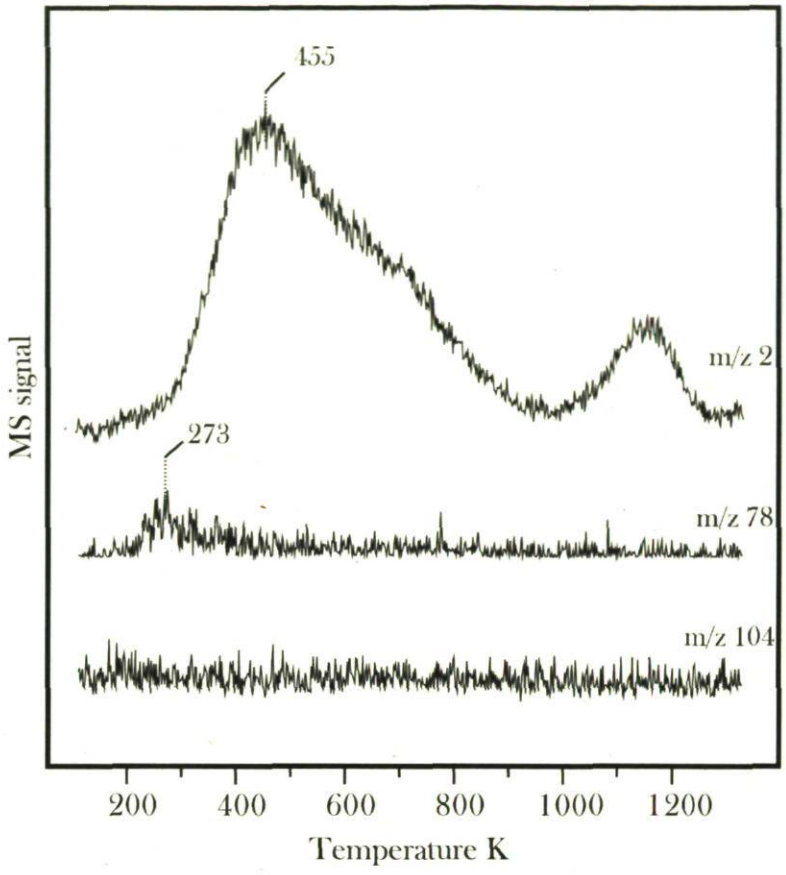

Figure 5-4 : TPD data for exposure of 20 L of acetylene on a clean surface. Data for H_2, C_6H_6 and C_8H_8 moieties desorption were recorded

The wide feature observed on the m/z=2 spectrum (H_2 desorption) with a maximum at 455 K, is due to molecular decomposition at higher temperatures. This implies that cyclo-oligomerization of acetylene on the surface of molybdenum carbide is active to that temperature, above which, molecular decomposition of acetylene leading to hydrogen desorption and carbon deposition on the surface takes place. This molecular decomposition has been already reported for a number of molecules adsorbed in this surface and is systematically observed in C(1s) spectra as a peak at 283.4 eV corresponding to undefined carbon deposition on the surface[17,20,21].

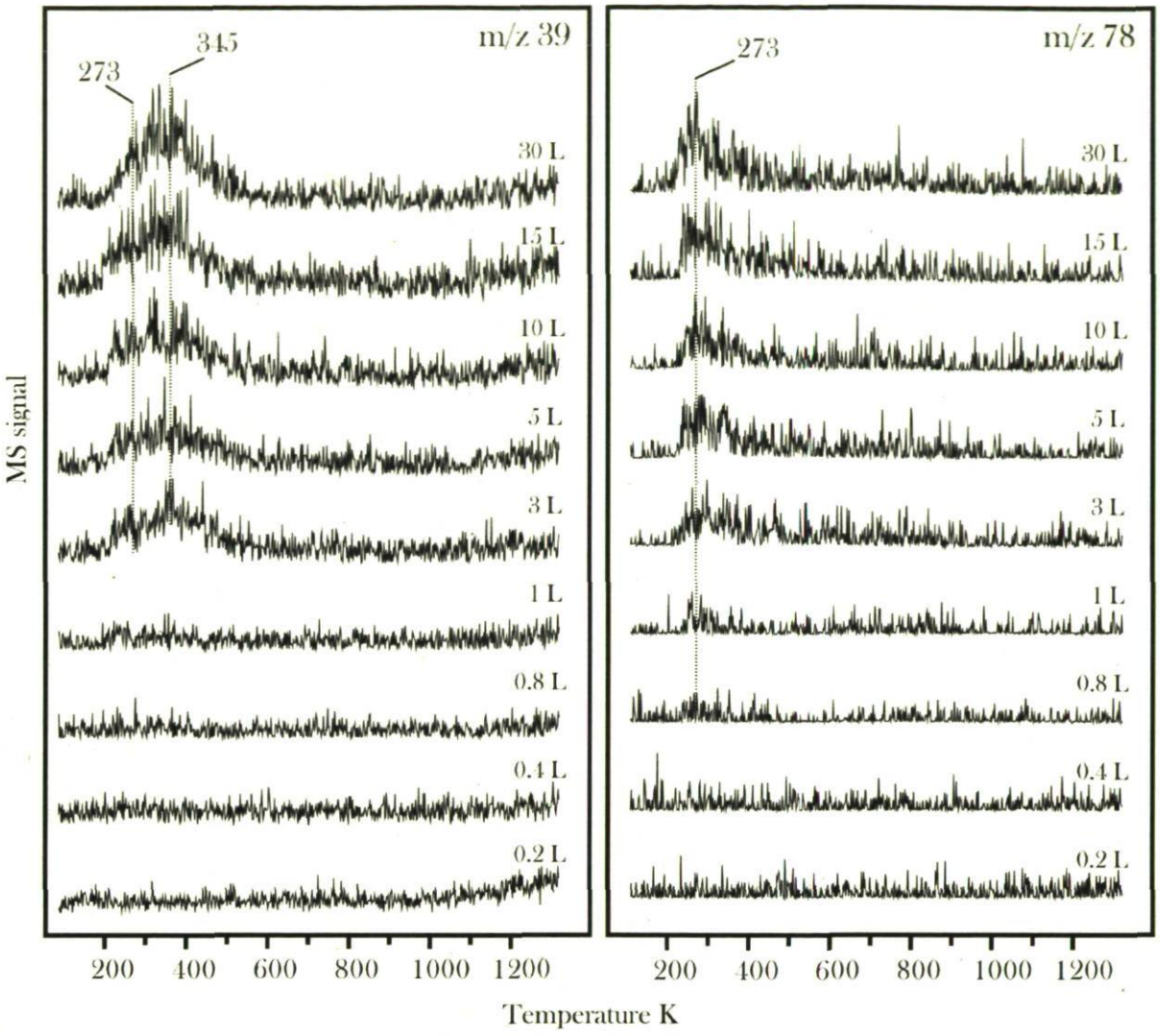

Figure 5-5 : TPD data for masses 39 and 78 as a function of exposure of acetylene at 100 K on the clean surface.

Spectra corresponding to m/z=39 as a function of exposure of acetylene (Figure 5-5) shows a double peak at coverages over 3 L (~1 monolayer) at 273 and 345 K. This doublet is not very well resolved since both peaks are very close together, but if we compare these results with data for m/z=78 it can be seen that the first peak, located at 273 K, is due to a benzene fragment matching the peak observed on the m/z=78 spectra at the same coverages. The second peak observed at 345 K is not observed however in the m/z=78 spectra, and can be attributed to surface butadiene species desorbing. This observation is supported by data in the literature. Abdelrehim et al.[59] have detected 1,3-butadiene peaks

appearing upon annealing a Pd(111) sample with adsorbed acetylene to 290 K, whereas Kyriakou et al.[44] have found traces of butadiene formation from acetylene coupling on Cu(111) at temperatures higher than 230 K.

Formation of butadiene provides direct chemical evidence for the formation of a C_4H_4 metallocycle intermediate for benzene formation. The coupling of two acetylene molecules to form a stable C_4 surface intermediate is the accepted mechanism for the acetylene cyclotrimerization towards benzene on the surface of Pd(111), being this the best characterized example of this reaction in heterogeneous catalysis[36,45-47]. Production of butadiene implies some C-H scission in the originally adsorbed acetylene to yield H_a that subsequently reacts with the C_4H_4 intermediate. The availability of this adsorbed hydrogen, though not directly observed, could arise from a complex interaction of acetylene with the surface, as it has been observed by Deng et al.[33] on acetylene adsorbed on Pt(111), and by Eng et al.[58] on clean and carbide-modified W(211) surfaces.

More information can be extracted from the H_2 desorption data displayed in Figure 5-6. In it, we can observe a first desorption peak from the submonolayer coverage centred at 345 K. This H_2 desorption is a direct observation of H_a produced on the surface as a consequence of C-H scission thereby providing the required adsorbed hydrogen for the formation and desorption of butadiene, since both hydrogen and butadiene desorption peaks appear at the same temperature. A second H_2 desorption peak is observed at 455 K indicating acetylene decomposition. This thermal decomposition has been observed at 450 K for acetylene adsorbed on carbide-modified W(211)[58], and at 496 K for acetylene adsorbed on Pt(111)[33].

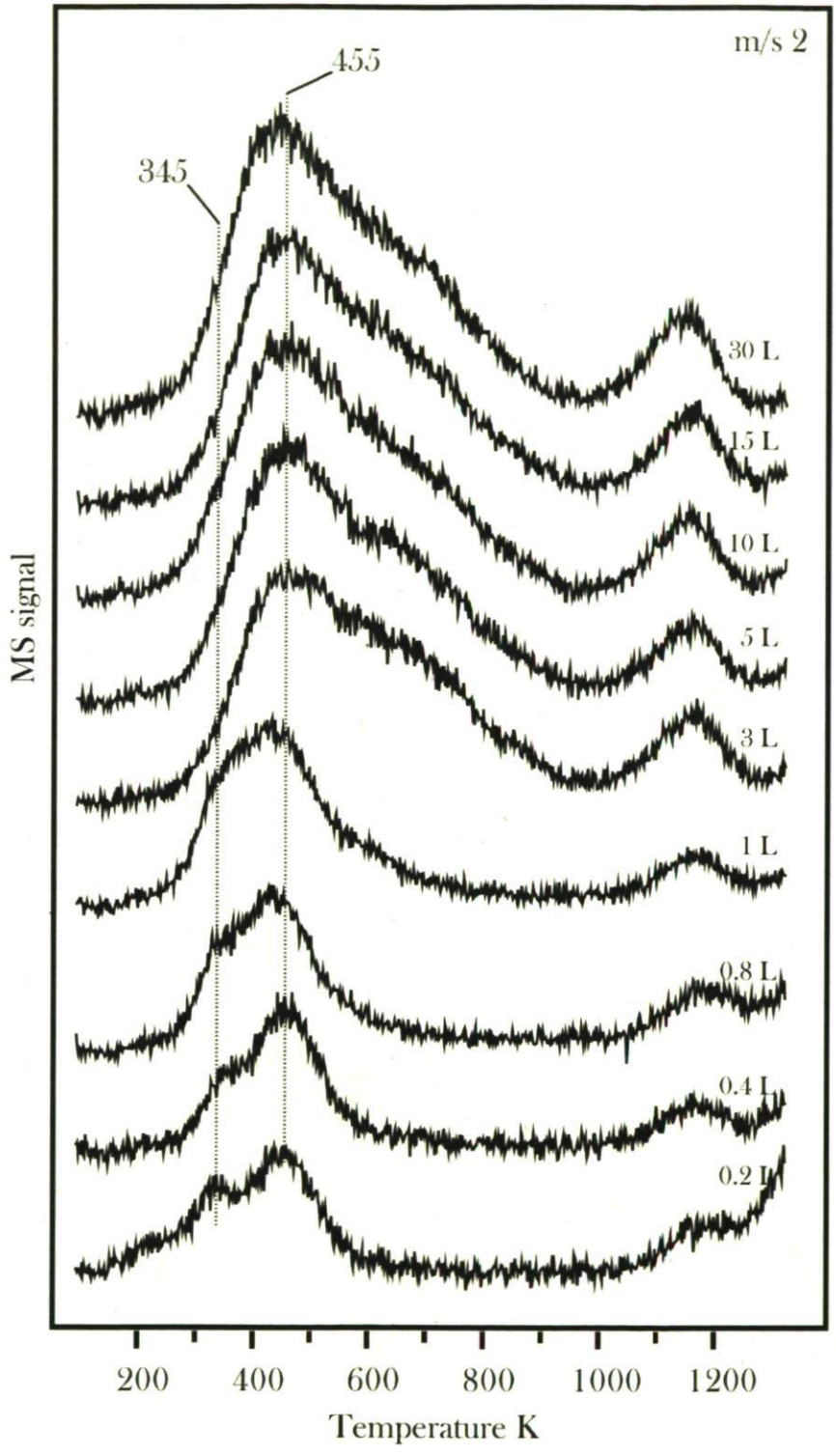

Figure 5-6 : TPD data for H_2 desorption as a function of acetylene exposure on a clean surface of molybdenum carbide.

5.4 Conclusion

Spectroscopic data of acetylene treatment on an alkylidene modified surface of molybdenum carbide show evidence of surface initiated acetylene metathesis polymerization under UHV conditions at near to room temperature. IR data at the C-H stretching region reveals that the formed polyacetylene is a mixture of *cis* and *trans* configurations, whereas XPS sequential spectra shows the evolution of the reaction with the exposure of the cyclopentylidene modified surface to increasing amounts of monomer, revealing the living character of this reaction. The latter provides the first insight of the formation of polyacetylene from the polymerization of acetylene directly bonded to a metallic surface.

Cyclo-oligomerization of acetylene has been also detected on the surface of β-Mo_2C. This is a well known reaction usually considered as a competing reaction of the polymerization itself. It is found that acetylene coupling occurs from low coverages to form butadiene and benzene at relatively low temperatures. The formation of butadiene reveals that the mechanism of the reaction, as in the case of Pd(111), is sequential, and the formation of benzene requires previous formation of surface C_4H_4 species. Cyclotetramerization leading to cyclooctatetraene was not recorded under these conditions.

5.5 Bibliography

(1) Natta, G.; Mazzanti, G.; Corradini, P. *Rend. Accad. Nazl. Lincei* **1958**, *25*, 2.

(2) Ito, T.; Shirakawa, H.; Ikeda, S. *J. Polym. Sci.* **1974**, *12*, 11.

(3) Luttinger, L. B. *J. Org. Chem.* **1962**, *27*, 1591.

(4) Soga, K.; Kobayashi, Y.; Ikeda, S.; Kawakami, S. *J. Chem. Soc. Chem. Commun.* **1980**, *19*, 931.

(5) Kambara, S.; Hatano, M.; Hosoe, T. *Kogyo Kagaku Zasshi* **1962**, *65*, 720.

(6) Merriwether, L. S. *J. Org. Chem.* **1961**, *26*, 5163.

(7) Cao, Y.; Qian, R. *Makromol. Chem. Rapid Commun.* **1982**, *3*, 687.

(8) Chen, Z.; Liu, M.; Shi, M.; Shen, Z.; Hummel, D. O. *Mackromol. Chem.* **1987**, *188*, 2687.

(9) Chen, z.; Liu, M.; Shi, M.; Shen, Z.; Hummel, D. O. *Mackromol. Chem.* **1987**, *188*, 2697.

(10) Aoky, K.; Kakudate, Y.; Yoshida, M.; Usuba, S.; Tanaka, K.; Fujiwara, S. *Synth. Metals* **1989**, *28*, 91.

(11) Woon, P. S.; Farona, M. F. *J. Polym. Sci. Chem. Ed.* **1974**, *12*, 1749.

(12) Schuehler, D. E.; Williams, J. E.; Sponsler, M. B. *Makromol.*. **2001**, *37*, 6255.

(13) Ren, F.; Feldman, A. K.; Carnes, M.; Steigerwald, M.; Nuckolls, C. *Makromol.*. **2007**, *40*, 8151.

(14) Scherman, O. A.; Grubbs, R. H. *Synth. Metals* **2001**, *124*, 431.

(15) Scherman, O. A.; Rutenberg, I. M.; Grubbs, R. H. *J. Am. Chem. Soc.* **2003**, *125*, 8515.

(16) Herisson, J. L.; Chauvin, Y. *Makromol. Chem.* **1971**, *141*, 161.

(17) Oudghiri-Hassani, H.; Siaj, M.; McBreen, P. H. *J. Phys. Chem. C* **2007**, *111*, 5954.

(18) Siaj, M.; Dubuc, N.; Temprano, I.; Maltais, C.; McBreen, P. H. *J. Phys. Chem.*, Article submitted.

(19) Siaj, M.; McBreen, P. H. *Science* **2005**, *309*, 588.

(20) Siaj, M.; Oudghiri-Hassani, H.; Maltais, C.; McBreen, P. H. *J. Phys. Chem. C* **2007**, *111*, 1725.

(21) Siaj, M.; Oudghiri-Hassani, H.; Zahidi, E. M.; McBreen, P. H. *Surf. Sci.* **2005**, *579*, 1.

(22) Siaj, M.; Reed, C.; Oyama, T.; Scott, S. L.; McBreen, P. H. *J. Am. Chem. Soc.* **2004**, *126*, 9514.

(23) Siaj, M.; Temprano, I.; Dubuc, N.; McBreen, P. H. *J. Organomet. Chem.* **2006**, *691*, 5497.

(24) Zahidi, E. M.; Oudghiri-Hassani, H.; McBreen, P. H. *Nature* **2001**, *409*, 1023.

(25) Kofranek, M.; Lischka, H.; Karpfen, A. *J. Chem, Phys.* **1992**, *96*, 982.

(26) Piaggio, P.; Dellepiane, G.; Piseri, L.; Tubino, R.; Taliani, C. *Sol. State Comm.* **1984**, *50*, 947.

(27) Shirakawa, H.; Ikeda, S. *Polym. J.* **1971**, *2*, 231.

(28) Will, F. G.; McDonald, R. S.; Gleim, R. D.; Winkle, M. R. *J. Chem, Phys.* **1983**, *78*, 5847.

(29) Rochet, F.; Bournel, F.; Gallet, J. J.; Dufour, G.; Lozzi, L.; Sirotti, F. *J. Phys. Chem. B* **2002**, *106*, 4967.

(30) Hitchcock, A. P.; Newbury, D. C.; Isii, I.; Stöhr, J.; Horsley, J. A.; Redwing, R. D.; Johnson, A. L.; Sette, F. *J. Chem, Phys.* **1986**, *85*, 4849.

(31) Solomon, J. L.; Madix, R. J.; Stöhr, J. *Surf. Sci.* **1991**, *255*, 12.

(32) Siaj, M.; Maltais, C.; Zahidi, E. M.; Oudghiri-Hassani, H.; Wang, J.; Rosei, F.; McBreen, P. H. *J. Phys. Chem. B* **2005**, *109*, 15376.

(33) Deng, R.; Jones, J.; Trenary, M. *J. Phys. Chem. C* **2007**, *111*, 1459.

(34) Ormerod, R. M.; Baddeley, C. J.; Lambert, R. M. *Surf. Sci. Lett.* **1991**, *259*, L710.

(35) Rucker, T. G.; Logan, M. A.; Gentle, T. M.; Muetterties, E. L.; Somorjai, G. A. *J. Phys. Chem.* **1986**, *90*, 2703.

(36) Sesselmann, W.; Woratschek, B.; Ertl, G.; Küppers, J.; Haberland, H. *Surf. Sci.* **1983**, *130*, 245.

(37) Vollhardt, K. P. C. *Acc. Chem. Res.* **1976**, *10*, 3344.

(38) Xu, C.; Peck, J. W.; Koel, B. E. *J. Am. Chem. Soc.* **1993**, *115*, 751.

(39) Berthelot, M. *C.R. Hebd. Seances Acad. Sci.* **1866**, *62*, 905.

(40) Badger, G. M.; Lewis, G. E.; Napier, I. M. *J. Chem. Soc.* **1960**, 2825.

(41) Reppe, W.; Schlichting, O.; Klager, K.; Toepel, T. *Justus Liebigs Ann. Chem.* **1948**, *560*, 1.

(42) Bertolini, J. C.; Massardier, J.; Dalmai-Imelik, G. *J. Chem. Soc. Faraday Trans.* **1978**, *1*, 1720.

(43) Colborn, R. E.; Volhardt, K. P. C. *J. Am. Chem. Soc.* **1986**, *108*, 5470.

(44) Kyriakou, G.; Kim, J.; Tikhov, M. S.; Macleod, N.; Lambert, R. M. *J. Phys. Chem. B* **2005**, *109*, 10952.

(45) Lee, A. F.; Baddeley, C. J.; Hardacre, C.; Lambert, R. M. *J. Am. Chem. Soc.* **1995**, *117*, 7719.

(46) Pacchioni, G.; Lambert, R. M. *Surf. Sci.* **1994**, *304*, 208.

(47) Rucker, T. G.; Logan, M. A.; Gentle, T. M.; Muetterties, E. L.; Somorjai, G. A. *J. Phys. Chem.* **1986**, *90*, 2703.

(48) Patterson, C. H.; Lambert, R. M. *J. Phys. Chem.* **1988**, *92*, 1266.

(49) Patterson, C. H.; Lambert, R. M. *J. Am. Chem. Soc.* **1988**, *110*, 6871.

(50) Hofmann, H.; Zaera, F.; Ormerod, R. M.; Lambert, R. M.; Wang, L. P.; Tysoe, W. T. *Surf. Sci.* **1990**, *232*, 259.

(51) Patterson, C. H.; Mundenar, J. M.; Timbrell, P. Y.; Gellman, A. J.; Lambert, R. M. *Surf. Sci.* **1989**, *208*, 93.

(52) Tysoe, W. T.; Nyberg, G. L.; Lambert, R. M. *Surf. Sci.* **1983**, *135*, 128.

(53) Avery, N. R. *Langmuir* **1988**, *4*, 445.

(54) Cremer, P. S.; Su, X.; Shen, Y. R.; Somorjai, G. A. *J. Phys. Chem. B* **1997**, *101*, 6474.

(55) Gates, J. A.; Kesmodel, L. L. *Surf. Sci.* **1983**, *124*, 68.

(56) Papageorgopoulos, D. C.; Ge, Q.; Nimmo, S.; king, D. A. *J. Phys. Chem. B* **1997**, *101*, 1999.

(57) Zhu, X. Y.; White, J. M. *Catal. Letters* **1988**, *1*, 247.

(58) Eng, J.; Chen, J. G.; Abdelrehim, I. M.; Madey, T. E. *J. Phys. Chem. B* **1998**, *102*, 9687.

(59) Abdelrehim, I. M.; Thornburg, N. A.; Sloan, J. T.; Caldwell, T. E.; Land, D. P. *J. Am. Chem. Soc.* **1995**, *117*, 9509.

6. General Conclusion

6.1 Conclusions

The present work was centred on the surface initiated metathesis growth of polyacetylene at alkylidene sites on the surface of molybdenum carbide. It is composed of two main parts.

The first part, the adsorption of aliphatic carbonyl molecules on molybdenum carbide, was studied in Chapter 3. Acetone and acrolein were found to adsorb at 100 K on the surface of β-Mo_2C in a η^1 adsorption state through the lone pair of the oxygen of the carbonyl group. This adsorption state is characterized by a perpendicular positioning of the molecular plane with respect to the surface. The annealing of these η^1 species to over 300 K led to the dissociative adsorption of these molecules yielding alkylidene species, dimethyl alkylidene in the case of acetone, and vinyl alkylidene in the case of acrolein (Scheme 6-1). The formation of these new species on the surface of molybdenum carbide was characterized by Reflection Absorption Infrared Spectroscopy (RAIRS), X-ray Photoelectron Spectroscopy (XPS), and Thermal Desorption Spectroscopy (TDS). It is believed that an intermediate η^2 adsorption state, with chemisorption bonding to both the oxygen and the carbon of the carbonyl group, is the responsible for such transformation, since a carbonyl-weakened parallel-to-the-surface species should be required for the C=O bond scission leading to surface alkylidene and surface oxo species. Although no spectroscopic evidences of such an adsorption state were found, examples of this species adsorbed on other metal surfaces are well established in the literature[1-11].

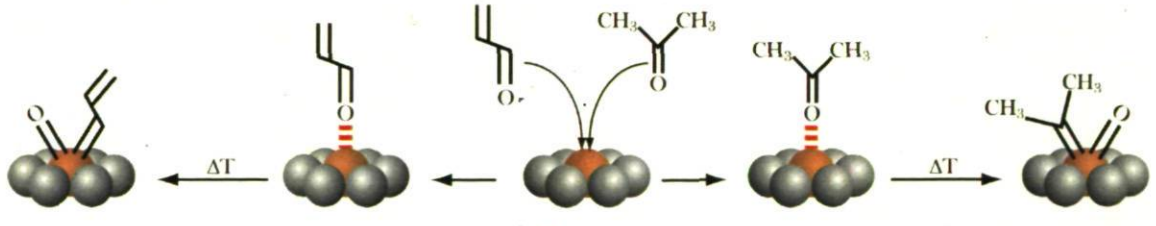

Scheme 6-1 : Formation of dimethyl alkylidene and vinyl alkylidene from the dissociative adsorption of acetone and acrolein respectively.

It was found, thus, that acetone and acrolein adsorption behaviour on molybdenum carbide matches that previously observed for cyclic ketones (cyclobutanone, cyclopentanone, and cyclohexanone) and acetaldehyde, reported by McBreen and co-workers[12-18] on the same surface under similar conditions.

The second part of this thesis deals with the formation of polyacetylene directly bonded to the surface through a double bond by metathesis reactions at alkylidene sites. Two polymerization methods were studied for the growth of polyene chains, the ring opening metathesis polymerization of 1,3,5,7-cyclooctatetraene, and the metathesis polymerization of acetylene (Scheme 6-2).

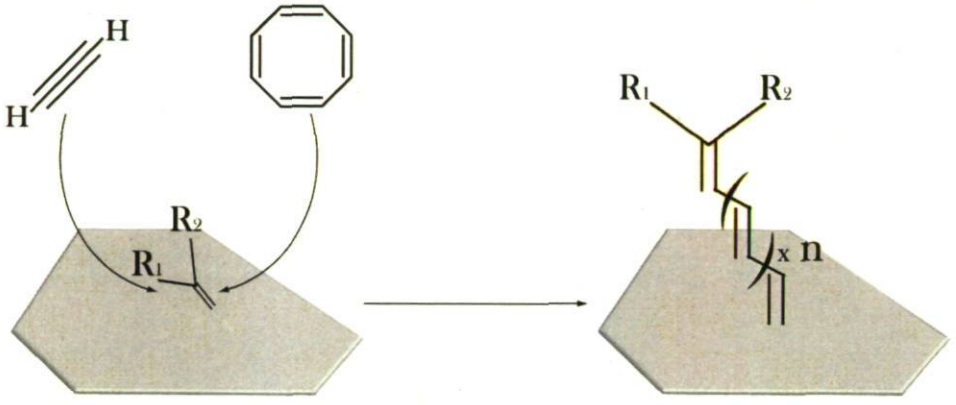

Scheme 6-2 : Metathesis polymerization of acetylene and cyclooctatetraene towards the formation of polyacetylene on the surface of alkylidene modified molybdenum carbide.

Ring opening metathesis polymerization of cyclooctatetraene at cyclopentylidene and vinyl alkylidene sites was discussed in Chapter 4. RAIRS and XPS data suggest the growth of polyene molecules on the surface of molybdenum carbide when an alkylidene functionalized surface is treated with cyclooctatetraene at temperatures above 350 K. Vibrational spectroscopy data suggest that short polyacetylene chains were formed. An analysis of the frequency of the C=C stretching band, together with the relative intensities of the different carbon species in the XPS spectra suggest that mainly one monomer insertion occurs, and essentially polyene chains of 4 double bonds are formed[19-23].

The low temperature required for this metathesis polymerization is remarkable since more strained olefins such as norbornene and cyclopentene undergo the same reaction only

at temperatures above 470 K[16,18]. An explanation for this phenomenon could arise from the adsorption characteristics of cyclooctatetraene. RAIRS data, in agreement with the literature[25-31], suggest that cyclooctatetraene undergoes planarization when adsorbed on molybdenum carbide with the four double bonds of the molecule taking part in the adsorption process. This fact could lead to two consequences that favour the polymerization reaction. One is the fact that a planar molecule with four double bonds interacts more strongly with the surface, and thus a higher sticking coefficient and a longer residence time should be expected. Second, the planarization of cyclooctatetraene adds strain tension to the cycle thereby increasing the driving force for ring opening metathesis polymerization.

As described in Chapter 5, acetylene metathesis then was studied following the same procedure as for the ROMP of cyclooctatetraene. It was found that acetylene insertion at alkylidene sites of the modified surface of molybdenum carbide leads to the growth of polyacetylene at similar conditions to those found for the polymerization of cyclooctatetraene. These results emphasize the high reactivity of this catalytic system for metathesis polymerizations leading to the formation of chemisorbed conjugated polymers. During this study it was found that acetylene adsorption on the clean surface of molybdenum carbide leads to benzene and butadiene formation at low temperatures (273 and 345 K respectively) under UHV conditions. This reaction, though novel for this material, has been previously observed for a number of heterogeneous catalytic systems[32-48].

Conformational differences between the polyacetylene chains formed by both methods were found. Although an exhaustive study on this subject would be required in order to firmly establish these differences and the conditions under which each conformation is obtained, RAIRS data suggest the formation of different proportions of *cis* and *trans* conformers of the surface-initiated polyene molecules depending the on synthetic method, the initiator species, and the reaction conditions.

Bromination of polyacetylene molecules formed on the surface was performed in order to further characterize the chemisorbed chain, by monitoring the Br(3d) region of the XPS spectra. Two peaks were found when the polyacetylene modified surface of molybdenum carbide was exposed to bromine. A low energy peak (68.5 eV) was assigned

to molecular Br atoms bonded to the conjugated chain, in agreement with observations in the literature[49,50]. A higher binding energy peak (76.3 eV) appears both when the surface is modified with polyacetylene and on the clean surface, and must be then assigned to surface bromine species.

The direct growth of alkylidene bonded polyene molecules reported in this work is the first observation of an intrinsically conducting polymer directly bonded to a metallic surface through a double bond.

6.2 Future works

Although studies of olefin metathesis on molybdenum carbide have been carried out from some time now, there is still a long way to fully understand the processes involved, and to fully develop the potential of this catalytic system. Hence, here I propose some studies that might be carried out in order to progress in the knowledge of the chemistry of the alkylidene modified surface of molybdenum carbide.

- A study of the conformational properties of the surface-initiated growth of polyacetylene on molybdenum carbide could be carried out by a careful vibrational characterization of the polyene chains formed under various conditions.

- The formation of polyacetylene on molybdenum carbide has been attempted on a polycrystalline material. However the study of metathesis reactions on monocrystalline materials with different faces could shed light on the activity of the different surface sites, and could help to further understand the properties of this catalytic system.

- Scanning Tunneling Microscopy (STM) studies would be interesting in order to precisely quantify the number of active surface alkylidene species on the surface of β-Mo_2C, as well as the number, length, and morphology of polymeric molecules formed from metathesis reactions.

- This microscopic technique could also help to further understand the mechanism of alkylidene formation by studying possible conformational changes of adsorbed carbonyl molecules as a function of temperature, and by investigating the possible creation of domains via intermolecular interactions.

- STM studies could also provide information on the electronic properties of the metal-molecule junction, as well as of the polyene chains and the effect of halogenation on these properties.

- Ultraviolet Photoelectron Spectroscopy (UPS) could help to characterize the band structure of the polyene molecules, and thus get insights of the electronic properties of these materials when directly grown from the surface of a metal.

- Studies under ambient conditions would have to be made in the future to investigate the possible utility of the alkylidene modified surface of molybdenum carbide as heterogeneous catalyst for industrial processes.

6.3 Bibliography

(1) Avery, N. R.; Weinberg, W. H.; Anton, A. B.; Toby, B. H. *Phys. Rev. Lett.* **1983**, *51*, 683.

(2) Jeffery, E. L.; Mann, R. K.; Hutchings, G. J.; Taylor, S. H.; Willock, D. J. *Catalysis Today* **2005**, *105*, 85.

(3) Vannice, M. A.; Erley, W.; Ibach, H. *Surf. Sci.* **1991**, *254*, 1.

(4) Villegas, I.; Weaver, M. J. *J. Am. Chem. Soc.* **1996**, *118*, 458.

(5) Anton, A. B.; Avery, N. R.; Toby, B. H.; Weinberg, W. H. *J. Am. Chem. Soc.* **1986**, *108*, 684.

(6) Davis, J. L.; Barteau, M. A. *Surf. Sci.* **1989**, *208*, 383.

(7) Houtman, C.; Barteau, M. A. *J. Phys. Chem.* **1991**, *95*, 3755.

(8) Sim, W.-S.; Li, T.-C.; Yang, P.-W.; Yeo, B.-S. *J. Am. Chem. Soc.* **2002**, *124*, 4970.

(9) Fujii, S.; Misono, Y.; Itoh, K. *Surf. Sci.* **1992**, *277*, 220.

(10) Fujii, S.; Osaka, N.; Akita, M.; Itoh, K. *J. Phys. Chem.* **1995**, *99*, 6994.

(11) Akita, M.; Osaka, N.; Itoh, K. *Surf. Sci.* **1998**, *405*, 172.

(12) Oudghiri-Hassani, H.; Siaj, M.; McBreen, P. H. *J. Phys. Chem. C* **2007**, *111*, 5954.

(13) Siaj, M.; Oudghiri-Hassani, H.; Zahidi, E. M.; McBreen, P. H. *Surf. Sci.* **2005**, *579*, 1.

(14) Siaj, M.; Reed, C.; Oyama, T.; Scott, S. L.; McBreen, P. H. *J. Am. Chem. Soc.* **2004**, *126*, 9514.

(15) Zahidi, E. M.; Oudghiri-Hassani, H.; McBreen, P. H. *Nature* **2001**, *409*, 1023.

(16) Siaj, M.; Dubuc, N.; Temprano, I.; Maltais, C.; McBreen, P. H. *J. Phys. Chem.*, Article submitted.

(17) Siaj, M.; Temprano, I.; Dubuc, N.; McBreen, P. H. *J. Organomet. Chem.* **2006**, *691*, 5497.

(18) Siaj, M.; McBreen, P. H. *Science* **2005**, *309*, 588.

(19) Shirakawa, H.; Ikeda, S. *Polym. J.* **1971**, *2*, 231.

(20) Parente, V.; Fredriksson, C.; Selmani, A.; Lazzaroni, R.; Bredas, J. L. *J. Phys. Chem. B* **1997**, *101*, 4193.

(21) Schettino, V.; Gervasio, F. L.; Cardini, G.; Salvi, P. R. *J. Chem. Phys.* **1999**, *110*, 3241.

(22) Takeuchi, H.; Furukawa, Y.; Harada, I.; Shirakawa, H. *J. Chem. Phys.* **1986**, *84*, 2882.

(23) Schaffer, H. E.; Chance, R. R.; Silbey, R. J.; Knoll, K.; Schrock, R. R. *J. Chem, Phys.* **1991**, *94*, 4161.

(24) Kofranek, M.; Lischka, H.; Karpfen, A. *J. Chem, Phys.* **1992**, *96*, 982.

(25) Hitchcock, A. P.; Newbury, D. C.; Isii, I.; Stöhr, J.; Horsley, J. A.; Redwing, R. D.; Johnson, A. L.; Sette, F. *J. Chem, Phys.* **1986**, *85*, 4849.

(26) Lee, A. F.; Baddeley, C. J.; Hardacre, C.; Lambert, R. M. *J. Am. Chem. Soc.* **1995**, *117*, 7719.

(27) Merrill, P. B.; Madix, R. J. *Surf. Sci.* **1996**, *365*, 701.

(28) Hovis, J. S.; Hamers, R. J. *J. Phys. Chem. B* **1998**, *102*, 687.

(29) Tegeder, P.; Danckwerts, M.; Hagen, S.; Hotzel, A.; Wolf, M. *Surf. Sci.* **2005**, *585*, 177.

(30) Rochet, F.; Bournel, F.; Gallet, J. J.; Dufour, G.; Lozzi, L.; Sirotti, F. *J. Phys. Chem. B* **2002**, *106*, 4967.

(31) Hostetler, M. J.; Nuzzo, R. G.; Girolami, G. S.; Dubois, L. H. *J. Phys. Chem.* **1994**, *98*, 2952.

(32) Deng, R.; Jones, J.; Trenary, M. *J. Phys. Chem. C* **2007**, *111*, 1459.

(33) Ormerod, R. M.; Baddeley, C. J.; Lambert, R. M. *Surf. Sci. Lett.* **1991**, *259*, L710.

(34) Sesselmann, W.; Woratschek, B.; Ertl, G.; Küppers, J.; Haberland, H. *Surf. Sci.* **1983**, *130*, 245.

(35) Xu, C.; Peck, J. W.; Koel, B. E. *J. Am. Chem. Soc.* **1993**, *115*, 751.

(36) Reppe, W.; Schlichting, O.; Klager, K.; Toepel, T. *Justus Liebigs Ann. Chem.* **1948**, *560*, 1.

(37) Bertolini, J. C.; Massardier, J.; Dalmai-Imelik, G. *J. Chem. Soc. Faraday Trans.* **1978**, *1*, 1720.

(38) Colborn, R. E.; Volhardt, K. P. C. *J. Am. Chem. Soc.* **1986**, *108*, 5470.

(39) Kyriakou, G.; Kim, J.; Tikhov, M. S.; Macleod, N.; Lambert, R. M. *J. Phys. Chem. B* **2005**, *109*, 10952.

(40) Lee, A. F.; Baddeley, C. J.; Hardacre, C.; Lambert, R. M. *J. Am. Chem. Soc.* **1995**, *117*, 7719.

(41) Pacchioni, G.; Lambert, R. M. *Surf. Sci.* **1994**, *304*, 208.

(42) Rucker, T. G.; Logan, M. A.; Gentle, T. M.; Muetterties, E. L.; Somorjai, G. A. *J. Phys. Chem.* **1986**, *90*, 2703.

(43) Patterson, C. H.; Lambert, R. M. *J. Phys. Chem.* **1988**, *92*, 1266.

(44) Patterson, C. H.; Lambert, R. M. *J. Am. Chem. Soc.* **1988**, *110*, 6871.

(45) Hofmann, H.; Zaera, F.; Ormerod, R. M.; Lambert, R. M.; Wang, L. P.; Tysoe, W. T. *Surf. Sci.* **1990**, *232*, 259.

(46) Patterson, C. H.; Mundenar, J. M.; Timbrell, P. Y.; Gellman, A. J.; Lambert, R. M. *Surf. Sci.* **1989**, *208*, 93.

(47) Tysoe, W. T.; Nyberg, G. L.; Lambert, R. M. *Surf. Sci.* **1983**, *135*, 128.

(48) Eng, J.; Chen, J. G.; Abdelrehim, I. M.; Madey, T. E. *J. Phys. Chem. B* **1998**, *102*, 9687.

(49) Ikemoto, I.; Cao, Y.; Yamada, M.; Kuroda, H.; Harada, I.; Shirakawa, H.; Ikeda, S. *Bull. Chem. Soc. Jpn.* **1982**, *55*, 721.

(50) Kang, E. T.; Neoh, K. G.; Tang, K. L.; Tang, B. T. G. *J. Polym. Sci. B* **1989**, *27*, 2061.